Experimental and Computational insight into Transition Metal Catalyzed Cascade Reactions

Thesis Submitted in fulfilment for the award of the degree of

Doctor of Philosophy

by

POOJA SOAM

(Reg. No. 901909010)

Under the supervision of

Dr. VIKAS TYAGI
Assistant Professor

Dr. DEBASISH MANDAL
Assistant Professor

DEPARTMENT OF CHEMISTRY AND BIOCHEMISTRY
Thapar Institute of Engineering & Technology
Patiala-147004, Punjab
India

2024

Dedicated to

my father

Mr. Vinit Kumar Soam

Acknowledgments

First and foremost, I want to express my sincere gratitude to ***LORD SHIVA*** *for all of the blessings he has bestowed upon me during my efforts to finish this successful research work of mine.*

This entire Ph.D. journey has been very transformative for me. Everything about my time at T.I.E.T. has been incredible. New chances have been given to me, and they have been beneficial to me. Without the help, motivation, and direction received from numerous people, I would not have been able to complete my Ph.D.

It gives me great pleasure to express my gratitude to my supervisors, ***Dr. Vikas Tyagi,*** *Assistant Professor, Department of Chemistry and Biochemistry, TIET, Patiala, and* ***Dr. Debasish Mandal,*** *Assistant Professor, Department of Chemistry and Biochemistry, TIET, Patiala for their unwavering support & guidance regarding fundamental principles, helpful ideas that enabled me to successfully begin and complete my research work. They gave me the motivation I needed to keep going, keep learning new things, and fix my mistakes as I went. Their assistance proved extremely valuable during the entire period of the research and thesis writing process. It was a wonderful learning experience to work under their supervision.*

I want to express my gratitude to ***Prof. Padmakumar Nair****, Director,* ***Prof. N.Tejo Prakash****, Dean of Research and Sponsored Projects, and* ***Dr. Bhupendra Kumar Chudasama,*** *Associate Dean of Research and Sponsored Projects, T.IE.T. Patiala. I would like to express my profound appreciation to* ***Prof. Manmohan Chhibber****, the head of the Department of Chemistry and Biochemistry, for giving me the chance to join this prestigious organization and being so helpful and supportive. I want to extend my sincere gratitude to my doctoral committee members,* ***Dr. Kamaldeep Paul, Dr. Bhupesh Goyal,*** *and* ***Dr. M. S. Reddy,*** *for their never-ending support, perceptive criticism, and insightful ideas during my research. I would also like to extend my gratitude to all the faculty members in the Department of Chemistry and Biochemistry for their invaluable support and wishes. I extend my heartfelt gratitude to* ***Mr. Chander Thakur, Mr. Hemant, Mr. Mayank Sharma****, and all the non-teaching staff of DCBC for their invaluable help and cooperation.*

I express my gratitude to our funding agencies, Department of Science and Technology (DST) and the Science and Engineering Research Board (SERB), Government of India, Center of Excellence in Emerging Materials (CEEMS-VT) for their financial support during the entire period of my doctoral research. I would like to thank, the DST-FIST-sponsored HR-MS, GC-MS and HPLC facilities available in the Department of Chemistry and Biochemistry. I would like to express my gratitude to ***Mr. Mukesh Aggarwal****, Senior Research Scientist, SAI Lab, for his friendly attitude during the operation of the NMR facility. I would like to thank Ministry of Human Resource Development (MHRD) sponsored Single Crystal X-ray Diffraction (SCXRD)*

facility at Central Analytical Facility (CAF), IISER, Mohali, Punjab, DST- FIST sponsored Single Crystal X-ray Diffraction (SCXRD) facility at Department of Chemistry, Panjab University, Chandigarh and Central Research Facility (CRF), National Institute of Technology, Rourkela, Odisha for providing crystal data.

I want to express my deepest gratitude to ***Dr. Priya Kamboj and Parmjeet Kaur****, for their unwavering support and encouragement throughout this challenging journey. Their insightful discussions and critical feedback have helped shape the direction of my research. They constantly served as a source of happiness, and inspiration and provided emotional support throughout this journey. This entire journey would not have been possible without their assistance and indispensable contributions. I would like to express my heartfelt gratitude to* ***Ms. Kirti Singh*** *and* ***Mr. Abinash Mohapatra*** *for their helpful character, and providing valuable suggestions, and for willingly helping me out with their abilities. They both always tried to uplift my spirits and ensure my well-being. I will always be thankful to all of them for making my PhD journey, an unforgettable and remarkable experience. I gratefully acknowledge the help and support I got from my seniors* ***Dr. Sunil Dutt*** *and* ***Dr. Meenakshi Budhiraja.*** *I would also like to express my gratitude to my other labmates* ***Akanksha Katoch, Lovleen Kaur, Anuva Mondal*** *and* ***Jasvinder Amul*** *for their help and support. I gratefully acknowledge the guidance, help, and support I got from my seniors and friends,* ***Dr. Priyanka Gautam, Dr. Dinesh Singla, Dr. Gaurav Sharma, Dr. Rajesh Kondabala, Dr. Abida, Dr. Aastha Palta, Anshu Tyagi, Mallika Phull, Akanksha Ranade, Yogesh Kumar*** *and other research fellows during my whole journey.*

Words are inefficient to express my gratitude towards ***Mrs. Leela Devi****, my grandmother,* ***Mr. Vinit Kumar Soam,*** *and* ***Mrs. Sudha Soam****, my parents, and my whole family, who love me, support me and inspire me to follow my dreams. They have always supported me whether it is emotionally or financially and their belief in me has always kept my spirits and motivation high in tough times. Without them, my success and the completion of my Ph.D. degree would not have been possible. I want to extend my sincere appreciation to my siblings and cousins,* ***Mr. Gaurav Soam, Mr. Sumit Soam, Mr. Shivam Soam, Mr. Mehul Soam, Mrs. Nisha Pundir, Mrs. Minakshi Raghav, Ms. Shivani Soam, Ms. Shraddha Soam and Ms. Yashika Soam*** *for continually offering firm support in various situations. Engaging in daily conversations with them resulted a relief on my soul and brought a broad smile every day. I am also gratefully thankful to my whole family for their emotional support, encouragement, and patience during my Ph.D. journey.*

Lastly, I would like to thank everyone in my life who encouraged me and helped me in whatever way possible.

Pooja Soam

Certificate

This is to certify that the thesis entitled **"Experimental and Computational insight into Transition Metal Catalyzed Cascade Reactions"**, being submitted by **Pooja Soam,** Department of Chemistry and Biochemistry, Thapar Institute of Engineering and Technology, Patiala for the award of the degree of Doctor of Philosophy, is a bonafide piece of research work carried out by her. Pooja Soam has worked under our guidance and supervision and has fulfilled the requirements for the submission of the thesis, which to our knowledge has reached the requisite standard. The results embodied in the thesis have not been submitted in part or full to any other University or Institute for the award of any degree or diploma.

Supervisors:

Dr. Vikas Tyagi
(Supervisor)
Assistant Professor
DCBC
TIET, Patiala

Dr. Debasish Mandal
(Supervisor)
Assistant Professor
DCBC
TIET, Patiala

Head:

Dr. Manmohan Chhibber
Professor and Head
DCBC
TIET, Patiala.

Candidate's Declaration

I, hereby declare that the work presented in the thesis entitled **"Experimental and Computational insight into Transition Metal Catalyzed Cascade Reactions"** in the fulfillment of the requirement for the award of the degree of Philosophy, Department of Chemistry and Biochemistry, Thapar Institute of Engineering and Technology, Patiala is an authentic record of my work carried out under the supervision of ***Dr. Vikas Tyagi***, Assistant Professor, and ***Dr. Debasish Mandal***, Assistant Professor, Department of Chemistry and Biochemistry, Thapar Institute of Engineering and Technology, Patiala, India. The matter embodied in the thesis has not been submitted in part or full to any other University or Institute for the award of any degree in India or abroad.

Pooja Soam

Contents

THF	Tetrahydrofuran
DMSO	Dimethyl sulfoxide
EtOH	Ethanol
MeOH	Methanol
DMF	Dimethylformamide
NaOH	Sodium hydroxide
K_2CO_3	Potassium carbonate
Cs_2CO_3	Cesium carbonate
KO^tBu	Potassium tert-butoxide
$Cu(OAc)_2$	Copper acetate
$Pd(OAc)_2$	Palladium acetate
$Rh_2(OAc)_4$	Rhodium acetate dimer
^1H NMR	Proton Nuclear Magnetic Resonance
^{13}C NMR	Carbon Nuclear Magnetic Resonance
TMS	Tetramethyl silane
D_2O	Deuterium oxide
$CDCl_3$	Deuterated chloroform
GC	Gas Chromatography
HPLC	High-Performance Liquid Chromatography
UV	Ultra-violet Spectroscopy
IR	Infrared Spectroscopy
GC-MS	Gas chromatography and Mass Spectrometry
LC-MS	Liquid chromatography with Mass Spectrometry
HRMS	High-resolution mass spectrometry
TLC	Thin Layer Chromatography
KMnO4	Potassium Permanganate
ppm	Parts per million
Mol	Mole
mmol	Millimole

kJ mol^{-1}	Kilo joule per mole
kJ mol K^{-1}	Kilo Joule per mole per kelvin
Min^{-1}	Per minute
h^{-1}	Per hour
mL	Millilitre
uL	Microlitre
mg	Milligram
nm	Nanometre
Mm	Millimeter
MHz	Megahertz
eV	Electron volt
v/v	Volume by volume
NR	No reaction
Equiv.	Equivalent
MM	Molar Mass
EW	Equivalent Weight

Symbols	Description
Å	Angstrom
C	Celsius
E*a*	Activation Energy
T	Temperature
ΔG‡	Gibb's free energy
g	gram
°	Degree
λ	Wavelength
Min	Minute
h	Hour
s	Second
%	Percentage
Y	Yield
C	Conversion
K	Kelvin
α	alpha
β	beta
μ	micro
ρ	Rho
σ	Sigma
γ	gamma
k	Rate constant
h	Plank's constant
v	frequency
mg	milligram
o	ortho
m	meta
p	para
L	litre

Great efforts have been devoted in the past many years to synthesizing clinically important novel heterocyclic compounds using transition metal-mediated reactions. Further, transition metal-catalyzed cascade or tandem reactions for the synthesis of crucial heterocyclic scaffolds have attracted a lot of attention in the last few years. These reactions can form multiple bonds in one pot without changing the reaction conditions and overall reduce the reaction steps and requirement of intermediate purifications. The reduction of reaction steps leads to saving reagents, energy and eliminates waste generation which makes the cascade reactions eco-friendly as well as highly economical. In this context, several transition metal catalysts like Rh, Pd, Cu, Ru, Ir, Fe, etc. have been employed to perform these kinds of reactions. In this view, carbenes or their precursors like diazo, hydrazones, etc. played an important role in making them more advantageous. On the other hand, computational chemistry is playing an important role and growing its roots in various fields of chemistry day by day. Particularly, in organic synthesis, DFT studies are widely used for mechanistic investigation and treated as an important tool for novel synthesis route detection. In the first chapter of this thesis, we are highlighting some appreciable efforts made in recent years towards the synthesis of highly important novel heterocyclic moieties by using palladium catalyzed cascade reactions including carbene transfer, isocyanide insertion, C-H activation, and cyclization as the vital steps. Also, mechanistic investigation via various experimental and computational studies, further transformation and applications, etc. are covered in these reports.

In the second chapter, we have described a divergent and selective synthesis of *(E)*-3-alkylidene oxindole, which is a highly valuable framework due to its presence in the biologically important molecules, via palladium-catalyzed multicomponent reaction of 3-diazo oxindole, isocyanide, and aniline has been developed. Further, the feasibility of the reaction was demonstrated by employing differently substituted 3-diazo oxindoles, isocyanides, and anilines as starting material and obtaining the corresponding products in 31-83% isolated yields. Besides, a plausible mechanism has been presented and further investigated using DFT calculations which suggest the formation of the Pd-carbene complex and ketenimine intermediate as the key step during the catalytic cycle.

In the third chapter of this thesis, we have reported a Pd-catalyzed multicomponent cascade reaction of 3-diazo oxindole and isocyanides to synthesize N-fused polycyclic indoles consisting of in-situ generated amide-assisted regioselective [3+1+1] annulation reaction provided yields up to 76% yield. Further, a good range of substrate libraries was also synthesized to check the feasibility of the protocol. The reaction includes carbene insertion

methodology for amide formation which subsequently assists the reaction for further double isocyanide insertion. Additionally, a mechanism is proposed and investigated using the DFT study that strongly favors the role of amide in assisting the annulation reaction, which was further confirmed using control experiments.

In the fourth chapter, we have synthesized (Z)-*N*-(tert-butyl)-2-oxo-3-(2-phenylhydrazono) indoline-1-carboxamide derivatives by using palladium-catalyzed isocyanide insertion methodology towards less reactive secondary N-H bond present in isatin phenyl hydrazone where phenyl hydrazone group act as a strong donating group enhancing the electron density at nitrogen atom to increase its nucleophilicity. These *N*-Carboxamide scaffolds can be used as valuable precursors for the synthesis of various biologically active moieties. A broad range of substrates have been synthesized in moderate to good yields by using different electron-withdrawing, electron-donating, and halogen substituents at isatin as well as hydrazone ring. Also, different isocyanides were incorporated to check the feasibility of the reaction.

In the fifth chapter**,** we have developed a Pd-catalyzed one-pot cascade consisting of C-C/C-O/N-N bond formation to access clinically important fused 1,2,3-triazole using N-aryl-α-(tosyl hydrazone)acetamides with isocyanide. Besides, various substitutions on the N-aryl part of acetamides along with different isocyanides show good compatibility in this protocol. Next, two plausible mechanistic routes were proposed, however, one of the routes was more favorable and involved the formation of the benzoxazine ring first followed by the realization of a triazole ring. Additionally, the more favorable mechanistic route was investigated using DFT studies which suggests Pd(II)-isocyanide complex and α-diazoimino intermediate formation were key steps in the catalytic cycle.

CHAPTER 1

Introduction & Literature Review

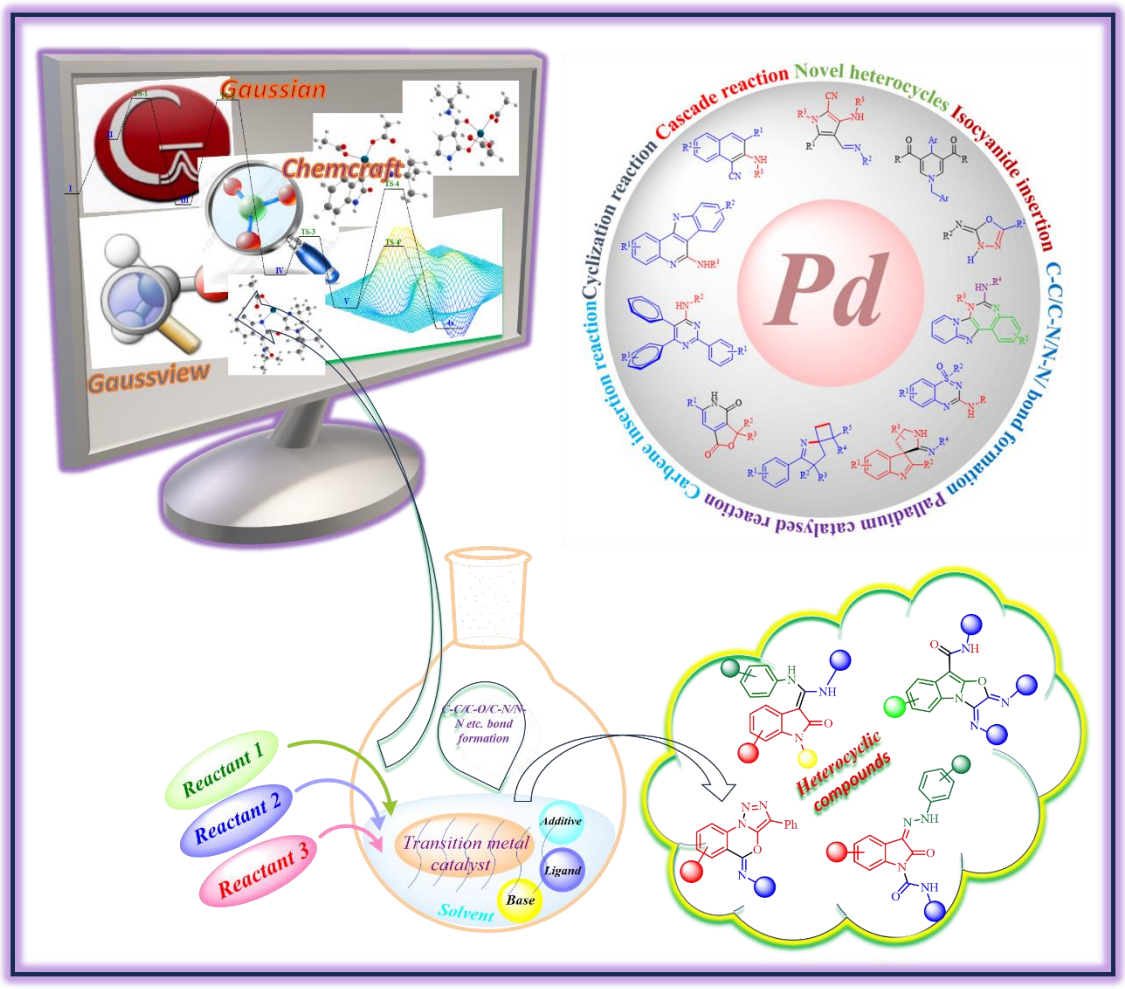

1.1 Introduction

The transition metal complexes have been considered as an imperative class of catalysts in the last decades due to their tremendous properties i.e., ability to adopt multiple oxidation states, having empty d-orbitals that can easily enable to accept or donate electrons from other molecules, showing the variability of co-ordination number and a high tolerance for various ligands.[1–3] Further, the homogeneous and heterogeneous nature of these catalysts provides an easy and fast approach towards the development of various novel organic molecules that possess various applications in several areas such as medicinal, environmental, energy storage, plastics, etc.[4,5] Particularly, transition metals are being used for catalyzing various types of reactions like coupling reactions, hydrogenation, alkylation, cyclopropanation, hydrogenolysis, annulation reactions, C-X activation, C-H activation, insertion reaction, cyclization, metathesis, carbene insertion reactions, etc (**Figure 1.1**).[6–10] Despite their long history in synthetic organic chemistry, the discovery of novel transition metal-catalyzed approaches is still an active and widely recognized area in the present era of research.[11,12]

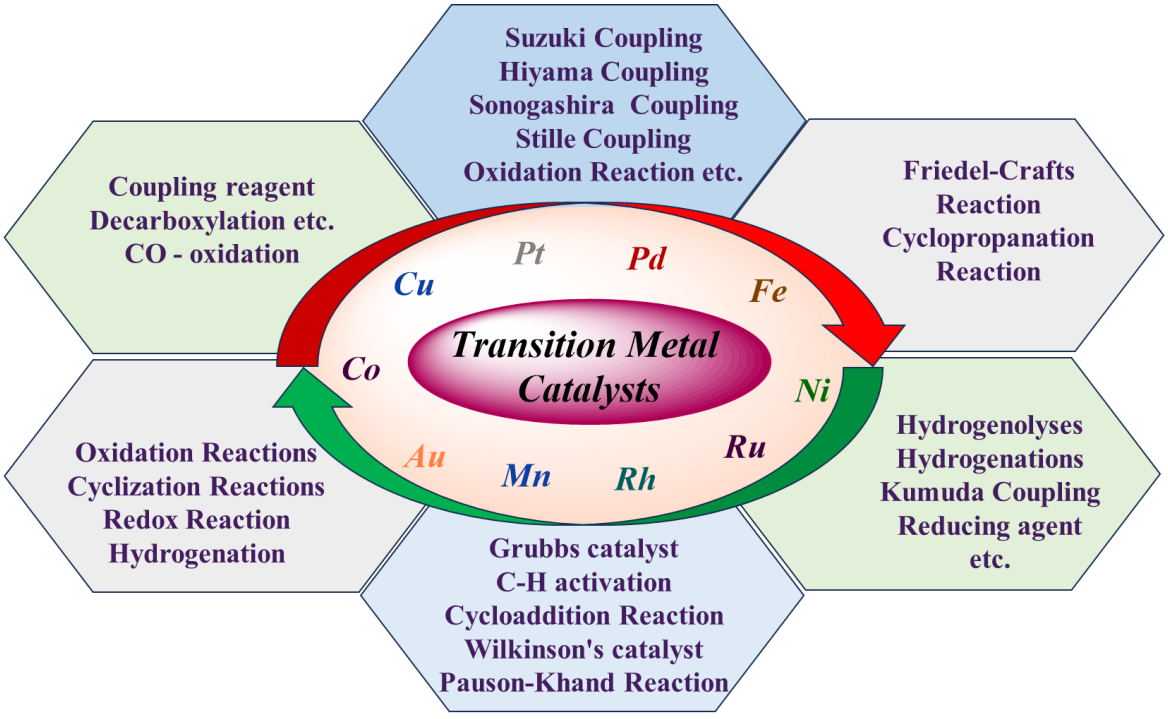

Figure 1.1: Traditional applications of transition metal catalysts

In this context, palladium-based catalysts are one of the most versatile catalysts used in organic synthetic chemistry from many past decades.[9,13,14] Other than some traditional approaches, a wide range of reactions such as; coupling reactions, multicomponent reactions, cyclization, and cascade reactions have been catalyzed by using palladium as a catalyst.[11] Further, Pd-based catalysts are majorly used for the tandem process in which more than one bond formation

occurs.[15] Due to its unachievable properties, palladium-catalyzed cross-coupling approaches between organic electrophilic species and organa-metal-based reagents to construct C-C/ C-N/ C-O bonds have emerged as a tremendously powerful tool for the development of novel molecules.[16–18]

Nowadays, cascade or tandem reactions play an important role in synthetic chemistry having lots of applications in various fields of mankind.[8,19,20] The major advantages of these reactions are their sustainability or ability to perform multiple steps in one single pot without purifying different intermediatory products and the formation of two or more bond formations in a single step under the same reaction conditions (**Figure 1.2**).[21,22] Nevertheless, there are some limitations too, i.e., compatibility of different substrates under the same reaction conditions, stability of intermediates, functional group tolerance, formation of side products, etc. So, some prior necessities for designing a cascade approach should be taken into consideration to avoid these limitations.[23,24] Yet, due to their massive advantageous properties, simplicity of protocols, energy and consumable saving ability, and space and time saving as compared to traditional step-by-step approaches this tandem process is more famed.[23] Many efforts are devoted to the development of such synthetic procedures.

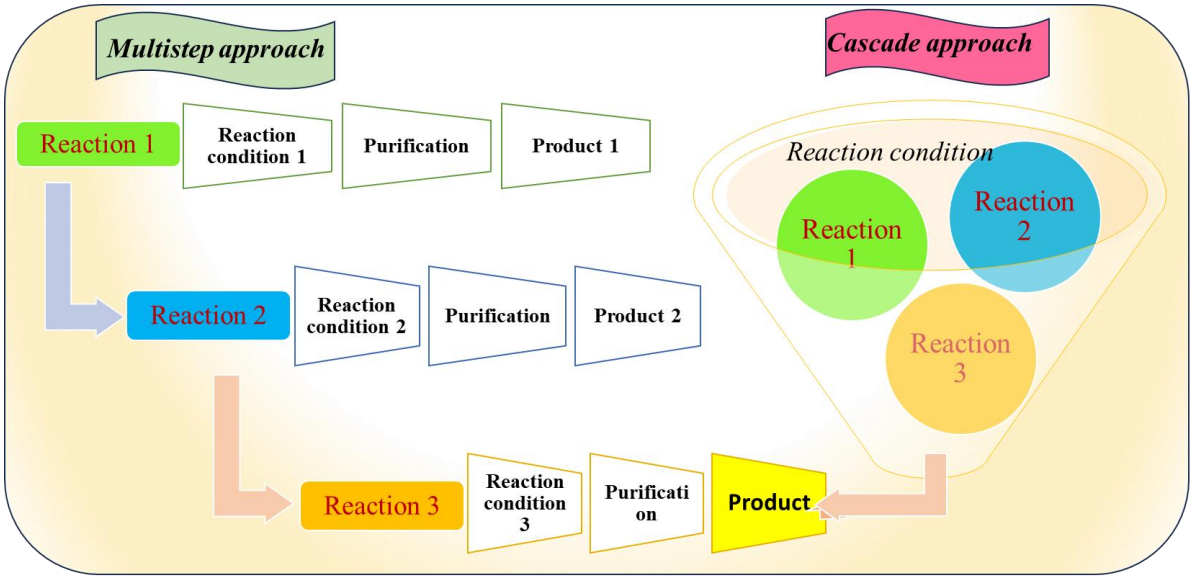

Figure 1.2: Cascade approach versus multistep approach

On the other hand, carbenes are an exceptional class of intermediate having diverse properties and unique structures having two unpaired electrons, formed *in situ* by various precursors like diazo compounds, *N*-tosyl hydrazones, *N*-sulphonyl-1,2,3-triazoles, etc. under various reaction conditions involving different transition metal catalysts.[2,25] Carbenes are generally classified as singlet and triplet carbene according to their tendency as donor or acceptor species.[26,27] Although, carbenes can undergo a variety of reactions i.e., rearrangement, dimerization,

insertion, etc. **(Figure 1.3)**. However, carbene insertion reactions are widely applicable for synthesis in various fields.[27–29] In this view, transition metals are generally treated as supporting partners for these reactive unstable species which makes them more versatile and reactive towards various reactions. They have lots of applications in organic synthetic chemistry due to their ability to insert into various C-X, C-H, N-H, O-H, Si-Si, C-O, etc. bonds and form selectively desired bonds.[30–32] After evidencing its massive role in organic synthesis, carbene-based methodologies are widely used in pharmaceutical industries for the development of precious active pharmaceutical agents (APIs), and late-stage modification of various advantageous drugs.[19,29,33–35]

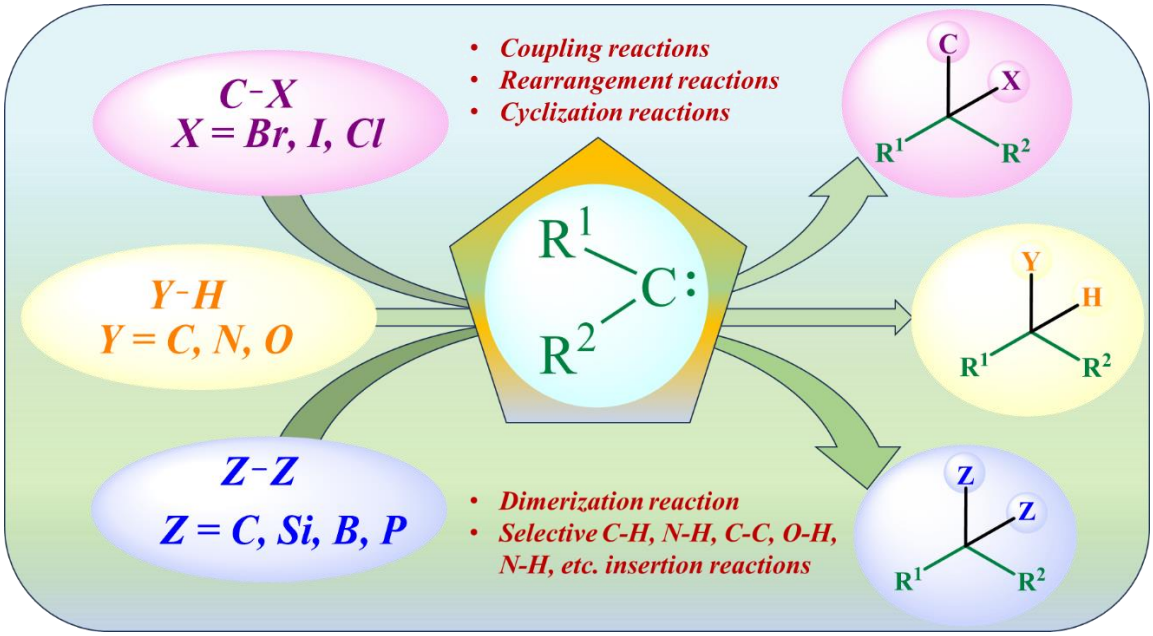

Figure 1.3: A few applications of carbene insertion reaction

In the last few decades, computational chemistry has played an important role in catalysis research and succeeded in establishing its place in the catalysis toolbox right after common laboratory techniques such as NMR, IR, XRD, etc.[36,37] Computational modeling and molecular simulations are continuously playing a substantial role in understanding mechanistic phenomena stirred in the reaction vessel and providing noteworthy information about the structural framework, spectroscopic characterization, stability, and comparability of substrates, mechanistic routes, etc. Theoretical chemistry also plays an important role in guiding the development of new and innovative catalytic directions.[38,39] Quantum chemical methodologies, such as semi-empirical methods, ab initio methods, Hartree folk (HF), and density functional theory (DFT), etc. are well-suited methodologies for understanding chemical kinetics, reactivity, and interpreting complex reaction paths. Out of these, DFT is widely used for the following purposes by many experimental chemists besides theoretical chemists (**Figure 1.4**).

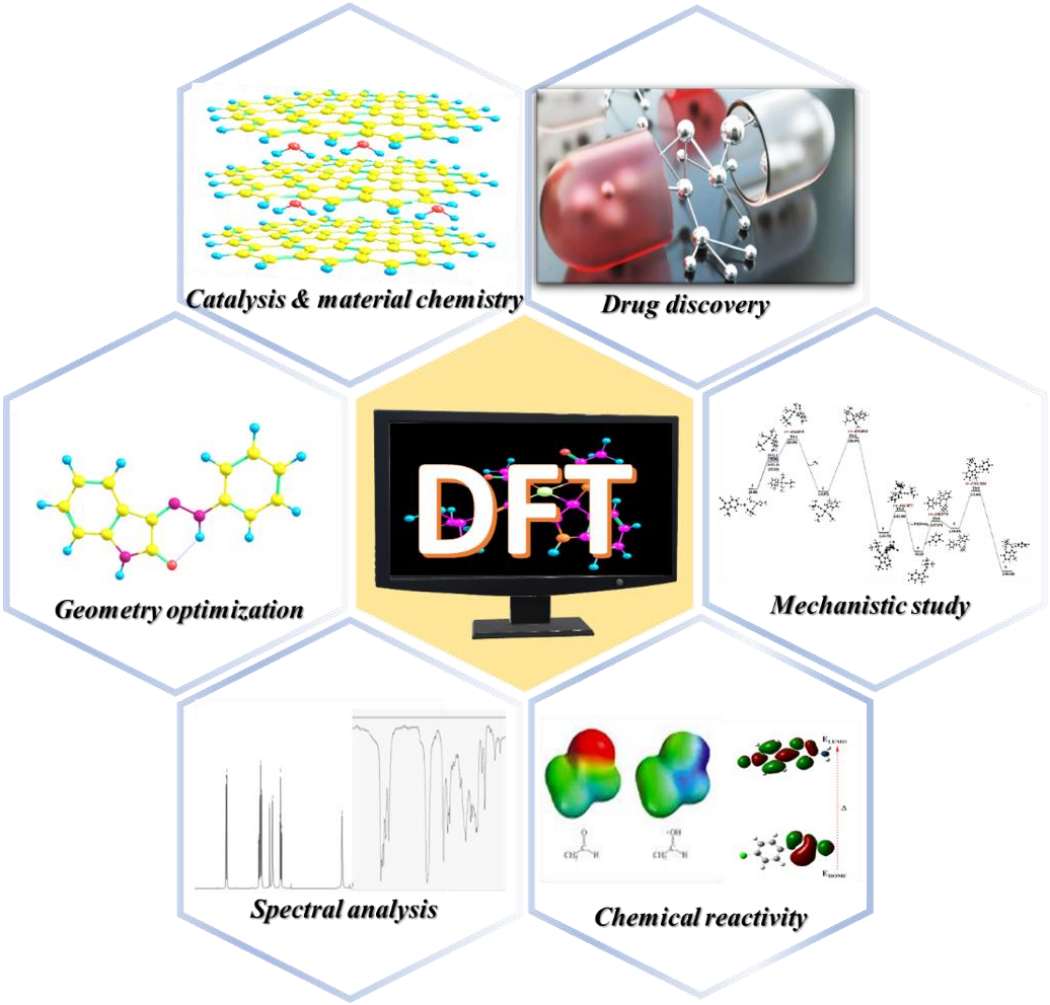

Figure 1.4: Schematic representation of applications of Density Functional Theory (DFT)

Various reports on DFT have been carried out in recent years which extends the role of mechanistic study in metal-catalyzed reactions.[38,40] Especially, it expands its applications for transition metal-catalyzed carbene insertion reactions. In this view, a combination of experimental results and theoretical study has become a more interesting technique for organic chemists to implement novel ideas.[39] Also, convenient programs and software to perform these computational studies, which can be achievable in the absence of advanced programming skills make them more efficient.[37,39–41]

1.2 Literature Survey

Sun *et al.* described a tandem approach via palladium-catalyzed intramolecular Heck-type coupling reaction of alkene-tethered carbamoyl chlorides with *N*-tosyl hydrazones to give 3-vinyl oxindoles (**Scheme 1.1a**).[42] A broad substrate scope for checking the generality of the reaction was also investigated with an electron-rich and deficient substituents on both the substrates i.e. carbamoyl chloride as well as tosyl hydrazone, which showed good functional group tolerance and provided 33-99% yields (**Scheme 1.1b**). The mechanistic studies revealed

that the reaction was initiated via an oxidative addition followed by alkene intramolecular insertion through 5-exo cyclization forming alkyl palladium. Further, the treatment of *N*-tosyl hydrazone with base generated diazo compound and the decomposition of diazo compound by Pd(II) species generated a palladium carbene intermediate followed by alkyl migratory insertion and finally *syn* β-hydride elimination process afforded the 3-vinyl oxindoles. To further demonstrate the practical utility of this process, two synthetic transformations were studied, where a hydrogenation reaction of N-protected 3-vinyloxindole proceeded to give 79% yield, and its deprotection by AIBN/NBS reagent afforded N-unprotected 3-vinyloxindoles in 82% yield (**Scheme 1.1c**).

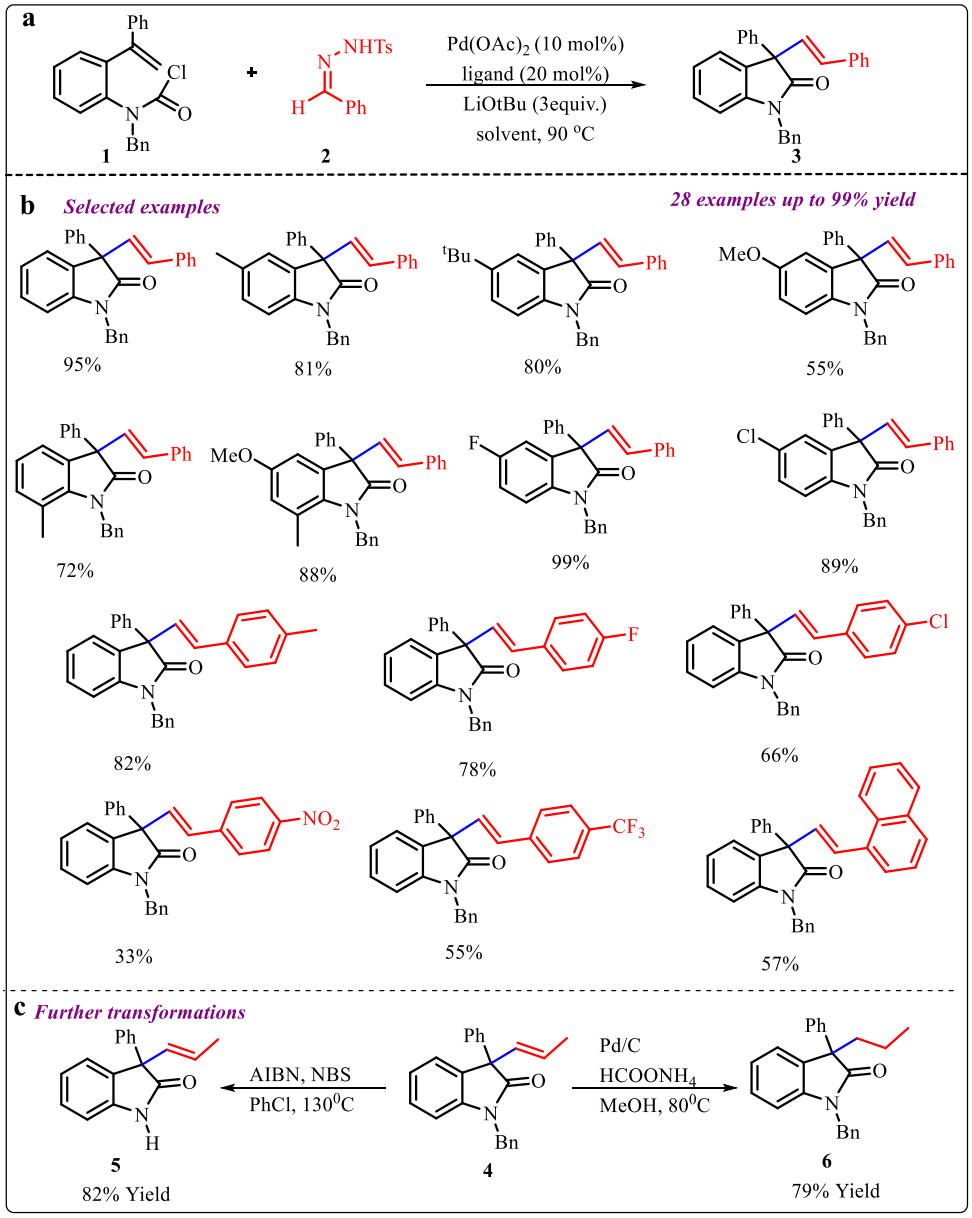

Scheme 1.1: Synthesis of 3- vinyl oxindoles via Pd- catalyzed cascade reaction

Fernandez's Group reported an intramolecular C-H functionalization of diazoester using transition metal-based catalysts for the synthesis of tetrahydroquinolines derivatives (**Scheme 1.2**).[43] Both the palladium and Grubbs catalysts showed effective results for this transformation, but the first-generation Grubbs catalyst was more effective in this process, although it did not always provide the maximum conversions/selectivity. The reaction was feasible with a broad substrate scope and was not only limited to N-isopropyl groups, but also the reaction occurred with substituted anilines having the secondary alkyl,N-tert-butyl,N-phenylanilines groups.

Further, the DFT studies were performed to get mechanistic insights which revealed that the nature of transition metal decides the process of sp^2 -C_{Ar}-H functionalization. Consequently, the reaction catalyzed by Pd(0)-catalyst comprises a Pd-mediated 1,6-H migration, followed by reductive elimination.

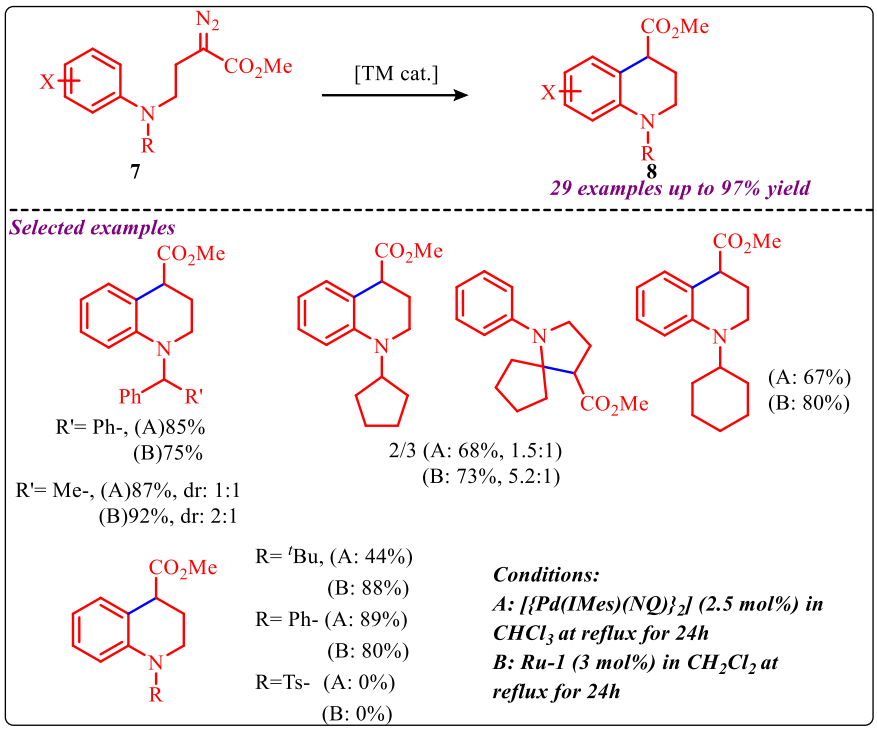

Scheme 1.2: Synthesis of tetrahydroquinolines derivatives via intramolecular C-H functionalization

Zhu's group described a valuable strategy for the synthesis of biologically active medium size lactones by site selective C-H bond functionalization via Pd-catalyzed carbene insertion reaction(**Scheme 1.3a**).[44] N-tosyl hydrazone was used as carbene precursor to react with 2-bromo benzaldehyde in presence of base and a palladium-based catalyst resulted the formation of seven membered lactones. Further, the DFT calculations shed light into mechanism followed by the reactions which revels the Pd-carbene migratory insertion step was found critical, as it

beared the palladium(II) intermediate having a fitted geometry which can experience 1,4-palladium shift. Also, de-diazonation was found as the rate-determining step for the formation of metal carbene species. This methodology was found to be efficient forlate stage functionalization of complex molecules, like in drug discovery (**Scheme 1.3b**). Next, o-Hydroxy -N- tosylhydrazones derived from bio- relevant compounds i.e. paracetamol, methyl paraben, carvacrol, thymol, estrone, eugenol etc. were also found competent diazo precursors which resulted the formation of various potentially bioactive lactones compounds.

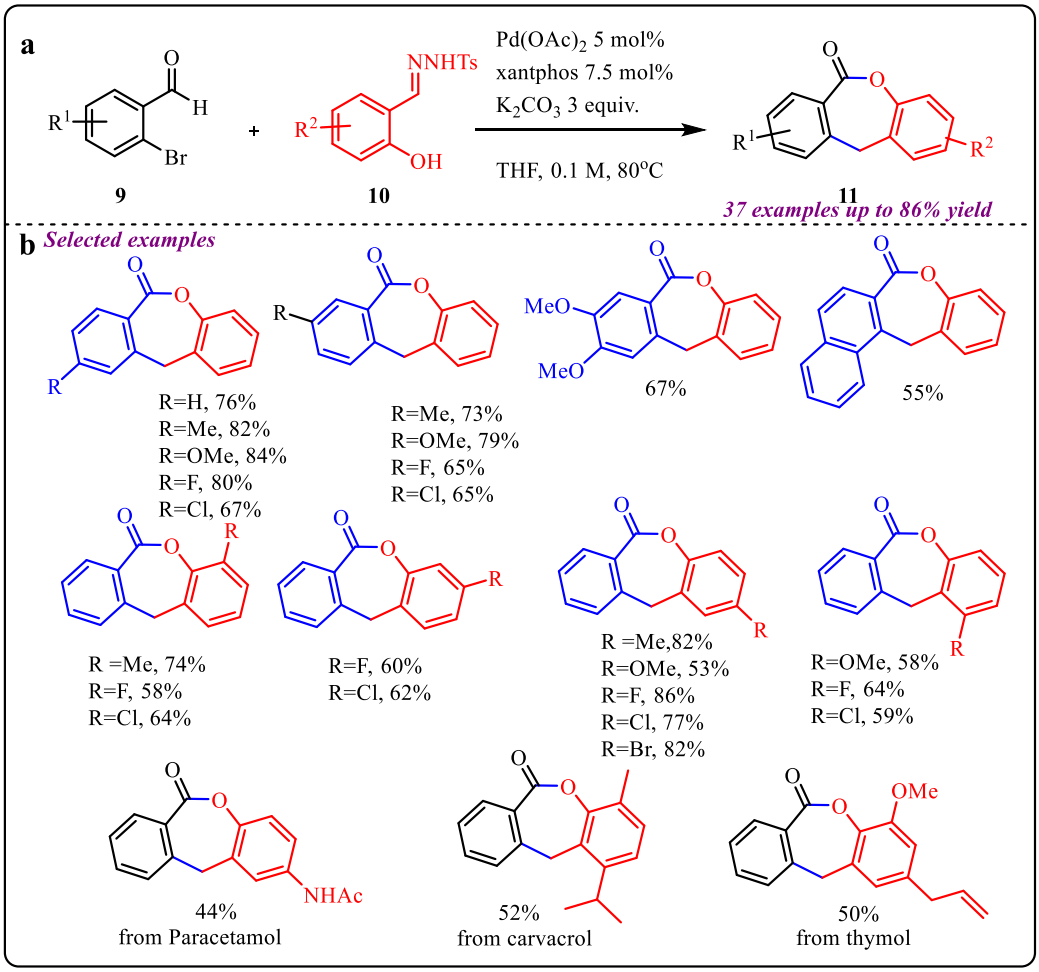

Scheme 1.3: Synthesis of 7-memebered lactones derivatives via palladium catalyzed reaction

Shun-Jun Ji and co-workers reported a simple and efficient tandem approach towards the synthesis of biologically relevant isoindolinone moiety via palladium-catalyzed isocyanide insertion into *o*-bromobenzaldehyde in high yield up to 98% and 78% for ketenimines and lactams based isoindolinone derivatives respectively (**Scheme 1.4a & 1.4c**).[45] The reaction was found suitable for various substituents at *o*-bromobenzaldehyde as well as isocyanides. Further, good to excellent yield was observed for electron-withdrawing and electron-donating

substituents at the *meta*-position of *o*- bromobenzaldehyde, while lower yield was observed when electron-donating substituents were employed at the *para*-position of *o*-bromobenzaldehyde as compared to electron-deficient and halogen substituents. Interestingly, this methodology was successfully applied for late-stage modification of some bioactive molecules such as methyl paraben and estrone. Also, this reaction methodology was successfully applied for gram-scale synthesis of model product in 80% yield. Based on some control experiments, a reaction mechanism was proposed that supports the concerted metalation-deprotonation (CMD) mechanism.

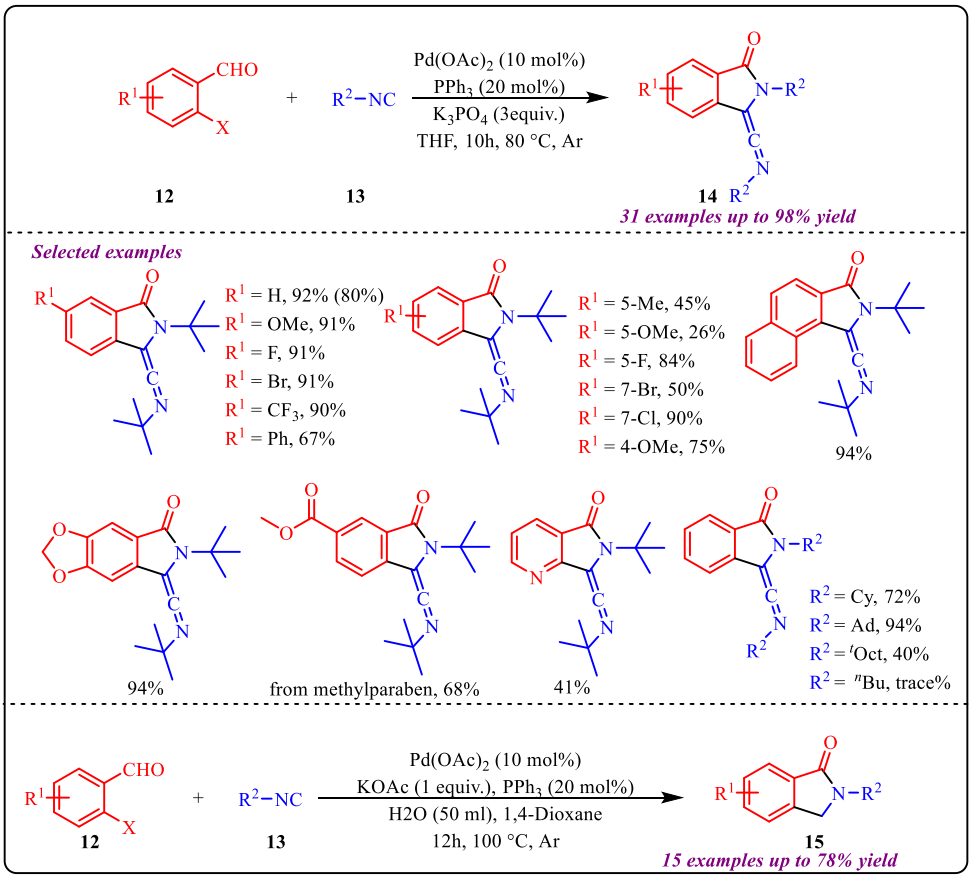

Scheme 1.4: Synthesis of ketenimines and lactams-based isoindolinone derivatives via Pd-catalysed isocyanide insertion

An interesting multicomponent approach toward the synthesis of biologically relevant 5-aminoimidazole scaffolds was reported by Pan et al (**Scheme 1.5**).[46] This Pd-catalyzed reaction involves amidoximes, isocyanides, and amines as a substrates for the tandem formation of C-C and C-N bonds to provide imidazole derivatives in moderate to good yields . After screening various palladium-based catalysts like $PdCl_2$, $Pd(acac)_2$, $PdBr_2$, $Pd(dba)_2$, $Pd(PPh_3)_4$, $Pd(OAc)_2$, $PdCl_2(PPh_3)_2$ etc., they found $Pd(OAc)_2$ along with PPh_3 ligand in DMSO as a best

catalyst to synthesized desired product within 6 h at elevated temperature. Further, various electron-donating and withdrawing functional groups were examined to explore the feasibility of the reaction and obtain corresponding products in good to excellent yield, which successfully define the applicability of the reported protocol. A gram-scale reaction was also performed, which appropriately justified the synthetic utility of the protocol.

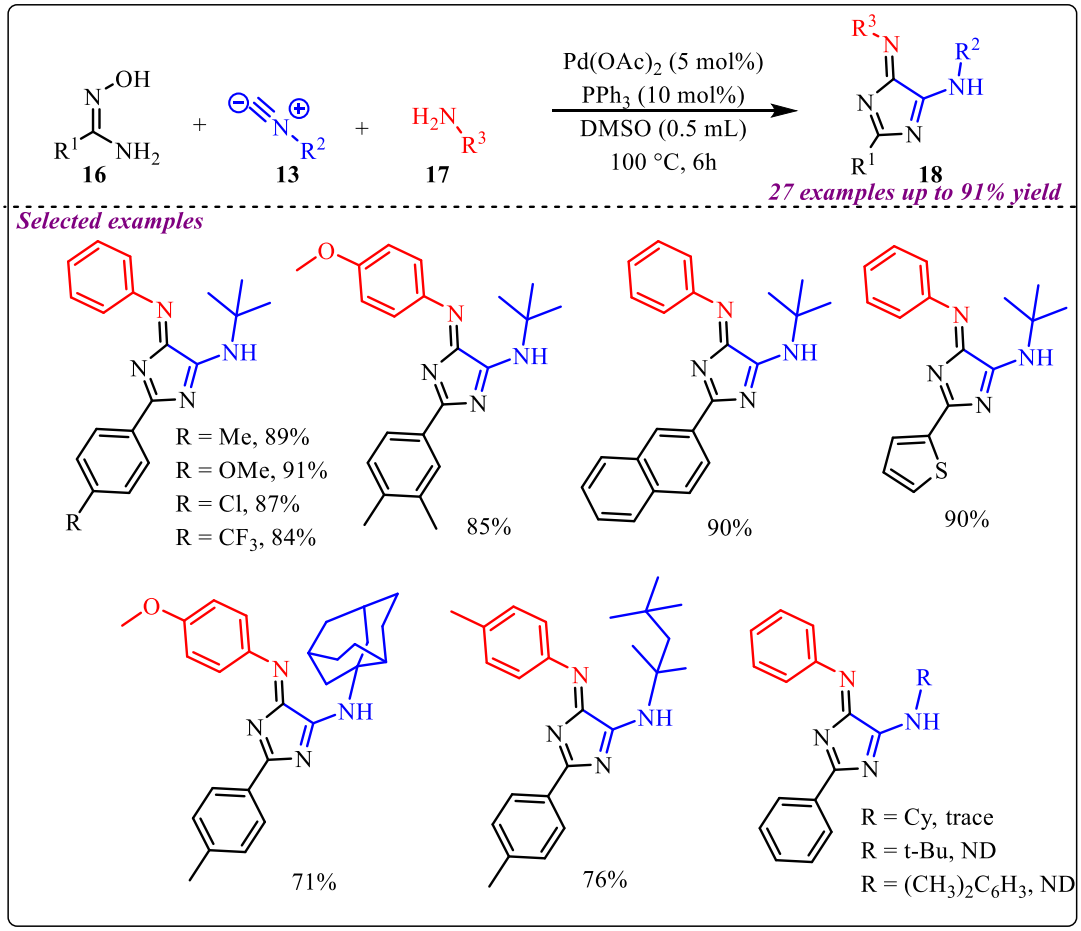

Scheme 1.5: Synthesis of biologically relevant 5-aminoimidazole scaffolds using Pd-catalyzed reaction

Next, Sharma et al. reported an efficient strategy for synthesis of 2,3- difunctionalized indole derivatives via palladium-catalyzed isocyanide insertion and triple bond-activation methodology (**Scheme 1.6a**).[47] During reaction conditions optimization, palladium acetate as a catalyst along with different ligands, bases, and additives was screened, however, they couldn't achieve more than 77% yield for the model reaction. Interestingly, the reaction worked well with freshly prepared 2-(2-phenylethynyl) phenyl isocyanides using a continuous flow process without direct exposure and odour. To check the synthetic feasibility of this protocol, a range of substituents were tested on both substrates 2-(2-phenylethynyl) phenyl isocyanide and *N*-(2-Iodophenyl)-*N*-methyl acrylamide. This protocol was found feasible for

electron-rich species over some electron-withdrawing substrates and provided moderate to good yield (**Scheme 1.6b**).

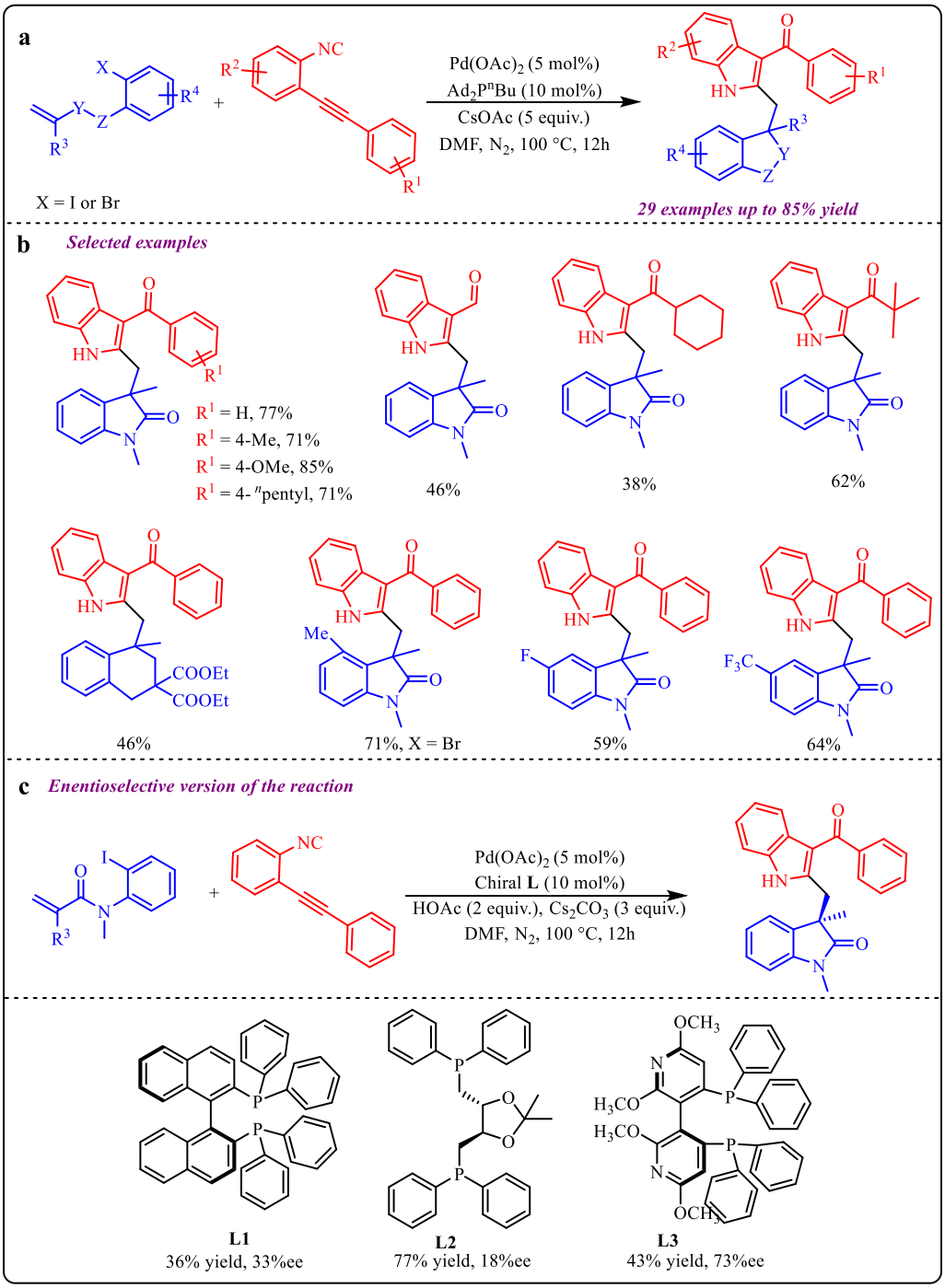

Scheme 1.6: Synthesis of 2,3- difunctionalized indole derivatives via palladium- catalysed isocyanide insertion

The optimized condition was also applied for enantioselective synthesis (**Scheme 1.6c**). However, this protocol provided enantioselective product only in 36-77% yield having low enantiomeric access while using chiral ligand. A plausible catalytic cycle evidenced the formation of palladium complex at C1- position of *N*-(2-Iodophenyl)-*N*-methyl acrylamide

which subsequently undergoes intramolecular carbopalladation, followed by isocyanide insertion and intramolecular addition to triple bond afforded the desired product.

Gabriele's group have demonstrated a novel stereoselective approach towards biologically relevant α, β -unsaturated γ-lactam derivatives via Pd-catalyzed multicomponent carbonylation reaction (**Scheme 1.7a**).[48] The reaction involves homopropargylic amines, alcohol, carbon monoxide and oxygen in the presence of palladium iodide and KI at high temperatures for 2 to 5 h and furnished the desired product in moderate to good yield. Further, the reaction provides good yields i.e. 85%, 82%, and 72% with methanol, ethanol, and isopropanol respectively, however, it provided a lower yield i.e. 33% with butanol (**Scheme 1.7b**).

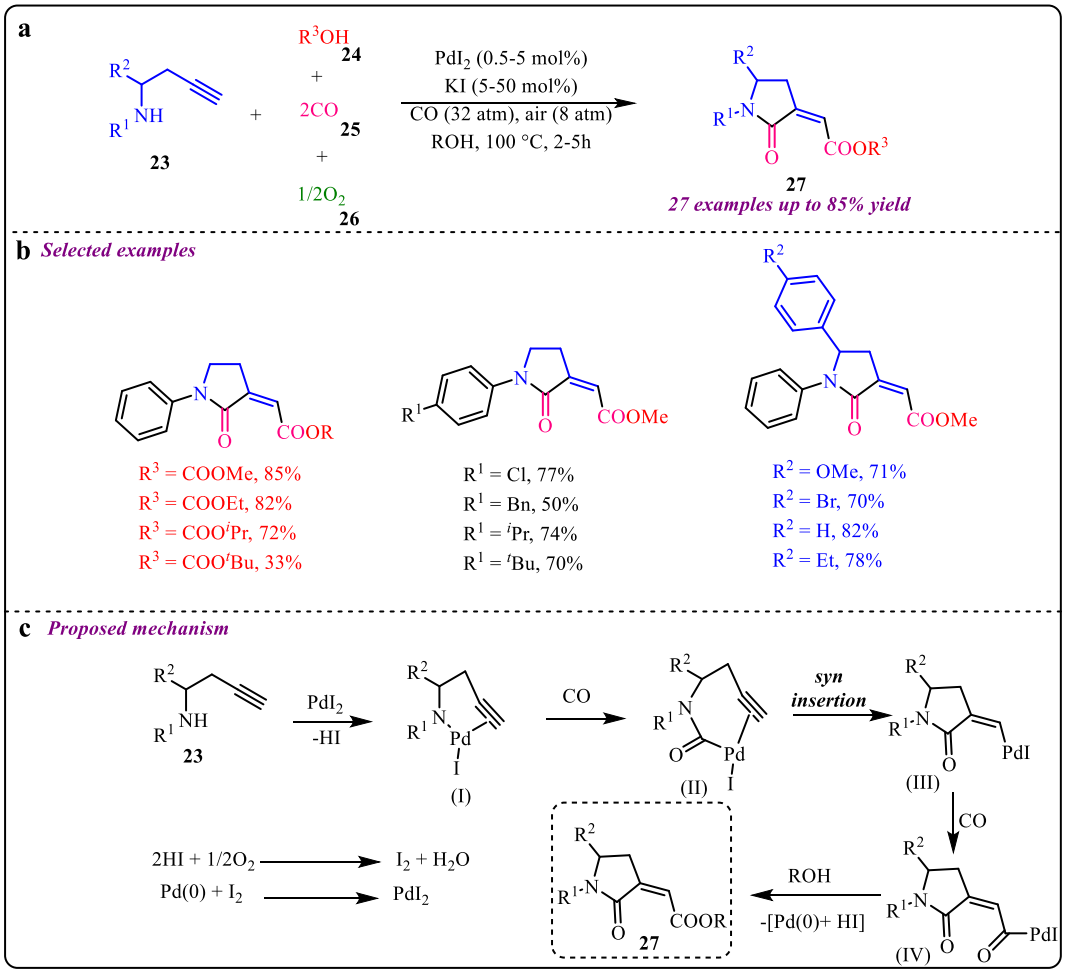

Scheme 1.7: Stereoselective approach towards biologically relevant α, β -unsaturated γ lactams derivatives via Pd-catalyzed multicomponent reaction

Also, various substituents at amine as well as alkyl position of homopropargylic amines were well tolerated and provided yield up to 82%. The reaction follows simple traditional N-H and alkyne activation methodology to provide intermediate I which upon carbon monoxide

insertion provides amide-Pd based intermediate II (**Scheme 1.7c**). After that, *syn* insertion into the alkyne bond takes place to provide 5-membered cyclic intermediate III, which further undergoes CO insertion to provide intermediate IV, nucleophilic replacement by alcohol provided corresponding product.

An interesting methodology towards the development of axially chiral 2-aryl and 2,3 -diaryl quinazolinones via Pd-catalysed atroposelective coupling-cyclization of 2-isocyanobenzamides and 2-iodo-3-mthylbenzoate substrates reported by Zhu et al (Scheme 1.8 (**Scheme 1.8a**).[49] This reaction provided a novel coupling strategy when sterically hindered coupling partners were taken into consideration for providing atroposelective biaryl derivatives. Before that, there was no report that described the C-aryl axial chirality of 2-aryl quinazolinones. To get the maximum enantiomeric excess, various SPINOL-derive phosphoramidite chiral ligands were tested. Out of five ligands, methyl and ethyl substituted ligands showed the best enantioselectivity of 94% and provided a maximum yield of 93% (**Scheme 1.8b**). It was observed that sterically hindered ligands were not found good for the reaction and diminished the atroposelectivity as well as the yield of the product.

. To examine the feasibility of the reaction, various 2-isocyanobenzamides having electron-rich, electron-deficient, and bulky substituents were tested and a negligible effect of substituents was observed on yield and enantioselectivity of the reaction. However, a significant effect on the yield of the product was observed while different substituents at 2-iodo-3-methyl benzoate were installed. This methodology was successfully applied for the synthesis of diastereoselective quinazolinone derivatives, and two desired derivatives were formed in 70% and 21% yield having 93% and 89% ee (**Scheme 1.8c**).

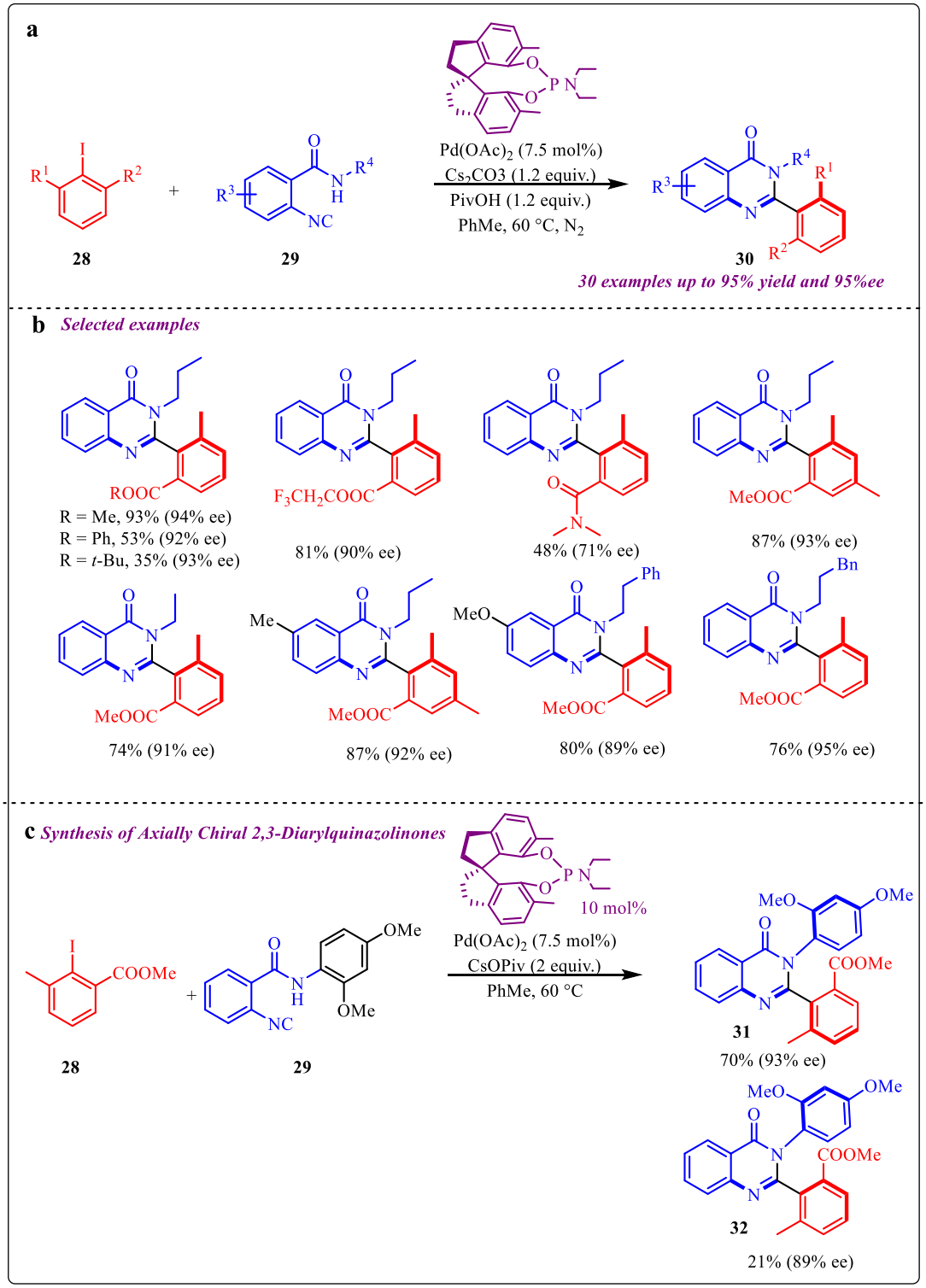

Scheme 1.8: Synthesis of axially chiral 2-aryl and 2,3 -diaryl quinazolinones via Pd-catalysed atroposelective coupling-cyclization reaction

Liang and co-workers reported a joint experimental and computational study about Pd-catalysed tandem strategy involving Narasaka-Heck coupling / C-H activation methodology to synthesize highly strained spirocyclobutane-pyrrolines in moderate to good yield (**Scheme**

1.9a &1.9b).[50] Interestingly, domino Heck coupling of alkene-tethered C(sp^2)-H bond was well reported, but activation of C(sp^3)-H was still challenging field which makes this strategy more identifiable. Initially, the reported domino reaction was performed using $Pd(OAc)_2$ as a catalyst along with Cs_2CO_3 base and $PCy_3.BF_4$ ligand in 1, 4-Dioxane at 140 °C to afford the desired product in 41% yield. After optimizing various reaction conditions, $Pd(OAc)_2$ as a catalyst, Cs_2CO_3 as a base, and $PCy_3.BF_4$ as a ligand remains the best choice for this reaction.

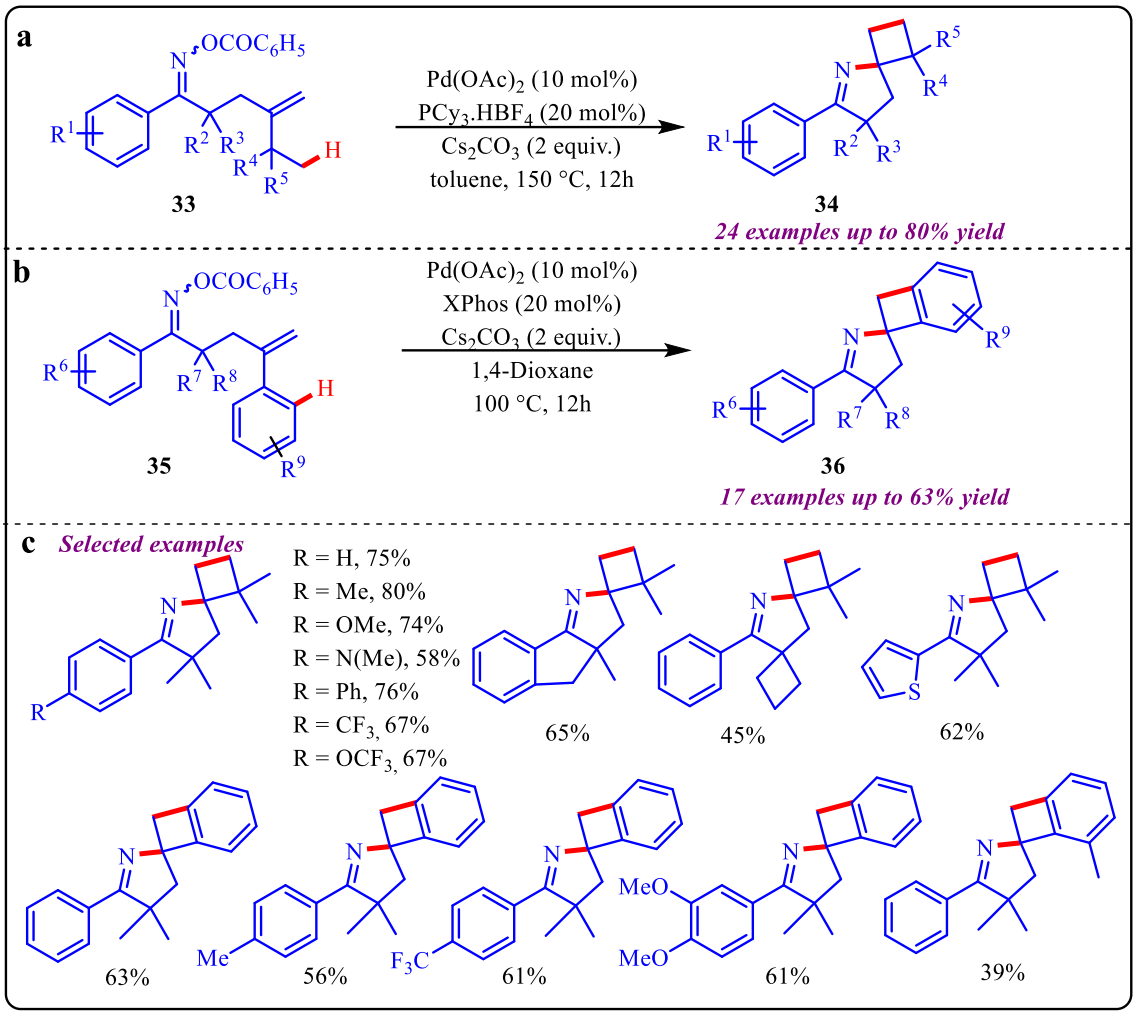

Scheme 1.9: Synthesis of highly strained spirocyclobutane- pyrrolines

After that, a broad range of substrate scope was developed, reaction worked well with each substrate independent of its electronic nature. However, substituent at *o*-position significantly reduces yield and provides only 20% product. Also, the reaction provides comparatively lower yields when aryl substituent was employed at alkenes (**Scheme 1.9c**). Further, DFT study was conducted to get deep overview about the reaction mechanism of reported Narasaka-Heck coupling (**Scheme 1.10**). Initially, palladium metal interacts with the substrate (**33**) and get inserted into N-O bond to form an intermediate (I). After coming into the promiscuity of the

substrate, the intermediate (I) undergoes chelation and further cyclization to provide intermediate (II) which undergoes a concerted metalation–demetallation (CMD) process followed by reductive elimination to provide product (**34**).

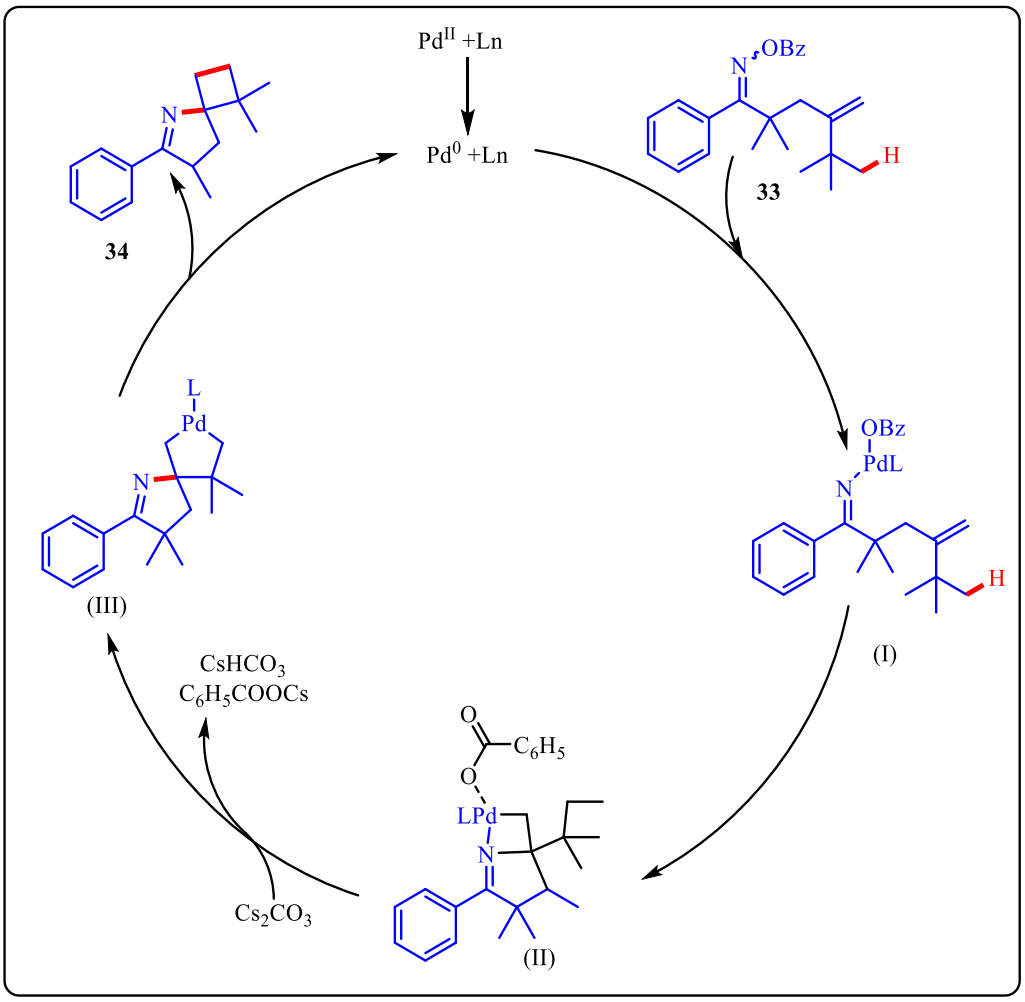

Scheme 1.10: Proposed mechanism for Narasaka- Heck coupling / C-H activation

Recently, Yao *et al.* reported a sequential Ugi-azide coupling along with palladium-catalyzed azide-isocyanide cross-coupling followed by cyclization without purifying intermediate species for the synthesis of biologically valuable precursors 4-tetrazolyl-3,4-dihydroquinazolines derivatives (**Scheme 1.11a**).[51] This reaction strategy involves two different isocyanide units for the Ugi reaction and Pd-coupling reaction. This multicomponent reaction showed good functional group tolerance and provided a yield of up to 90%. However, the reaction provided lower yields when strong electron-donating substituents were employed at benzaldehyde. Similarly, the reaction was feasible with both aliphatic and aromatic amines, but a lower yield was observed in the case of electron-donating amines (**Scheme 1.11b**). To evaluate the biological potential of the synthesized moiety, the anticancer activity of the

synthesized compound was tested with the least cytotoxicity. The Edu method detected its activity via the proliferation of breast cancer cells treated with synthesized molecules. It also shows comparable results for apoptosis of glioma cells. A gram-scale synthesis was also performed to check the synthetic applicability of the reaction, which provides an 80% yield, proving the synthetic role of the reported strategy.

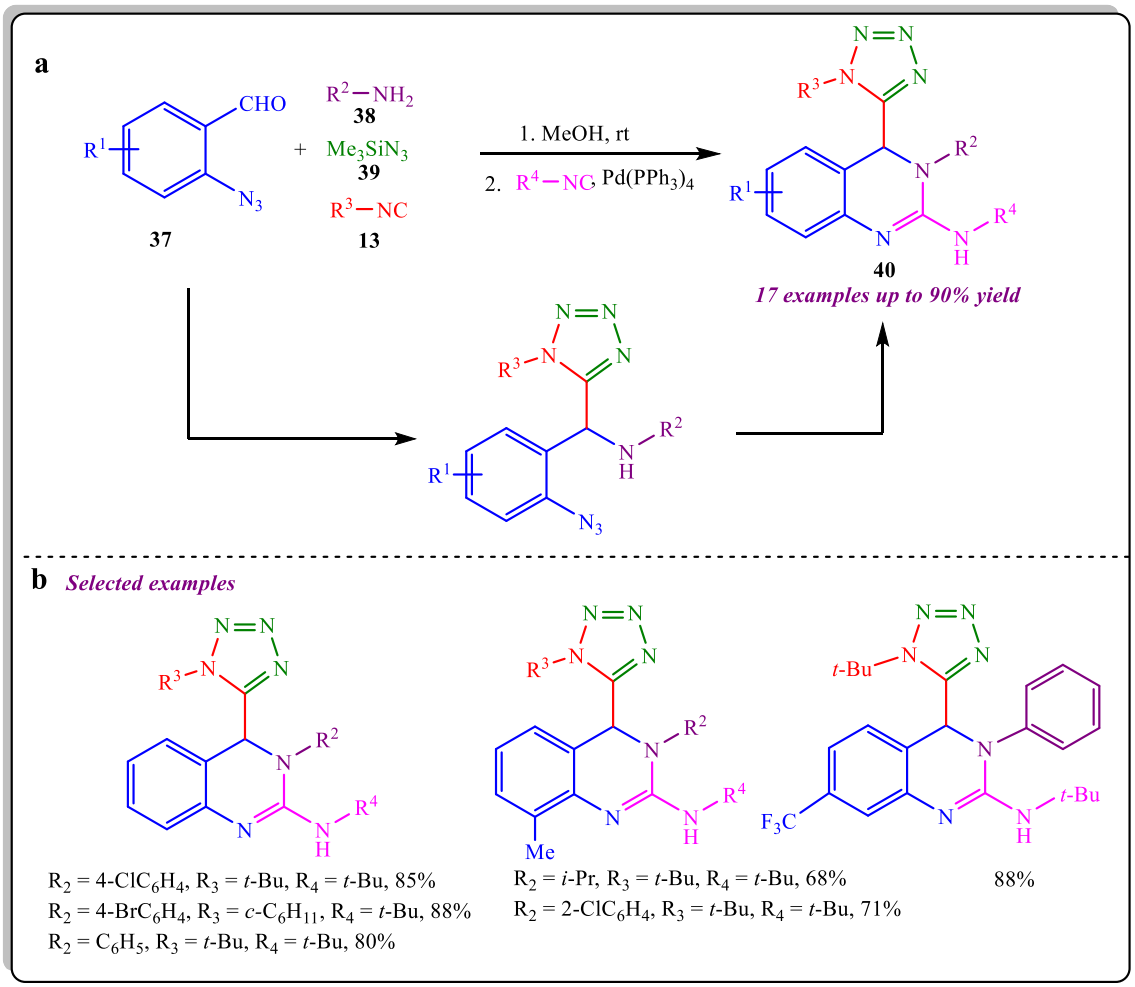

Scheme 1.11: Synthesis of biologically valuable precursors 4-tetrazolyl-3,4-dihydroquinazolines derivatives

Zhang and co-workers reported another palladium catalysed isocyanide insertion approach to synthesize N-substituted benz[*c,d*]indol-2-imines and N-substituted amino -1-napthylamides derivatives in absence and presence of water molecule respectively (**Scheme 1.12a**).[52] After optimizing various palladium based catalysts, such as $Pd(OAc)_2$, $Pd(TFA)_2$, $Pd(PPh_3)_4$, $Pd_2(dba)_3$ etc., $Pd(TFA)_2$ was found superior than other catalysts. Also, DCE was found best solvent among the solvents screened for this reaction. The reaction provided moderate to good yield in case of both the substrates and found slightly dependent on electronic nature of the substituents (**Scheme 1.12b**). This methodology was successfully applied for the synthesis of antiproliferative agents i.e. N-substituted –(benzo[c,d]-indol 2 (*1H*)-ylidene)-4-nitroanilines in

56% and 73% yield, respectively (**Scheme 1.12c**). Further transformation towards synthesis of BET bromodomain inhibitor was successfully achieved, which showed the synthetic applicability of the protocol.

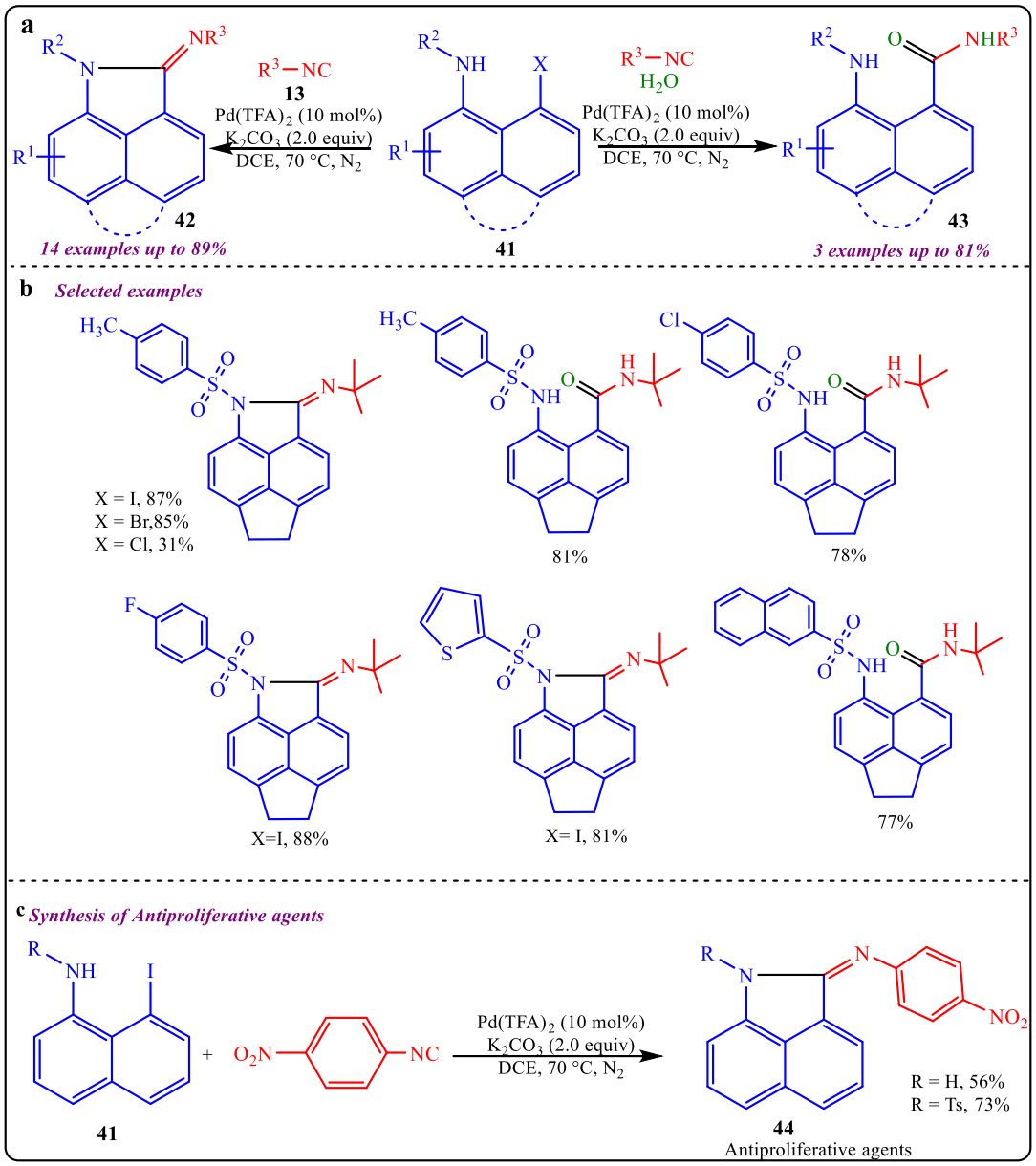

Scheme 1.12: Synthesis of N-substituted benz[*c,d*]indol-2-imines and N-substituted amino -1-napthylamides derivatives

A novel and diverse synthesis of polysubstituted fused tetracyclic heterocyclic scaffolds reported by Wu's group (**Scheme 1.13a**).[53] This methodology was dependent on the nature of Pd-catalyst to provide two different types of products via mono or double-isocyanide insertion. A wide range of substrates having electron-rich and electron-deficient substitutions was tested for synthesizing both types of heterocycles (**Scheme 1.13b**). Also, different isocyanides unit

were tested and observed that steric hindrance played an important role and as a result reaction provided lower yields. To demonstrate the practical utility of the reaction, a gram-scale reaction was performed, which provided 58% and 55% for corresponding poly heterocycles. Further, DFT study was also performed to get an overview about the mechanistic route flowed by the reaction. This study supported that sequential isocyanide insertion was considered as rate-determining step for the following reaction. Next, further transformation was performed to check the synthetic potential of the protocol and successfully synthesized various modified products in moderate to good yields (**Scheme 1.14**).

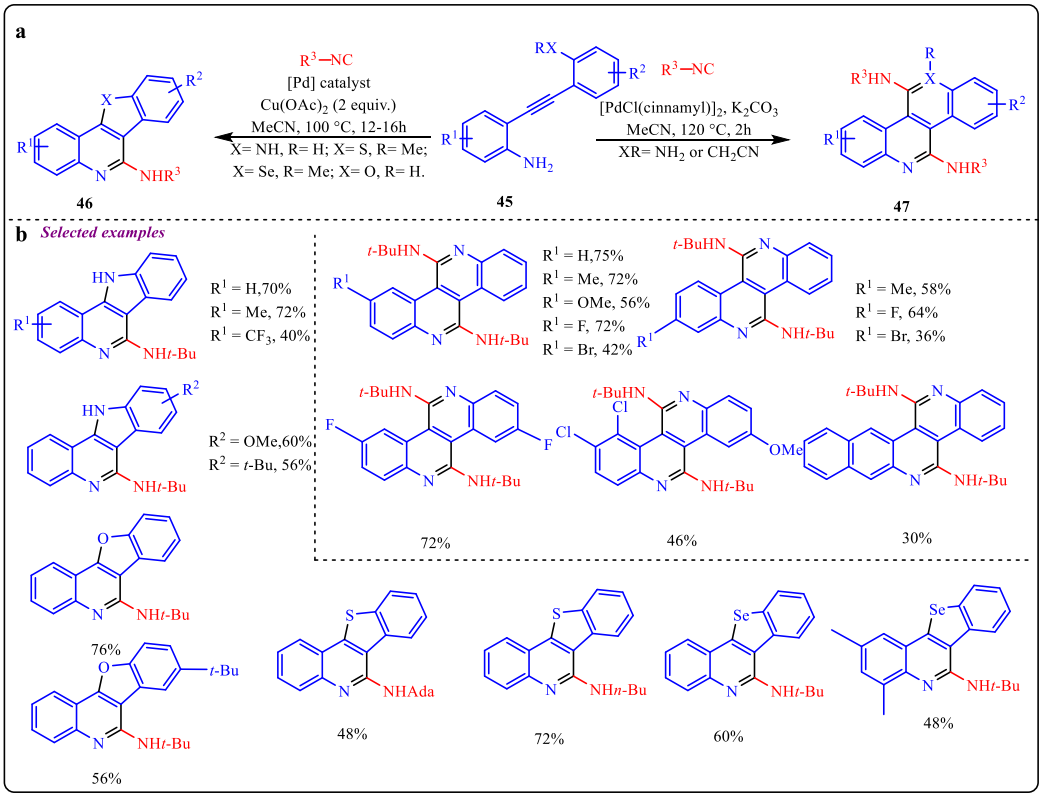

Scheme 1.13: Synthesis of polysubstituted fused tetracyclic heterocyclic scaffolds

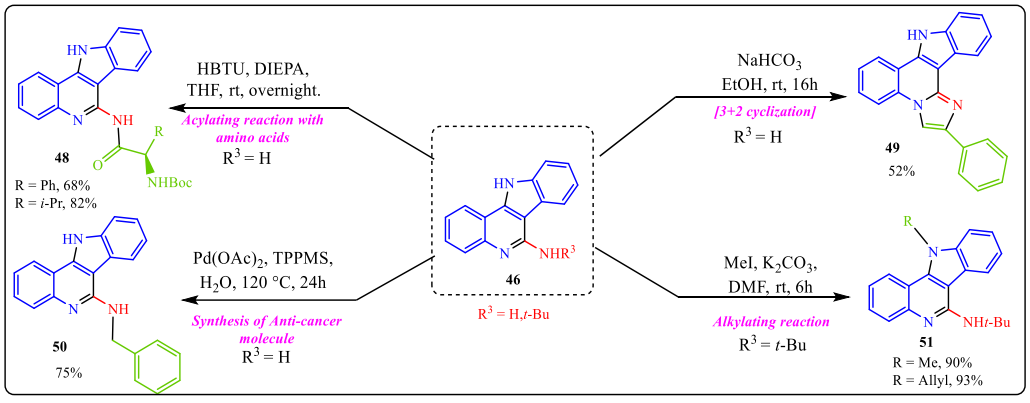

Scheme 1.14: Further transformations

Guchhait *et al.* reported an intramolecular cascade cyclization/ isocyanide insertion strategy to synthesize bicyclic indolylisoindolinones motifs involving indolyl migration, redox-neutral process in presence of palladium acetate and P(*o*-tolyl)$_3$ ligand (**Scheme 1.15a**).[54] Interestingly, for the first time, an alkyl isocyanide C-H act a hydride source for promoting rearrangement occurred in the reaction. A good range of substrate scope showed good functional group tolerance and found independent from electronic nature of the substituents (**Scheme 1.15b**). Also, various isocyanides were compatible in this reaction. However, reaction didn't work with aromatic isocyanide substrates. Further modification via de-*tert* butylation of synthesized heterocycle also provide moderate yields up to 47% (**Scheme 1.15c**). Also, reaction yield was not so much affected when reaction was performed at gram-scale level.

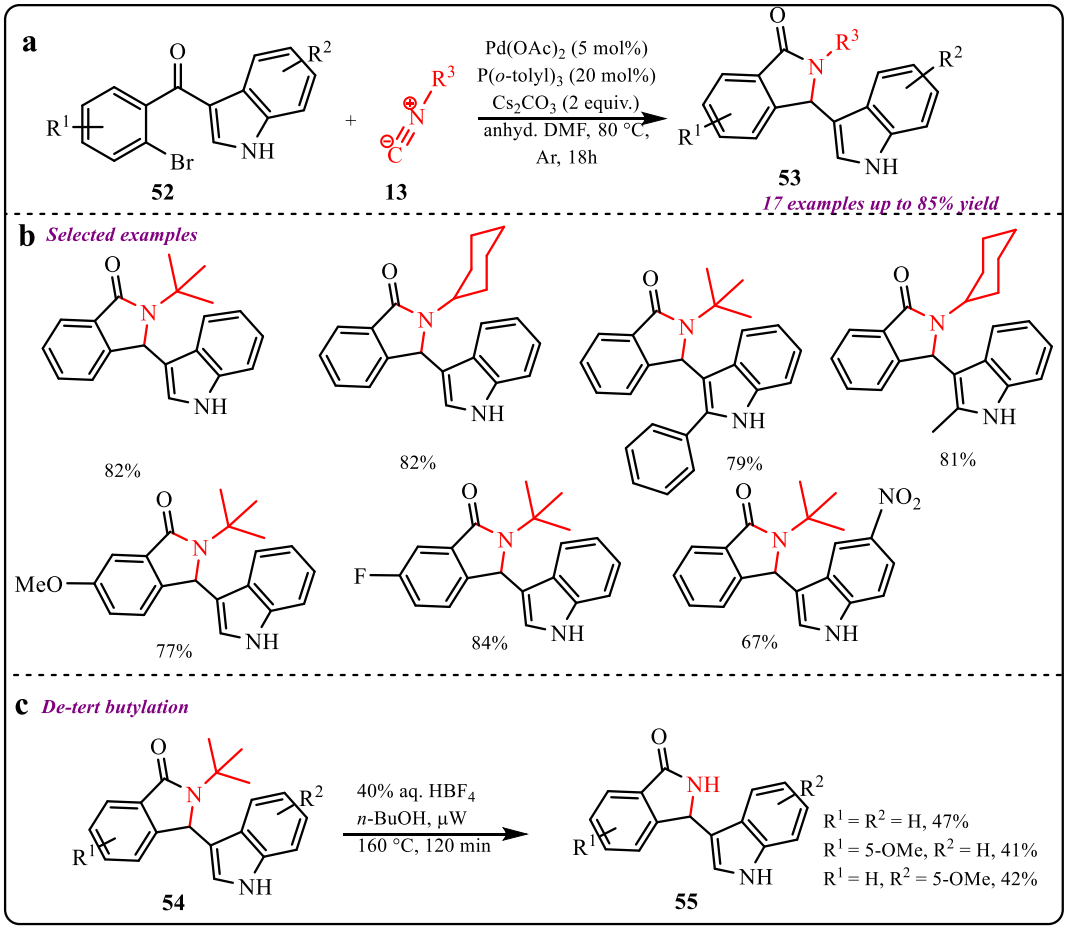

Scheme 1.15: Synthesis of bicyclic indolylisoindolinones

A novel proximal C-H activation strategy using isocyanide insertion was reported by Huang and co-workers (**Scheme 1.16**).[55] The reaction provided three different types of products under slightly different reaction conditions. Also, the role of the palladium catalyst along with different ligands and additives directs the reaction route as a result reaction yielded different products. Interestingly, when palladium acetate was employed as a catalyst with CsF as a base

and PivOH as an additive, a mono isocyanide insertion took place and provided a 3-unsubstituted isoindolinone derivative in moderate to good yield. Next, when $[Pd_2(dba)_3]CHCl_3$ with PPh_3 as a ligand, cesium carbonate as a base and PivOH as a ligand were used then a double isocyanide insertion product i.e. 3-cyano-substituted isoindolinone derivatives were obtained in excellent yield. In the last, when only $(4\text{-}CF_3C_6H_6)_3P$ ligand was used, disubstituted isoindolinone derivatives were formed in good yield.

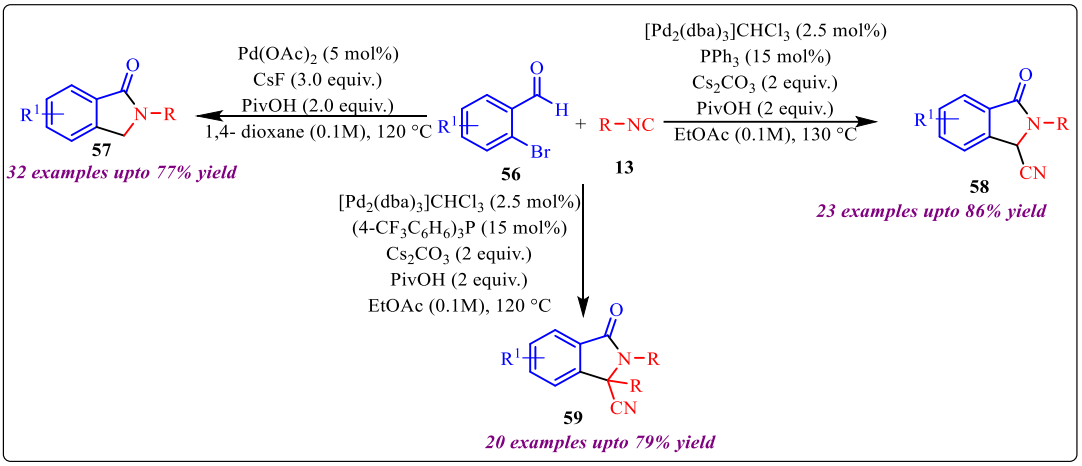

Scheme 1.16: Synthesis of Isoindolinone derivative via C-H activation

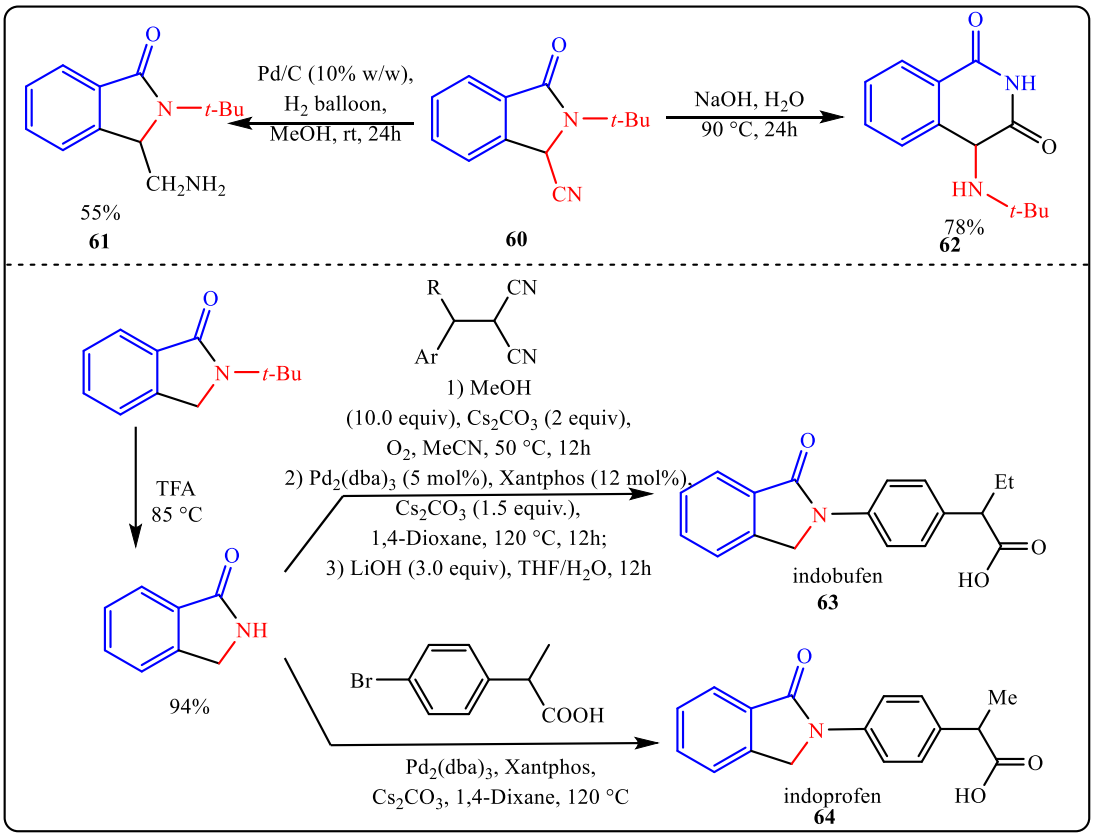

Scheme 1.17: Further transformations

Further transformation of 3-cyano substituted isoindolinone derivative by hydrogenation reaction in presence of Pd/C and ring expansion in presence of NaOH was performed, which provided 55% and 78% of the desired product. Also, 3-unsubstituted isoindolinone was further modified to access biologically relevant indobufen and indoprofen molecules (**Scheme 1.17**).

Wang and co-workers recently extended isocyanide insertion methodology towards the synthesis of biologically active naphthalen-2-amines in moderate to high yield via Pd-catalysed tandem cyclization reaction of 2-(2-vinylarene) acetonitriles with *tert*-butyl isocyanide (**Scheme 1.18a**).[56] Interestingly, this methodology worked well with various electron-rich and electron-poor groups containing 2-(2-vinylarene) acetonitriles along with differently substituted isocyanides. Besides, the in vitro antitumor activity of synthesized derivatives was tested against various tumor cell lines i.e., U87, 4T1, HeLa, PC-3, HCT116, HepG-2, and A549. Among them, compounds showed significant antitumor activity in comparison of 5-fluorouracil (5-FU) and amonafide as positive control (**Scheme 1.18b)**.

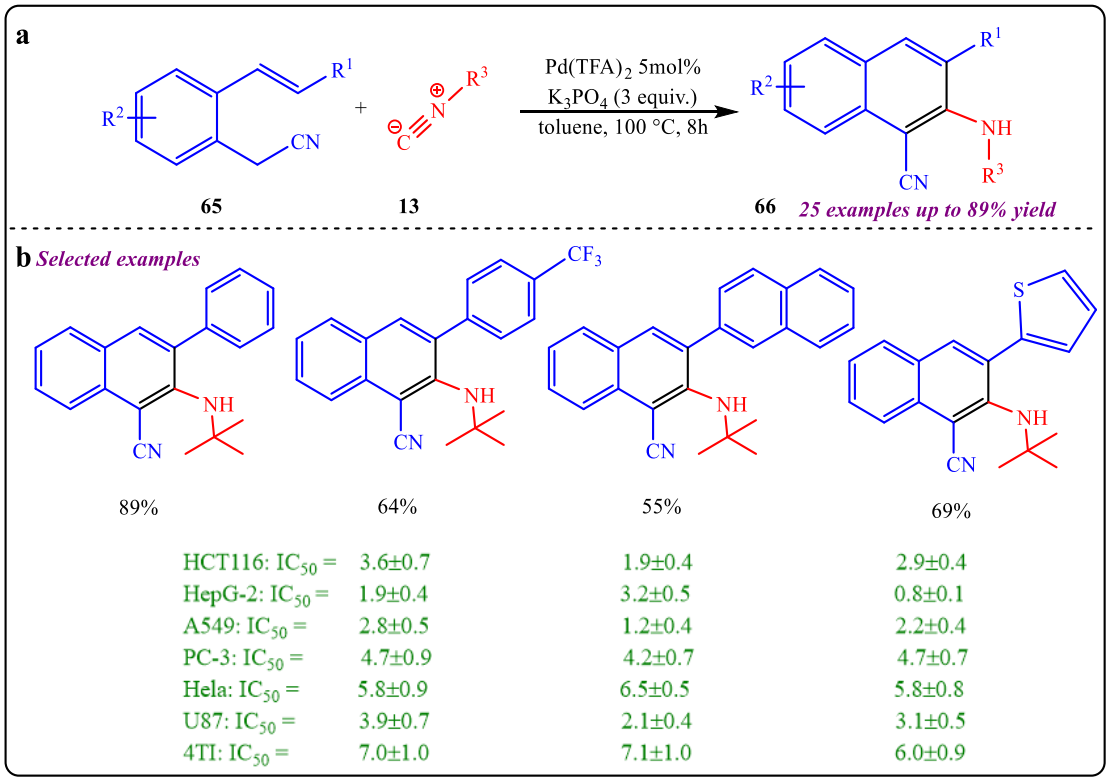

Scheme 1.18: Synthesis of naphthalen-2-amines derivative via isocyanide insertion

Next, Balalaie's group reported an interesting ring-expanding approach to afford polysubstituted pyrimidines heterocycles via palladium-catalyzed cascade consisting C-C and C-N bond formation through ring opening of *2H*-azirines and simultaneous insertion of isocyanide species (**Scheme 1.19**).[57] This methodology was applicable to successfully

synthesize 20 derivatives in moderate to excellent yield by using substituted azirines having different electron withdrawing and electron donating groups. However, they observed that the electronic effect on azirines doesn't provide any significant effect on the reaction outcome. Moreover, various aliphatic isocyanides were found superior to this cyclization reaction, while, aromatic isocyanides provide lower yields.

An interesting reaction mechanism was also proposed which goes through a four-membered palladacyclic intermediate (A) formed by oxidative addition of palladium (0) species into the azirine (**67**) bond (**Scheme 1.20**). After that, isocyanide insertion takes place into A to form five membered intermediate (B), which simultaneously attached with another azirine (**67**) species to form intermediate C. After subsequent reductive elimination of palladium catalyst, a zwitterionic species named D formed which upon aqueous workup formed the desired product (**68**).

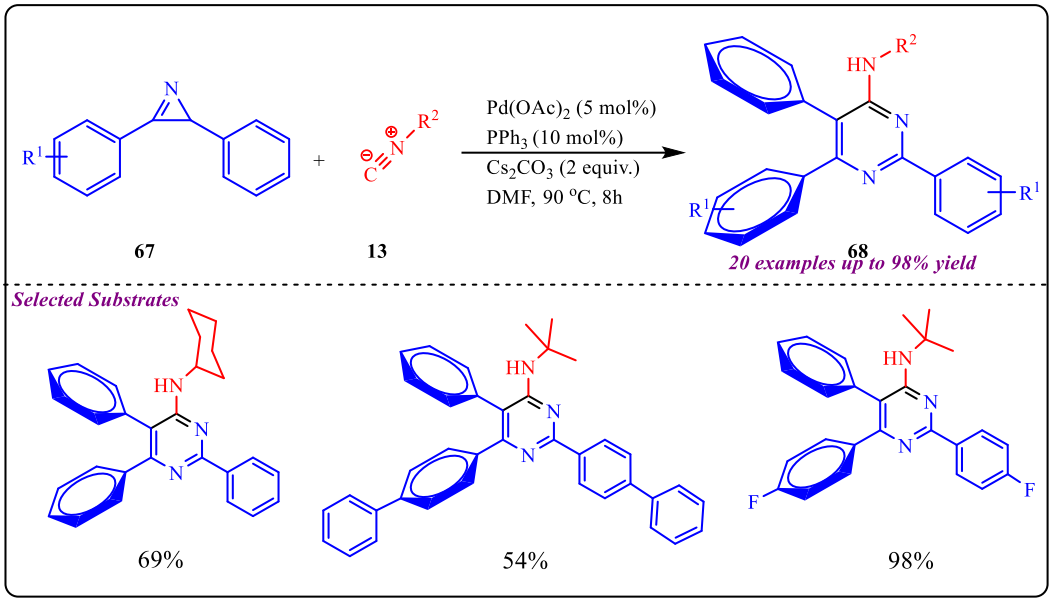

Scheme 1.19: Synthesis of polysubstituted pyrimidines heterocycles via palladium-catalyzed reaction

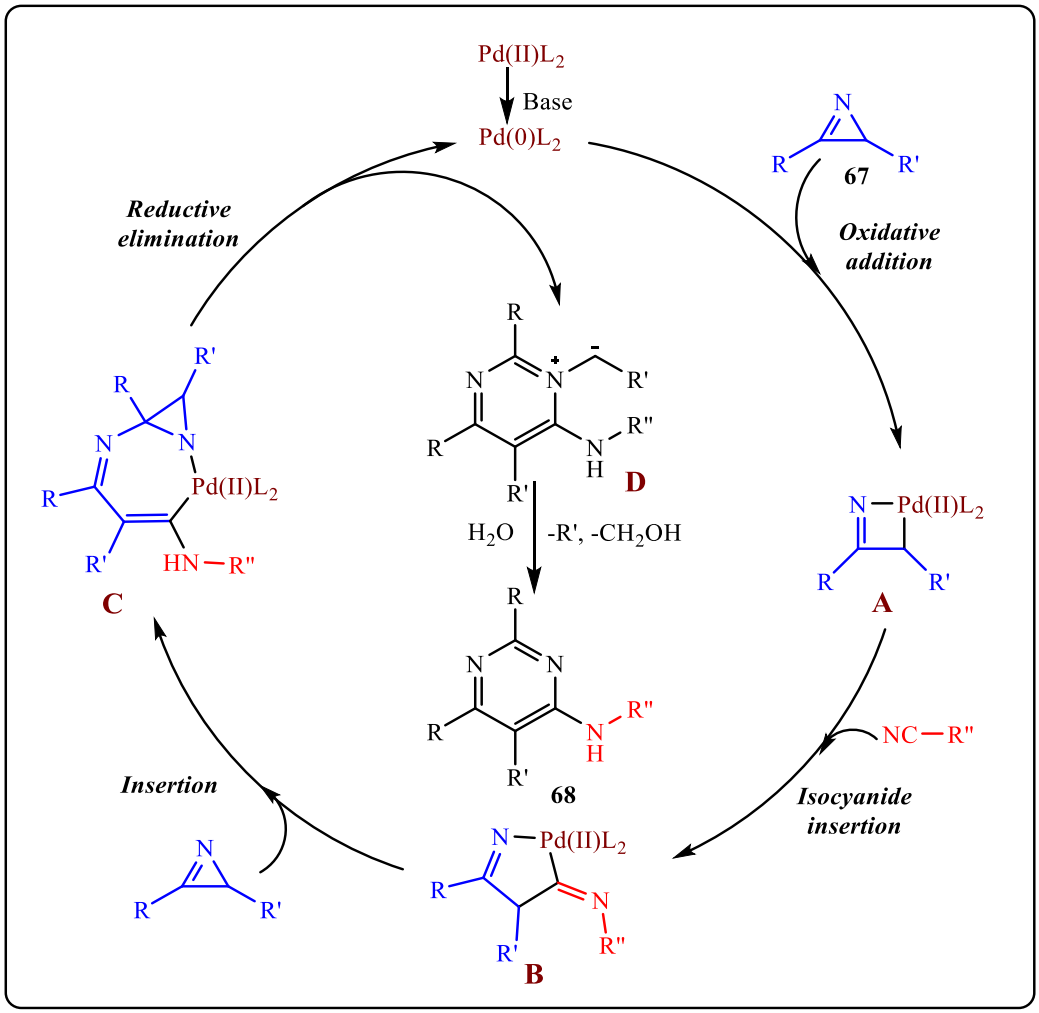

Scheme 1.20: Proposed mechanism

Bolm's et al. developed a green and novel approach to synthesize 3-amino substituted benzothiadiazine oxides in good to excellent yield via Pd-catalyzed tandem reaction of 2-azido sulfoximines with isonitriles (**Scheme 1.21a**).[58] Interestingly, the reaction was getting completed in very short time in the presence of 0.25 mol% of Pd-catalyst at room temperature, which makes this protocol more efficient and economical. However, the reaction was found slightly selective towards 2-azido sulfoximines substrates. The reaction involved isocyanide insertion into N-H and azide bond involving multiple intermediatory key steps. The applicability of the derived product was explored by further transformations via removal of the *tert*-butyl group to form amine-substituted derivatives which can be easily transformed through various simple organic reactions (**Scheme 1.21c**).

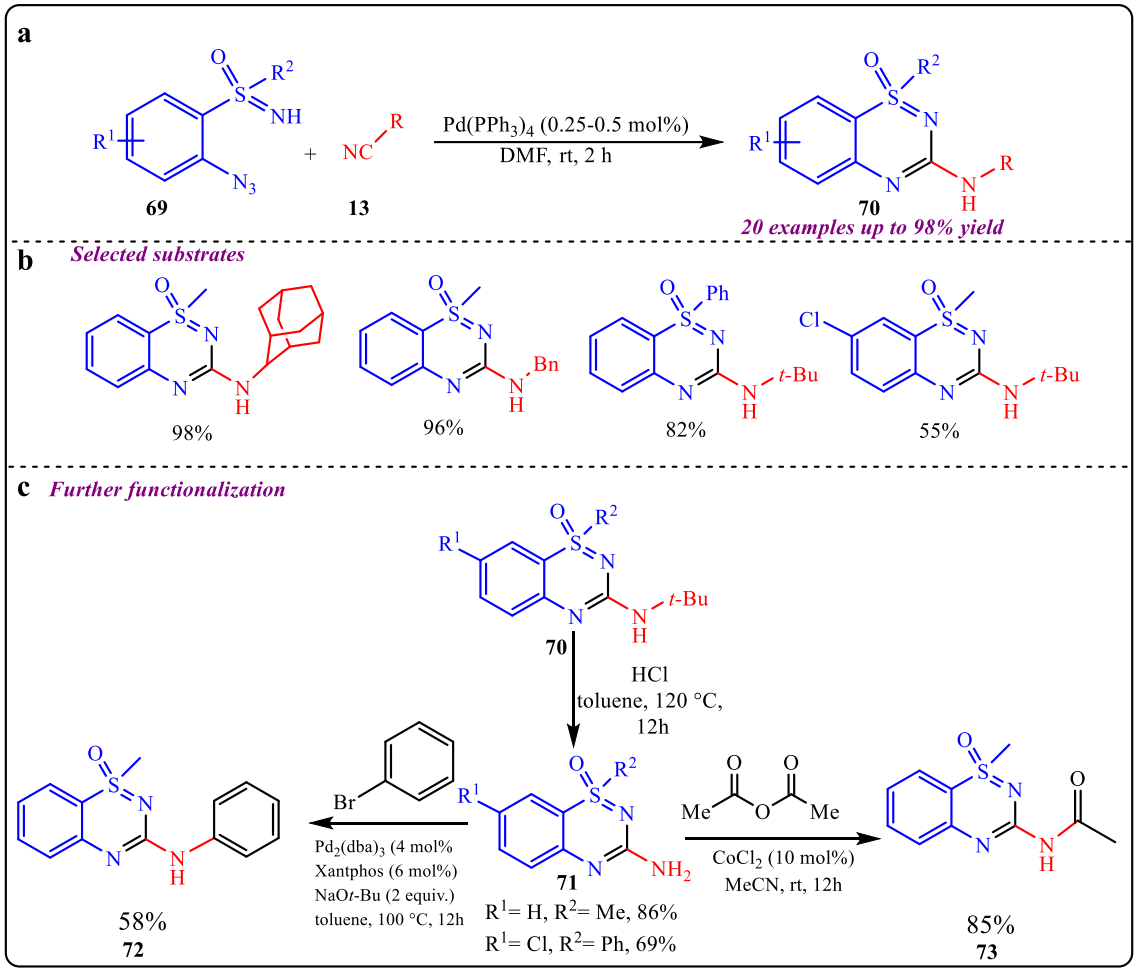

Scheme 1.21: Synthesis of 3-amino substituted benzothiadiazine oxides via palladium-catalyzed reaction

Further, a novel Pd-catalyzed coupling reaction between azide and isocyanides was reported by Xiong's group (**Scheme 1.22a**).[59] The reaction involves Groebke-Blackburn-Bienayme multicomponent reaction followed by azide-isocyanide coupling by using another substrate of isocyanide to afforded imidazo [1,2-a] pyridine-fused 1,3-benzodiazepine heterocycles in moderate to excellent yield. A number of substrates were screened having different electron-donating and withdrawing substituents at amino pyridines and benzaldehydes along with different isocyanides to prove the generality of the protocol (**Scheme 1.22b**). In addition, synthesized derivatives were screened for their anticancer activities and the results showed good activity of the compound (a) toward apoptosis of glioma cells which makes this methodology more attractive for drug development and synthetic chemistry. Interestingly, the gram-scale synthesis of compound (a) provided 78% yield which successfully defined the applicability of the developed methodology (**Scheme 1.22c**).

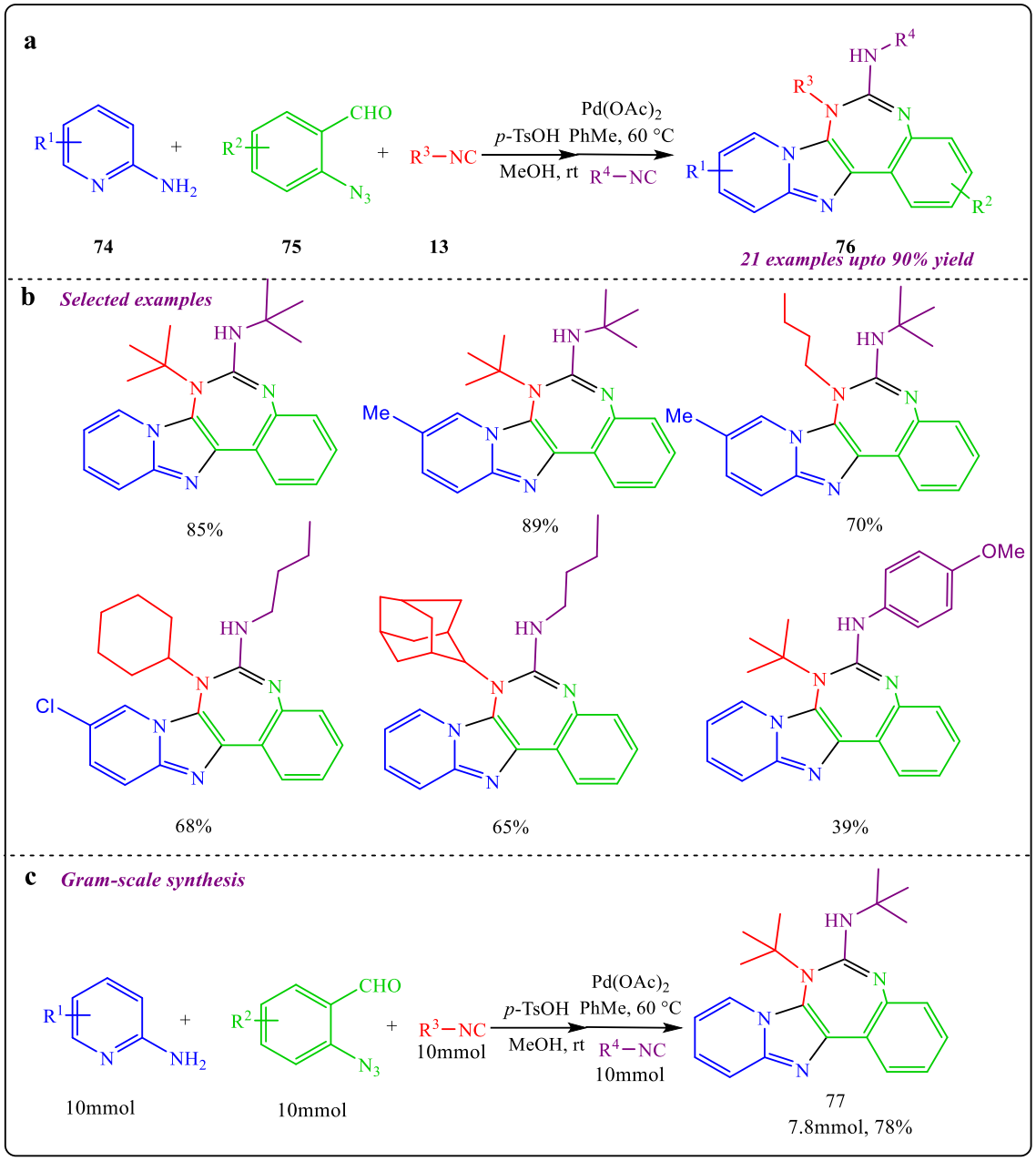

Scheme 1.22: Synthesis of Imidazo [1,2-a] pyridine-Fused 1,3-Benzodiazepine heterocycles

Ren et al. reported an imine directed triple isocyanide insertion approach to synthesize poly substituted pyrroles derivative involving palladium catalysed aza- Nazarov cyclization reaction of alkenyl bromide, isocyanides and amines (**Scheme 1.23**).[60] A broad range of substrate scope was done by employing diverse substituted substrates and observed that the reaction underwent smoothly with various electron donating and withdrawing substituent at alkenyl bromide and provide good yields of corresponding products. However, reaction didn't work when alkyl group was taken in place of aromatics at alkenyl bromide. Similarly, a trace amount of product formation was observed when aliphatic amines were employed in the reaction. Also, various

aromatic and aliphatic rings containing isocyanides worked well for the proposed reaction and provided good to moderate yield. A proposed reaction mechanism suggested the formation of four-membered palladacyclic intermediate which enforced the reaction to proceed through consecutive triple-isocyanide insertion via seven membered transition state which is further supported via DFT studies and various control experiments.

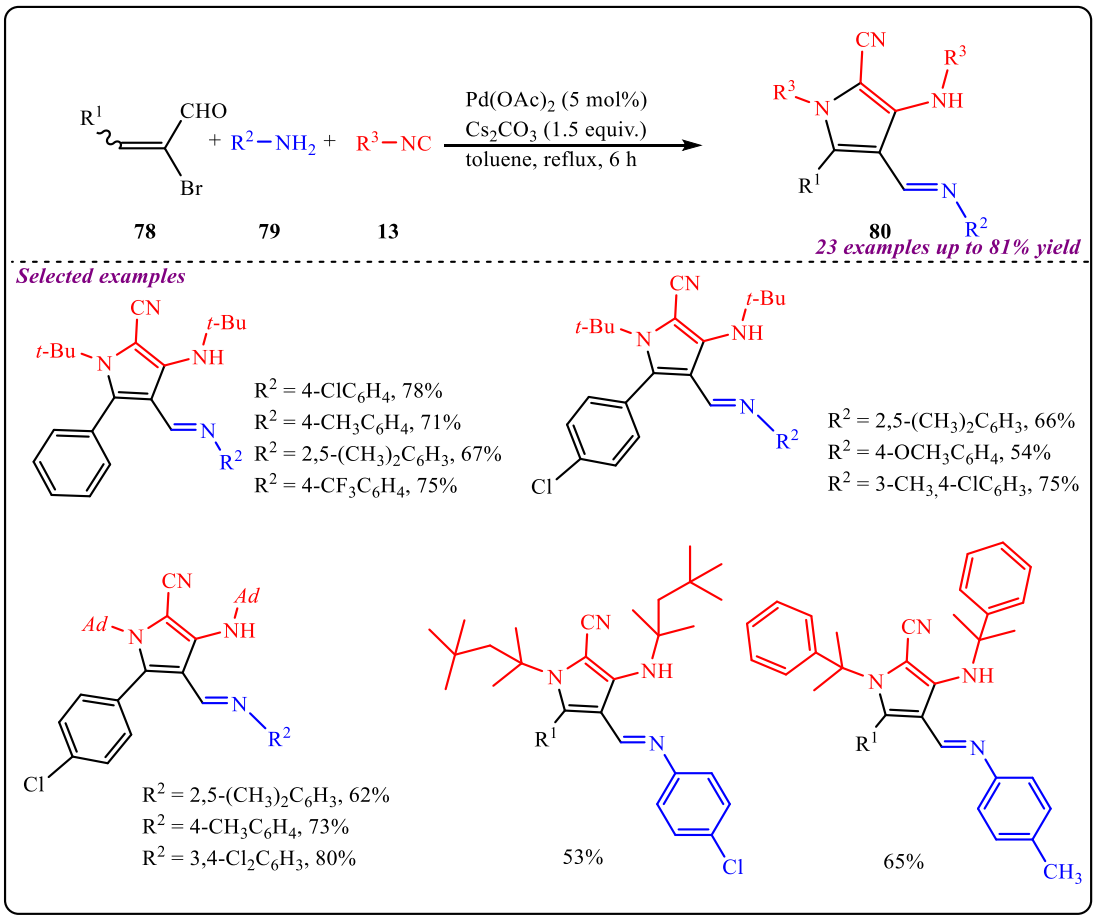

Scheme 1.23: Synthesis of poly-substituted pyrroles derivative via an imine-directed triple isocyanide insertion

1.3: Conclusion

Transition metal catalyzed cascade reactions are widely used method methodology for the synthesis of various novel heterocyclic molecules in organic synthesis. Cascade or tandem reactions are considered as sustainable approach due to their ability to perform multiple steps in one single vessel which makes them more efficient than multistep approaches. We can reduce the wastage of expensive solvents and reagents which required for the purification of intermediate steps by using tandem approaches. That's why, these reactions are time-saving approach and provide the desired product in a highly selective manner. In recent years, various novel approaches have been reported in this direction to synthesize highly applicable

heterocyclic molecules. In summary, we have discussed here some recent advancements in the palladium-catalyzed cascade approach applied for the synthesis of various novel heterocyclic scaffolds. These reactions involve carbene insertion, isocyanide insertion, cyclization, etc as key steps.

1.4: References

(1) Gardner, B. M.; Johansson Seechurn, C. C. C.; Colacot, T. J. Industrial Milestones in Organometallic Chemistry, *Organometallic Chemistry in Industry: A Practical Approach.* **2020**, 1-22.

(2) Xia, Y.; Qiu, D.; Wang, J. Transition-Metal-Catalyzed Cross-Couplings through Carbene Migratory Insertion. *Chem. Rev*. **2017**, *117*, 13810–13889.

(3) Jana, R.; Pathak, T. P.; Sigman, M. S. Advances in Transition Metal (Pd,Ni,Fe)-Catalyzed Cross-Coupling Reactions Using Alkyl-Organometallics as Reaction Partners. *Chem. Rev*. **2011**, *111*, 1417–1492.

(4) Crawley, M. L.; Trost, B. M. *Applications of Transition Metal Catalysis in Drug Discovery and Development : An Industrial Perspective*; John Wiley & Sons, **2012**.

(5) Piontek, A.; Bisz, E.; Szostak, M. Eisenkatalysierte Kreuzkupplungen in Der Synthese von Pharmazeutika: Streben Nach Nachhaltigkeit. *Angew. Chem.* **2018**, *130*, 11284–11297.

(6) Liu, Z. K.; Zhao, Q. Q.; Gao, Y.; Hou, Y. X.; Hu, X. Q. Organic Azides: Versatile Synthons in Transition Metal-Catalyzed C(Sp2)−H Amination/Annulation for N-Heterocycle Synthesis. *Adv. Synth. Catal*. **2021**, *363*, 411–424.

(7) Das, S.; Dutta, A. Rhodium-Catalyzed Annulation for the Construction of Indole Core: An Update. *Tetrahedron*. **2023**, *146*, 133633.

(8) Dhakshinamoorthy, A.; Garcia, H. Cascade Reactions Catalyzed by Metal Organic Frameworks. *ChemSusChem*. **2014**, *7*, 2392–2410.

(9) Vlaar, T.; Ruijter, E.; Maes, B. U. W.; Orru, R. V. A. Palladium-Catalyzed Migratory Insertion of Isocyanides: An Emerging Platform in Cross-Coupling Chemistry. *Angew. Chem. Int. Ed.* **2013**, *52*, 7084–7097.

(10) Hu, F.; Wang, J. Synthesis of Heterocyclic Compounds Based on Transition-Metal-Catalyzed Carbene Coupling Reactions. In *Advances in Transition-Metal Mediated Heterocyclic Synthesis*; Elsevier, **2018**, *2018*, 129–191.

(11) Biajoli, A. F. P.; Schwalm, C. S.; Limberger, J.; Claudino, T. S.; Monteiro, A. L. Recent Progress in the Use of Pd-Catalyzed C-C Cross-Coupling Reactions in the Synthesis of Pharmaceutical Compounds. *J.Braz. Chem. Soc*. **2014**, *25*, 2186–2214.

(12) Lauria, A.; Delisi, R.; Mingoia, F.; Terenzi, A.; Martorana, A.; Barone, G.; Almerico, A. M. 1,2,3-Triazole in Heterocyclic Compounds, Endowed with Biological Activity, through 1,3-Dipolar Cycloadditions. *Eur. J. Org. Chem*. **2014**, 2014, 3289–3306.

(13) Solé, D.; Fernández, I. Controlling Selectivities in Palladium-Catalyzed Cyclization Reactions Leading to Heterocycles. In *Advances in Transition-Metal Mediated Heterocyclic Synthesis*; Elsevier, **2018**, 311–337.

(14) Rio, J.; Liang, H.; Perrin, M. E. L.; Perego, L. A.; Grimaud, L.; Payard, P. A. We Already Know Everything about Oxidative Addition to Pd(0): Do We? *ACS Catal.* **2023**, *13*, 11399–11421.

(15) Sehnal, P.; Taylor, R. J. K.; Fairlamb, L. J. S. Emergence of Palladium(IV) Chemistry in Synthesis and Catalysis. *Chem. Rev.* **2010**, *110*, 824–889.

(16) Wu, X. F.; Neumann, H.; Beller, M. Synthesis of Heterocycles via Palladium-Catalyzed Carbonylations. *Chem. Rev*. **2013**, *113*, 1–35.

(17) Chinchilla, R.; Nájera, C. Chemicals from Alkynes with Palladium Catalysts. *Chem. Rev*. **2014**, *114*, 1783–1826.

(18) Poli, G.; Giambastiani, G.; Heumann, A. Palladium in Organic Synthesis: Fundamental Transformations and Domino Processes. Tetrahedron. **2000**, 56, 5959-5989.

(19) Li, L.; Mi, C.; Huang, G.; Huang, M.; Zhu, Y.; Ni, S. F.; Wang, Z.; Huang, Y. A Carbene Relay Strategy for Cascade Insertion Reactions. *Angew. Chem. Int. Ed.* **2023**, *135*, e202312793.

(20) Barluenga, J.; Rodréguez, F.; Fañáns, F. J. Recent Advances in the Synthesis of Indole and Quinoline Derivatives through Cascade Reactions. *Chem. Asian J*. **2009**, 4, 1036–1048.

(21) Lu, L. Q.; Chen, J. R.; Xiao, W. J. Development of Cascade Reactions for the Concise Construction of Diverse Heterocyclic Architectures. *Acc. Chem. Res.* **2012**, *45*, 1278–1293.

(22) Wang, Y.; Lu, H.; Xu, P. F. Asymmetric Catalytic Cascade Reactions for Constructing Diverse Scaffolds and Complex Molecules. *Acc. Chem. Res.* **2015**, *48*, 1832–1844.

(23) Parsons, P. J.; Penkett, C. S.; Shell, A. J. *Tandem Reactions in Organic Synthesis: Novel Strategies for Natural Product Elaboration and the Development of New Synthetic Methodology. Chem. Rev*. **1996**, *96*, 195-206.

(24) Grondal, C.; Jeanty, M.; Enders, D. Organocatalytic Cascade Reactions as a New Tool in Total Synthesis. *Nat. Chem*. **2010**, *2*, 167–178.

(25) Epping, R. F. J.; Vesseur, D.; Zhou, M.; de Bruin, B. Carbene Radicals in Transition-Metal-Catalyzed Reactions. *ACS Catal*. **2023**, *13,* 5428–5448.

(26) Bourissou, D.; Guerret, O.; Gabbaï, F. P.; Bertrand, G. Stable Carbenes. *Chem. Rev.* **2000**, *100*, 39–91.

(27) de Frémont, P.; Marion, N.; Nolan, S. P. Carbenes: Synthesis, Properties, and Organometallic Chemistry. *Coord. Chem. Rev*. **2009**, *253*, 862–892.

(28) Skander, M.; Retailleau, P.; Bourrié, B.; Schio, L.; Mailliet, P.; Marinetti, A. N-Heterocyclic Carbene-Amine Pt(II) Complexes, a New Chemical Space for the Development of Platinum-Based Anticancer Drugs. *J. Med. Chem.* **2010**, *53*, 2146–2154.

(29) Singh, G. S. Progress in Classical Chemistry of Metal-Carbenoids from α-Diazocarbonyls. *Arkivoc*. **2023**, *1*, 202312072.

(30) Huang, M. Y.; Zhu, S. F. Uncommon Carbene Insertion Reactions. *Chem. Sci.* **2021**, *12*, 15790–15801.

(31) Cardin, D. J.; Cetinkaya, B.; Lappert, M. F. Transition metal-carbene complexes. *Chem. Rev*. **1972**, *72*, 545-574.

(32) Wentrup, C. Carbene Und Nitrene: Aktuelle Entwicklungen in Der Grundlagenchemie. *Angew. Chem.* **2018**, *130*, 11680–11693.

(33) Xie, Z. Y.; Xuan, J. Advances in Heterocycle Synthesis through Photochemical Carbene Transfer Reactions. *Chem. Commun.* **2024**, 60, 2125-2136.

(34) Barluenga, J.; Santamaría, J.; Tomás, M. Synthesis of Heterocycles via Group VI Fischer Carbene Complexes. *Chem. Rev.* **2004**, *104*, 2259–2283.

(35) Nhat, N.; Le, T. Digital Commons @ Colby Generation and Reactions of Cyclopropyl Vinylidene Carbenes. *Honors. Theses.* **2019**, 991.

(36) Vogiatzis, K. D.; Polynski, M. V.; Kirkland, J. K.; Townsend, J.; Hashemi, A.; Liu, C.; Pidko, E. A. Computational Approach to Molecular Catalysis by 3d Transition Metals: Challenges and Opportunities. *Chem. Rev*. **2019**, *4*, 2453–2523.

(37) Duan, A.; Xiao, F.; Lan, Y.; Niu, L. Mechanistic Views and Computational Studies on Transition-Metal-Catalyzed Reductive Coupling Reactions. *Chem. Soc. Rev*. **2022**, *119*, 9986–10015.

(38) Cheng, G. J.; Zhang, X.; Chung, L. W.; Xu, L.; Wu, Y. D. Computational Organic Chemistry: Bridging Theory and Experiment in Establishing the Mechanisms of Chemical Reactions. *J. Am. Chem. Soc*. **2015**, *137*, 1706–1725.

(39) Zhang, X.; Chung, L. W.; Wu, Y. D. New Mechanistic Insights on the Selectivity of Transition-Metal-Catalyzed Organic Reactions: The Role of Computational Chemistry. *Acc. Chem. Res.* **2016**, *49*, 1302–1310.

(40) Xiong, Q.; Chen, H.; Zhang, T.; Shan, C.; Bai, R.; Lan, Y. On the Mechanism of Palladium-Catalyzed Unsaturated Bond Transformations: A Review of Theoretical Studies. *Asian J. Org. Chem*. **2019**, 8, 1194–1206.

(41) Samec, J. S. M.; Bäckvall, J. E.; Andersson, P. G.; Brandt, P. Mechanistic Aspects of Transition Metal-Catalyzed Hydrogen Transfer Reactions. *Chem. Soc. Rev.* **2006**, *35*, 237–248.

(42) Sun, W.; Chen, C.; Qi, Y.; Zhao, J.; Bao, Y.; Zhu, B. Palladium-Catalyzed Cascade Reactions of Alkene-Tethered Carbamoyl Chlorides with: N-Tosyl Hydrazones: Synthesis of Alkene-Functionalized Oxindoles. *Org. Biomol. Chem.* **2019**, *17*, 8358–8363.

(43) Solé, D.; Amenta, A.; Bennasar, M. L.; Fernández, I. Palladium- and Ruthenium-Catalyzed Intramolecular Carbene CAr−H Functionalization of γ-Amino-α-Diazoesters for the Synthesis of Tetrahydroquinolines. *Chem. Eur. J.* **2019**, *25*, 10239–10245.

(44) Yu, Y.; Chakraborty, P.; Song, J.; Zhu, L.; Li, C.; Huang, X. Easy Access to Medium-Sized Lactones through Metal Carbene Migratory Insertion Enabled 1,4-Palladium Shift. *Nat. Commun.* **2020**, *11*, 461.

(45) Zhu, Y. M.; Fang, Y.; Li, H.; Xu, X. P.; Ji, S. J. Divergent Reaction of Isocyanides with O-Bromobenzaldehydes: Synthesis of Ketenimines and Lactams with Isoindolinone Cores. *Org. Lett.* **2021**, *23*, 7342–7347.

(46) Wang, X.; Fu, J. P.; Mo, J. H.; Tian, Y. H.; Liu, C. Y.; Tang, H. T.; Sun, Z. J.; Pan, Y. M. Assembly of 5-Aminoimidazoles via Palladium-Catalysed Double Isocyanide Insertion Reaction. *Adv. Synth. Catal.* **2021**, *363*, 2762–2766.

(47) Chen, S.; Oliva, M.; Van Meervelt, L.; Van der Eycken, E. V.; Sharma, U. K. Palladium-Catalyzed Domino Synthesis of 2,3-Difunctionalized Indoles via Migratory Insertion of Isocyanides in Batch and Continuous Flow. *Adv. Synth. Catal.* **2021**, *363*, 3220–3226.

(48) Mancuso, R.; Ziccarelli, I.; Brindisi, M.; Altomare, C. D.; Frattaruolo, L.; Falcicchio, A.; Della Ca', N.; Cappello, A. R.; Gabriele, B. A Stereoselective, Multicomponent Catalytic Carbonylative Approach to a New Class of α,β-Unsaturated γ-Lactam Derivatives. *Catalysts*. **2021**, *11*, 1–18.

(49) Teng, F.; Yu, T.; Peng, Y.; Hu, W.; Hu, H.; He, Y.; Luo, S.; Zhu, Q. Palladium-Catalyzed Atroposelective Coupling-Cyclization of 2-Isocyanobenzamides to Construct Axially Chiral 2-Aryl- And 2,3-Diarylquinazolinones. *J. Am. Chem. Soc.* **2021**, *143*, 2722–2728.

(50) Wei, W. X.; Li, Y.; Wen, Y. T.; Li, M.; Li, X. S.; Wang, C. T.; Liu, H. C.; Xia, Y.; Zhang, B. S.; Jiao, R. Q.; Liang, Y. M. Experimental and Computational Studies of Palladium-Catalyzed Spirocyclization via a Narasaka-Heck/C(Sp3or Sp2)-H Activation Cascade Reaction. *J. Am. Chem. Soc.* **2021**, *143*, 7868–7875.

(51) Xiong, J.; He, H. T.; Yang, H. Y.; Zeng, Z. G.; Zhong, C. R.; Shi, H.; Ouyang, M. L.; Tao, Y. Y.; Pang, Y. L.; Zhang, Y. H.; Hu, B.; Fu, Z. X.; Miao, X. L.; Zhu, H. L.; Yao, G. Synthesis of 4-Tetrazolyl-Substituted 3,4-Dihydroquinazoline Derivatives with Anticancer Activity via a One-Pot Sequential Ugi-Azide/Palladium-Catalyzed Azide-Isocyanide Cross-Coupling/Cyclization Reaction. *J. Org. Chem.* **2022**, *87*, 9488–9496.

(52) Zhang, Y.; Liu, T.; Liu, L.; Guo, H.; Zeng, H.; Bi, W.; Qiu, G.; Gao, W.; Ran, X.; Yang, L.; Du, G.; Zhang, L. Palladium-Catalyzed Preparation of N-Substituted Benz[c, d]Indol-2-Imines and N-Substituted Amino-1-Naphthylamides. *J. Org. Chem.* **2022**, *87*, 8515–8524.

(53) Li, M.; Zhang, R.; Gao, Q.; Jiang, H.; Lei, M.; Wu, W. Divergent Synthesis of Fused Tetracyclic Heterocycles from Diarylalkynes Enabled by the Selective Insertion of Isocyanide. *Angew. Chem. Int. Ed.* **2022**, *61*, e202208203.

(54) Sisodiya, S.; Acharya, A.; Nagpure, M.; Roy, N.; Giri, S. K.; Yadav, H. R.; R. Choudhury, A.; Guchhait, S. K. A Cascade Reaction of Indolyl-Migratory Isocyanide Insertion, Scaffold Rearrangement and Redox-Neutral Event with Isocyanide as a C(Sp3)H-N Synthon Efficiently Constructs Indolylisoindolinones. *Chem. Commun.* **2022**, *58*, 11827–11830.

(55) Zhang, F.; Zhao, R.; Zhu, L.; Yu, Y.; Liao, S.; Wang, Z. X.; Huang, X. Divergent Isoindolinone Synthesis through Palladium-Catalyzed Isocyanide Bridging C–H Activation. *Cell Rep.* **2022**, *3*, 100776.

(56) Lin, H.; Pan, Y.; Fu, J.; Yi, Y.; Tang, H.; Pan, Y.; Yu, W.; Wang, X. Palladium-Catalyzed Tandem C(Sp3)-H Insertion Cyclization of 2-(2-Vinylarene)Acetonitriles with Isocyanides to Access Naphthalen-2-Amines. *J. Org. Chem.* **2023**, *88*, 12409–12420.

(57) Saeifard, L.; Amiri, K.; Rominger, F.; Müller, T. J. J.; Balalaie, S. Synthesis of Polysubstituted Pyrimidines through Palladium-Catalyzed Isocyanide Insertion to 2H-Azirines. *J. Org. Chem.* **2023**, *88*, 12519–12525.

(58) Hommelsheim, R.; Bausch, S.; van Nahl, R.; Ward, J. S.; Rissanen, K.; Bolm, C. Synthesis of 3-Amino-Substituted Benzothiadiazine Oxides by a Palladium-Catalysed Cascade Reaction. *Green Chem.* **2023**, *25*, 3021–3026.

(59) Zhong, C. R.; Zhang, Y. H.; Yao, G.; Zhu, H. L.; Hu, Y. Di; Zeng, Z. G.; Liao, C. Z.; He, H. T.; Luo, Y. T.; Xiong, J. Synthesis of Imidazo[1,2-a]Pyridine-Fused 1,3-Benzodiazepine Derivatives with Anticancer Activity via a One-Pot Cascade GBB-3CR/Pd(II)-Catalyzed Azide-Isocyanide Coupling/Cyclization Process. *J. Org. Chem.* **2023**, *88*, 13125–13134.

(60) Li, J.; Zhao, Z. W.; Zheng, S.; He, P.; Qiu, J. Y.; Zhou, Q. Q.; Ren, Z. L. Pd-Catalyzed Imine-Directed One-Pot Access to Polysubstituted Pyrroles via Tandem Triple Isocyanide Insertion/Aza-Nazarov Cyclization Reactions. *Org. Chem. Front.* **2023**, *10*, 3252–3258.

Literature gaps:

After reviewed the literature in detail, following gaps are found in the present study. It has been found that following areas have not been much explored till now:

a) One pot strategy leading to biologically important heterocyclic rings are highly interested in synthetic organic chemistry due to a number of advantages over the step-wise protocols. In this context, development of novel and resourceful methods for getting biologically important heterocycles in one operation i.e., domino or tandem reactions are extremely required.
b) Computational chemistry is well suited to the study of various organic reaction mechanism. In this perspective, the mechanistic investigation using computational methods may assist in the exploration of newly developed cascade reactions and also opens the door to develop new organic transformations.

Objectives:

Based on the gaps found in this study, we are proposing the following objectives here:

1. Development of novel transition-metal catalyzed cascade reactions using diazo compounds or their equivalents to synthesize biologically important heterocycles.
2. Mechanistic investigation of newly developed cascade reactions mentioned in objective 1 using computational methods.

CHAPTER 2

Divergent and selective synthesis of 3-alkylidene oxindoles using Pd-catalysed multicomponent reaction

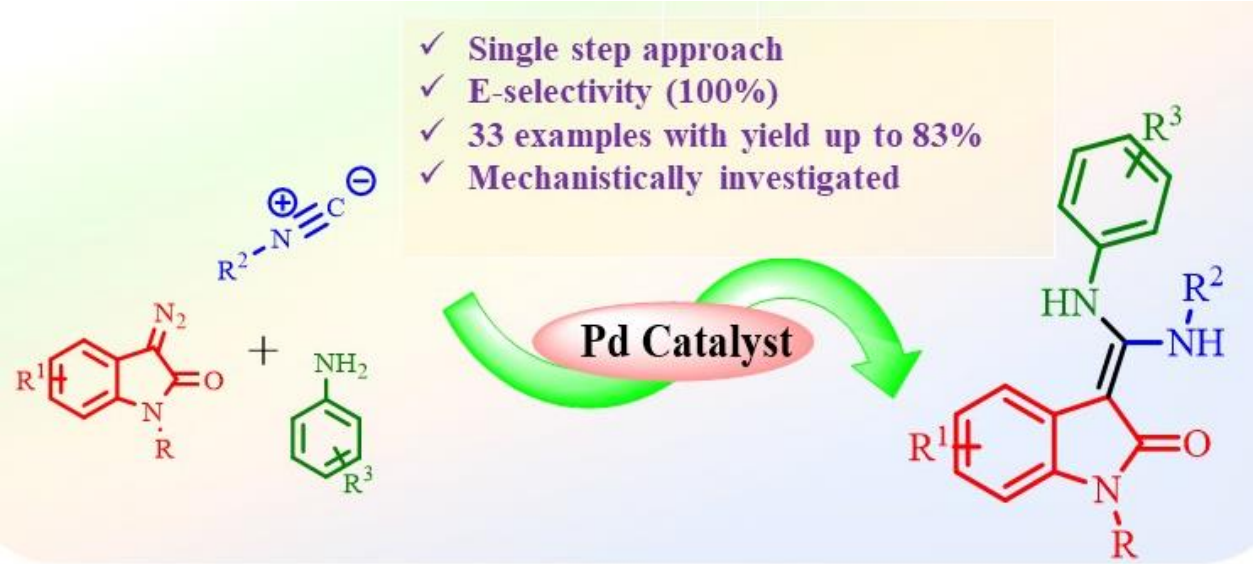

2.1: Introduction

Oxindole is a valuable scaffold found in a number of natural products and clinically important molecules.[1] Moreover, oxindole derivatives show a broad range of biological activities such as anti-cancer, anti-fungal, anti-bacterial, anti-tubercular, anti-convulsant, anti-glycation, antioxidant, anti-inflammatory, analgesic, anti-anxiety, anti-diabetic and anti-HIV, etc.[2a-2f] Besides, they have several other applications such as being used as corrosion inhibitors, fluorescent sensors, and in the dye industry.[2g-2h] In particular, 3-alkylidene oxindole is an extremely crucial framework and has gained lots of attention in recent years due to its presence in several drug molecules (**Figure 2.1**).[3]

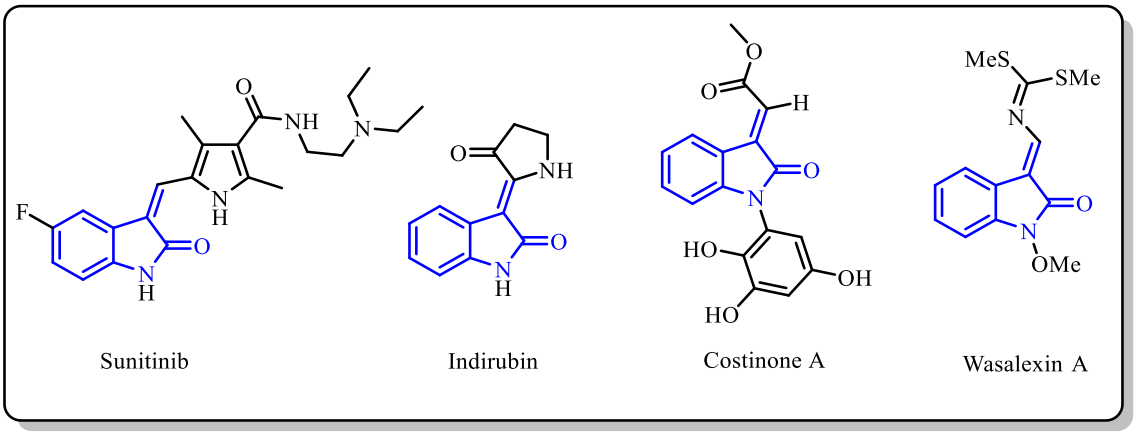

Figure 2.1: Example of 3-alkylidene oxindole containing biologically active molecules

The most successful example of a 3-alkylidene oxindole-containing drug is sunitinib, which is used as tyrosine kinase inhibitor and exhibits potent antiangiogenic and antitumor activities.[4] Also, 3-alkylidene oxindole scaffolds is a part of various natural products such as costinone A and wasalexin A those having anticancer and antifungal activities respectively (**Figure 2.1**).[5] Previously, a number of approaches have been developed to synthesize 3-alkylidene oxindole scaffold.[6] In this context, Li *et al.* reported a method to synthesized biologically valuable (*E*)-oxindolylidene derivatives via Pd-catalyzed Heck reaction followed by alkoxycarbonylation of N-substituted propiolamides with CO and alcohol (**Scheme 2.1a**).[7a] Further, Gnanaprakasam and group members has synthesized (*Z*)-3-(aminobenzylidene/aminoalkylidene)indolin-2-ones using 2-oxindole and alkyl/aryl nitrile in the presence of strong base i.e. LiO*t*Bu and 2,2'-bipyridine as a ligand (**Scheme 2.1b**).[7b] An approach to synthesize unsymmetrically substituted *E*-selective 3-allylideneoxindole using Pd- nanoparticles as a catalyst was reported by Sekar's group (**Scheme 2.1c**).[7c] Next, Chen's group developed a method to construct α-amidoacrylates containing a 3-ylideneoxindole using 3-flourooxindoles and α-iminoacetates (**Scheme 2.1d**)[7d]. Recently, Hanusek et al. developed a modular approach to construct (*Z*)-3-[amino

(phenyl/methyl)methylidene]-1,3-dihydro-2H-indol-2-ones using easily available 3-bromooxindoles or (2-oxoindolin-3-yl)triflate and thioacetamides or thiobenzamides (**Scheme 2.1e**).[7e] Nevertheless, most of the previously reported methods have certain limitations like narrow substrate scope and formation of the mixture of E/Z isomers, etc. To overcome the previous limitations and keep in view the biological importance of 3-alkylidene oxindole scaffold, a divergent and highly selective synthesis is extremely required, which is also very important from the medicinal chemistry perspective.

On the other hand, multicomponent reactions (MCR) are perhaps the most convenient and practical approach for the construction of biologically valuable frameworks.[8] Despite a lot of development in the past decades, transition metals catalyzed multicomponent reactions are still heavily investigated for synthesizing heterocycles.[9] Next, diazo compounds which are vital precursors for the *in-situ* formation of metal carbenoids, have been vastly implemented in the transition metal-catalyzed multicomponent reactions.[10] In this context, Zhao and co-workers reported rhodium catalyzed tandem methodology to synthesize trifluoromethyl substituted isoquinoline, imidates, and amidines derivatives by using triflourodiazoethanes as carbene precursor along with isocyanides and nucleophiles like alcohols, amines, etc.[11a] Similarly, a multicomponent approach was reported by Liu's group to synthesize 1.3- bis(β-amino acrylate) substituted 2-mercaptoimidazole scaffolds by using α-diazoacetates, isocyanides and 2-mercaptoimidazoles [11b] Recently, Xia et al. reported the synthesis of amidines via cobalt catalysed MCR consisting diazo ester, isocyanides and amines (**Scheme 2.1f**).[11c] Besides, palladium-catalyzed MCR's consisting of the diazo compound, isocyanide along with amine have been investigated to construct heterocyclic compounds.[12] By drawing encouragement from the attractive therapeutic applications of 3- alkylidene oxindole[5] and our previous work on the metal-catalyzed reaction of diazo compounds,[13] herein, we reported a multi-component approach for the diverse synthesis of *E*-selective 3-alkylidene oxindole derivatives via Pd-catalyzed reaction of 3-diazo oxindole, isocyanide and aniline (**Scheme 2.1g**).

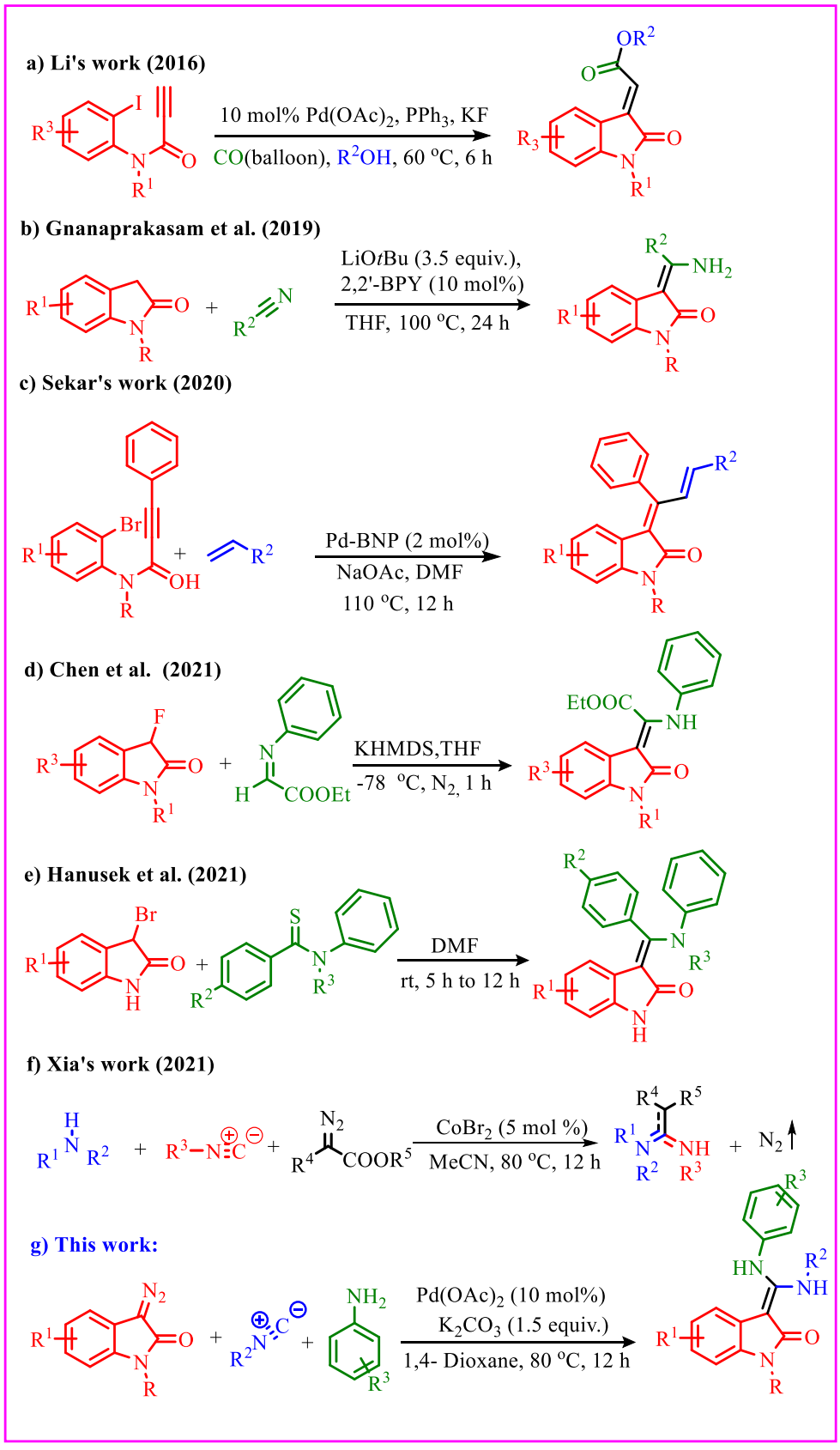

Scheme 2.1: Recent approaches to synthesize 3-(aminoaryl/alkylidene) oxindole derivatives (**a-e**). Recent multicomponent approach using diazoesters, amine and isocyanide (**f**). Our approach (**g**).

2.2: Results and discussion

2.2.1: Optimization of the reaction conditions

We began our investigation by selecting 3-diazo-1-methyl oxindole (1a), *tert*-butyl isocyanide (2a) and aniline (3a) as the model substrates for the multicomponent reaction and screened $PdCl_2$, $Cu(OAc)_2$ and $Rh_2(OAc)_4$ as a metal catalyst (**Table 2.1, entries 1-3**). Interestingly, the model reaction furnished desired product (4a) in 64% yield when 10 mol% of $PdCl_2$ along with 1.5 equiv. of K_2CO_3 in 1,4-dioxane as a solvent was used (**Table 2.1, entry 1**). However, no product formation was observed when $Cu(OAc)_2$, and $Rh_2(OAc)_4$ were employed as a catalyst in the model reaction (**Table 2.1, entries 2 & 3**). Next, to improve the yield of the model reaction, various palladium salts such as $Pd(OAc)_2$, $PdCl_2(NCC_6H_5)_2$, $Pd(DPPF)Cl_2$, $Pd(dba)_3$, and $Pd(PPh_3)_4$ were screened (**Table 2.1, entries 4-8**). Unfortunately, there was no significant improvement in the outcome of the reaction and only up to 75% isolated yield could be achieved while using $Pd(OAc)_2$ as a catalyst (Table 2.1, entries 4). Also, reaction did not provide any desired product in the absence of $Pd(OAc)_2$ (**Table 2.1, entry 9**). Next, we screened various bases like Cs_2CO_3, Na_2CO_3, KO*t*-Bu, NEt_3, etc., in the presence of $Pd(OAc)_2$ as a catalyst and found that K_2CO_3 was the best base for this reaction (**Table 2.1, entries 10-13**). It was clearly evident that mild base provides a higher yield in comparison to a strong base like KO*t*Bu which afforded only 24% isolated yield. However, when we tried the reaction in absence of base it gave the product (4a) only in 26% isolated yield, which shows the importance of K_2CO_3 in this multicomponent reaction (**Table 2.1, entry 19**). Noticeably, when we tried solvents such as toluene, DMF, DMSO, and THF instead of 1,4-dioxane, no improvement in the results was observed (**Table 2.1, entries 14-17**). Moreover, the yield of the reaction was diminished when the amount of palladium salt reduced from 10 mol% to 5 mol% (**Table 2.1, entry 18**). Finally, the substrate ratio was changed from 1:1.2:1 to 1:1:1 or1:1.5:1.5 for 3-diazo-1-methyl oxindole (1a), *tert*-butyl isocyanide (2a) and aniline (3a) respectively, however, the yield of the reaction did not improve. Also, it was noticed that increasing the temperature or reaction time does not make any improvement in the outcome of the model reaction.

Table 2.1: Optimization of the reaction conditions[a]

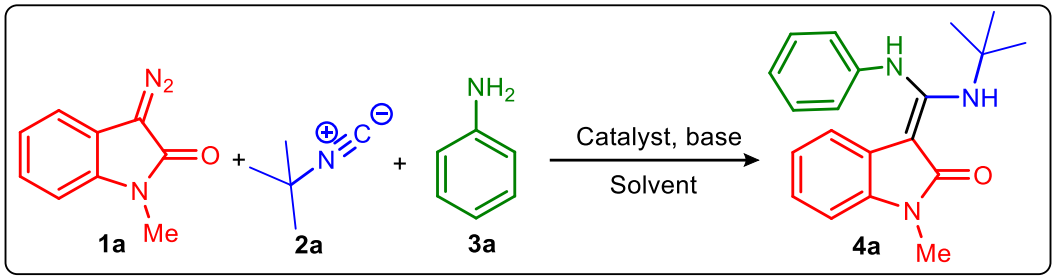

entry	catalyst	base	solvent	yield[b] (%)
1	$PdCl_2$	K_2CO_3	1,4-dioxane	64
2	$Cu(OAc)_2$	K_2CO_3	1,4-dioxane	-
3	$Rh(OAc)_2$	K_2CO_3	1,4-dioxane	-
4	$Pd(OAc)_2$	K_2CO_3	1,4-dioxane	75
5	$PdCl_2(NCC_6H_5)_2$	K_2CO_3	1,4-dioxane	70
6	$Pd(DPPF)Cl_2$	K_2CO_3	1,4-dioxane	72
7	$Pd(dba)_3$	K_2CO_3	1,4-dioxane	67
8	$Pd(PPh_3)_4$	K_2CO_3	1,4-dioxane	54
9	-	K_2CO_3	1,4-dioxane	-
10	$Pd(OAc)_2$	Cs_2CO_3	1,4-dioxane	56
11	$Pd(OAc)_2$	Na_2CO_3	1,4-dioxane	43
12	$Pd(OAc)_2$	KO*t*-Bu	1,4-dioxane	24
13	$Pd(OAc)_2$	NEt_3	1,4-dioxane	45
14	$Pd(OAc)_2$	K_2CO_3	Toluene	48
15	$Pd(OAc)_2$	K_2CO_3	DMF	63
16	$Pd(OAc)_2$	K_2CO_3	DMSO	39
17	$Pd(OAc)_2$	K_2CO_3	THF	30
18[c]	$Pd(OAc)_2$	K_2CO_3	1,4-dioxane	51
19[d]	$Pd(OAc)_2$	-	1,4-dioxane	26

[a]**Reaction conditions**: 3-diazo-1-methyloxindole (1a) (1.0 equiv., 100 mg, 0.58 mmol), *tert*-butyl isocyanide (2a) (1.2 equiv., 57.6 mg, 79 µL, 0.70 mmol), aniline (3a) (1.0 equiv., 54 mg, 53 µL, 0.58 mmol), Pd-catalyst=10 mol%, base (1.5 equiv.), solvent = 2 mL, [b]isolated yield, [c]Pd-catalyst = 5 mol%, [d]no base, 12 h, 80 °C.

2.2.2: Substrate Scope

After having optimal reaction conditions in hands (**Table 2.1, entry 4**), next, we tested the substrate scope for the Pd-catalyzed multicomponent reaction. Initially, *tert*-butyl isocyanide was replaced by 1,1,3,3-tetramethyl butyl isocyanide or cyclohexyl isocyanide, as a result, 80% and 74% isolated yields were obtained for the corresponding products (**4b-c**, **Scheme 2.2**). These results indicated that the outcome of the multicomponent reaction does not significantly depend on the structural diversity of isocyanide. Further, different 3-diazo oxindoles bearing either electron-withdrawing or electron-donating groups were tested. In this context, 3-diazo oxindoles bearing electron-donating groups like -OMe at C-5 position afforded the corresponding products in 78%, 75% and 68% isolated yields (**4d-f**, **Scheme 2.2**). Similarly, 3-diazo-1,5-dimethyl oxindoles afforded the products in good yields when employed with *tert*-butyl isocyanide, 1,1,3,3-tetramethyl butyl isocyanide and cyclohexyl isocyanide, (**4g-i**, **Scheme 2.2**). Also, substitution at other position of 3-diazo oxindoles like 6-OMe worked well and provided 73% yield of desired product **(4j, Scheme 2.2)**. Although, 3-diazo oxindoles bearing electron-withdrawing group like -NO_2 at C-5 position afforded the corresponding products in the inferior yield than the electron-donating group (**4k-m**, **Scheme 2.2**). It might be due to either the low solubility of NO_2-containing 3-diazo oxindoles or lower stability in the reaction conditions. Next, electron-withdrawing group such as 7-CF_3 at 3-diazo oxindoles was employed and obtained 54% yield of product (**4n, Scheme 2.2**) which was slightly higher than yield obtained in the case of 5-NO_2 substitutions at 3-diazo oxindoles. We have also examined the effect of halide substitution at 3-diazo oxindoles and obtained 51% yield of product with 7-flouro substituted 3-diazo oxindoles and 76-83% isolated yields in the case of 5–Cl substitution (**4o-r**, **Scheme 2.2**). However, the reaction gave a lower yield when 5–Br substitution was used (**4s-u**, **Scheme 2.2**), and it might be due to the formations of the side products those could not purified and characterized. Next, we replaced the –CH_3 group at the N-1 position of 3-diazo oxindoles with a phenyl group, which decreased the yield of the reaction and was probably due to an increment in the steric hindrance at the N-1 position (**4v**, **Scheme 2.2**). After checking the effect of substituents on 3-diazo oxindoles, we further investigated the scope of substituted anilines (**4w-4h'**, **Scheme 2.2**). In this context, we obtained moderate to good yield when different halide-substituted anilines were employed in the multicomponent reaction (**4w-y**, **Scheme 2.2**). However, when aniline containing a strong electron-withdrawing group like -NO_2 at the *para*-position was employed, the reaction almost

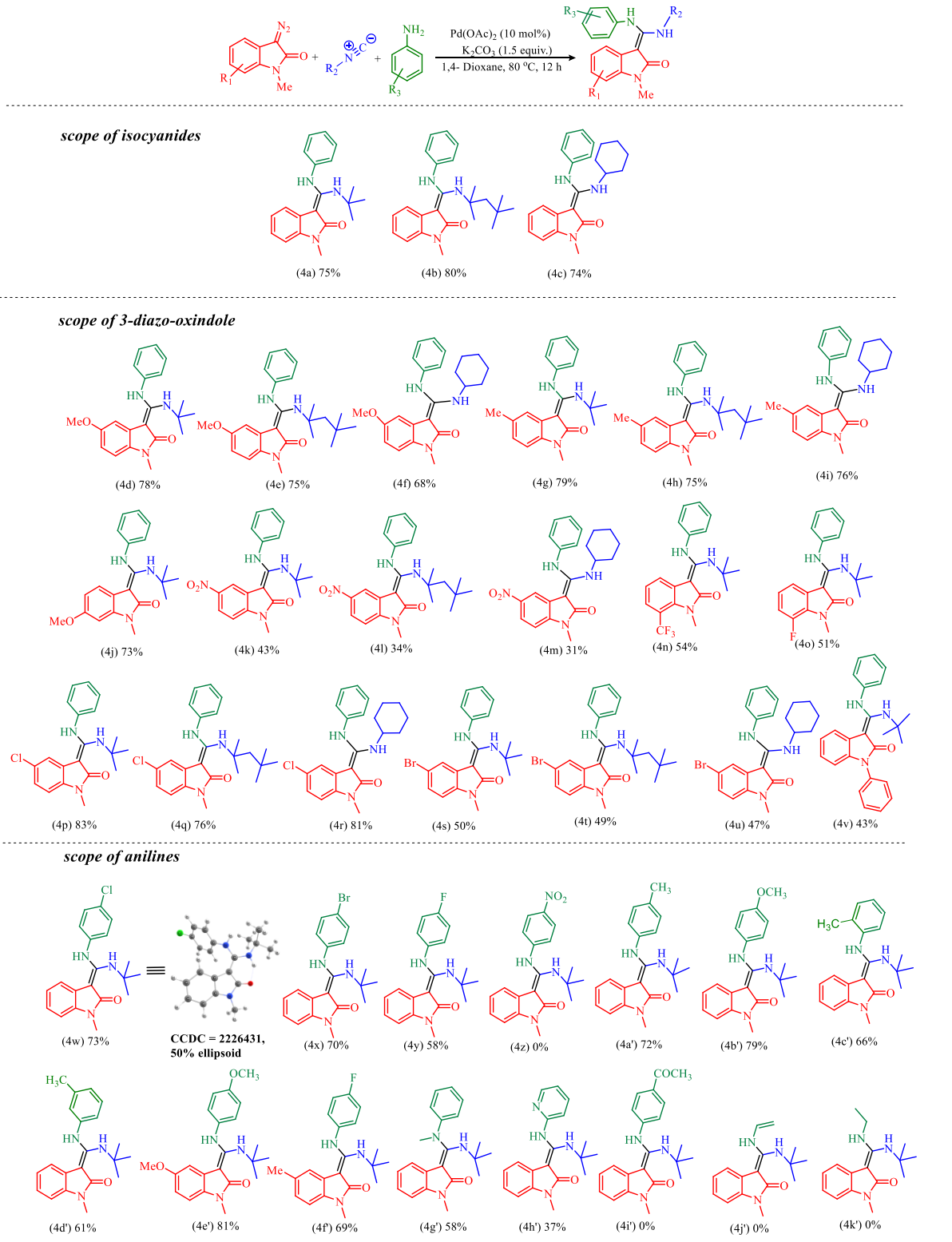

Reaction conditions: 3-diazo oxindoles (1) (1.0 equiv.), isocyanides (2) (1.2 equiv.), anilines (3) (1.0 equiv.), $Pd(OAc)_2$ (10 mol%), K_2CO_3 (1.5 equiv.), 1,4-dioxane (2 mL), 12 h, 80 °C.

Scheme 2.2: The substrate scopes of Pd-catalyzed multicomponent reaction

diminished. (**4z**, **Scheme 2.2**). Next, we incorporate different electron-donating groups at *o*- and *p*- positions of aniline. Pleasantly, we obtained the corresponding products (**4a'-b'**) in good

yields i.e. 72% and 79% respectively, when 4-CH_3 or 4-OMe groups were employed on the aniline (**Scheme 2.2**). However, in case of 2-methyl aniline and 3-methyl aniline, the desired products (**4c'** & **4d'**) were obtained in a slightly lower yield i.e., 66% and 61% respectively (**Scheme 2.2**). Afterwards, we have checked the reactivity of 4-methoxy aniline and 4-fluoro aniline in combination of 5-OMe and 5-CH_3 substituted 3-diazo oxindoles and interestingly we obtained 81% and 69% isolated yield for (**4e'**) & (**4f'**) respectively. Besides, N-methyl aniline was tested in the multicomponent reaction which provided the product in 58% isolated yield (**4g'**, **Scheme 2.2**), and it might be due to an increment in the steric hindrance at the nitrogen atom of aniline. We have also checked the effect of a hetero atom containing amino pyridine, gratifyingly, the reaction work well and provided the product (**4h'**) in 37 % isolated yield (**Scheme 2.2**). We have also tried *p*-amino acetophenone as amine substituent, unfortunately reaction didn't work with such electron withdrawing group (**4i'**, **Scheme 2.2**). Next, we have examined the reaction with aliphatic amines like vinyl amine and ethyl amine, unfortunately reaction didn't work with aliphatic amines (**4j'**&**4k'**, **Scheme 2.2**).

2.2.3: Plausible mechanism and DFT calculations

On the basis of literature precedence, a plausible catalytic cycle for the Pd(II)-catalyzed multicomponent reaction is proposed and investigated using DFT calculations.[14] The possible schematic mechanism and the corresponding computational potential energy surface have been presented in figure 2.2 and figure 2.3, respectively.

Initially, the Pd(II)-isocyanide complex (**I**) which is chosen as starting point, coupled with 3-diazo-1-methyl oxindole (**1a**) substrate to form a square planer complex (**II**) (**Figure 2.2**). After that subsequent dissociation of N_2 from **II** produces a Pd-carbene complex (**III**) via **TS-1** with the energy of activation $\Delta G^{\ddagger}$= 7.43 kcal/mol (**Figures 2.2 & 2.3**). Next, migratory insertion of isocyanide into the Pd-carbene complex takes place through a three-membered ring transition state (**TS2**) which possesses $\Delta G^{\ddagger}$= 25.49 kcal/mol energy with respect to complex **(I)** and forms intermediate (**IV**). Then, intermediate **(IV)** immediately releases the catalyst i.e. $Pd(OAc)_2$, and forms an unstable ketenimine intermediate (**V**) (**Figure 2.2**). This process is followed via **TS3** with 11.8 kcal/mol energy of activation (**Figure 2.3**). Next, nucleophilic attack by aniline (**3a**) to the central electrophilic carbon of ketenimine intermediate (**V**), followed by concerted proton transfer from aniline to the nitrogen of isocyanide unit takes place to form the final product (**4a**) via **TS4** (route 1, **Figure 2.3**) which exists at 31.12 kcal/mole higher than intermediate (**V).**

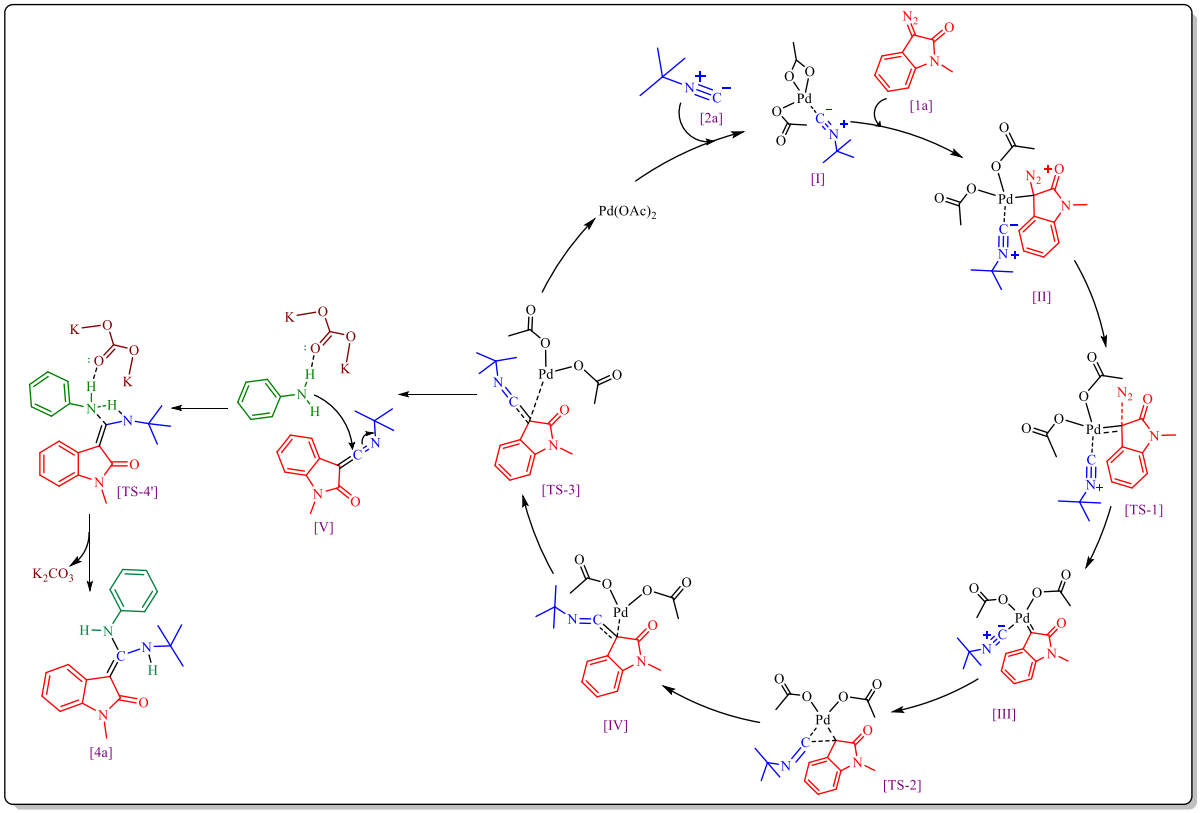

Figure 2.2: The plausible mechanism for Pd-catalyzed multicomponent reaction

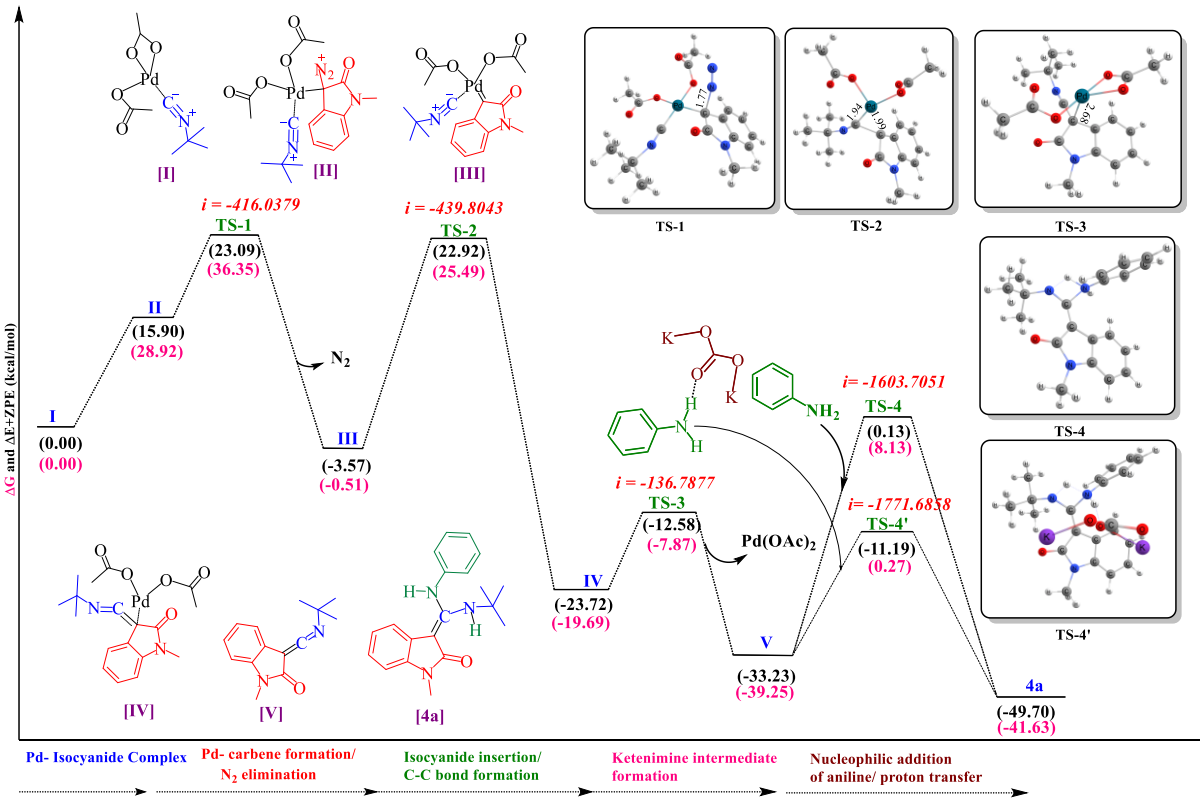

Figure 2.3: Computational investigation of the Pd-catalyzed multicomponent reaction

Besides, in the presence of base (route 2, **Figure 2.3**), nucleophilic attack by aniline (**3a**) to the central electrophilic carbon of ketenimine intermediate (**V**) followed by concerted proton transfer from aniline to the nitrogen of isocyanide unit is facilitated by K_2CO_3 and hence become more favorable since it exists at only 11.19 kcal/mole higher than intermediate (**V**) to form the final product (**4a**) via **TS4'.** This phenomenon suggests that the presence of base is enhancing the rate of the reaction which was also validated by experimental results (**Table 2.1, entry 19**). Also, it was observed that Pd(II) preserved its oxidation state during the whole catalytic process.

2.2.4: Application of the methodology

To show further application of our methodology, we set-up different experiments as depicted in scheme (2.3a-c)

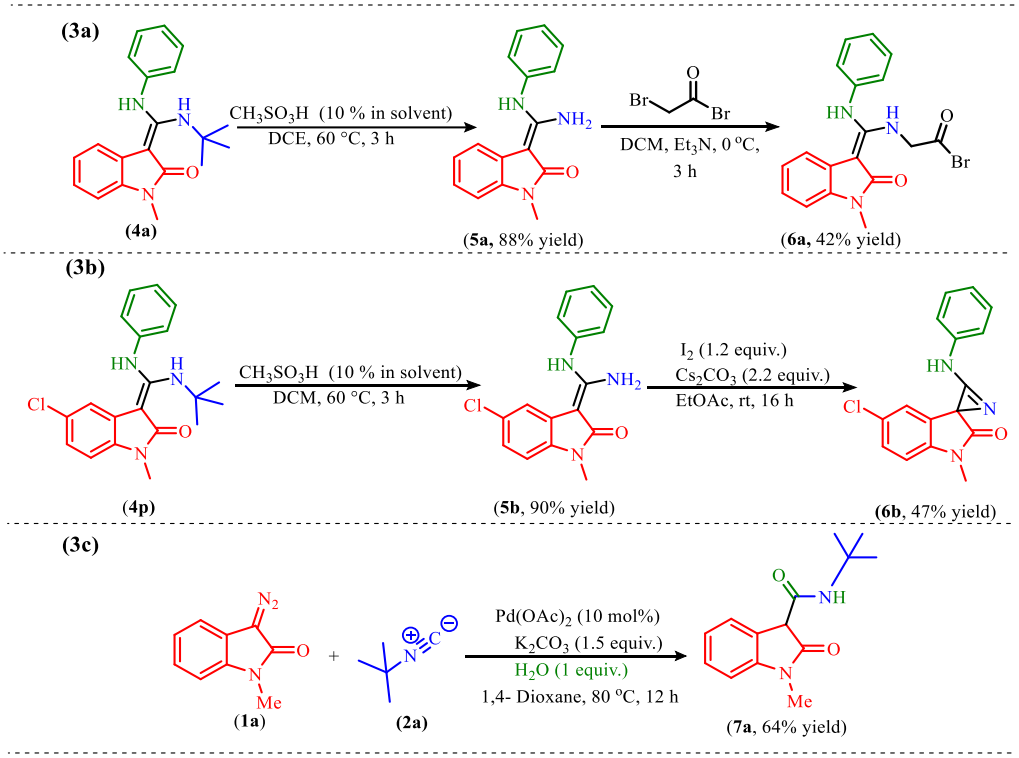

[a]**Reaction conditions: (3a)** (E)-3-((tert-butylamino)(phenylamino)methylene)-5-chloro-1-methylindolin-2-one (4m) (1 equiv.), CH_3SO_3H (10% in solvent), DCM (3 mL), 3 h, 60 °C, 3-(amino(phenyl)methylene)-1-methylindolin-2-one (5a) (1.0 equiv.), bromo acetyl bromide (1.5 equiv.), triethylamine (1.2 equiv.), dichloromethane (2 ml), 3h, 0 °C. **(3b)** (E)-3-(amino(phenylamino)methylene)-5-chloro-1-methylindolin-2-one (1.0 equiv.), iodine (1.2 equiv.), Cs_2CO_3 (2.2 equiv.), EtOAc (2 mL), 16 h, rt. and **(3c)** Reaction conditions: 3-diazo oxindoles (1) (1.0 equiv.), isocyanides (2) (1.2 equiv.), H_2O (1.0 equiv.), $Pd(OAc)_2$ (10 mol%), K_2CO_3 (1.5 equiv.), 1,4-dioxane (2 mL), 12 h, 80 °C.

Scheme 2.3: Application of the methodology

First, we performed *de-tertiary* butylation of 3-(aminoarylidene) oxindole derivative (**4a**) & (**4p**) under mild reaction conditions[15a] and obtained the corresponding products (**5a**) & (**5b**) in 88 & 90% yields respectively. Afterward, a reaction of (**5a**) was performed with bromoacetyl bromide to functionalize amino functionality and obtained the product (**6a**) in 42% isolated yield which proves that the presence of extra amino group is useful for adding more diversity in 3-alkylidene oxindole derivatives. Also, we have set up a reaction of 3-(amino(phenylamino)methylene)-1-methylindolin-2-one (**5b'**) with iodine and Cs_2CO_3 in ethyl acetate as a solvent at room temperature[15b] and got 1'-methyl-3-(phenylamino) spiro[azirine-2,3'-indolin]-2'-one derivative (**6b**) in 47% isolated yield. Moreover, we observed the formation of amide at C-3 position of oxindole during the mechanistic investigation. To investigate this observation, we performed a reaction in the presence of water rather than aniline, and delightedly, the reaction provided product (**7a**) in 64% yield which clearly indicates that the reaction goes through the formation of unstable ketenimine (**v**) intermediate as depicted in **figure 2.2**.

2.3: Experimental section:

2.3.1: General procedure to synthesize (*E*)-3-alkylidene oxindole (4a-4h')

In a sealed tube having a stirrer bar added 3-diazo-1-methyloxindole (1.0 equiv., 100 mg, 0.58 mmol), isocyanide (1.2 equiv., 57.6 mg, 0.70 mmol), aniline (1.0 equiv., 54 mg, 0.58 mmol), $Pd(OAc)_2$ (10 mol%, 13 mg) and K_2CO_3 (1.5 equiv., 120 mg, 0.87 mmol) in 2 mL anhydrous 1,4-dioxane as a solvent. The resulting reaction mixture was stirred at 80 °C in a preheated oil bath for 12 h. and the progress of the reaction was monitored using TLC. After completion of the reaction as indicated by TLC, volatiles were evaporated under reduced pressure and the obtained residue was purified by column chromatography using ethyl acetate in hexane as eluents affording the corresponding (*E*)-3-alkylidene oxindole derivatives (**4a-4h'**) in 31- 83% yields.

2.3.2: General method for the synthesis of 3-diazo-1-methylindolin-2-one(1a-1i)[20]

A mixture of isatin (1.0 equiv., 1g, 6.80 mmol) and *para*- tosylhydrazones (1.1 equiv., 1.39 gm, 7.48 mmol) were added in methanol (~ 20 mL) at 60 °C in a preheated oil bath and stirred the resulting mixture for 6 h which afforded a highly yellow colored solid of 3-(2-(p-tolyl) hydrazono) indolin-2-one (B) after filtration. The filtered solid of (B) and NaOH (2.0 equivalent, 2.4 mmol) were dissolved in a mixture of THF and water in a ratio of 1:2, and stirred the mixture at room temperature for 5 h. Upon complete conversion of the starting

materials, workup of the reaction using ethyl acetate and distilled water in a 2:1 ratio was done, and the volatiles were removed using a high vacuum. The orange-red solid of 3-diazo oxindoles (C) (83%, 900 mg, 5.65 mmol) was obtained which directly used for the next step without further purification. To the solution of NaH (60% in mineral oils, 1.05 equiv., 79 mg, 3.29 mmol) in 5 ml dry DMF under argon atmosphere at 0 ^{o}C, a solution of 3-diazo oxindoles (C) (500 mg, 3.14 mmol) in 7.5 ml of DMF was added dropwise and the resulted mixture was allowed to stir at 0 ^{o}C for 30 min. Then, alkyl halide (1.2 equiv., 235 µL, 3.76 mmol) was added slowly, and the resulting mixture was slowly brought to room temperature and allowed it to stir overnight. The reaction progress was monitored by TLC and upon complete consumption of the reactants, the reaction mixture was poured into cold water and extracted with ethyl acetate, then the volatiles were removed and, the resulting residue was purified by column chromatography to obtain the desired 3-diazo-1-methylindolin-2-one (1a) (50% yield, 270 mg, 1.56 mmol) in moderate to good yield. The purity of the synthesized compounds (**1a-1i**) was confirmed either 1H-NMR or HPLC chromatogram.

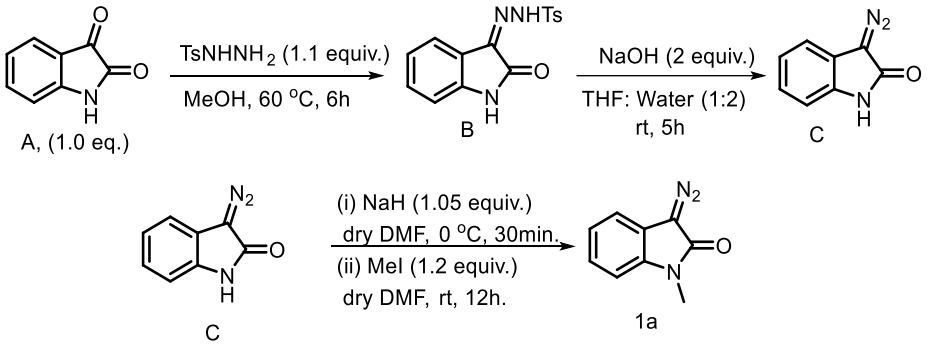

Scheme 2.4: Synthesis of 3-diazo-1-methylindolin-2-one.

2.3.3: General method for the synthesis of 3-diazo-1-phenylindolin-2-one (1j)[21]

A mixture of isatin (100 mg, 1.0 equiv., 0.68mmol), phenylboronic acid (207 mg, 2.5 equiv., 1.7 mmol), anhydrous $Cu(OAc)_2$ (247 mg, 2 equiv., 1.36 mmol), pyridine (137 µL, 2.5 equiv., 1.7 mmol) in 25 mL DCM was stirred at room temperature for 24 h at room temperature. The progress of the reaction was monitored by TLC. The reaction mixture was poured into water and extracted with DCM then volatiles were removed and the resulting residue was purified by column chromatography to obtain the desired 1-phenylindolin-2-one (1g) (bright orange, 70%, 106 mg, 0.48 mmol). After that 3-diazo-1-phenylindolin-2-one was synthesized as aforementioned procedure.

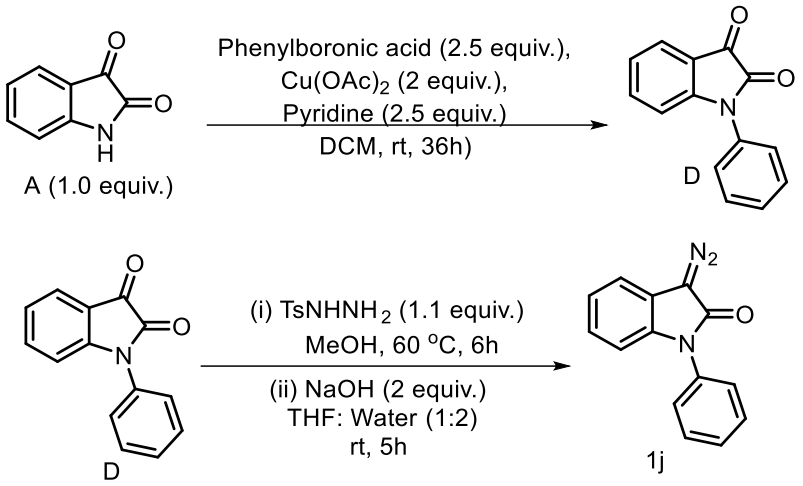

Scheme 2.5: Synthesis of 3-diazo-1-phenylindolin-2-one.

2.3.4: Computational details

All the calculations were performed using density functional theory (DFT) implemented in the Gaussian 16 software.[16] Most widely used B3LYP hybrid functional which uses Becke's three-parameter hybrid exchange-correlation functional along with the Lee, Yang, and Parr (LYP) correlation functional was used to calculate optimized geometries and frequencies.[17] The 6-31+G** and SDD basis sets were used for main group atoms such as C, H, N, O, and palladium, respectively. All the optimized structures have confirmed either minima (no imaginary frequencies) or transition states (one imaginary frequency) at the same level of theory. To inspect the connectivity of reactants and products with their respective transition states, intrinsic reaction coordinate (IRC) calculations have also been performed. The Minnesota continuum solvation model, SMD, was used to check the influence of 1,4- dioxane as solvent using the same method and basis set as earlier.[18] The 3D structures used in the calculation were prepared and analyzed via the Chemcraft visualization program.[19]

2.3.5: Characterization data

(*E*)-3-((tert-butylamino) (phenylamino)methylene)-1-methylindolin-2-one (4a)

Purification by column chromatography (mobile phase: EtOAc/Hexane, 1:8 v/v, stationary phase: Silica 60-120 mesh) afforded 4a; Solid, yield = 75% (140 mg, 0.44 mmol), ^{1}H NMR (400 MHz, $CDCl_3$): δ 9.34 (s, 1H), 7.21(t, *J* = 8.0 Hz, 2H), 6.97-6.92 (m, 4H), 6.83(d, *J* = 8.0 Hz, 1H), 6.66 (t, *J* = 7.2 Hz, 1H), 6.45(d, *J* = 6.4 Hz, 1H), 6.13(s, 1H), 3.37(s, 3H), 1.48(s, 9H) ppm. ^{13}C{^{1}H} NMR (100 MHz, $CDCl_3$): δ 169.8, 154.4, 140.2, 136.4, 129.7, 123.1, 122.6,

121.7, 120.4, 119.5, 118.1, 106.8, 88.5, 53.8, 31.4, 25.8 ppm. HRMS (ESI-TOF) m/z: $[M + H]^+$ calcd. for $C_{20}H_{23}N_3O$ 322.1875; found 322.1876.

(*E*)-1-methyl-3-((phenylamino)((2,4,4-trimethylpentan-2-yl)amino)methylene)indolin-2-one (4b)

Purification by column chromatography (mobile phase: EtOAc/Hexane, 1:9 v/v, stationary phase: Silica 60-120 mesh) afforded 4b; Solid, yield = 80% (143 mg, 0.47 mmol), ^{1}H NMR (400 MHz, $CDCl_3$): δ 9.53 (s, 1H), 7.21(t, *J* = 8.4 Hz, 2H), 6.96-6.91 (m, 4H), 6.83 (d, *J* = 7.6 Hz, 1H), 6.65 (t, *J* = 7.6 Hz, 7.2 Hz, 1H), 6.43 (d, *J* = 7.2 Hz, 1H), 6.12 (s, 1H), 3.38 (s, 3H), 1.75 (s, 2H), 1.53 (s, 6H), 1.05 (s, 9H) ppm. ^{13}C{^{1}H} NMR (100 MHz, $CDCl_3$): δ 169.7, 154.1, 140.0, 136.3, 129.7, 123.1, 122.5, 121.5, 120.3, 119.5, 117.9, 106.7, 88.1, 57.3, 55.6, 32.1, 31.8, 31.7, 25.9 ppm. HRMS (ESI-TOF) m/z: $[M + H]^+$ calcd. for $C_{24}H_{31}N_3O$ 378.2538; found 378.2502.

(*E*)-3-((cyclohexylamino)(phenylamino)methylene)-1-methylindolin-2-one (4c)

Purification by column chromatography (mobile phase: EtOAc/Hexane, 1:9 v/v, stationary phase: Silica 60-120 mesh) afforded 4c; Solid, yield = 74% (150 mg, 0.42 mmol) ^{1}H NMR (400 MHz, d^6 -DMSO): δ 9.44 (s, 1H), 8.83 (s, 1H), 7.19 (t, *J* = 8.4 Hz, 2H), 6.97 (d, *J* = 7.6 Hz, 2H), 6.89-6.79 (m, 3H), 6.61-6.57(m, 2H), 3.59-3.57 (m, 1H), 3.22 (s, 3H), 1.78-1.09 (m, 10H) ppm. ^{13}C{^{1}H} NMR (100 MHz, d^6 -DMSO): δ 169.1, 154.7, 141.9, 136.1, 129.8, 123.7, 122.1, 121.2, 120.2, 118.5, 107.2, 86.1, 51.2, 33.4, 25.9, 25.5, 24.8 ppm. HRMS (ESI-TOF) m/z: $[M + H]^+$ calcd. for $C_{22}H_{25}N_3O$ 348.2076; found 348.2043.

(*E*)-3-((tert-butylamino)(phenylamino)methylene)-5-methoxy-1-methylindolin-2-one (4d)

Purification by column chromatography (mobile phase: EtOAc/Hexane, 1:9 v/v, stationary phase: Silica 60-120 mesh) afforded 4d; Solid, yield = 78% (135 mg, 0.38 mmol), ^{1}H NMR (400 MHz, $CDCl_3$): δ 9.46 (s, 1H), 7.21 (t, *J* = 8.0 Hz, 2H), 6.96-6.93 (m, 3H), 6.83 (d, *J* = 8.4 Hz, 1H), 6.50 (dd, *J* = 8.4 Hz, 2 Hz, 1H), 6.22 (s,1H), 6.02 (s, 1H), 3.33 (s, 3H), 3.30 (s, 3H), 1.49 (s, 9H) ppm. ^{13}C{^{1}H} NMR (100 MHz, $CDCl_3$): δ 169.8, 154.4, 154.3, 140.0, 130.6, 129.8, 123.8, 122.6, 118.2, 108.5, 107.0, 105.4, 88.1, 55.6, 53.7, 31.4, 25.9 ppm. HRMS (ESI-TOF) m/z: $[M + H]^+$ calcd. for $C_{21}H_{25}N_3O_2$ 352.1980; found 352.1982.

(*E*)-5-methoxy-1-methyl-3-((phenylamino)((2,4,4-trimethylpentan-2-yl)amino)methylene)indolin-2-one (4e)

Purification by column chromatography (mobile phase: EtOAc/Hexane, 1:9 v/v, stationary phase: Silica 60-120 mesh) afforded 4e; Solid, yield = 75% (151 mg, 0.37 mmol), ^{1}H NMR (400 MHz, $CDCl_3$): δ 9.63 (s, 1H), 7.21 (t, *J* = 8.4 Hz, 2H), 6.97-6.93 (m, 3H), 6.70 (d, *J* = 8.4 Hz, 1H), 6.50 (dd, *J* = 8.4 Hz, 2.4 Hz, 1H), 6.17 (s, 1H), 6.02 (d, *J* = 2.4 Hz, 1H), 3.34 (s, 3H), 3.30 (s, 3H), 1.75 (s, 2H), 1.54 (s, 6H), 1.05 (s, 9H) ppm. ^{13}C{^{1}H} NMR (100 MHz, $CDCl_3$): δ 169.7, 154.4, 154.0, 139.9, 130.5, 129.8, 123.6, 122.6, 118.1, 108.4, 106.9, 105.4, 88.2, 57.2, 55.6, 32.0, 31.9, 31.7, 25.9 ppm. HRMS (ESI-TOF) m/z: $[M + H]^+$ calcd. $C_{25}H_{33}N_3O_2$ 408.2651; found 408.2669.

(*E*)-3-((cyclohexylamino)(phenylamino)methylene)-5-methoxy-1-methylindolin-2-one (4f)

Purification by column chromatography (mobile phase: EtOAc/Hexane, 1:9 v/v, stationary phase: Silica 60-120 mesh) afforded 4f; Solid, yield = 68% (126 mg, 0.33 mmol), ^{1}H NMR (400 MHz, d^6 -DMSO): δ 9.60 (s, 1H), 8.82 (s, 1H), 7.19 (t, *J* = 8.4 Hz, 2H), 6.95 (d, *J* = 7.6 Hz, 2H), 6.88 (t, *J* = 7.2 Hz, 1H), 6.71 (d, *J* = 8.4 Hz, 1H), 6.37 (dd, *J* = 8.0, 2.4 Hz, 1H), 6.09 (s, 1H), 3.69 -3.66 (m, 1H), 3.30 (s, 3H), 3.18 (s, 3H), 1.80-1.21 (m, 10H) ppm. ^{13}C{^{1}H} NMR (100 MHz, d^6 -DMSO): δ 169.3, 154.6, 154.2, 141.9, 130.4, 129.9, 124.3, 122.1, 118.6, 107.2, 105.0, 86.3, 55.4, 51.1, 33.5, 26.1, 25.5, 24.2 ppm. HRMS (ESI-TOF) m/z: $[M + H]^+$ calcd. for $C_{23}H_{27}N_3O_2$ 378.2137; found 378.2139.

(*E*)-3-((tert-butylamino)(phenylamino)methylene)-1,5-dimethylindolin-2-one (4g)

Purification by column chromatography (mobile phase: EtOAc/Hexane, 1:9 v/v, stationary phase: Silica 60-120 mesh) afforded 4g; Solid, yield = 79% (150 mg, 0.44 mmol), ^{1}H NMR (400 MHz, $CDCl_3$): δ 9.32 (s, 1H), 7.22(t, *J* = 8.0 Hz, 2H), 6.97-6.93 (m, 3H), 6.75-6.70 (m, 2H), 6.22 (s,1H), 6.14 (s, 1H), 3.34 (s, 3H), 2.01 (s, 3H), 1.48 (s, 9H) ppm. ^{13}C{^{1}H} NMR (100 MHz, $CDCl_3$): δ 169.9, 154.4, 140.3, 134.4, 129.6, 129.5, 123.1, 122.5, 122.1, 120.5, 118.3, 106.4, 88.3, 53.7, 31.4, 25.8, 21.4 ppm. HRMS (ESI-TOF) m/z: $[M + H]^+$ calcd. for $C_{21}H_{25}N_3O$ 336.2031; found 336.2035.

(*E*)-1,5-dimethyl-3-((phenylamino)((2,4,4-trimethylpentan-2-yl)amino)methylene)indolin-2-one (4h)

Purification by column chromatography (mobile phase: EtOAc/Hexane, 1:9 v/v, stationary phase: Silica 60-120 mesh) afforded 4h; White Solid, yield = 75% (166 mg, 0.42 mmol), ^{1}H NMR (400 MHz, $CDCl_3$): δ 9.52 (s, 1H), 7.22(t, *J* = 8.0 Hz, 2H), 6.97-6.92 (m, 3H), 6.71 (s, 1H), 6.19 (s, 1H), 6.11 (s, 1H), 3.35 (s, 3H), 2.00 (s, 3H), 1.75 (s, 2H), 1.53 (s, 6H), 1.05 (s, 9H) ppm. $^{13}C\{^{1}H\}$ NMR (100 MHz, $CDCl_3$): δ 169.8, 154.1, 140.1, 134.2, 129.6, 129.4, 123.1, 122.5, 121.8, 120.6, 118.2, 106.3, 87.9, 57.3, 55.6, 32.0, 31.8, 31.7, 25.9, 21.4 ppm. HRMS (ESI-TOF) m/z: $[M + H]^+$ calcd. for $C_{25}H_{33}N_3O$ 392.2702; found 392.2708.

(*E*)-3-((cyclohexylamino)(phenylamino)methylene)-1,5-dimethylindolin-2-one (4i)

Purification by column chromatography (mobile phase: EtOAc/Hexane, 1:9 v/v, stationary phase: Silica 60-120 mesh) afforded 4i; White Solid, yield = 76% (154 mg, 0.43 mmol), ^{1}H NMR (400 MHz, d^6 -DMSO): δ 9.44 (s, 1H), 8.81 (s, 1H), 7.21 (t, *J* = 8.0 Hz, 2H), 6.98 (d, *J* = 8.0 Hz, 2H), 6.81 (t, *J* = 7.2 Hz, 1H), 6.71 (d, *J* = 7.6 Hz, 1H), 6.62 (d, *J* = 8.0 Hz, 1H), 6.44 (s, 1H), 3.54 -3.52 (m, 1H), 3.19 (s, 3H), 1.99 (s, 3H), 1.77-1.20 (m, 10H) ppm. $^{13}C\{^{1}H\}$ NMR (100 MHz, d^6 -DMSO): δ 169.2, 154.7, 141.9, 132.1, 129.7, 129.2, 128.4, 123.8, 122.2, 121.7, 121.4, 119.5, 118.8, 117.9, 106.8, 86.0, 51.2, 33.3, 26.0, 25.5, 24.2, 21.7 ppm. HRMS (ESI-TOF) m/z: $[M + H]^+$ calcd. for $C_{23}H_{27}N_3O$ 362.2232; found 362.2245.

(*E*)-3-((tert-butylamino)(phenylamino)methylene)-6-methoxy-1-methylindolin-2-one (4j)

Purification by column chromatography (mobile phase: EtOAc/Hexane, 1:9 v/v, stationary phase: Silica 60-120 mesh) afforded 4j; Solid, yield = 73% (126 mg, 0.36 mmol), ^{1}H NMR (400 MHz, $CDCl_3$): 9.03(s, 1H), 7.21 (t, *J* = 8.0 Hz, 2H), 6.96-6.88 (m, 3H), 6.43 (d, *J* = 8.0 Hz, 1H), 6.31-6.22 (m, 2H), 6.03 (s, 1H), 3.73 (s, 3H), 3.33 (s, 3H), 1.46 (s, 9H) ppm. $^{13}C\{^{1}H\}$ NMR (100 MHz, $CDCl_3$): δ 170.3, 156.1, 153.1, 140.2, 137.9, 129.6, 122.2, 120.2, 117.8, 116.4, 105.4, 94.4, 55.6, 53.7, 31.5, 25.8 ppm. HRMS (ESI-TOF) m/z: $[M + H]^+$ calcd. for $C_{21}H_{26}N_3O_2$ 352.2025; found 352.2032.

(*E*)-3-((tert-butylamino)(phenylamino)methylene)-1-methyl-5-nitroindolin-2-one (4k)

Purification by column chromatography (mobile phase: EtOAc/Hexane, 1:9 v/v, stationary phase: Silica 60-120 mesh) afforded 4j; Solid, yield = 43% (74 mg, 0.14 mmol), ^{1}H NMR (400 MHz, $CDCl_3$): δ 9.54 (s, 1H), 7.82 (dd, *J* = 8.8, 2.4Hz, 1H), 7.23 (t, *J* = 8.8, 2H), 7.18 (s, 1H), 7.00 (t, *J* = 8.4, 3H), 6.78 (d, *J* = 8.4Hz, 1H), 6.38 (s, 1H), 3.40 (s, 3H), 1.55 (s, 9H)ppm. $^{13}C\{^{1}H\}$ NMR (100 MHz, $CDCl_3$): δ 170.1, 155.8, 141.7, 140.2, 139.0, 130.0, 124.2, 123.1,

119.6, 117.8, 114.5, 105.7, 85.3, 53.8, 31.2, 26.2 ppm. HRMS (ESI-TOF) m/z: $[M + H]^+$ calcd. for $C_{20}H_{23}N_4O_3$ 367.1770; found 367.1803.

(*E*)-1-methyl-5-nitro-3-((phenylamino)((2,4,4-trimethylpentan-2-yl)amino)methylene)indolin-2-one (4l)

Purification by column chromatography (mobile phase: EtOAc/Hexane, 1:9 v/v, stationary phase: Silica 60-120 mesh) afforded 4k; Solid, yield = 34% (68 mg, 0.16 mmol), ^{1}H NMR (400 MHz, $CDCl_3$): δ 9.63 (s, 1H), 7.83 (dd, *J* = 8.0, 2.0Hz, 1H), 7.26-7.22 (m, 2H), 7.17 (d, *J* = 2.0Hz, 1H), 7.02-6.98 (m, 3H), 6.79 (s, *J* = 8.8Hz, 1H), 6.36 (s, 1H), 3.40 (s, 3H), 1.79 (s, 2H), 1.60 (s, 6H), 1.07 (s, 9H) ppm. ^{13}C{^{1}H} NMR (100 MHz, $CDCl_3$): δ 170.0, 155.5, 141.7, 140.2, 138.9, 123.0, 124.2, 123.1, 119.5, 117.7, 114.6, 105.6, 85.1, 57.4, 55.2, 32.1, 31.6, 26.2 ppm. HRMS (ESI-TOF) m/z: $[M + H]^+$ calcd. for $C_{24}H_{31}N_4O_3$ 423.2351; found 423.2352.

(*E*)-3-((cyclohexylamino)(phenylamino)methylene)-1-methyl-5-nitroindolin-2-one (4m)

Purification by column chromatography (mobile phase: EtOAc/Hexane, 1:9 v/v, stationary phase: Silica 60-120 mesh) afforded 4l; Solid, yield = 31% (56 mg, 0.14 mmol), ^{1}H NMR (400 MHz, d^6-DMSO): δ 9.48 (d, *J* = 8.4Hz, 1H), 9.22 (s, 1H), 7.22 (dd, *J* = 8.4, 2.4 Hz, 1H), 7.28 (d, *J* = 2.0Hz, 1H), 7.22 (t, *J* = 7.2, 2H), 7.02 (t, *J* = 7.2, 3H), 6.94 (t, *J* = 7.2, 1H), 3.75- 3.68 (m, 1H), 3.30 (s, 3H), 1.83- 1.22 (m, 10H)ppm. ^{13}C{^{1}H} NMR (100 MHz, d^6-DMSO): δ 169.3, 157.2, 155.7,141.2, 140.9, 140.4, 129.9, 124.0, 123.4, 120.1, 117.3, 113.0, 106.7, 83.8, 51.3, 33.9, 33.2, 26.4, 25.8, 25.4, 25.0, 24.2 ppm. HRMS (ESI-TOF) m/z: $[M + H]^+$ calcd. for $C_{22}H_{24}N_4O_3$ 393.1927; found 393.1950.

(*E*)-3-((tert-butylamino)(phenylamino)methylene)-1-methyl-7-(trifluoromethyl)indolin-2-one (4n)

Purification by column chromatography (mobile phase: EtOAc/Hexane, 2:8 v/v, stationary phase: Silica 60-120 mesh) afforded 4n; solid, yield = 54% (87.2 mg, 0.22 mmol), ^{1}H NMR (400 MHz, $CDCl_3$): 9.64 (s, 1H), 7.23-7.17 (m, 3H), 6.97 (t, *J* = 7.6 Hz, 1H), 6.91 (d, *J* = 8.0 Hz, 2H), 6.69-6.62 (m, 2H), 6.20 (s, 1H), 3.57 (q, *J* = 2.4 Hz, 1H), 1.52 (s, 9H) ppm. ^{13}C{^{1}H} NMR (100 MHz, $CDCl_3$): δ 170.0, 155.1, 139.7, 132.9, 129.8, 125.9, 125.3, 123.2, 123.1, 122.3, 119.3, 119.25, 119.19, 119.12, 119.07, 116.3, 111.1, 110.8, 110.5, 110.2, 86.2, 53.6, 31.3, 28.3 ppm. HRMS (ESI-TOF) m/z: $[M + H]^+$ calcd. for $C_{21}H_{23}F_3N_3O$ 390.1793; found 390.1801.

(*E*)-3-((tert-butylamino)(phenylamino)methylene)-7-fluoro-1-methylindolin-2-one (4o)

Purification by column chromatography (mobile phase: EtOAc/Hexane, 2:8 v/v, stationary phase: Silica 60-120 mesh) afforded 4o; solid, yield = 51% (91 mg, 0.27 mmol), ^{1}H NMR (400 MHz, $CDCl_3$): 9.51(s, 1H), 7.21 (t, *J* = 8.0 Hz, 2H), 6.98-6.91(m, 3H), 6.64-6.59(m, 1H), 6.54-6.50 (m, 1H), 6.23-6.16 (m, 2H), 3.58 (d, *J* =2.4 Hz, 3H), 1.49(s, 9H) ppm. $^{13}C\{^{1}H\}$ NMR (100 MHz, $CDCl_3$): δ 169.4, 155.0, 149.0, 146.6, 139.9, 129.7, 126.2, 122.9, 120.3, 118.2, 115.2, 108.9, 108.7, 87.9, 53.8, 31.3, 28.33, 28.28 ppm. HRMS (ESI-TOF) m/z: $[M + H]^+$ calcd. for $C_{20}H_{22}FN_3O$ 340.1825; found 340.1834.

(*E*)-3-((tert-butylamino)(phenylamino)methylene)-5-chloro-1-methylindolin-2-one (4p)

Purification by column chromatography (mobile phase: EtOAc/Hexane, 1:9 v/v, stationary phase: Silica 60-120 mesh) afforded 4m; Solid, yield = 83% (140 mg, 0.40 mmol), ^{1}H NMR (400 MHz, $CDCl_3$): δ 9.49 (s, 1H), 7.24 (t, *J* = 8.0 Hz, 2H), 7.02-6.93 (m, 3H), 6.85 (dd, *J* = 8.4, 1.6 Hz, 1H), 6.66 (d, *J* = 8.4Hz, 1H), 6.29 (s, 1H), 6.21 (s, 1H), 3.33 (s, 3H), 1.50 ppm (s, 9H), $^{13}C\{^{1}H\}$ NMR (100 MHz, $CDCl_3$): δ 169.6, 155.0, 139.6, 134.5, 129.8, 125.7, 124.4, 123.3, 120.9, 119.2, 118.7, 107.3, 86.9, 53.7, 31.3, 25.9 ppm. HRMS (ESI-TOF) m/z: $[M + H]^+$ calcd. for $C_{20}H_{22}ClN_3O$ 356.1530; found 356.1560.

(*E*)-5-chloro-1-methyl-3-((phenylamino)((2,4,4-trimethylpentan-2-yl)amino)methylene)indolin-2-one (4q)

Purification by column chromatography (mobile phase: EtOAc/Hexane, 1:9 v/v, stationary phase: Silica 60-120 mesh) afforded 4n; Solid, yield = 76% (149 mg, 0.36 mmol), ^{1}H NMR (400 MHz, $CDCl_3$): δ 9.65 (s, 1H), 7.24 (t, *J* = 8.4, 2H), 7.02-6.93 (m, 3H), 6.84 (dd, *J* = 8.0, 2.0 Hz, 1H), 6.69 (d, *J* = 8.0Hz, 1H), 6.27 (s, 1H), 6.19 (s, 1H), 3.34 (s, 3H), 1.75 (s, 2H), 1.55 (s, 6H), 1.05 (s, 9H) ppm. $^{13}C\{^{1}H\}$ NMR (100 MHz, $CDCl_3$): δ 169.4, 154.7, 139.4, 134.7, 129.8, 124.9, 123.4, 123.3, 122.1, 118.7, 113.2, 107.7, 86.9, 57.5, 55.4, 32.0, 31.8, 31.6, 25.9 ppm. HRMS (ESI-TOF) m/z: $[M + H]^+$ calcd. for $C_{24}H_{31}ClN_3O$ 412.2155; found 412.2184.

(*E*)-5-chloro-3-((cyclohexylamino)(phenylamino)methylene)-1-methylindolin-2-one (4r)

Purification by column chromatography (mobile phase: EtOAc/Hexane, 1:9 v/v, stationary phase: Silica 60-120 mesh) afforded 4o; Solid, yield = 81% (150 mg, 0.38 mmol), ^{1}H NMR (400 MHz, d^6 -DMSO): δ 9.52 (d, *J* = 3.6 Hz, 1H), 8.97 (s, 1H), 7.23 (t, *J* = 8.0 Hz, 2H), 6.94 (t, *J* = 7.2, 1H), 6.83 (d, *J* = 8.4 Hz, 1H), 6.79 (dd, *J* = 8.4, 2.0 Hz, 1H), 3.64 -3.57 (m, 1H), 3.21 (s, 3H), 1.79-1.16 (m, 10H) ppm. $^{13}C\{^{1}H\}$ NMR (100 MHz, d^6 -DMSO): δ 169.0, 155.3,

141.4, 134.4, 129.9, 125.4, 124.5, 122.8, 120.1, 119.3, 117.8, 108.1, 85.0, 51.2, 33.3, 26.1, 25.5, 24.2 ppm. HRMS (ESI-TOF) m/z: $[M + H]^+$ calcd. for $C_{22}H_{24}ClN_3O$ 382.1686; found 382.1699.

(*E*)-5-bromo-3-((tert-butylamino)(phenylamino)methylene)-1-methylindolin-2-one (4s)

Purification by column chromatography (mobile phase: EtOAc/Hexane, 1:9 v/v, stationary phase: Silica 60-120 mesh) afforded 4p; Solid, yield = 50% (80 mg, 0.20 mmol), ^{1}H NMR (400 MHz, $CDCl_3$): δ 9.51 (s, 1H), 7.25 (t, *J* = 8.0 Hz, 2H), 7.04-6.94 (m, 4H), 6.66 (d, *J* = 8.4Hz, 1H), 6.41 (s, 1H), 6.18 (s, 1H), 3.34 (s, 3H), 1.51 ppm (s, 9H), ^{13}C{^{1}H} NMR (100 MHz, $CDCl_3$): δ 169.5, 155.0, 139.5, 134.8, 129.8, 124.8, 123.6, 123.4, 122.1, 118.8, 113.3, 107.8, 86.6, 53.7, 32.0, 31.3, 25.9 ppm. HRMS (ESI-TOF) m/z: $[M + H]^+$ calcd. for $C_{20}H_{23}BrN_3O$ 400.1025; found 400.1042.

(*E*)-5-bromo-1-methyl-3-((phenylamino)((2,4,4-trimethylpentan-2-yl)amino)methylene)indolin-2-one (4t)

Purification by column chromatography (mobile phase: EtOAc/Hexane, 1:9 v/v, stationary phase: Silica 60-120 mesh) afforded 4q; Solid, yield = 49% (90 mg, 0.20 mmol), ^{1}H NMR (400 MHz, $CDCl_3$): δ 9.65 (s, 1H), 7.25 (t, *J* = 7.6Hz, 2H), 7.04-6.93 (m, 4H), 6.66 (d, *J* = 8.0Hz, 1H), 6.40 (s, 1H), 6.18 (s, 1H), 3.34 (s, 3H), 1.76 (s, 2H), 1.55 (s, 6H), 1.05 (s, 9H) ppm. ^{13}C{^{1}H} NMR (100 MHz, $CDCl_3$): δ 169.4, 154.7, 139.35, 134.7, 129.8, 124.9, 123.4, 123.3, 122.1, 118.7, 113.2, 107.7, 86.3, 57.3, 55.4, 32.0, 31.8, 31.6, 25.9 ppm. HRMS (ESI-TOF) m/z: $[M + H]^+$ calcd. for $C_{24}H_{31}BrN_3O$ 457.1550; found 457.1556.

(*E*)-5-bromo-3-((cyclohexylamino)(phenylamino)methylene)-1-methylindolin-2-one (4u)

Purification by column chromatography (mobile phase: EtOAc/Hexane, 1:9 v/v, stationary phase: Silica 60-120 mesh) afforded 4r; Solid, yield = 47% (80 mg, 0.18 mmol), ^{1}H NMR (400 MHz, d^6-DMSO): δ 9.53 (s, 1H), 8.99 (s, 1H), 7.23 (t, *J* = 8.0 Hz, 2H), 7.00-0.90 (m, 4H), 6.77 (d, *J* = 8.4 Hz, 1H), 6.62 (s, 1H), 3.62 -3.60 (m, 1H), 3.20 (s, 3H), 1.77-1.18 (m, 10H) ppm. ^{13}C{^{1}H} NMR (100 MHz, d^6-DMSO): δ 168.8, 155.3, 141.4, 134.7, 129.9, 129.2, 125.8, 122.9, 122.8, 120.6, 119.3, 118.0, 112.6, 108.7, 84.8, 51.2, 33.3, 26.0, 25.5, 24.2 ppm. HRMS (ESI-TOF) m/z: $[M + H]^+$ calcd. for $C_{22}H_{25}BrN_3O$ 426.1181; found 426.1189.

(*E*)-3-((tert-butylamino)(phenylamino)methylene)-1-phenylindolin-2-one (4v)

Purification by column chromatography (mobile phase: EtOAc/Hexane, 1:9 v/v, stationary phase: Silica 60-120 mesh) afforded 4s; Solid, yield = 43% (70 mg, 0.18 mmol), ^{1}H NMR (400 MHz, $CDCl_3$): δ 9.53 (s, 1H), 7.53-7.48 (m, 4H), 7.39-7.35 (m, 1H), 7.28-7.24 (m, 2H), 7.00

(t, *J* = 7.6, 3H), 6.88-6.83 (m, 2H), 6.71 (t, *J* = 5.6 Hz, 1H), 6.53 (d, *J* = 5.6 Hz 1H), 6.21 (s, 1H), 1.49 (s, 9H). $^{13}C\{^{1}H\}$ NMR (100 MHz, $CDCl_3$): δ 169.4, 155.0, 140.1, 136.1, 135.7, 129.8, 129.5, 127.4, 127.4, 123.3, 122.8, 121.6, 120.9, 119.5, 118.2, 108.2, 87.9, 53.8, 31.4 ppm. HRMS (ESI-TOF) m/z: $[M + H]^+$ calcd. for $C_{25}H_{25}N_3O$ 384.2075; found 384.2052.

(*E*)-3-((tert-butylamino)((4-chlorophenyl)amino)methylene)-1-methylindolin-2-one (4w)

Purification by column chromatography (mobile phase: EtOAc/Hexane, 1:9 v/v, stationary phase: Silica 60-120 mesh) afforded 4t; Solid, yield = 73% (152 mg, 0.43 mmol), ^{1}H NMR (400 MHz, $CDCl_3$): δ 9.29 (s, 1H), 7.16 (d, *J* = 8.8 Hz, 2H), 6.96 (t, *J* = 7.6, 1H), 6.84 (d, *J* = 7.6, 3H), 6.70 (t, *J* = 7.6, 1H), 6.46 (d, *J* = 7.2 Hz, 1H), 6.06 (s, 1H), 3.36 (s, 3H), 1.46 (s, 9H) ppm. $^{13}C\{^{1}H\}$ NMR (100 MHz, $CDCl_3$): δ 169.8, 154.4, 140.2, 136.4, 129.7, 123.1, 122.6, 121.7, 120.4, 119.5, 118.1, 106.8, 88.5, 53.8, 31.4, 25.8 ppm. HRMS (ESI-TOF) m/z: $[M + H]^+$ calcd. for $C_{20}H_{22}ClN_3O$ 356.1530; found 356.1542.

(*E*)-3-(((4-bromophenyl)amino)(tert-butylamino)methylene)-1-methylindolin-2-one (4x)

Purification by column chromatography (mobile phase: EtOAc/Hexane, 1:9 v/v, stationary phase: Silica 60-120 mesh) afforded 4u; Solid, yield = 70% (159 mg, 0.41 mmol), ^{1}H NMR (400 MHz, $CDCl_3$): δ 9.29 (s, 1H), 7.31 (d, *J* = 8.8, 2H), 6.97 (t, *J* = 7.2 Hz, 1H), 6.85-6.78 (m, 3H), 6.72 (t, *J* = 7.2 Hz, 1H), 6.47 (d, *J* = 6.8 Hz, 1H), 6.07 (s, 1H), 3.36 (s, 3H), 1.46 (s, 9H) ppm. $^{13}C\{^{1}H\}$ NMR (100 MHz, $CDCl_3$): δ 169.7, 153.7, 139.5, 136.7, 132.6, 122.7, 122.1, 120.7, 119.5, 119.2, 114.7, 107.0, 89.1, 53.8, 31.4, 25.8 ppm. HRMS (ESI-TOF) m/z: $[M + H]^+$ calcd. for $C_{20}H_{23}BrN_3O$ 401.0926; found 401.0928.

(*E*)-3-((tert-butylamino)((4-fluorophenyl)amino)methylene)-1-methylindolin-2-one (4y)

Purification by column chromatography (mobile phase: EtOAc/Hexane, 1:9 v/v, stationary phase: Silica 60-120 mesh) afforded 4v; Solid, yield = 58% (114 mg, 0.33 mmol), ^{1}H NMR (400 MHz, $CDCl_3$): δ 9.32 (s, 1H), 6.96-6.90 (m, 5H), 6.84 (d, *J* = 7.6 Hz, 1H), 6.69 (s, 1H), 6.45 (s, 1H), 6.17 (s, 1H), 3.36 (s, 3H), 1.46 (s, 9H) ppm. $^{13}C\{^{1}H\}$ NMR (100 MHz, $CDCl_3$): δ 169.7, 159.6, 154.7, 136.1, 122.9, 121.8, 120.5, 119.6, 119.2, 116.5, 116.2, 106.9, 88.0, 53.8, 31.3, 25.8 ppm. HRMS (ESI-TOF) m/z: $[M + H]^+$ calcd. for $C_{20}H_{22}FN_3O$ 340.1825; found 340.1845.

(*E*)-3-((tert-butylamino)(p-tolylamino)methylene)-1-methylindolin-2-one (4a')

Purification by column chromatography (mobile phase: EtOAc/Hexane, 1:9 v/v, stationary phase: Silica 60-120 mesh) afforded 4x; Solid, yield = 72% (140 mg, 0.42 mmol), ^{1}H NMR

(400 MHz, $CDCl_3$): δ 9.34 (s, 1H), 7.01 (d, 2H), 6.94 (t, *J* = 7.6, 1H), 6.84 (t, 3H), 6.68 (t, *J* = 8.4, 1H), 6.49 (s, 1H), 6.12 (s, 1H), 3.37 (s, 3H), 2.25 (s, 3H), 1.47 (s, 9H) ppm. $^{13}C\{^1H\}$ NMR (100 MHz, $CDCl_3$): δ 169.8, 154.9, 137.7, 136.3, 132.2, 130.2, 123.3, 121.5, 120.4, 119.4, 118.3, 106.7, 88.0, 53.7, 31.4, 25.8, 20.8 ppm. HRMS (ESI-TOF) m/z: $[M + H]^+$ calcd. for $C_{21}H_{25}N_3O$ 336.2076; found 336.2082.

(*E*)-3-((tert-butylamino)((4-methoxyphenyl)amino)methylene)-1-methylindolin-2-one (4b')

Purification by column chromatography (mobile phase: EtOAc/Hexane, 1:9 v/v, stationary phase: Silica 60-120 mesh) afforded 4y; Solid, yield = 79% (162 mg, 0. 49mmol), ^1H NMR (400 MHz, $CDCl_3$): δ 9.34 (s, 1H), 6.93 (m, 3H), 6.83 (d, *J* = 8.0 Hz, 1H), 6.76 (m, 2H), 6.68 (s, 1H), 6.47 (s, 1H), 6.08 (s, 1H), 3.72 (s, 3H), 3.37 (s, 3H), 1.47 (s, 9H) ppm. $^{13}C\{^1H\}$ NMR (100 MHz, $CDCl_3$): δ 169.7, 155.5, 136.2, 133.5, 123.2, 121.3, 120.4, 120.1, 119.1, 114.9, 106.7, 87.2, 55.5, 31.3, 25.8 ppm. HRMS (ESI-TOF) m/z: $[M + H]^+$ calcd. for $C_{21}H_{25}N_3O_2$ 352.2034; found 352.2025.

(*E*)-3-((tert-butylamino)(o-tolylamino)methylene)-1-methylindolin-2-one (4c')

Purification by column chromatography (mobile phase: EtOAc/Hexane, 1:9 v/v, stationary phase: Silica 60-120 mesh) afforded 4z; Solid, yield = 66% (128 mg, 0.38 mmol), ^1H NMR (400 MHz, $CDCl_3$): δ 9.48 (s, 1H), 7.24 (s, 1H), 6.90 (m, 5H), 6.63 (s, 1H), 6.21 (s, 1H), 5.89 (s, 1H), 3.37 (s, 3H), 3.41 (s, 3H), 1.48 (s, 9H) ppm. $^{13}C\{^1H\}$ NMR (100 MHz, $CDCl_3$): δ 169.7, 155.2, 138.5, 136.4, 130.8, 127.4, 125.9, 123.1, 122.8, 121.5, 120.4, 118.9, 118.2, 106.8, 87.9, 53.5, 31.5, 25.8, 18.1 ppm. HRMS (ESI-TOF) m/z: $[M + H]^+$ calcd. for $C_{21}H_{25}N_3O$ 336.2076; found 336.2081.

(E)-3-((tert-butylamino)(m-tolylamino)methylene)-1-methylindolin-2-one (4d')

Purification by column chromatography (mobile phase: EtOAc/Hexane, 2:8 v/v, stationary phase: Silica 60-120 mesh) afforded 4d'; solid, yield = 61% (119 mg, 0.35 mmol), ^1H NMR (400 MHz, $CDCl_3$): 9.33(s, 1H), 7.06 (t, *J* = 8.0 Hz, 1H), 6.94 (t, *J* = 7.6 Hz, 1H), 6.81 (d, *J* = 7.6 Hz, 1H), 6.77-6.67 (m, 4H), 6.49 (s, 1H), 6.09 (s, 1H), 3.37 (s, 3H), 2.24 (s, 3H), 1.49 (s, 9H) ppm. $^{13}C\{^1H\}$ NMR (100 MHz, $CDCl_3$): δ 169.7, 154.6, 140.2, 139.5, 136.4, 129.4, 123.5, 123.2, 121.6, 120.4, 119.5, 118.8, 115.2, 106.8, 88.5, 31.4, 25.8, 21.6 ppm. HRMS (ESI-TOF) m/z: $[M + H]^+$ calcd. for $C_{21}H_{25}N_3O$ 336.2076; found 336.2086.

(E)-3-((tert-butylamino)((4-methoxyphenyl)amino)methylene)-5-methoxy-1-methylindolin-2-one (4e')

Purification by column chromatography (mobile phase: EtOAc/Hexane, 1:9 v/v, stationary phase: Silica 60-120 mesh) afforded 4e'; Solid, yield = 81% (152 mg, 0.40 mmol),^{1}H NMR (400 MHz, $CDCl_3$): 9.45 (s, 1H), 6.94 (d, *J* = 8.4 Hz, 2H), 6.77 (d, *J* = 8.8 Hz, 2H), 6.70 (d, *J* = 8.4 Hz, 1H), 6.49 (d, *J* = 6.4 Hz, 2H), 6.07 (s, 1H), 3.71 (s, 3H), 3.38 (s, 3H), 3.33 (s, 3H), 1.48 (s, 9H) ppm. $^{13}C\{^{1}H\}$ NMR (100 MHz, $CDCl_3$): δ 169.8, 155.6, 155.3, 154.4, 133.4, 130.5, 123.8, 120.3, 115.0, 108.1, 106.8, 105.2, 87.2, 55.7,55.6, 31.4, 25.8 ppm. HRMS (ESI-TOF) m/z: $[M + H]^+$ calcd. for $C_{22}H_{28}N_3O_3$ 382.2130; found 382.2138.

(E)-3-((tert-butylamino)((4-fluorophenyl)amino)methylene)-1,5-dimethylindolin-2-one (4f')

Purification by column chromatography (mobile phase: EtOAc/Hexane, 2:8 v/v, stationary phase: Silica 60-120 mesh) afforded PS-442; solid, yield = 69% (130 mg, 0.37 mmol), ^{1}H NMR (400 MHz, $CDCl_3$): 9.31 (s, 1H), 6.92 (d, *J* = 6.4 Hz, 4H), 6.76-6.70 (m, 2H), 6.22 (s, 1H), 6.07 (s, 1H), 3.71 (s, 3H), 3.33 (s, 3H), 2.04 (s, 1H), 1.47 (s, 9H) ppm. $^{13}C\{^{1}H\}$ NMR (100 MHz, $CDCl_3$): 169.8, 154.6, 136.4, 134.4, 129.6, 123.0, 122.3, 120.2, 119.9, 116.4, 116.1, 106.5, 87.7, 53.7, 31.3, 25.8, 21.4, δ HRMS (ESI-TOF) m/z: $[M + H]^+$ calcd. for $C_{21}H_{25}FN_3O$ 354.1982; found 354.1971.

(*E*)-3-((tert-butylamino)(methyl(phenyl)amino)methylene)-1-methylindolin-2-one (4g')

Purification by column chromatography (mobile phase: EtOAc/Hexane, 1:9 v/v, stationary phase: Silica 60-120 mesh) afforded 4a'; Solid, yield = 58% (114 mg, 0.34 mmol), ^{1}H NMR (400 MHz, $CDCl_3$): δ 9.59 (s, 1H), 7.36 (s, 1H), 7.11 (s, 1H), 7.00 (td, *J* = 7.6, 1.2 Hz, 1H), 6.86-6.82 (m, 4H), 6.79 (td, *J* = 8.0, 1.2 Hz, 1H), 6.69 (d, *J* = 8 Hz, 1H), 3.38 (s, 3H), 3.39 (s, 3H), 1.31 (s, 9H) ppm. $^{13}C\{^{1}H\}$ NMR (100 MHz, $CDCl_3$): δ 170.0, 158.9, 145.9, 137.0, 129.4, 122.8, 122.7, 121.1, 119.6, 118.6, 116.3, 112.2, 107.3, 93.8, 54.8, 38.3, 31.1, 25.9 ppm. HRMS (ESI-TOF) m/z: $[M + H]^+$ calcd. for $C_{21}H_{25}N_3O$ 336.2076; found 336.2102.

(*E*)-3-((tert-butylamino)(pyridin-2-ylamino)methylene)-1-methylindolin-2-one (4h')

Purification by column chromatography (mobile phase: EtOAc/Hexane, 1:9 v/v, stationary phase: Silica 60-120 mesh) afforded 4b'; Solid, yield = 37% (71 mg, 0.22mmol), ^{1}H NMR (400 MHz, $CDCl_3$): δ 9.35 (s, 1H), 8.28 (d, *J* = 4.4 Hz, 1H), 7.38 (td, *J* = 8.4, 1.6 Hz, 1H), 6.97 (t, *J* = 8.0, 1H), 6.86-6.82(m, 3H), 6.71 (t, *J* = 5.6 Hz, 1H), 6.62 (d, *J* = 8.0, 1H), 6.51 (d, *J* = 7.2 Hz, 1H), 3.37 (s, 3H), 1.48 (s, 9H) ppm. $^{13}C\{^{1}H\}$ NMR (100 MHz, $CDCl_3$): δ 169.6, 153.1, 152.5, 148.5, 138.6, 136.9, 122.9, 122.3, 120.7, 119.5, 117.2, 110.2, 107.0, 90.5, 53.8, 31.2, 25.8 ppm. HRMS (ESI-TOF) m/z: $[M + H]^+$ calcd. for $C_{19}H_{23}N_4O$ 323.1872; found 323.1887.

(E)-3-(amino(phenylamino)methylene)-1-methylindolin-2-one (5a)

Purification by work-up (EtOAc:H_2O, 1:2 v/v) afforded 5a; Solid, yield = 88% (76 mg, 0.29mmol), ^{1}H NMR (400 MHz, $CDCl_3$): δ 11.53 (s, 1H), 7.42 (t, *J* = 7.6 Hz, 2H), 7.27 (d, *J* = 7.6 Hz, 3H), 7.16-7.13 (m, 1H), 7.08-7.00 (m, 2H), 6.95 (d, *J* = 7.2 Hz, 1H), 5.27 (s, 2H), 3.39 (s, 3H) ppm. ^{13}C{^{1}H} NMR (100 MHz, $CDCl_3$): δ 167.4, 154.2, 134.9, 129.0, 125.5, 123.8, 122.9, 119.8, 119.5, 114.3, 106.4, 79.4, 24.7 ppm. HRMS (ESI-TOF) m/z: $[M + H]^+$ calcd. for $C_{16}H_{16}N_3O$ 266.1293; found 266.1304.

(E)-3-(amino(phenylamino)methylene)-5-chloro-1-methylindolin-2-one (5b)

Purification by work-up (EtOAc: H_2O, 1:2 v/v) afforded 5b; Solid, yield = 91% (77 mg, 0.26mmol) ^{1}H NMR (400 MHz, $CDCl_3$): δ 7.46 (dt, *J* = 8.4, 2.0 Hz, 2H), 7.33-7.30 (m, 3H), 7.10 (s, 1H), 6.95 (dd, *J* = 8.4, 2.0 Hz, 1H), 6.85 (d, *J* = 8.4 Hz, 1H), 3.37 (s, 3H), 2.65 (s, 1H) ppm. ^{13}C{^{1}H} NMR (100 MHz, $CDCl_3$): 169.9, 167.2, 154.6, 134.2, 129.2, 126.1, 124.8, 124.2, 124.1, 119.4, 114.2, 107.1, 76.2, 24.8 ppm. HRMS (ESI-TOF) m/z: $[M + H]^+$ calcd. for $C_{16}H_{15}ClN_3O$ 300.0904; found 300.0922.

(*E*)-((1-methyl-2-oxoindolin-3-ylidene)(phenylamino)methyl)glycinoyl bromide (6a)

Purification by column chromatography (mobile phase: EtOAc/Hexane, 2:8 v/v, stationary phase: Silica 60-120 mesh) Solid, yield = 42% (61 mg, 0.16mmol) ^{1}H NMR (400 MHz, *d*^{6} -DMSO): δ 7.67 (d, *J* = 7.2 Hz, 1H), 7.52-7.48 (m, 2H), 7.44-7.37 (m, 2H), 7.30-7.27 (m, 2H), 7.21 (s, 1H), 7.14-7.10 (m, 1H), 7.09 (s, 1H), 6.96 (s, 1H), 5.72 (s, 2H), 3.17 (s, 3H) ppm. ^{13}C{^{1}H} NMR (100 MHz, DMSO- *d*$_6$): δ 174.8, 173.6, 173.4, 145.2, 132.6, 130.3, 129.7, 129.4, 127.5, 124.8, 123.6, 109.8, 57.1, 55.5, 27.3. HRMS (ESI-TOF) m/z: $[M + H]^+$ calcd. for $C_{18}H_{17}BrN_3O_2$ 385.0426; found 385.0413

5'-chloro-1'-methyl-3-(phenylamino)spiro[azirine-2,3'-indolin]-2'-one (6b)

Purification by column chromatography (mobile phase: EtOAc/Hexane, 3:7 v/v, stationary phase: Silica 60-120 mesh) Solid, yield = 47% (46 mg, 0.16mmol), ^{1}H NMR (400 MHz, $CDCl_3$): δ 7.74 (s, 1H), 7.55 (d, *J* = 2.4 Hz, 1H), 7.27-7.25 (m, 3H), 7.03 (t, *J* = 7.6 Hz, 1H), 6.97-6.95 (m, 2H), 6.67 (d, *J* = 8.4 Hz, 1H), 3.18 (s, 3H) ppm. ^{13}C{^{1}H} NMR (100 MHz, $CDCl_3$): δ 171.8, 151.5, 147.5, 143.4, 130.4, 129.6, 129.1, 126.6, 124.5, 123.4, 120.9, 109.8, 62.9, 26.7. HRMS (ESI-TOF) m/z: $[M + H]^+$ calcd. for $C_{16}H_{13}ClN_3O$ 280.0669; found 280.0657.

N-(tert-butyl)-1-methyl-2-oxoindoline-3-carboxamide (7a)

Purification by column chromatography (mobile phase: EtOAc/Hexane, 2:8 v/v, stationary phase: Silica 60-120 mesh) Solid, yield = 64% (91 mg, 0.37 mmol), ^{1}H NMR (400 MHz, $CDCl_3$): δ 7.73 (d, *J* = 7.2 Hz, 1H), 7.46 (s, 1H), 7.31 (t, *J* = 6.8 Hz, 1H), 7.13 (t, *J* = 7.6 Hz, 1H), 6.83 (d, *J* = 7.6 Hz, 1H), 4.16 (s, 1H), 3.22 (s, 3H), 1.37 (s, 9H) ppm. $^{13}C\{^{1}H\}$ NMR (100 MHz, $CDCl_3$): δ 173.7, 162.6, 143.4, 128.5, 127.1, 123.7, 123.3, 108.3, 51.6, 51.0, 28.8, 26.6. HRMS (ESI-TOF) m/z: $[M + H]^+$ calcd. for $C_{14}H_{18}N_2O_2$ 247.1447; found 247.1464.

2.4: Conclusion

In summary, a Pd-catalyzed multicomponent reaction using 3-diazo oxindole as a carbene precursor along with isocyanide and aniline to provide clinically relevant (*E*)-3-al oxindoles has been reported. This simple protocol was found compatible with various electron-rich, and electron-deficient groups containing 3-diazo oxindole, aniline, and isocyanides which in turn provided (*E*)-3-alkylidene oxindole derivatives in moderate to good yields. Also, (*E*)-3-alkylidene oxindole derivatives containing two amine-substituents were synthesized for the first time. Next, DFT calculations were used to investigate the plausible route that suggested the formation of Pd(II)-carbene complex which undergoes migratory insertion into isocyanide to produce ketenimine intermediate, followed by nucleophilic addition of aniline to provide (*E*)-3-alkylidene oxindole. The nucleophilic addition of aniline was considered to be a rate-determining step as it exists at the highest energy barrier.

2.5: References

1. (a) Varun; Sonam; Kakkar, R. Isatin and Its Derivatives: A Survey of Recent Syntheses, Reactions, and Applications. *Med. Chem. Commun*. **2019**, *10*, 351–368. (b) Trost, B. M.; Brennan, M. K. Asymmetric Syntheses of Oxindole and Indole Spirocyclic Alkaloid Natural Products. *Synthesis*. **2009**, *18*, 3003–3025. (c) Dhokne, P.; Sakla, A. P.; Shankaraiah, N. Structural Insights of Oxindole Based Kinase Inhibitors as Anticancer Agents: Recent Advances. *Eur. J. Med. Chem*. **2021**, *216*, 113334.
2. (a) Wan, Y.; Li, Y.; Yan, C.; Yan, M.; Tang, Z. Indole: A Privileged Scaffold for the Design of Anti-Cancer Agents. *Eur. J. Med. Chem*. **2019,** *183*, 111691. (b) Dhuguru, J.; Skouta, R. Role of Indole Scaffolds as Pharmacophores in the Development of Anti-Lung Cancer Agents. *Molecules*. MDPI AG **2020**, *25*, 1615. (c) Yu, B.; Yu, D. Q.; Liu, H. M. Spirooxindoles: Promising Scaffolds for Anticancer Agents. *Eur. J. Med. Chem*. **2015**, *97*, 673–698. (d) Badillo, J. J. Enantioselective Synthesis of Substituted Oxindoles and Spirooxindoles with Applications in Drug Discovery. *Curr. Opin. Drug. Discov. Devel*. **2010**, *13*, 758–776. (e) Khetmalis, Y. M.; Shivani, M.; Murugesan, S.; Chandra Sekhar, K.

V. G. Oxindole and Its Derivatives: A Review on Recent Progress in Biological Activities. *Biomed. Pharmacother*. **2021**. (f) Sakla, A. P.; Kansal, P.; Shankaraiah, N. Syntheses and Applications of Spirocyclopropyl Oxindoles: A Decade Review. *Eur. J. Org. Chem.* **2021**, 2021, 757–772. g) Kundu, A.; Pathak, S.; Pramanik, A. Synthesis and Fluorescence Properties of Isatin-Based Spiro Compounds: Switch off Chemosensing of Copper(II) Ions. *Asian. J. Org. Chem.* **2013**, *2*, 869–876. (h) Ansari, K. R.; Quraishi, M. A.; Singh, A. Isatin Derivatives as a Non-Toxic Corrosion Inhibitor for Mild Steel in 20% H_2SO_4. *Corros. Sci.* **2015**, *95*, 62–70.

3. (a) Hassan, A. S.; Moustafa, G. O.; Awad, H. M.; Nossier, E. S.; Mady, M. F. Design, Synthesis, Anticancer Evaluation, Enzymatic Assays, and a Molecular Modeling Study of Novel Pyrazole-Indole Hybrids. *ACS Omega.* **2021**, *6*, 12361–12374. (b) Dalpozzo, R. Catalytic Asymmetric Synthesis of Hetero-Substituted Oxindoles. *Org. Chem. Front*. **2017**, *4*, 2063–2078. (c) Fu, W.; Zhou, Y.; Song, Q. Copper/Diboron-Mediated Intramolecular Oxygenation and Allylation/Benzylation of Nitroalkynes for the Synthesis of C2-Quaternary Indolin-3-Ones. *Chem. Asian. J.* **2018**, *13*, 2511–2515. (d) Prakash, C. R.; Raja, S.; Saravanan, G. Design and Synthesis of 4-(1-(4-Chlorobenzyl)-2,3-Dioxoindolin-5-Yl)-1-(4- Substituted/Unsubstituted Benzylidene) Semicarbazide: Novel Agents with Analgesic, Anti-Inflammatory and Ulcerogenic Properties. *Chinese Chemical Letters.* **2012**, *23*, 541–544. (e) Millemaggi, A.; Taylor, R. J. K. 3-Alkylidene-Oxindoles: Natural Products, Pharmaceuticals, and Recent Synthetic Advances in Tandem/Telescoped Approaches. *Eur. J. Org. Chem.* **2010**, *2010*, 4527–4547. (f) Cheng, D.; Ling, F.; Zheng, C.; Ma, C. Tuning of Copper-Catalyzed Multicomponent Reactions toward 3-Functionalized Oxindoles. *Org. Lett.* **2016**, *18*, 2435–2438. (g) Sharma, P. K.; Balwani, S.; Mathur, D.; Malhotra, S.; Singh, B. K.; Prasad, A. K.; Len, C.; van der Eycken, E. v.; Ghosh, B.; Richards, N. G. J.; Parmar, V. S. Synthesis and Anti-Inflammatory Activity Evaluation of Novel Triazolyl-Isatin Hybrids. *J. Enzyme. Inhib. Med. Chem.* **2016**, *31*, 1520–1526. (h) Chiyanzu, I.; Clarkson, C.; Smith, P. J.; Lehman, J.; Gut, J.; Rosenthal, P. J.; Chibale, K. Design, Synthesis and Anti-Plasmodial Evaluation in Vitro of New 4-Aminoquinoline Isatin Derivatives. *Bioorg. Med. Chem.* **2005**, *13*, 3249–3261. (i) Chiou, C. T.; Lee, W. C.; Liao, J. H.; Cheng, J. J.; Lin, L. C.; Chen, C. Y.; Song, J. S.; Wu, M. H.; Shia, K. S.; Li, W. T. Synthesis and Evaluation of 3-Ylideneoxindole Acetamides as Potent Anticancer Agents. *Eur. J. Med. Chem.* **2015**, *98*, 1–12.. (j) Andreani, A.; Burnelli, S.; Granaiola, M.; Leoni, A.; Locatelli, A.; Morigi, R.; Rambaldi, M.; Varoli, L.; Cremonini, M. A.; Placucci, G.; Cervellati, R.; Greco, E. New Isatin Derivatives with Antioxidant

Activity. *Eur. J. Med. Chem.* **2010**, *45*, 1374–1378. (k) Duan, S. W.; Lu, H. H.; Zhang, F. G.; Xuan, J.; Chen, J. R.; Xiao, W. J. Organocatalytic Conjugate Additions of Acetylacetone to 3-Ylideneoxindoles: A Direct Access to Highly Enantioenriched Oxindole Derivatives. *Synthesis.* **2011**, *12*, 1847–1852. (l) Zou, H.; Zhang, L.; Ouyang, J.; Giulianotti, M. A.; Yu, Y. Synthesis and Biological Evaluation of 2-Indolinone Derivatives as Potential Antitumor Agents. *Eur. J. Med. Chem.* **2011**, *46*, 5970–5977. (m) Pedras, M. S. C.; Chumala, P. B.; Suchy, M. Phytoalexins from Thlaspi Arvense, a Wild Crucifer Resistant to Virulent Leptosphaeria Maculans: Structures, Syntheses and Antifungal Activity. *Phytochemistry.* **2003**, *64*, 949–956.

4. (a) Christensen, J. G. A Preclinical Review of Sunitinib, a Multitargeted Receptor Tyrosine Kinase Inhibitor with Anti-Angiogenic and Antitumour Activities. In *Annals of Oncology*; Oxford University Press, **2007**; *18*, 3-10. (b) Hauf, S.; Cole, R. W.; LaTerra, S.; Zimmer, C.; Schnapp, G.; Walter, R.; Heckel, A.; van Meel, J.; Rieder, C. L.; Peters, J. M. The Small Molecule Hesperadin Reveals a Role for Aurora B in Correcting Kinetochore-Microtubule Attachment and in Maintaining the Spindle Assembly Checkpoint. *Journal of Cell Biology.* **2003**, *161*, 281–294. (c) Hilberg, F.; Roth, G. J.; Krssak, M.; Kautschitsch, S.; Sommergruber, W.; Tontsch-Grunt, U.; Garin-Chesa, P.; Bader, G.; Zoephel, A.; Quant, J.; Heckel, A.; Rettig, W. J. BIBF 1120: Triple Angiokinase Inhibitor with Sustained Receptor Blockade and Good Antitumor Efficacy. *Cancer Res.* **2008**, *68*, 4774–4782. (d) Roth, G. J.; Heckel, A.; Colbatzky, F.; Handschuh, S.; Kley, J.; Lehmann-Lintz, T.; Lotz, R.; Tontsch-Grunt, U.; Walter, R.; Hilberg, F. Design, Synthesis, and Evaluation of Indolinones as Triple Angiokinase Inhibitors and the Discovery of a Highly Specific 6-Methoxycarbonyl-Substituted Indolinone (BIBF 1120). *J. Med. Chem.* **2009**, *52*, 4466–4480.
5. (a) Girgis, A. S.; Panda, S. S.; Srour, A. M.; Abdelnaser, A.; Nasr, S.; Moatasim, Y.; Kutkat, O.; El Taweel, A.; Kandeil, A.; Mostafa, A.; Ali, M. A.; Fawzy, N. G.; Bekheit, M. S.; Shalaby, E. S. M.; Gigli, L.; Fayad, W.; Soliman, A. A. F. 3-Alkylidene-2-Oxindoles: Synthesis, Antiproliferative and Antiviral Properties against SARS-CoV-2. *Bioorg. Chem.* **2021**, *114*, 105131. (b) Wisastra, R.; Dekker, F. J. Inflammation, Cancer and Oxidative Lipoxygenase Activity Are Intimately Linked. *Cancers*. **2014**, 1500–1521.
6. (a) You, Y.; Quan, B. X.; Wang, Z. H.; Zhao, J. Q.; Yuan, W. C. Divergent Synthesis of Oxindole Derivatives: Via Controllable Reactions of Isatin-Derived Para-Quinone Methides with Sulfur Ylides. *Org. Biomol. Chem.* **2020**, *18*, 4560–4565. (b) Zhao, Y. L.; Cao, Z. Y.; Zeng, X. P.; Shi, J. M.; Yu, Y. H.; Zhou, J. Asymmetric Sequential Au(i)/Chiral

Tertiary Amine Catalysis: An Enone-Formation/Cyanosilylation Sequence to Synthesize Optically Active 3-Alkylideneoxindoles from Diazooxindoles. *Chem. Commun.* **2016**, *52*, 3943–3946. (c) Cantagrel, G.; de Carné-Carnavalet, B.; Meyer, C.; Cossy, J. Iron Trichloride-Promoted Cyclization of o-Alkynylaryl Lsocyanates: Synthesis of 3-(Chloromethylene)Oxindoles. *Org. Lett.* **2009**, *11*, 4262–4265. (d) Miura, T.; Toyoshima, T.; Takahashi, Y.; Murakami, M. Stereoselective Oxindole Synthesis by Palladium-Catalyzed Cyclization Reaction of 2-(Alkynyl)Aryl Isocyanates with Amides. *Org. Lett.* **2009**, *11*, 2141–2143. (e) Gurry, M.; Allart-Simon, I.; McArdle, P.; Gérard, S.; Sapi, J.; Aldabbagh, F. Photochemical Aryl Radical Cyclizations to Give (E)-3-Ylideneoxindoles. *Molecules.* **2014**, *19*, 15891–15899. (f) Yuan, W. K.; Cui, T.; Liu, W.; Wen, L. R.; Li, M. When Ethyl Isocyanoacetate Meets Isatins: A 1,3-Dipolar/Inverse 1,3-Dipolar/Olefination Reaction for Access to 3-Ylideneoxindoles. *Org. Lett.* **2018**, *20*, 1513–1516. (g) Kamalraja, J.; Babu, T. H.; Muralidharan, D.; Perumal, P. T. A Facile Method for the Synthesis of 3-(Aminomethylene)Oxindoles from Isatylidene Malononitriles and α-Azido Ketones. *Synlett.* **2012**, *23*, 1950–1954. (h) Parveen, N.; Sekar, G. Palladium Nanoparticle-Catalyzed Stereoselective Domino Synthesis of 3-Allylidene-2(3 H)-Oxindoles and 3-Allylidene-2(3 H)-Benzofuranones. *J. Org. Chem.* **2020**, *85*, 4682–4694. (i) Jiang, L.; Li, Y. G.; Li, H.; Yuan, M. W.; Chuan, Y. M.; Li, H. L.; Yuan, M. L. Catalyst-Free Synthesis of 3-Alkylideneoxindoles from Isatin-Derived Morita-Baylis-Hillman Carbonates. *J Chem Res.* **2017**, *41*, 160–164.

7. (a) Lin, W. J.; Shia, K. S.; Song, J. S.; Wu, M. H.; Li, W. T. Synthesis of (E)-Oxindolylidene Acetate Using Tandem Palladium-Catalyzed Heck and Alkoxycarbonylation Reactions. *Org Biomol Chem* **2015**, *14*, 220–228. (b) Song, S.; Li, Y.; Chen, D. Y.; Wang, X. P.; Liu, Y. L.; Chen, L. Y. Synthesis of α-Amidoacrylates Containing a 3-Ylideneoxindole Motif. *ChemistrySelect.* **2021**, *6*, 3187–3191. (c) Parveen, N.; Sekar, G. Palladium Nanoparticle-Catalyzed Stereoselective Domino Synthesis of 3-Allylidene-2(3 H)-Oxindoles and 3-Allylidene-2(3 H)-Benzofuranones. *Journal of Organic Chemistry* **2020**, *85*, 4682–4694. (d) Bisht, G. S.; Gnanaprakasam, B. Transition-Metal-Free Addition Reaction for the Synthesis of 3-(Aminobenzylidene/Aminoalkylidene)Indolin-2-Ones and Its Synthetic Applications. *J. Org. Chem.* **2019**, *84*, 13516–13527. (e) Marek, L.; Kolman, L.; Váňa, J.; Svoboda, J.; Hanusek, J. Synthesis of (Z)-3-[Amino(Phenyl)Methylidene]-1,3-Dihydro-2Hindol-2-Ones Using an Eschenmoser Coupling Reaction. *Beilstein J. Org. Chem.* **2021**, *17*, 527–539.

8. (a) Younus, H. A.; Al-Rashida, M.; Hameed, A.; Uroos, M.; Salar, U.; Rana, S.; Khan, K. M. Multicomponent Reactions (MCR) in Medicinal Chemistry: A Patent Review (2010-2020). *Expert Opinion on Therapeutic Patents*. **2021**, *31*, 267–289. (b) Fairoosa, J.; Neetha, M.; Anilkumar, G. Recent Developments and Perspectives in the Copper-Catalyzed Multicomponent Synthesis of Heterocycles. *RSC Advances*. **2021**, *11*, 3452–3469. (c) Sharma, U. K.; Ranjan, P.; van der Eycken, E. v.; You, S. L. Sequential and Direct Multicomponent Reaction (MCR)-Based Dearomatization Strategies. *Chem. Soc. Rev.* **2020**, *49*, 8721–8748.
9. (a) Ruan, S.; Zhong, X.; Chen, Q.; Feng, X.; Liu, X. An Asymmetric Hydrocyanation/Michael Reaction of α-Diazoacetates: Via Cu(i)/Chiral Guanidine Catalysis. *Chem. Commun.* **2020**, *56*, 2155–2158. (b) Audic, B.; Cramer, N. Rhodium(III)-Catalyzed Cyclopropane C-H/C-C Activation Sequence Provides Diastereoselective Access to α-Alkoxylated γ-Lactams. *Org. Lett.* **2020**, *22*, 5030–5034. (c) Zhou, C.; Jiang, J.; Wang, J. Three-Component Synthesis of Isoquinoline Derivatives by a Relay Catalysis with a Single Rhodium(III) Catalyst. *Org. Lett.* **2019**, *21*, 4971–4975. (d) Yu, Y.; Zhang, Y.; Wang, Z.; Liang, Y. X.; Zhao, Y. L. A Rhodium-Catalyzed Three-Component Reaction of Arylisocyanides, Trifluorodiazoethane, and Activated Methylene Isocyanides or Azomethine Ylides: An Efficient Synthesis of Trifluoroethyl-Substituted Imidazoles. *Org. Chem. Front.* **2019**, *6*, 3657–3662.
10. (a) Bakulina, O.; Inyutina, A.; Dar'in, D.; Krasavin, M. Multicomponent Reactions Involving Diazo Reagents: A 5-Year Update. *Molecules*. **2021,** *26*, 6563. (b) Xiang, Y.; Wang, C.; Ding, Q.; Peng, Y. Diazo Compounds: Versatile Synthons for the Synthesis of Nitrogen Heterocycles via Transition Metal-Catalyzed Cascade C–H Activation/Carbene Insertion/Annulation Reactions. *Adv. Synth. Catal.* **2019**, *361*, 919–944. (c) Yamakawa, Y.; Ikuta, T.; Hayashi, H.; Hashimoto, K.; Fujii, R.; Kawashima, K.; Mori, S.; Uchida, T**.;** Katsuki, T. Iridium(III)-Catalyzed Asymmetric Site-Selective Carbene C–H Insertion during Late-Stage Transformation *J. Org. Chem.* **2022**, *87*, 6769–6780. (d) Li, C.; Wang, R.; Huang, L.; Chen, J.; Jin, J.; Yan, Q.; Wang, H.; Chen, F. TfOH-Catalyzed Regioselective S–H Insertion of Cyclic Thioamide Derivatives with Diazo Compounds at Room Temperature. *J. Am. Chem. Soc.* **2022**, *144*, 23275–23279. (e) Wu, Y.; Cao, S.; Douair, I.; Maron, L.; Bi. Computational Insights into Different Mechanisms for Ag-, Cu-, and Pd-Catalyzed Cyclopropanation of Alkenes and Sulfonyl Hydrazones. *Chem. Eur. J.* **2021**, *27*, 5999. (f) Ning, Y.; Zhang, X.; Gai, Y.; Dong, Y.; Sivaguru, P.; Wang, Y.; Reddy, B. R. P.; Zanoni, G.; Bi, X. Difluoroacetaldehyde *N*-Triftosylhydrazone

(DFHZ-Tfs) as a Bench-Stable Crystalline Diazo Surrogate for Diazoacetaldehyde and Difluorodiazoethane. *Angew. Chem. Int. Ed*. **2020**, *59*, 6473. (g) Shanshan, C.; Zhaohong, L.; Haiyan, Y.; Liu, Y.; Jingping, Z.; Xihe, B. Computational Studies on Reaction Mechanism of the Catalyst-Controlled Selective Insertion of Metal Carbenoids into C-C and C-H Bonds of 1,3-Dicarbonyl Compounds. *Chin. J. Org. Chem.* **2020**, *40*, 2468. (h) Zhang, X.; Liu, Z.; Yang, X.; Dong, Y.; Virelli, M.; Zanoni, G.; Anderson, E. A.; Bi, X. Use of trifluoroacetaldehyde N-tfsylhydrazone as a trifluorodiazoethane surrogate and its synthetic applications. *Nat. Commun.* **2019**, *10*, 284. https://doi.org/10.1038/s41467-018-08253-z. (i) Gava, R.; Olmos, A.; Noverges, B.; Varea, T.; Alvarez, E.; Belderrain, T. R.; Caballero, A.; Asensio, G.; Perez, P. J. Discovering Copper for Methane C–H Bond Functionalization. *ACS Catal.*, **2015**, *5*, 3726-3730.

11. (a) Bu, X. bin; Wang, Z.; Wang, X. di; Meng, X. H.; Zhao, Y. L. Rhodium-Catalyzed Tandem Reaction of Isocyanides with Trifluorodiazoethane and Nucleophiles: Divergent Synthesis of Trifluoroethyl-Substituted Isoquinolines, Imidates, and Amidines. *Adv. Synth. Catal.* **2018**, *360*, 2945–2951. (b) Luo, J.; Chen, G. S.; Chen, S. J.; Li, Z. D.; Zhao, Y. L.; Liu, Y. L. One-Pot Tandem Protocol for the Synthesis of 1,3-Bis(β-Aminoacrylate)-Substituted 2-Mercaptoimidazole Scaffolds. *Adv. Synth. Catal.* **2020**, *362*, 3635–3643. (c) Gu, Z. Y.; Han, H.; Li, Z. Y.; Ji, S. J.; Xia, J. B. Catalytic Synthesis of Functionalized Amidines: Via Cobalt-Carbene Radical Coupling with Isocyanides and Amines. *Org. Chem. Front.* **2021**, *8*, 1544–1550.
12. (a) Collet, J. W.; Roose, T. R.; Weijers, B.; Maes, B. U. W.; Ruijter, E.; Orru, R. V. A. Recent Advances in Palladium-Catalyzed Isocyanide Insertions. *Molecules*. **2020**, 25, 4906. (b) Pálinkás, N.; Kollár, L.; Kégl, T. Palladium-Catalyzed Synthesis of Amidines via Tert-Butyl Isocyanide Insertion. *ACS Omega.* **2018**, *3*, 16118–16126. (c) Kato, H.; Musha, I.; Komatsuda, M.; Muto, K.; Yamaguchi, J. Catalytic Three-Component C-C Bond Forming Dearomatization of Bromoarenes with Malonates and Diazo Compounds. *Chem. Sci*. **2020**, *11*, 8779–8784. (d) Huang, K.; Liu, J. B.; Chen, Z. F.; Wang, Y. C.; Yadav, S.; Qiu, G. Palladium-Catalyzed Imidoylation-Triggered [2 + 2 + 1] Cyclization of Internal Alkyne with Isocyanides. *Org. Lett.* **2020**, *22*, 5931–5935. (e) Sun, S.; Hu, W. M.; Gu, N.; Cheng, J. Palladium-Catalyzed Multi-Component Reactions of N-Tosylhydrazones, 2-Iodoanilines and CO2towards 4-Aryl-2-Quinolinones. *Chem. Eur. J.* **2016**, *22*, 18729–18732. (f) Zhou, F.; Ding, K.; Cai, Q. Palladium-Catalyzed Amidation of N-Tosylhydrazones with Isocyanides. *Chem. Eur. J.* **2011**, *17*, 12268–12271. (g) Jiang, X.; Tang, T.; Wang, J. M.; Chen, Z.; Zhu, Y. M.; Ji, S. J. Palladium-Catalyzed One-Pot

Synthesis of Quinazolinones via Tert-Butyl Isocyanide Insertion. *J. Org. Chem.* **2014**, *79*, 5082–5087. (h) Ali, W.; Dahiya, A.; Patel, B.K. Cascade Synthesis of Dihydrobenzofurans and Aurones *via* Palladium-Catalyzed Isocyanides Insertion into 2-Halophenoxy Acrylates. *Adv. Synth. Catal.* **2018**, *360*, 1232-1239. (i) Dahiya, A.; Das, B.; Sahoo, A. K.; Patel, B. K. Visible-Light-Driven Isocyanide Insertion to *o*-Alkylideneanilines: A Route to Isoindolinone Synthesis**.** *Adv. Synth. Catal.* **2022**, *364*, 966-973.

13. (a) Kamboj, P.; Dutt, S.; Chakroborty, S.; Tyagi, V. CuI-Catalyzed Highly Regioselective C-H Functionalization of Indoles Using Indole-3-Tosylhydrazones as Carbene Precursor: An Efficient Synthesis of 3,3-Bis(Indolyl)Methane Derivatives. *Tetrahedron. Lett.* **2019**, *60*, 151162. (b) Soam, P.; Gaba, H.; Mandal, D.; Tyagi, V. A Pd-Catalyzed One-Pot Cascade Consisting of C-C/C-O/N-N Bond Formation to Access Benzoxazine Fused 1,2,3-Triazoles. *Org. Biomol. Chem.* **2021**, *19*, 9936–9945.
14. (a) Bi, X.; Liu, Z.; Cao, S.; Wu, J.; Zanoni, G.; Sivaguru, P. Palladium(II)-Catalyzed Cross-Coupling of Diazo Compounds and Isocyanides to Access Ketenimines. *ACS Catal.* **2020**, *10*, 12881–12887. (b) Hui Zhang, X.; Yuan Geng, Z.; Tai Wang, K. Theoretical Studies on the Mechanism of Palladium(II)-Catalysed Ortho-Carboxylation of Acetanilide with CO. *J. Chem. Sci.* **2014**, *126*, 265-272. (c) Gu, H.; Qiu, Z.; Zhang, Z.; Li, J.; Yan, B. A Mechanistic Study of Pd(OAc)2-Catalyzed Intramolecular C-H Functionalization Reaction Involving CO/Isonitrile Insertion. *Dalton Trans.* **2015**, *44*, 9839–9846. (d) Liu, Y.; Luo, Z.; Zhang, J. Z.; Xia, F. DFT Calculations on the Mechanism of Transition-Metal-Catalyzed Reaction of Diazo Compounds with Phenols: O-H Insertion versus C-H Insertion. *J. Phys. Chem. A* **2016**, *120*, 6485–6492. (e) He, X.; Zhu, L.; Heng, D.; Liu, F.; Liu, S.; Zhong, K.; Shan, C.; Bai, R.; Lan, Y. Mechanistic Insights into the Rhodium-Copper Cascade Catalyzed Dual C-H Annulation of Indoles. *Org. Chem. Front.* **2021**, *8*, 1739–1746. (g) Lu, B.; Liang, X.; Zhang, J.; Wang, Z.; Peng, Q.; Wang, X. Dirhodium(II)/Xantphos-Catalyzed Relay Carbene Insertion and Allylic Alkylation Process: Reaction Development and Mechanistic Insights. *J. Am. Chem. Soc.* **2021**, *143*, 11799–11810.
15. (a) Olimpieri, F.; Bellucci, M. C.; Volonterio, A.; Zanda, M. A. Mild, Efficient Approach for the Synthesis of 1,5-Disubstituted Hydantoins. *Eur. J. Org. Chem.* **2009**, *2009*, 6179–6188. (b) Bisht, G. S.; Dunchu, T. D.; Gnanaprakasam, B.; Synthesis of Quaternary Spirooxindole *2H*-Azirines under Batch and Continuous Flow Condition and Metal Assisted Umpolung Reactivity for the Ring-Opening Reaction. *Chem Asian J.* **2021**, *16*, 656–665.

16. Gaussian 16, Revision C.01, Frisch, M. J.; Trucks, G. W.; Schlegel, H. B.; Scuseria, G. E.; Robb, M. A.; Cheeseman, J. R.; Scalmani, G.; Barone, V.; Petersson, G. A.; Nakatsuji, H.; Li, X.; Caricato, M.; Marenich, A. V.; Bloino, J.; Janesko, B. G.; Gomperts, R.; Mennucci, B.; Hratchian, H. P.; Ortiz, J. V.; Izmaylov, A. F.; Sonnenberg, J. L.; Williams-Young, D.; Ding, F.; Lipparini, F.; Egidi, F.; Goings, J.; Peng, B.; Petrone, A.; Henderson, T.; Ranasinghe, D.; Zakrzewski, V. G.; Gao, J.; Rega, N.; Zheng, G.; Liang, W.; Hada, M.; Ehara, M.; Toyota, K.; Fukuda, R.; Hasegawa, J.; Ishida, M.; Nakajima, T.; Honda, Y.; Kitao, O.; Nakai, H.; Vreven, T.; Throssell, K.; Montgomery, J. A., Jr.; Peralta, J. E.; Ogliaro, F.; Bearpark, M. J.; Heyd, J. J.; Brothers, E. N.; Kudin, K. N.; Staroverov, V. N.; Keith, T. A.; Kobayashi, R.; Normand, J.; Raghavachari, K.; Rendell, A. P.; Burant, J. C.; Iyengar, S. S.; Tomasi, J.; Cossi, M.; Millam, J. M.; Klene, M.; Adamo, C.; Cammi, R.; Ochterski, J. W.; Martin, R. L.; Morokuma, K.; Farkas, O.; Foresman, J. B.; Fox, D. J. Gaussian, Inc., Wallingford CT, **2016**.
17. (a) Lee, C.; Yang, eitao; Parr, R. G. Development of the Colic-Salvetti Correlation-Energy Formula into a Functional of the Electron Density. Phys. Rev. B. **1988**, *37*, 785. (b) Sylaja, B.; Srinivasan, S. Ab Initio and Density Functional Theory (DFT) Study on Clonazepam. *Open. J. Biophys.* **2012**, *02*, 80–87. (c) Andrae, D.; Iubermann, U. H.; Dolg, M.; Stoll, H.; Preub, H. Theoretica Chimica Acta Energy-Adjusted Ab Initio Pseudopotentials for the Second and Third Row Transition Elements. *Theoretica chimica acta*. **1990**, *77*, 121-143. (d) Becke, A. D. Density-Fnnctional Exchange-Energy Approximation with Correct Asymptotic Behavior. *Phys. Rev. A.* **1988**, *38*, 3098. (e) Parr, Y. A.; Miehlich, B.; Savin, A.; Stoll, H.; Preuss, H. Results obtained with the Correlation Energy Density Functionals of Becke and Lee, Yang and Parr. *Chem. Phys. Lett*. **1989**, *157*, 200-206.
18. Marenich, A. v.; Cramer, C. J.; Truhlar, D. G. Universal Solvation Model Based on Solute Electron Density and on a Continuum Model of the Solvent Defined by the Bulk Dielectric Constant and Atomic Surface Tensions. *J. Phys. Chem.* **2009**, *113*, 6378–6396.
19. Andrienko, G. A.ChemCraft, http://www.chemcraftprog.com.
20. (a) Muthusamy, S.; Gunanathan, C.; Nethaji, M. Multicomponent Reactions of Diazoamides: Diastereoselective Synthesis of Mono- and Bis-Spirofurooxindoles. *J. Org. Chem.* **2004**, *69*, 5631–5637. (b) Murphy, G. K.; Abbas, F. Z.; Poulton, A. v. α,α-Dichlorination of Oxindole Derivatives Using (Dichloroiodo)Benzene. *Adv. Synth. Catal.* **2014**, *356*, 2919–2923. (c) Jeankumar, V. U.; Alokam, R.; Sridevi, J. P.; Suryadevara, P.; Matikonda, S. S.; Peddi, S.; Sahithi, S.; Alvala, M.; Yogeeswari, P.; Sriram, D. Discovery

and Structure Optimization of a Series of Isatin Derivatives as Mycobacterium Tuberculosis Chorismate Mutase Inhibitors. *Chem. Biol. Drug. Des.* **2014**, *83*, 498–506.

21. Chan, D. M. T.; Monaco, K. L.; Wang, R.-P.; Winters, M. P. New N-and O-Arylations with Phenylboronic Acids and Cupric Acetate. *Tetrahedron Lett*. **1998**, *39*, 2933-2936.

CHAPTER 3

Synthesis of N-Fused Polycyclic Indoles via Pd-Catalyzed Multicomponent Cascade Reaction Consisting of Amide-Directed [3+1+1] Annulation Reaction of 3-Diazo Oxindole and Isocyanides

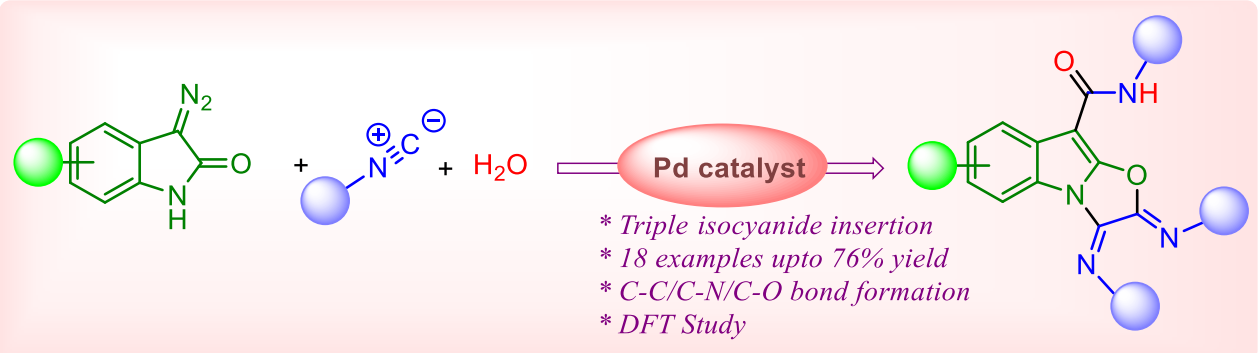

3.1: Introduction

N-fused polycyclic indoles have attracted great attention in synthetic chemistry due to their ubiquitous presence in a number of natural products and pharmaceutical agents (**Figure 3.1**). They displayed a wide range of biological activities such as anticancer, anti-inflammatory, antimicrobial, antiatherogenic, and antihypertensive, etc. Moreover, indole-fused heterocycles are imperative structural units of various agrochemicals, plastics and dyes that are integrated into everyday life.[1a-g]

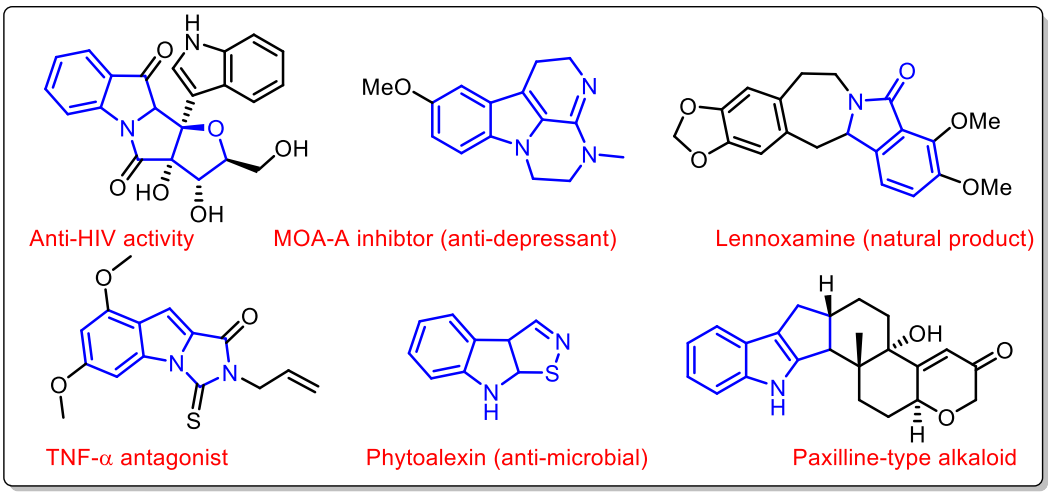

Figure 3.1. Biologically important indole-fused heterocycles

In this context, various combinations of polycyclic indole-fused heterocycles have been designed and synthesized in the past.[2a-e] However, the production of these moieties is very challenging due to the requirement of multistep synthesis which is associated with their own disadvantages. So, the development of novel and efficient methodologies to synthesize indole-fused heterocyclic scaffolds is highly admirable in synthetic chemistry. Throughout the significant progress made in this area, different methods have been developed to synthesize tricyclic oxazolo[3,2-*a*] indole moiety. In this context, Zhu et al. synthesized oxazolo[3,2-*a*] indolones via visible light-induced aerobic dearomative reaction of *N*-substituted indoles in the presence of Ru-catalyst (**Scheme 3.1a**).[3] Next, a metal and solvent-free approach to synthesize oxazolo[3,2-*a*] indolones using propargylic alcohols and indole derivatives was developed by Oparina's group (**Scheme 3.1b**).[4] Recently, Wang and co-workers reported a cascade approach to synthesized oxazolo[3,2-*a*] indolones along with indolo [2,3-*b*] indoles in the presence of rhodium catalyst at 130 °C (**Scheme 3.1c**).[5] However, most of these approaches are associated with certain limitations such as complex starting materials, longer reaction time, lower efficiency, and substrate scope.

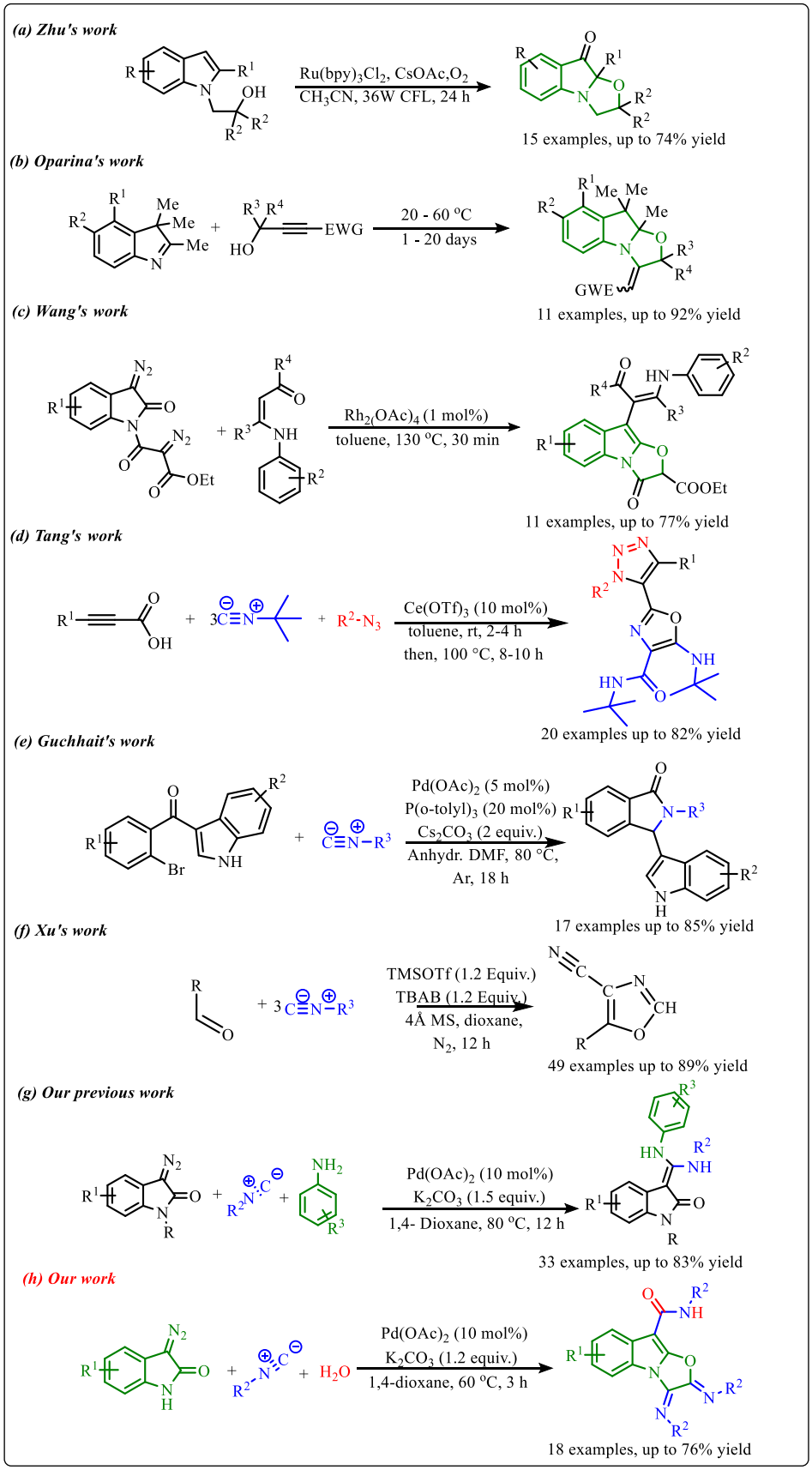

Scheme 3.1. (a-c) Recent approaches to synthesizing tricyclic oxazolo[3,2-*a*] indole derivatives, **(d-f)** recent isocyanide insertion approaches, (**g**) our previous work, (**h**) recent work

On the other hand, cascade or tandem reactions have been found very advantageous to improve synthetic efficiency in modern organic chemistry.[6a-e] Further, cascade reaction involves multiple bonds forming reactions in one-pot, representing an attractive strategy towards the facile synthesis of novel molecular frameworks with less wastage of resources. In particular, transition metal-catalyzed one-pot cascade reactions are being used to generate novel fused heterocycles.[7a-c] Interestingly, isocyanides have been considered as an important substrate for transition metal-catalysed one-pot cascade reactions since they can react both as a nucleophile or an electrophile in chemical reactions.[8a-e] In this context, several cascade reactions using isocyanides have been developed in the past. Recently, Tang's group reported a cerium triflate catalysed triple isocyanide insertion approach to develop a library of oxazole derivatives.[9] Next, Guchhait *et al.* developed a cascade C-H activation methodology to construct bicyclic indolyl motifs via intramolecular isocyanide insertion using Pd-catalyst.[10] Another efficient approach towards consecutive triple isocyanide insertion into aldehydes to synthesize a broad library of 4-cyano oxazole derivatives was reported by Xu and co-workers. (**Scheme 3.1d-3.1f**)[11] Also, we have developed a Pd-catalysed one-pot cascade reaction to access benzoxazine fused 1,2,3-triazoles using *N*-aryl-α-(tosylhydrazone)acetamides with isocyanide.[12] In continuation of our efforts to develop novel cascade reactions by the use of isocyanide and diazo compounds (**Scheme 3.1g**)[13], herein, we have developed a Pd-catalysed multicomponent cascade reaction of 3-diazo oxindole, isocyanide, and H_2O to generate tricyclic oxazolo [3,2-*a*] indole scaffolds (**Scheme 3.1h**).

3.2: Results and discussion

3.2.1: Optimization of the reaction conditions

Initially, we envisioned the synthesis of indole-3-acetamide via the formation of indole-based ketenimines intermediate by the reaction of isocyanide and 3-diazo oxindole as previously reported by our group and others. To actualize our hypothesis, we set up a reaction of *tert*-butyl isocyanide, water, and 3-diazo oxindole using 10 mol% of $Pd(PPh_3)_4$, 1.2 equivalent of Na_2CO_3 in toluene as a solvent at 80 °C and obtained the product in 30% isolated yield. However, characterization techniques such as ^{1}H-NMR, ^{13}C-NMR, HRMS, and X-ray confirm the unprecedented formation of tricyclic oxazolo[3,2-*a*] indole derivative (**Scheme 3.2**).

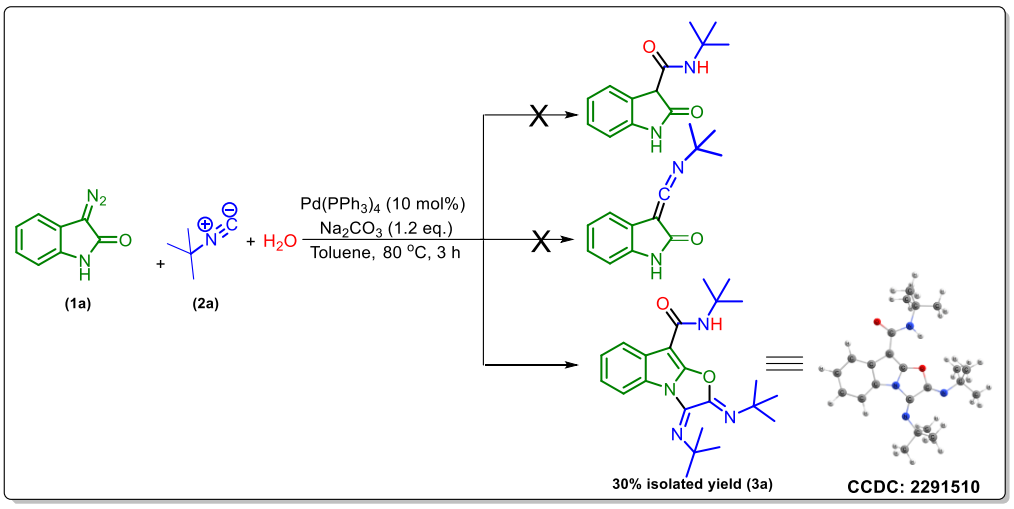

Scheme 3.2. Possible structures under Pd-catalyzed reaction

Drawing encouragement from these findings, next, we decided to optimize the reaction conditions to improve the yield of the multicomponent cascade reaction by selecting 3-diazo oxindole (**1a**), *tert*-butyl isocyanide (**2a**), and H_2O as model substrates. Initially, we screened different transition metal catalysts such as $Cu(OAc)_2$ and $Rh_2(OAc)_4$ in addition to $Pd(PPh_3)_4$, and unexpectedly reaction worked only with Pd-catalyst (**Table 3.1, entries 1-3**). Afterward, we examined different palladium-based catalysts like $Pd(OAc)_2$, $Pd(TFA)_2$, $Pd(OPiv)_2$, $PdCl_2$, $PdCl_2(NCC_6H_5)_2$, $Pd(DPPF)Cl_2$,$Pd_2(dba)_3$ etc. and obtained the product (**3a**) in maximum yield i.e. 56% when 10 mmol% of $Pd(OAc)_2$ was added as a catalyst (**Table 3.1, entry 4-6) & (Table 3.1, entries 7-10**). However, on decreasing the amount of $Pd(OAc)_2$ from 10 mol% to 5 mol%, the yield of the model reaction got decreased (**Table 3.1, entry 11**). Also, it must be noticed that the reaction didn't work in the absence of a palladium catalyst (**Table 3.1, entry 12**). Next, we screened different bases and found that the reaction provided maximum yield in the case of K_2CO_3 as compared to other bases such as Na_2CO_3, Cs_2CO_3, KO*t*-Bu, NEt_3 & DBU (**Table 3.1, entries 13-17**). Also, it was observed that in the absence of a base the yield of the product (**3a**) got decreased up to 27% yield (**Table 3.1, entry 18**). Further, toluene was replaced by various solvents like 1,4-dioxane, CH_3CN, DMF, DMSO, and THF, however, 1,4-dioxane was found as the best solvent (**Table 3.1, entry 19) & (Table 3.1, entries 20-23**). Besides, there was no improvement in the outcome of the model reaction observed while adding different additives like AgOAc & CsOAc (**Table 3.1, entries 24-25**). Moreover, temperature variation significantly affected the outcome of the model reaction. In particular, decreasing the temperature from 80 °C to 60 °C increases the yield of (**3a**) up to 71% (**Table 3.1, entry 26**). Then, the yield of (**3a**) was reduced by further decreasing the temperature up to 50 °C (**Table**

3.1, entry 27). The reaction was almost diminished below 50 °C and the product was observed only in trace amount at 40 °C (**Table 3.1, entries 28-29**). Subsequently, increasing the equivalents of water slightly decreased the yield up to 60% (**Table 3.1, entry 30**). Noticeably, in the absence of water, only 20% yield of product (**3a**) was observed, which suggests the requirement of water in an equimolar amount in this transformation (**Table 3.1, entry 31**). Also, the molar ratio of substrates was varied, however, 1:3.2:1 of 3-diazo oxindole, tert-butyl isocyanide, and water respectively remained the best ratio (**Table 3.1, entries 32-35**).

Table 3.1. Optimization of the reaction conditions[a]

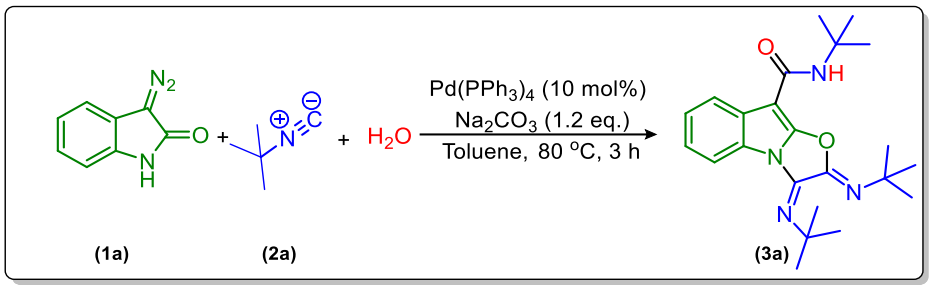

entry	deviation from standard conditions	yield[b] (%)
1.	No deviation	30
2.	$Cu(OAc)_2$ instead of $Pd(PPh_3)_4$	-
3.	$Rh_2(OAc)_4$ instead of $Pd(PPh_3)_4$	-
4.	$Pd(OAc)_2$ instead of $Pd(PPh_3)_4$	56
5.	$Pd(TFA)_2$ instead of $Pd(PPh_3)_4$	38
6.	$Pd(OPiv)_2$ instead of $Pd(PPh_3)_4$	31
7.	$PdCl_2$ instead of $Pd(PPh_3)_4$	44
8.	$PdCl_2(NCC_6H_5)_2$ instead of $Pd(PPh_3)_4$	37
9.	$Pd(DPPF)Cl_2$ instead of $Pd(PPh_3)_4$	41
10.	$Pd(dba)_3$ instead of $Pd(PPh_3)_4$	32
11.	$Pd(OAc)_2$ (5 mol% instead of 10 mol%).	48
12.	No catalyst	-
13.	Cs_2CO_3 instead of Na_2CO_3	51
14.	K_2CO_3 instead of Na_2CO_3	59
15.	KO*t*-Bu instead of Na_2CO_3	35
16.	NEt_3 instead of Na_2CO_3	43
17.	DBU instead of Na_2CO_3	39
18.	In absence of base	27
19.	1,4-dioxane instead of toluene	64
20.	CH_3CN instead of toluene	53
21.	DMF instead of toluene	57
22.	DMSO instead of toluene	54
23.	THF instead of toluene	50
24.	Added AgOAc as an additive	58
25.	Added CsOAc as an additive	63
26.	60 °C	71
27.	50 °C	36
28.	40 °C	trace
29.	rt	-

30.	2 equiv. of H_2O	60
31.	No H_2O	20
32.	*tert*-butyl isocyanide (1.5 equiv.)	31
33.	*tert*-butyl isocyanide (2.0 equiv.)	43
34.	*tert*-butyl isocyanide (3.5 equiv.)	62
35.	*tert*-butyl isocyanide (4.0 equiv.)	60

[a]**Reaction conditions:** 3-diazo oxindole 1a (1.0 equiv., 0.31 mmol, 50 mg), *tert*-butyl isocyanide 2a (3.2 equiv., 113 µL, 0.99 mmol), H_2O (1.0 equiv., 5.6 µL), Pd-catalyst (10 mol%), base (1.2 equiv.), solvent (2 ml), 3 h. [b]isolated yield.

3.2.2: Substrate Scope

After having optimized reaction conditions in hands, we have evaluated the feasibility of the reaction with different isocyanides as well as 3-diazo oxindole as revealed in **Scheme 3.3**. Firstly, we have replaced *tert*-butyl isocyanide with 1,1,3,3-tetramethyl butyl isocyanide or cyclohexyl isocyanide, as a result, corresponding products (**3b** & **3c**) were obtained in slightly lower yield in comparison of the product (**3a**) (**Scheme 3.3**). These results represent the structural role of isocyanides as the steric hindrance increases, the yield of the reaction decreases. Also, we have tried reactions with other isocyanides like p-methoxy phenyl isocyanide and *p*-toluene sulphonyl methyl-isocyanide, however, no product formation was observed with these substrates. Next, we have examined the effect of various electron-donating, electron-withdrawing, and halide substituents at different positions of 3-diazo oxindole. Initially, a range of electron-donating groups at different positions of the phenyl ring of 3-diazo oxindole was tested. Noticeably, in the case of 5-OMe substituted 3-diazo oxindole, the reaction provided products (**3d**) and (**3e**) in 76% and 68% yields respectively whereas the reaction provided moderate to a good yield of desired products when 5-CH_3 substituted 3-diazo oxindole was employed with *tert*-butyl isocyanide, 1,1,3,3-tetramethyl butyl isocyanide, and cyclohexyl isocyanide respectively (**3f-h,** Scheme 3.3). Also, 6-OMe substituted 3-diazo oxindole provided products (**3i**) and (**3j**) in slightly lower yield i.e., 59 and 53% (**Scheme 3.3**). It should be noticed that the reaction diminished when the electron-donating group i.e. -CH_3 incorporated at the 7-position of 3-diazo oxindole and it might be due to hindrance enhancement near the fringe where the reaction occurred (**3k**, **Scheme 3.3**).

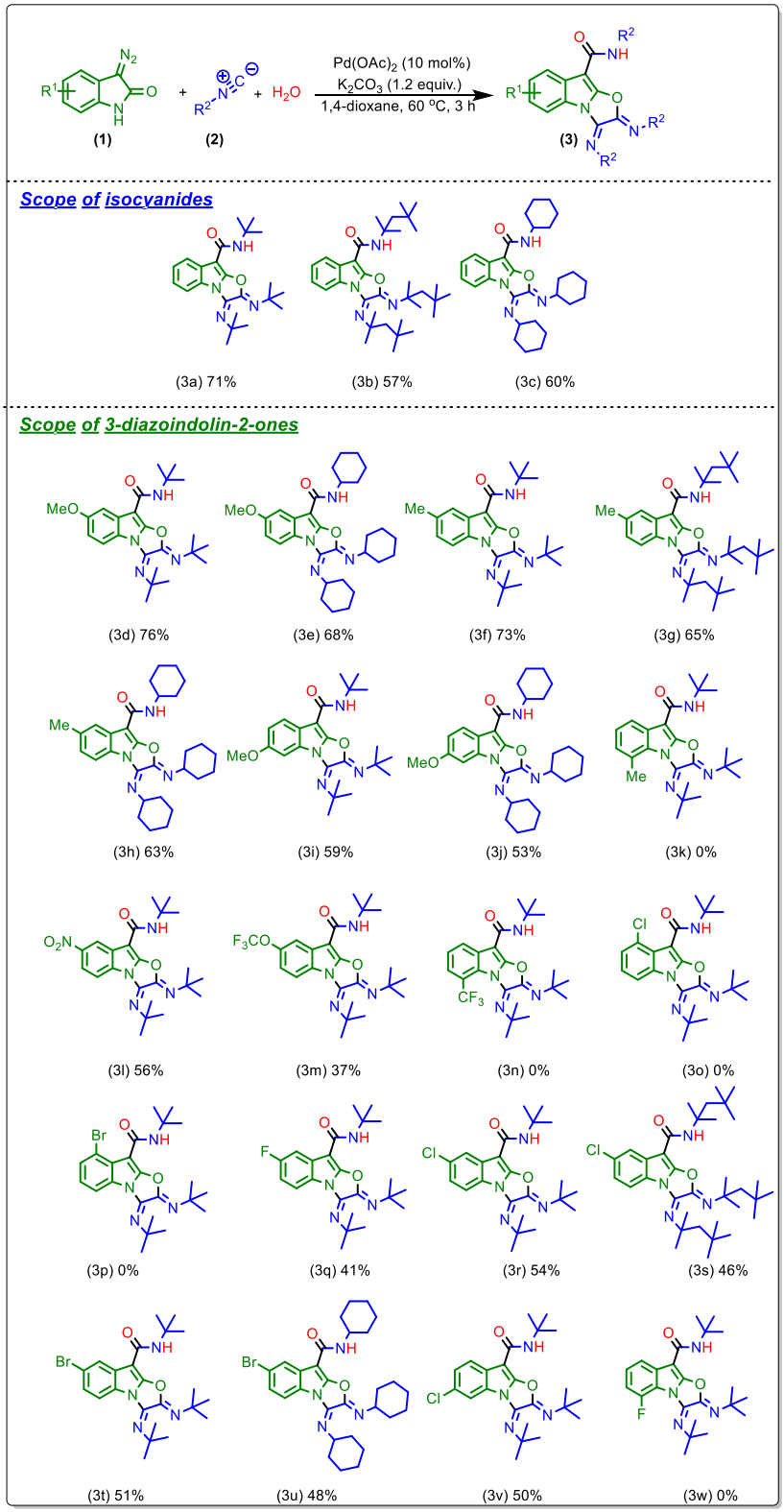

Reaction conditions: 3-diazo oxindoles (1) (1.0 equiv.), isocyanides (2) (3.2 equiv.), H_2O (3) (1.0 equiv.), $Pd(OAc)_2$ (10 mol%), K_2CO_3 (1.2 equiv.), 1,4-dioxane (2 mL), 3 h, 60 °C.

Scheme 3.3. The substrate scopes of Pd-catalyzed multicomponent cascade reaction

This abatement of yield indicated the significance of the electronic and steric effect of the substituent at different positions of 3-diazo oxindole. Next, the electron-withdrawing groups

i.e., 5-nitro & 5-OCF_3 substituted 3-diazo oxindole implemented in the reaction and attained the product (**3l &3m**) in 56 % and 37% isolated yield (**Scheme 3.3**) which was slightly lower in comparison to 3-diazo oxindole having an electron-donating group at the same position. However, there was no product formation observed when 7-CF_3 contained 3-diazo oxindole employed in the reaction (**3n, Scheme 3.3**). Afterward, we examined the effect of halides at different positions of 3-diazo oxindoles and found that in the case of 4-Cl and 4-Br substitutions reaction almost diminished (**3o-3p, Scheme 3.3**). Next, 5-F substituted 3-diazo oxindole provides product (**3q)** in a lower yield as compared to 3-diazo oxindole having electron-withdrawing and -donating groups. Next, 5-Cl and 5-Br substituted 3-diazo oxindole was employed in the reaction, and obtained the corresponding products (**3r-3u**) in the lower yields i.e., 46 to 54% as compared to electron-donating and electron-withdrawing substitutions at 3-diazo oxindole. However, the reaction provided product in moderate yield when 6-Cl substituted 3-diazo oxindole was used in the reaction (**3v, Scheme 3.3**). Again, halide substitution at the 7-position of 3-diazo oxindole didn't work (**3w, Scheme 3.3**).

3.2.3: Hammet Study

Besides, a Hammet study was performed to get further information about the effect of substituents on the rate of the reaction.[14]

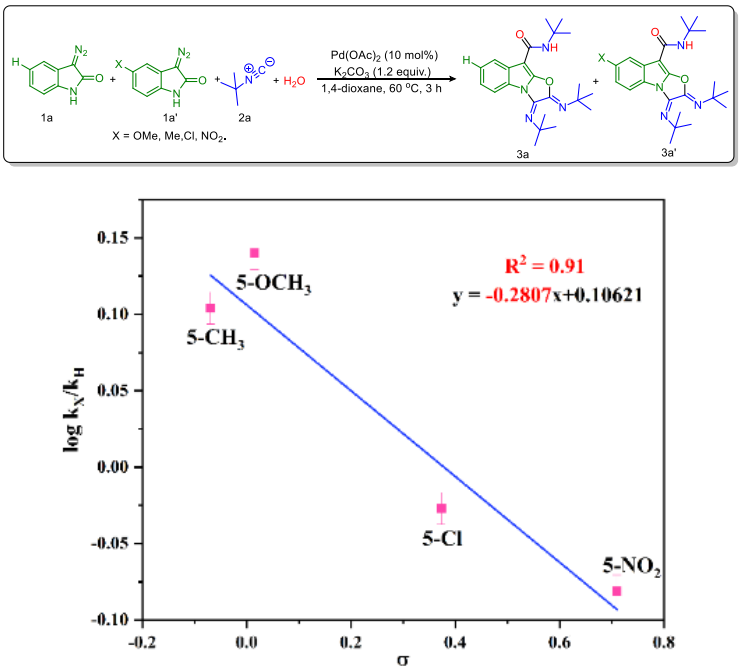

[a]**Reaction conditions**: 3-diazo oxindole 1a (1.0 equiv., 0.31 mmol), substituted 3-diazo oxindole 1a' (1.0 equiv., 0.31 mmol), *tert*-butyl isocyanide 2a (3.2 equiv., 0.99 mmol), H_2O (1.0 equiv.), $Pd(OAc)_2$ (10 mol%), K_2CO_3 (1.2 equiv.), 1,4-dioxane (2 mL), 3 h, 60 °C.

Scheme 3.4: Hammett plot for the reaction of isocyanide with electronically varied 3-diazo oxindole[a]

In this view, 3-diazo oxindole having substituents like 5- OMe, 5-Me, 5-Cl & and 5-NO_2 along with unsubstituted 3-diazo oxindole were employed in the multicomponent reaction **(Scheme 3.4)**. The best linear fit ($R^2 = 0.91$) was achieved using the standard σ_p parameters vs log k_X/k_H, providing a ρ value (slope value) of -0.28. The value of ρ is less than 1, which indicates that a positive charge is built up during the rate-determining (slope value) of -0.28. The value of ρ is less than 1, which indicates that a positive charge is built up during the rate-determining step. Also, the positive slope value suggests that the rate of reaction accedes in the presence of the electron-donating group.

3.2.4: Plausible mechanism and DFT calculations

Next, we have presented a plausible mechanism for the synthesis of tricyclic oxazolo [3,2-a] indole scaffolds as shown in **Figure 3.2**.[15] Initially, *tert*-butyl isocyanide reacts with $Pd(OAc)_2$ to generate complex (**I**).[12, 16a-d] Then, *tert*-butyl isocyanide acts as a neutral ligand in complex (**I**), and palladium remains in its divalent oxidation state. The complex (**I**) was then linked with the 3-diazo oxindole (**1a**) substrate to generate the square planer complex (**II**) that serves as our starting complex. In this context, **Figure 3.2** shows the overall mechanism's steps, and **Figure 3.3(a)** displays the associated DFT-computed potential free energy profile in relation to the energies of the initial complex (I+1a). Further, **Figure 3.3(b)** depicted optimized transition states computed at B3LYP/ 6-31+G(d, p) level of theory.

Further, the elimination of N_2 from complex (**II**) took place and generated Pd-carbene complex (**III)** via **TS1** (**Figure 3.3(b)**) with the free energy of activation $\Delta G^{\ddagger}$= 29.2 kcal mol^{-1}. The next step is the migration of isocyanide into the Pd-carbene complex through the three-membered ring transition state, **TS2** (**Figure 3.3(b)**), which has a 21.5 kcal mol^{-1} activation free energy and produces the Pd-ketenimine complex (**IV**), which readily releases $Pd(OAc)_2$ to form a highly unstable ketenimine intermediate (**V**). Furthermore, H_2O is connected to the central electrophilic carbon of ketenimine intermediate (**V**) with simultaneous proton transfer to the nitrogen of the isocyanide unit via **TS3** (**Figure 3.3(b)**) with $\Delta G^{\ddagger}$= 13.3 kcal mol^{-1} to form the intermediate **VI**, which is stabilized by -37.2 kcal mol^{-1} from **TS3** (**Figure 3.3(b)**). After that, the tautomerization step takes place via proton transfer to C-3 carbon of **VI** from the OH group to form amide intermediate (N-(tert-butyl)-2-oxoindoline-3-carboxamide) **4**, through **TS4** (**Figure 3.3(b)**) with a barrier of 40.3 kcal mol^{-1}.[17a-b] Afterward, N-(tert-butyl)- 2-oxoindoline-3-carboxamide (**4)** interacts with palladium acetate to form six-membered complex **VII** which releases the proton from the C-3 position and acetate group from the palladium catalyst as acetic acid to form complex **VIII** via transition state **TS5** (**Figure 3.3(b)**) with $\Delta G^{\ddagger}$= 14.6 kcal

mol^{-1}. During this step, the oxidation state of Pd remains unchanged which is further coordinated with second *tert*-butyl isocyanide to form a highly stabilized (-80.0 kcal mol^{-1})

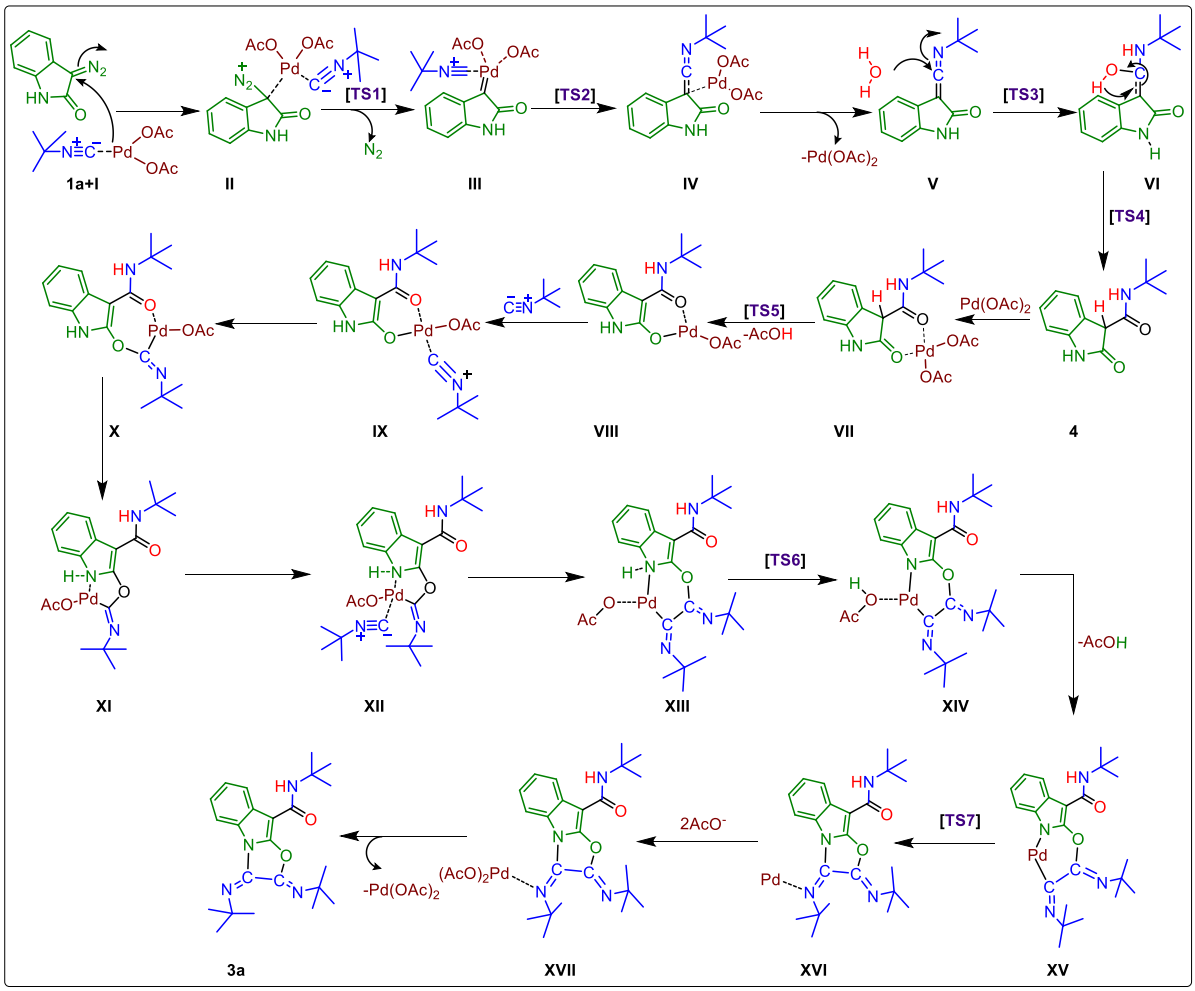

Figure 3.2. The plausible mechanism for Pd-catalyzed multicomponent cascade reaction

tetravalent Pd-containing intermediate **IX**. Then, the amidic C=O group at the C2-position gets activated and an isocyanide unit is inserted into Pd-O bond to form a seven-membered complex **X** which readily converted to a five-membered palladacyclic intermediate complex **XI** having energy of 22.3 kcal mol^{-1} higher than the complex **X**. Next, third *tert*-butyl isocyanide proceeds to linked to the Pd atom of complex (**XI**) to form a stable tetravalent complex **XII**. Again, this isocyanide is inserted into Pd-C bond and regains its six-membered intermediate to form intermediate **XIII**, having higher energy of 8.6 kcal mol^{-1} from complex **XII**. The acetate group present at palladacyclic intermediate (**XIII**) abstracts the N-H proton via the transition state, **TS6** (**Figure 3.3(b)**), which is located at the point of -35.8 kcal mol^{-1} in the PES and form another complex **XIV** which possesses 44.6 kcal mol^{-1} less energy from the starting complex. Afterward, complex **XIV** releases AcOH and forms another complex **XV** having slightly higher energy (3.8 kcal mol^{-1}) than complex **XIII**. In the last, C-N bond formation takes place via the

transition state, **TS7** (**Figure 3.3(b)**), having $\Delta G^{\ddagger}$ = 19.4 kcal mol^{-1} from complex **XV** and formed complex **XVI**. Afterward, reductive elimination of palladium occurs in the form of palladium acetate to give the final product (**3a**) through the intermediate **XVII**.

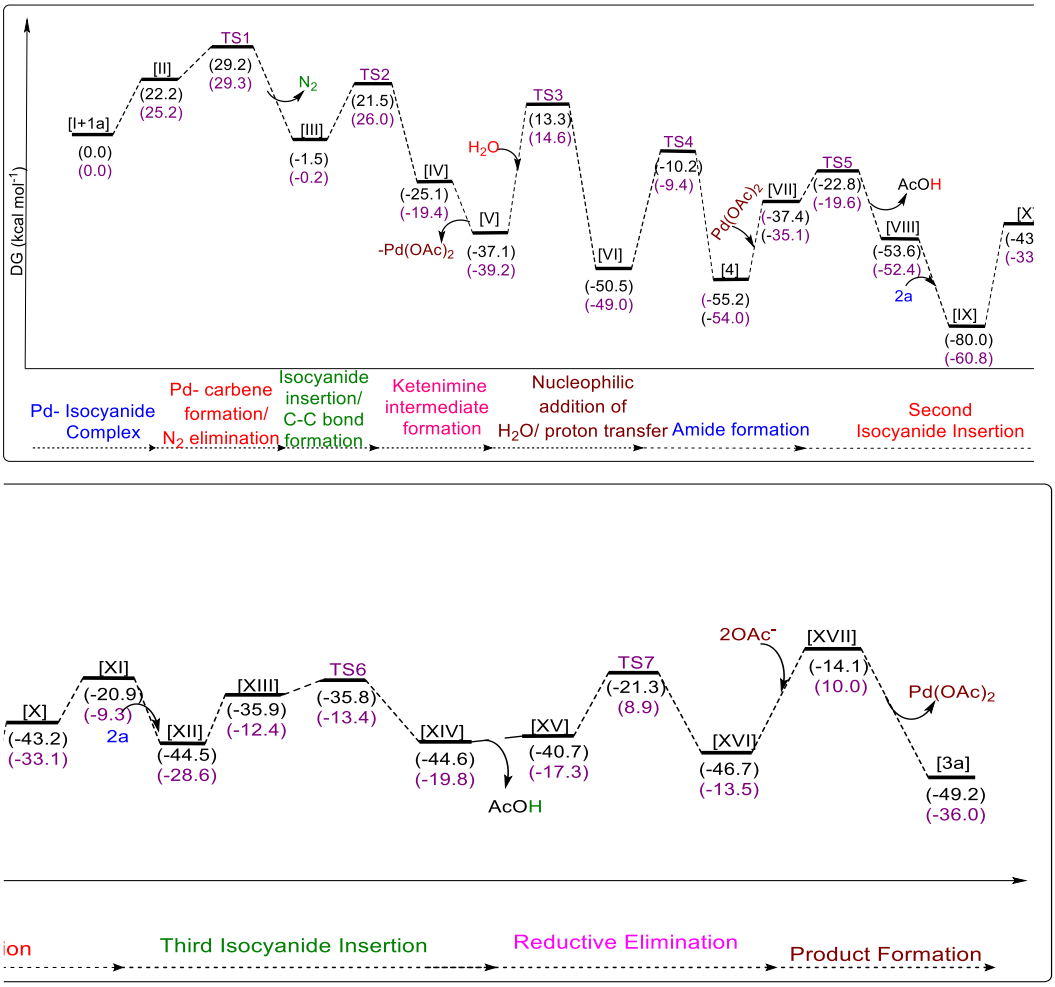

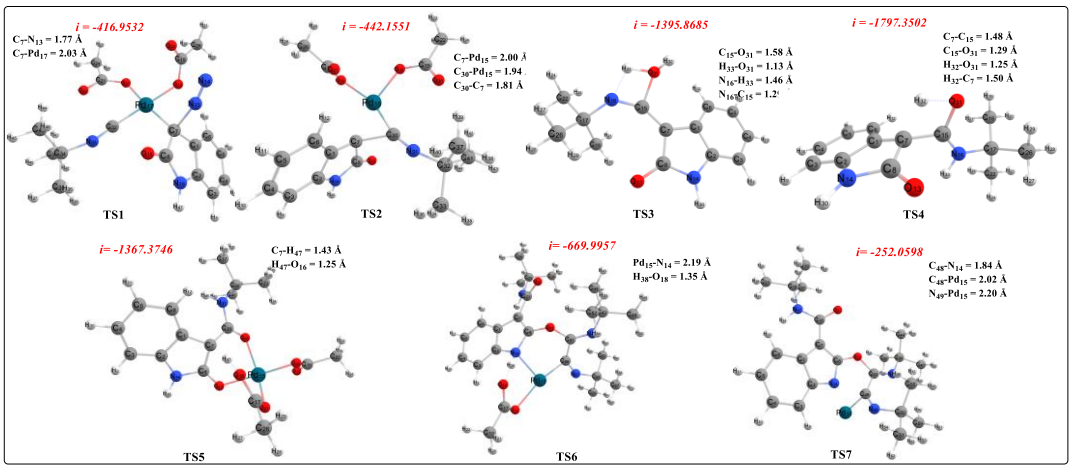

Figure 3.3. (a) The potential energy profiles computed at M06/6-31++G(2d, 2p)/ B3LYP/ 6-31+G(d, p level of theory related to the plausible mechanism represented in Figure 3.2. **(b)** Optimized transition states computed at B3LYP/ 6-31+G(d, p) level of theory.

3.2.5: Control experiments

In the last, several control studies were carried out to confirm the role of amide in this synthesis. We set up a reaction using *tert*-butyl 3-diazo-2-oxoindoline-1-carboxylate (**1p**) with *tert*-butyl isocyanide under standard reaction conditions (**Scheme 3.5-i**) and got the product N-(tert-butyl)-2-oxoindoline-3-carboxamide (**4**) in 78% yield. In continuation, we performed a reaction of N-(tert-butyl)-2-oxoindoline-3-carboxamide (**4**) with *tert*-butyl isocyanide under the same reaction conditions. Delightedly, we got the desired product (**3a**) in good yield (**Scheme 3.5-ii**) which confirms the formation of N-(tert-butyl)-2-oxoindoline-3-carboxamide (**4**) as an intermediate in this transformation. To further confirm the role of *in-situ* generated amide, we have tried the reaction with three different oxindole derivatives such as ethyl 2-oxoindoline-3-carboxylate (**5**), indolin-2-one (**6**), and 3-hydroxy-3-(2-oxopropyl)indolin-2-one (**7**). Surprisingly there was no reaction with these substrates {**Scheme 3.5 (iii-v)**}. So, these control experiments suggest that the amide group at the C-3 position of oxindole is required to assist the reaction for further steps.[8,18] Next, we have tried reaction with D_2O in place of H_2O and product formation was confirmed with HRMS analysis. HRMS data of crude reaction mixture showed a peak at 398.2648, equivalent to deuterated amide-based product. Hence, this experiment suggests the participation of H_2O molecules in the formation of amide {**Scheme 3.5 (vi)**}.

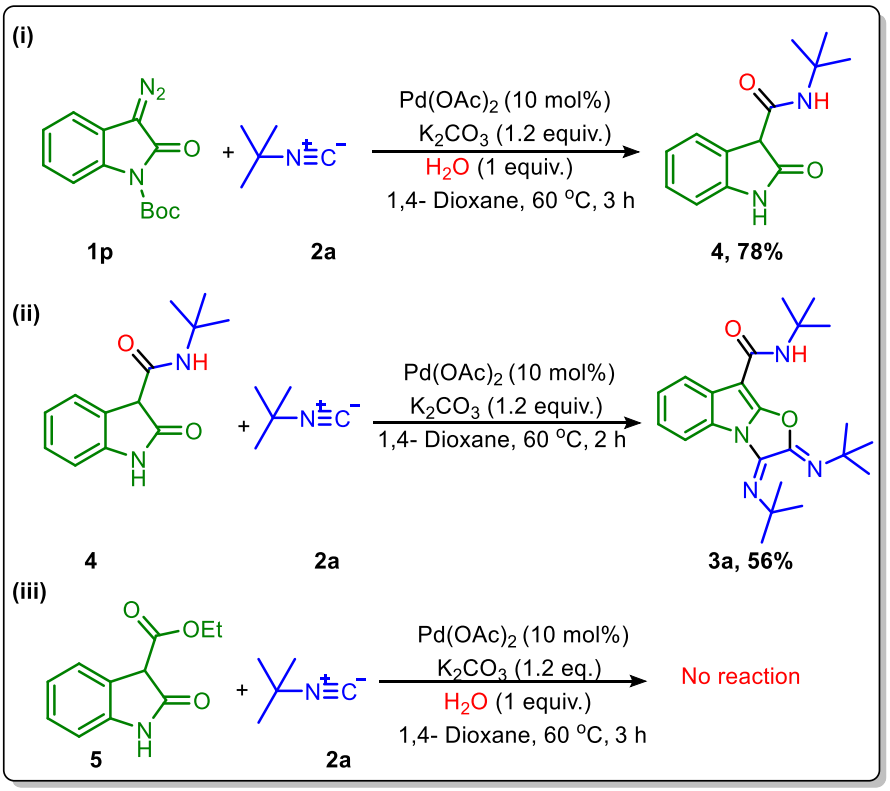

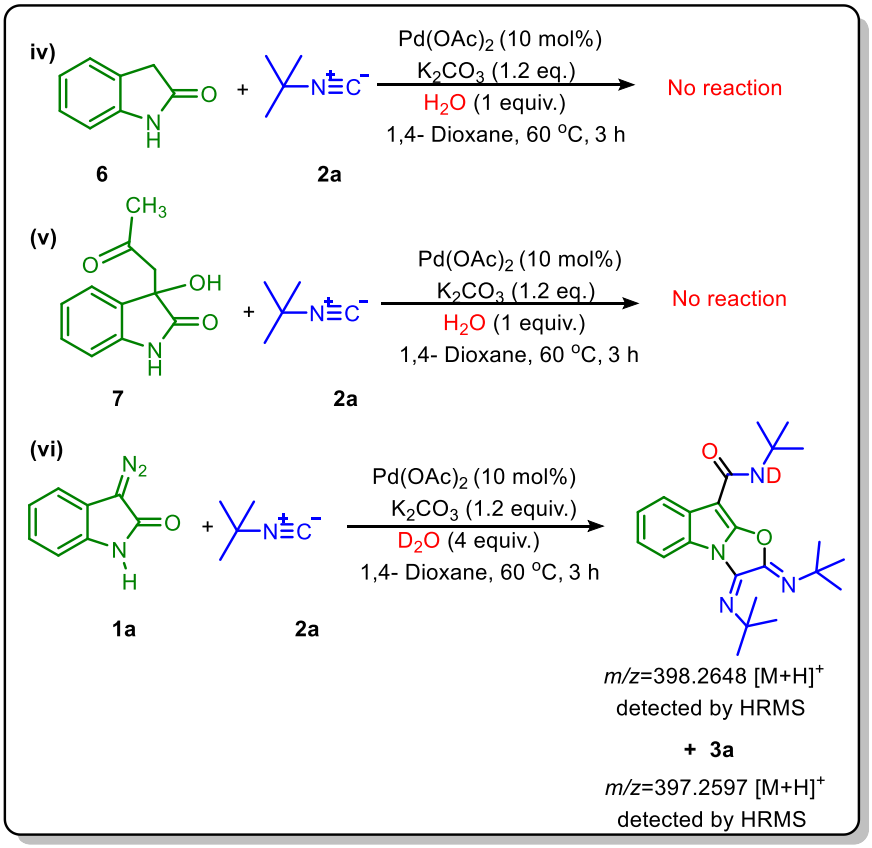

Reaction conditions for **(i) to (v):** Substrate; 1p/4/5/6 or 7 (1equiv.), isocyanides (2) (3.2 equiv.), H_2O (1.0 equiv.), $Pd(OAc)_2$ (10 mol%), K_2CO_3 (1.2 equiv.), 1,4-dioxane (2 mL), 3 h, 60°C. **(vi)** 1a (1equiv.), isocyanides (2) (3.2 equiv.), D_2O (4.0 equiv.), $Pd(OAc)_2$ (10 mol%), K_2CO_3 (1.2 equiv.), 1,4-dioxane (2 mL), 3 h, 60°C.

Scheme 3.5. Control experiments

3.3: Experimental section:

3.3.1: General procedure to synthesize (*2Z,3E*)-N-(tert-butyl)-2,3-bis(tert-butylimino)-2,3-dihydrooxazolo[3,2-a]indole-9-carboxamide (3a-3q)

In a glass tube equipped with a stirrer bar added 3-diazo oxindole (1.0 equiv., 50 mg, 0.31 mmol), H_2O (1.0 equiv., 5.6 µL, 0.31 mmol), $Pd(OAc)_2$ (10 mol%, 7 mg), K_2CO_3 (1.5 equiv., 65 mg, 0.47 mmol) and 2 mL of 1,4-dioxane as a solvent. Then, the resulting reaction mixture was allowed to be stirred at 60 °C in a preheated oil bath and added *tert*-butyl isocyanide (3.2 equiv., 116 µL, 0.99 mmol) slowly with the help of a syringe. After completion of the reaction as indicated by TLC, work-up of the reaction mixture was done using ethyl acetate and distilled water in a 2:1 ratio followed by the evaporation of volatiles under reduced pressure. Next, the crude mixture was purified by column chromatography using ethyl acetate in hexane as eluents affording the corresponding (*2Z,3E*)-N-(tert-butyl)-2,3-bis(tert-butylimino)-2,3-dihydrooxazolo[3,2-a]indole-9 carboxamide (3a-3w) in 37- 76 % yields.

3.3.2: General method for the synthesis of 3-diazo oxindoles (1a-1p)[19-20]

A mixture of isatin (1.0 equiv., 1g, 6.80mmol) and *para*-tosyl hydrazones (1.1 equiv., 1.39 gm, 7.48 mmol) were added in methanol as solvent (~ 20 mL) at 60 °C and stirred the resulting mixture for 5 to 6 h, a highly yellow colored solid 3-(2-(p-tolyl) hydrazono) indolin-2-one intermediates was filtered. The filtered solid and NaOH (2.0 equiv., 13.6mmol) were dissolved in a mixture of THF and water in a ratio of 1:2 and stirred the mixture at room temperature for 5 h. Upon complete conversion of the starting materials, work-up of the reaction with ethyl acetate and distilled water in a 2:1 ratio was done and the volatiles were removed using a high vacuum. The 3-diazo oxindole (83%, 900 mg) was obtained as an orange-red solid and used for the next step without further purification. *(Substrates 5 and 7 were synthesized using previously reported methods)*[21-22]

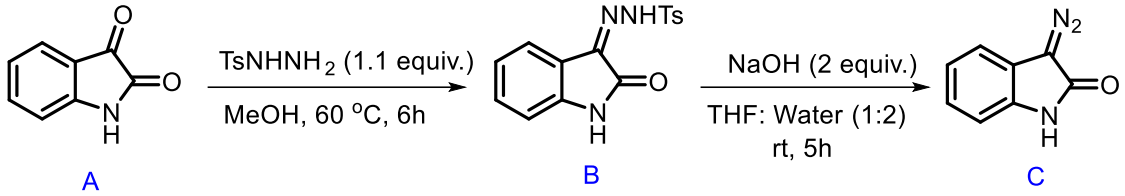

Scheme 3.6: Synthesis of 3-diazo oxindole

3.3.3: Computational details

All of the structures in the study were optimized using the DFT-B3LYP[23] method with the 6-31+G(d,p)[24] basis set for all atoms except for Pd, which uses the SDD method with its own electrostatic potential[25]. The optimization has been conducted in presence of solvent 1,4-Dioxane using solvation model density (SMD) approximation[26]. At the same level of theory, frequency studies were also done to make sure that the stationary points were either local minimums (with no imaginary frequencies) or transition states (with one imaginary frequency). Further energy refinement was also done using single-point calculations on the optimized geometries at the Minnesota density functional M06[27] with a larger basis set 6-31++G(2d,2p)[28] for all non-metal atoms. The previous level's basis for Pd and solvent corrections was maintained. The solvated Gibbs free energy, which was utilized for discussion, was determined by adding thermal correction to the Gibbs energy with the single-point electronic energy. The visualization and results analysis were carried out by using Chemcraft visualization Software.[29] All the DFT calculations were performed using Gaussian 16 program.[30]

3.3.4: Characterization data

^{1}H NMR (400 MHz, $CDCl_3$) and $^{13}C\{^{1}H\}$ NMR (100 MHz, $CDCl_3$) spectra of (*2Z,3E*)-N-(tert-butyl)-2,3-bis(tert-butylimino)-2,3-dihydrooxazolo[3,2-a]indole-9-carboxamide (3a)

Purification by column chromatography (EtOAc: Hexane v/v 1:19) afforded 3a; yellow solid, yield = 71% (88 mg, 0.223mmol), ^{1}H NMR (400 MHz, $CDCl_3$): 8.20 (d, *J*= 7.2 Hz, 1H), 7.89 (d, *J*= 7.6 Hz, 1H), 7.27-7.18 (m, 2H), 5.70 (s, 1H), 1.52 (s, 9H), 1.50 (s, 9H), 1.47 (s, 9H) ppm. $^{13}C\{^{1}H\}$ NMR (100 MHz, $CDCl_3$): δ 162.3, 148.8, 136.5, 133.0, 128.9, 127.4, 124.2, 123.1, 121.9, 112.6, 87.8, 57.6, 55.9, 51.4, 30.0, 29.5, 29.4 ppm. HRMS (ESI-TOF) m/z: $[M + H]^+$ calcd. for $C_{23}H_{33}N_4O_2$ 397.2604; found 397.2601.

^{1}H NMR (400 MHz, $CDCl_3$) and $^{13}C\{^{1}H\}$ NMR (100 MHz, $CDCl_3$) spectra of (*2Z,3E*)-N-(2,4,4-trimethylpentan-2-yl)-2,3-bis((2,4,4-trimethylpentan-2-yl)imino)-2,3-dihydrooxazolo[3,2-a]indole-9-carboxamide (3b)

Purification by column chromatography (EtOAc: Hexane v/v 1:19) afforded 3b; Yellow solid, yield = 57% (101mg, 0.179mmol), ^{1}H NMR (400 MHz, $CDCl_3$): 8.24 (d, *J*= 8 Hz, 1H), 7.94 (d, *J*= 8 Hz, 1H), 7.28-7.19 (m, 2H), 5.62 (s, 1H), 2.01 (s, 2H), 1.92 (s, 4H), 1.58 (s, 6H), 1.55 (s, 6H), 1.51 (s, 6H), 1.03 (s, 9H), 1.00 (s, 9H), 1.00 (s, 9H) ppm. $^{13}C\{^{1}H\}$ NMR (100 MHz, $CDCl_3$): δ 162.3, 148.4, 136.2, 131.8, 129.0, 127.5, 124.2, 123.1, 122.1, 112.5, 87.7, 61.4, 60.0, 55.3, 54.3, 54.1, 51.1, 32.2, 32.1, 32.0, 31.9, 31.7, 31.6, 31.0, 30.3, 30.2 ppm. HRMS (ESI-TOF) m/z: $[M + H]^+$ calcd. for $C_{35}H_{57}N_4O_2$ 565.4487; found 565.4487.

^{1}H NMR (400 MHz, $CDCl_3$) and $^{13}C\{^{1}H\}$ NMR (100 MHz, $CDCl_3$) spectra of (*2Z,3E*)-N-cyclohexyl-2,3-bis(cyclohexylimino)-2,3-dihydrooxazolo[3,2-a]indole-9-carboxamide (3c)

Purification by column chromatography (EtOAc: Hexane v/v 1:19) afforded 3c; Yellow solid, yield = 60% (89mg, 0.188mmol), ^{1}H NMR (400 MHz, $CDCl_3$): 8.11 (d, *J*= 8.0 Hz, 1H), 7.87 (d, *J*= 8.0 Hz, 1H), 7.27-7.19 (m, 2H), 5.78 (d, *J*= 8.0 Hz, 1H), 4.78-4.71 (m, 1H), 4.09-3.97 (m, 2H), 2.00-1.26 (m, 30H) ppm. $^{13}C\{^{1}H\}$ NMR (100 MHz, $CDCl_3$): δ 160.7, 148.1, 138.2, 133.3, 127.6, 126.1, 123.1, 122.1, 120.5, 111.6, 86.7, 56.3, 55.3, 46.2, 32.9, 32.1, 32.0, 24.8, 24.7, 24.6, 23.4, 23.3, 22.7 ppm. HRMS (ESI-TOF) m/z: $[M + H]^+$ calcd. for $C_{29}H_{39}N_4O_2$ 475.3069; found 475.3073.

^{1}H NMR (400 MHz, $CDCl_3$) and $^{13}C\{^{1}H\}$ NMR (100 MHz, $CDCl_3$) spectra of (*2Z,3E*)-N-(tert-butyl)-2,3-bis(tert-butylimino)-7-methoxy-2,3-dihydrooxazolo[3,2-a]indole-9-carboxamide (3d)

Purification by column chromatography (EtOAc: Hexane v/v 1:19) afforded 3d; Yellow solid, yield = 76% (86mg, 0.201mmol), ^{1}H NMR (400 MHz, $CDCl_3$): δ 7.77 (d, *J*= 2.4 Hz, 1H), 7.74 (s, 1H), 6.80 (dd, *J*= 8.8, 2.8 Hz, 1H), 5.70 (s, 1H), 3.86 (s, 3H), 1.50 (s, 9H), 1.49 (s, 9H), 1.46 (s, 9H) ppm. ^{13}C{^{1}H} NMR (100 MHz, $CDCl_3$): δ 162.6, 157.1, 149.2, 136.4, 132.8, 130.0, 121.8, 113.3, 112.2, 104.5, 87.8, 57.6, 55.8, 51.4, 30.0, 29.5, 29.4 ppm. HRMS (ESI-TOF) m/z: $[M + H]^+$ calcd. for $C_{24}H_{35}N_4O_3$ 427.2709; found 427.2712.

^{1}H NMR (400 MHz, $CDCl_3$) and ^{13}C{^{1}H} NMR (100 MHz, $CDCl_3$) spectra of (2Z,3E)-N-cyclohexyl-2,3-bis(cyclohexylimino)-7-methoxy-2,3-dihydrooxazolo[3,2-a]indole-9-carboxamide (3e)

Purification by column chromatography (EtOAc: Hexane v/v 1:19) afforded 3e; Yellow solid, yield = 68% (137 mg, 0.272mmol), ^{1}H NMR (400 MHz, $CDCl_3$): 7.75-7.73 (m, 2H), 6.81 (dd, *J*= 8.4, 2.4 Hz, 1H), 5.74 (d, *J*= 8.0 Hz, 1H), 4.76-4.69 (m, 1H), 3.86 (s, 3H), 2.00-1.27 (m, 30H) ppm. ^{13}C{^{1}H} NMR (100 MHz, $CDCl_3$): δ 162.0, 157.1, 149.4, 139.2, 134.3, 130.0, 121.7, 113.5, 112.1, 104.7, 87.7, 57.4, 56.4, 55.7, 47.3, 34.0, 33.2, 33.1, 29.8, 25.85, 25.77, 25.72, 24.5, 24.4, 23.8 ppm. HRMS (ESI-TOF) m/z: $[M + H]^+$ calcd. for $C_{30}H_{41}N_4O_3$ 505.3179; found 505.3179.

^{1}H NMR (400 MHz, $CDCl_3$) and ^{13}C{^{1}H} NMR (100 MHz, $CDCl_3$) spectra of (*2Z,3E*)-N-(tert-butyl)-2,3-bis(tert-butylimino)-7-methyl-2,3-dihydrooxazolo[3,2-a]indole-9-carboxamide (3f)

Purification by column chromatography (EtOAc: Hexane v/v 1:19) afforded 3f; Yellow solid, yield = 73% (86.5 mg, 0.211mmol), ^{1}H NMR (400 MHz, $CDCl_3$): 8.04 (s,1H), 7.75 (d, *J*= 8.0 Hz, 1H), 7.01 (dd, *J*= 1.2, 8.4 Hz, 1H), 5.69 (s, 1H), 2.41 (s, 3H), 1.51 (s, 9H), 1.49 (s, 9H), 1.46 (s, 9H) ppm. ^{13}C{^{1}H} NMR (100 MHz, $CDCl_3$): δ 162.6, 148.9, 136.6, 133.9, 132.9, 129.0, 125.6, 124.2, 122.1, 112.2, 87.6, 57.6, 55.8, 51.4, 30.0, 29.5, 29.3, 21.8 ppm. HRMS (ESI-TOF) m/z: $[M + H]^+$ calcd. for $C_{24}H_{35}N_4O_2$ 411.2760; found 411.2755.

^{1}H NMR (400 MHz, $CDCl_3$) and ^{13}C{^{1}H} NMR (100 MHz, $CDCl_3$) spectra of (*2Z,3E*)-7-methyl-N-(2,4,4-trimethylpentan-2-yl)-2,3-bis((2,4,4-trimethylpentan-2-yl)imino)-2,3-dihydrooxazolo[3,2-a]indole-9-carboxamide (3g)

Purification by column chromatography (EtOAc: Hexane v/v 1:19) afforded 3g; Yellow solid, yield = 65% (108mg, 0.188mmol), ^{1}H NMR (400 MHz, $CDCl_3$): 8.08 (s, 1H), 7.80 (d, *J*= 8.0 Hz, 1H), 7.02 (dd, *J*= 8.0 Hz, 1.2 Hz, 1H), 5.61 (s, 1H), 2.42 (s, 3H), 2.00 (s, 2H), 1.92 (s, 2H), 1.91 (s, 2H), 1.57 (s, 6H), 1.54 (s, 6H), 1.51 (s, 6H), 1.02 (s, 9H), 1.00 (s, 9H), 0.99 (s, 9H) ppm. ^{13}C{^{1}H} NMR (100 MHz, $CDCl_3$): δ 162.5, 148.6, 136.3, 133.9, 131.7, 129.2, 125.6, 124.2, 122.2, 112.1, 87.4, 61.4, 59.9, 55.3, 54.4, 54.1, 51.0, 32.2, 32.1, 32.0, 31.9, 31.7, 31.6,

31.0, 30.3, 30.1, 29.8, 21.8 ppm. HRMS (ESI-TOF) m/z: $[M + H]^+$ calcd. for $C_{36}H_{59}N_4O_2$ 579.4638; found 579.4632.

^{1}H NMR (400 MHz, $CDCl_3$) and $^{13}C\{^1H\}$ NMR (100 MHz, $CDCl_3$) spectra of (*2Z,3E*)-N-cyclohexyl-2,3-bis(cyclohexylimino)-7-methyl-2,3-dihydrooxazolo[3,2-a]indole-9-carboxamide (3h)

Purification by column chromatography (EtOAc: Hexane v/v 1:19) afforded 3h; Yellow solid, yield = 63% (88.8mg, 0.182mmol), ^{1}H NMR (400 MHz, $CDCl_3$): 7.95 (s, 1H), 7.73 (d, 1H), 7.03 (dd, *J*= 8.4, 1.2 Hz, 1H), 5.75 (d, *J*= 7.6 Hz, 1H), 4.77-4.71 (m, 1H), 4.08-3.96 (m, 2H), 2.43 (s, 3H), 1.82-1.24 (m, 30H) ppm. $^{13}C\{^1H\}$ NMR (100 MHz, $CDCl_3$): δ 160.8, 148.1, 138.3, 133.3, 132.8, 127.8, 124.3, 123.2, 120.8, 111.3, 86.4, 56.3, 55.3, 46.2, 32.9, 32.1, 32.0, 28.6, 24.74, 24.67, 24.6, 23.4, 23.3, 22.7, 20.8 ppm. HRMS (ESI-TOF) m/z: $[M + H]^+$ calcd. for $C_{30}H_{41}N_4O_2$ 489.3230; found 489.3224.

^{1}H NMR (400 MHz, $CDCl_3$) and $^{13}C\{^1H\}$ NMR (100 MHz, $CDCl_3$) spectra of (*2Z,3E*)-N-(tert-butyl)-2,3-bis(tert-butylimino)-6-methoxy-2,3-dihydrooxazolo[3,2-a]indole-9-carboxamide (3i)

Purification by column chromatography (EtOAc: Hexane v/v 1:19) afforded 3i; Yellow solid, yield = 59% (66.5mg, 0.156mmol), ^{1}H NMR (400 MHz, $CDCl_3$): δ 8.06 (d, *J*= 8.8 Hz, 1H), 7.49 (d, *J*= 2.4 Hz, 1H), 6.86 (dd, *J*= 8.8 Hz, 2.4 Hz, 1H), 5.67 (s, 1H), 3.83 (s, 3H), 1.51 (s, 9H), 1.49 (s, 9H), 1.46 (s, 9H) ppm. $^{13}C\{^1H\}$ NMR (100 MHz, $CDCl_3$): δ 162.4, 156.7, 147.9, 136.8, 133.1, 128.1, 122.5, 122.4, 111.6, 98.2, 87.7, 57.5, 55.9, 55.7, 51.3, 30.0, 29.5, 29.4 ppm. HRMS (ESI-TOF) m/z: $[M + H]^+$ calcd. for $C_{24}H_{35}N_4O_3$ 427.2709; found 427.2714.

^{1}H NMR (400 MHz, $CDCl_3$) and $^{13}C\{^1H\}$ NMR (100 MHz, $CDCl_3$) spectra of (*2Z,3E*)-N-cyclohexyl-2,3-bis(cyclohexylimino)-6-methoxy-2,3-dihydrooxazolo[3,2-a]indole-9-carboxamide (3j)

Purification by column chromatography (EtOAc: Hexane v/v 1:19) afforded 3j; Yellow solid, yield = 53% (70mg, 0.140mmol), ^{1}H NMR (400 MHz, $CDCl_3$): δ 8.00 (d, *J*= 8.0 Hz, 1H), 7.45 (d, *J*= 2.4 Hz, 1H), 6.88 (dd, *J*= 8.8 Hz, 2.4 Hz), 4.77-4.71 (m, 1H), 4.08-3.95 (m, 1H), 3.85 (s, 3H), 2.00-1.24 (m, 30H) ppm. $^{13}C\{^1H\}$ NMR (100 MHz, $CDCl_3$): δ 170.8, 161.9, 156.9, 148.2, 139.5, 134.5, 128.0, 122.3, 122.2, 111.7, 98.3, 87.6, 57.3, 56.4, 55.8, 47.3, 34.0, 33.2, 29.8, 25.9, 25.8, 25.7, 24.5, 24.4, 23.8, 23.1 ppm. HRMS (ESI-TOF) m/z: $[M + H]^+$ calcd. for $C_{30}H_{40}N_4O_3$ 505.3179; found 505.3177.

^{1}H NMR (400 MHz, $CDCl_3$) and $^{13}C\{^1H\}$ NMR (100 MHz, $CDCl_3$) spectra of (*2Z,3E*)-N-(tert-butyl)-2,3-bis(tert-butylimino)-7-nitro-2,3-dihydrooxazolo[3,2-a]indole-9-carboxamide (3l)

Purification by column chromatography (EtOAc: Hexane v/v 1:19) afforded 3l; Yellow solid, yield = 56% (60.5mg, 0.137mmol), ^{1}H NMR (400 MHz, $CDCl_3$): δ 9.15 (d, *J*= 2.0 Hz, 1H), 8.13 (td, *J*= 8.8, 2.0 Hz, 1H), 7.96 (d, *J*= 8.8 Hz, 1H), 5.68 (s, 1H), 1.53 (s, 9H), 1.51 (s, 9H), 1.47 (s, 9H) ppm. ^{13}C{^{1}H} NMR (100 MHz, $CDCl_3$): δ 161.2, 149.7, 144.8, 135.0, 132.3, 130.3, 129.2, 119.0, 118.5, 112.4, 88.7, 58.2, 56.6, 51.7, 30.0, 29.34, 29.27, 28.8 ppm. HRMS (ESI-TOF) m/z: $[M + H]^+$ calcd. for $C_{23}H_{32}N_5O_4$ 442.2454; found 442.2463.

^{1}H NMR (700 MHz, $CDCl_3$), ^{13}C{^{1}H} NMR (175 MHz, $CDCl_3$) and ^{19}F{^{1}H} NMR (376 MHz, $CDCl_3$) spectra of (*2Z,3E*)-N-(tert-butyl)-2,3-bis(tert-butylimino)-7-(trifluoromethoxy)-2,3-dihydrooxazolo[3,2-a]indole-9-carboxamide (3m)

Purification by column chromatography (EtOAc: Hexane v/v 1:19) afforded 3m; Yellow solid, yield = 37% (36.5mg, 0.076mmol), ^{1}H NMR (700 MHz, $CDCl_3$): 8.17 (d, *J*= 1.4 Hz, 1H), 7.91 (d, *J*= 9.1 Hz, 1H), 7.11 (dd, *J*= 8.4, 1.4 Hz, 1H), 5.70 (s, 1H), 1.55 (s, 9H), 1.54 (s, 9H), 1.50 (s, 9H) ppm. ^{13}C{^{1}H} NMR (175 MHz, $CDCl_3$): δ 161.8, 149.4, 145.97, 145.96, 135.7, 132.5, 129.9, 125.6, 121.37, 119.91, 116.7, 115.1, 113.1, 88.0, 57.8, 56.0, 51.4, 29.9, 29.3, 29.2 ppm. ^{19}F{^{1}H} NMR (376 MHz, $CDCl_3$): -57.86 ppm. HRMS (ESI-TOF) m/z: $[M + H]^+$ calcd. for $C_{24}H_{32}F_3N_4O_3$ 481.2427; found 481.2430.

^{1}H NMR (700 MHz, $CDCl_3$), ^{13}C{^{1}H} NMR (175 MHz, $CDCl_3$) and ^{19}F{^{1}H} NMR (376 MHz, $CDCl_3$) spectra of (2Z,3E)-N-(tert-butyl)-2,3-bis(tert-butylimino)-7-fluoro-2,3-dihydrooxazolo[3,2-a]indole-9-carboxamide (3q)

Purification by column chromatography (EtOAc: Hexane v/v 1:19) afforded 3q; Yellow solid, yield = 41% (48mg, 0.116mmol), ^{1}H NMR (700 MHz, $CDCl_3$): δ 7.96 (dd, *J*= 9.8 Hz, 2.8 Hz, 1H), 7.84 (q, *J*= 4.2 Hz, 1H), 6.95 (td, *J*= 8.4 Hz, 2.1 Hz, 1H), 5.69 (s, 1H), 1.55 (s, 9H), 1.53 (s, 9H), 1.50 (s, 9H) ppm. ^{13}C{^{1}H} NMR (175 MHz, $CDCl_3$): δ 162.0, 160.9, 159.5, 149.4, 135.9, 132.6, 130.2, 130.1, 123.7, 113.3, 113.2, 110.6, 110.5, 108.6, 108.4, 87.9, 57.7, 56.0, 51.4, 29.9, 29.4, 29.3 ppm. ^{19}F{^{1}H} NMR (376 MHz, $CDCl_3$): -117.66 ppm. HRMS (ESI-TOF) m/z: $[M + H]^+$ calcd. for $C_{23}H_{32}FN_4O_2$ 415.2509; found 415.2513.

^{1}H NMR (400 MHz, $CDCl_3$) and ^{13}C{^{1}H} NMR (100 MHz, $CDCl_3$) spectra of (*2Z,3E*)-N-(tert-butyl)-2,3-bis(tert-butylimino)-7-chloro-2,3-dihydrooxazolo[3,2-a]indole-9-carboxamide (3r)

Purification by column chromatography (EtOAc: Hexane v/v 1:19) afforded 3r; Yellow solid, yield = 54% (60mg, 0.140mmol), ^{1}H NMR (400 MHz, $CDCl_3$): 8.25 (d, *J*= 2.0 Hz, 1H), 7.78 (d, *J*= 8.0 Hz, 1H), 7.16 (dd, *J*= 2.0, 8.0 Hz, 1H), 5.66 (s, 1H), 1.51 (s, 9H), 1.50 (s, 9H), 1.46 (s, 9H) ppm. ^{13}C{^{1}H} NMR (100 MHz, $CDCl_3$): δ 161.9, 149.2, 135.9, 132.6, 130.2, 130.0,

125.7, 123.3, 121.9, 113.4, 87.6, 57.8, 56.1, 51.5, 30.0, 29.4, 29.3 ppm. HRMS (ESI-TOF) m/z: $[M + H]^+$ calcd. for $C_{23}H_{32}ClN_4O_2$ 431.2214; found 431.2212.

^{1}H NMR (400 MHz, $CDCl_3$) and $^{13}C\{^1H\}$ NMR (100 MHz, $CDCl_3$) spectra of (*2Z,3E*)-7-chloro-N-(2,4,4-trimethylpentan-2-yl)-2,3-bis((2,4,4-trimethylpentan-2-yl)imino)-2,3-dihydrooxazolo[3,2-a]indole-9-carboxamide (3s)

Purification by column chromatography (EtOAc: Hexane v/v 1:19) afforded 3s; Yellow solid, yield = 46% (71mg, 0.119mmol), ^{1}H NMR (400 MHz, $CDCl_3$): δ 8.28 (d, *J*= 4.0 Hz, 1H), δ 7.83 (d, *J*= 8.4 Hz, 1H), 7.18 (dd, *J*= 8.4, 2.0 Hz, 1H), 5.58 (s, 1H), 1.99 (s, 2H), 1.91 (s, 4H), 1.57 (s, 6H), 1.54 (s, 6H), 1.50 (s, 6H), 1.02 (s, 9H), 1.00 (s, 9H), 0.99 (s, 9H) ppm. $^{13}C\{^1H\}$ NMR (100 MHz, $CDCl_3$): δ 161.8, 148.9, 135.5, 131.4, 130.3, 129.9, 125.7, 123.4, 122.0, 113.3, 87.5, 61.6, 60.2, 55.4, 54.3, 54.1, 51.0, 32.14, 32.09, 32.05, 31.9, 31.7, 31.6, 31.0, 30.2, 30.1 ppm. HRMS (ESI-TOF) m/z: $[M + H]^+$ calcd. for $C_{35}H_{56}ClN_4O_2$ 599.4092; found 599.4091.

^{1}H NMR (400 MHz, $CDCl_3$) and $^{13}C\{^1H\}$ NMR (100 MHz, $CDCl_3$) spectra of (*2Z,3E*)-7-bromo-N-(tert-butyl)-2,3-bis(tert-butylimino)-2,3-dihydrooxazolo[3,2-a]indole-9-carboxamide (3t)

Purification by column chromatography (EtOAc: Hexane v/v 1:19) afforded 3t; Yellow solid, yield = 51% (51mg, 0.107mmol), ^{1}H NMR (400 MHz, $CDCl_3$): 8.41 (d, *J*= 2.0 Hz, 1H), 7.73 (d, *J*= 8.0 Hz, 1H), 7.30 (dd, *J*= 2.0, 8.0 Hz, 2H), 5.66 (s, 1H), 1.51 (s, 9H), 1.50 (s, 9H), 1.46 (s, 9H) ppm. $^{13}C\{^1H\}$ NMR (100 MHz, $CDCl_3$): δ 161.9, 149.1, 135.8, 132.6, 130.6, 126.1, 126.0, 124.8, 117.7, 113.8, 87.4, 57.8, 56.1, 51.5, 30.0, 29.4, 29.3 ppm. HRMS (ESI-TOF) m/z: $[M + H]^+$ calcd. for $C_{23}H_{32}BrN_4O_2$ 475.1709; found 475.1709.

^{1}H NMR (400 MHz, $CDCl_3$) and $^{13}C\{^1H\}$ NMR (100 MHz, $CDCl_3$) spectra of (2Z,3E)-7-bromo-N-cyclohexyl-2,3-bis(cyclohexylimino)-2,3-dihydrooxazolo[3,2-a]indole-9-carboxamide (3u)

Purification by column chromatography (EtOAc: Hexane v/v 1:19) afforded 3u; Yellow solid, yield = 48% (56mg, 0.101mmol), ^{1}H NMR (400 MHz, $CDCl_3$): δ 8.32 (d, *J*= 2.0 Hz, 1H), 7.71 (d, *J*= 8.4 Hz, 1H), 7.31 (dd, *J*= 8.4 Hz, 2.0 Hz, 1H), 5.71 (d, *J*= 7.6 Hz, 1H), 4.76-4.70 (m, 1H), 4.08-3.96 (m, 1H), 2.00-1.24 (m, 30H) ppm. $^{13}C\{^1H\}$ NMR (100 MHz, $CDCl_3$): δ 161.3, 149.3, 138.7, 134.1, 130.5, 126.1, 125.8, 124.7, 117.7, 114.0, 87.4, 57.6, 56.6, 47.5, 33.9, 33.2, 33.1, 29.8, 25.81, 25.76, 25.7, 24.5, 24.4, 23.8 ppm. HRMS (ESI-TOF) m/z: $[M + H]^+$ calcd. for $C_{29}H_{38}BrN_4O_2$ 553.2178; found 553.2180.

^{1}H NMR (700 MHz, $CDCl_3$) and $^{13}C\{^{1}H\}$ NMR (175 MHz, $CDCl_3$) spectra of (2Z,3E)-N-(tert-butyl)-2,3-bis(tert-butylimino)-6-chloro-2,3-dihydrooxazolo[3,2-a]indole-9-carboxamide (3v)

Purification by column chromatography (EtOAc: Hexane v/v 1:19) afforded 3v; Yellow solid, yield = 50% (56mg, 0.129mmol), ^{1}H NMR (700 MHz, $CDCl_3$): δ 8.17 (d, *J*= 8.4 Hz, 1H), 7.90 (d, *J*= 2.1 Hz, 1H), 7.26 (dd, *J*= 8.4, 1.4 Hz, 1H), 5.71 (s, 1H), 1.55 (s, 9H), 1.53 (s, 9H), 1.50 (s, 9H) ppm. $^{13}C\{^{1}H\}$ NMR (175 MHz, $CDCl_3$): δ 161.9, 148.6, 135.9, 132.5, 128.7, 124.50, 122.8, 112.1, 87.8, 57.8, 56.1, 51.4, 29.9, 29.3, 29.2 ppm. HRMS (ESI-TOF) m/z: $[M + H]^+$ calcd. for $C_{23}H_{33}N_4O_2$ 431.2213; found 431.2214.

^{1}H NMR (400 MHz, $CDCl_3$) and $^{13}C\{^{1}H\}$ NMR (100 MHz, $CDCl_3$) spectra of N-(tert-butyl)-2-oxoindoline-3-carboxamide (4)

Purification by column chromatography (EtOAc: Hexane v/v 1:9) afforded 4; Off white solid, yield = 78% (70mg, 0.301mmol), ^{1}H NMR (400 MHz, $CDCl_3$): δ 8.25 (s, 1H), 7.69 (d, *J*= 7.2 Hz, 1H), 7.33 (s, 1H), 7.24 (t, *J*= 6.8 Hz, 1H), 7.10 (t, *J*= 7.6 Hz, 1H), 6.87 (d, *J*= 7.2, 1H), 4.18 (s, 1H), 1.37 (s, 9H) ppm. $^{13}C\{^{1}H\}$ NMR (100 MHz, $CDCl_3$): δ 175.7, 162.5, 140.5, 128.6, 127.4, 124.4, 123.2, 109.8, 51.7, 51.4, 28.8 ppm. HRMS (ESI-TOF) m/z: $[M + H]^+$ calcd. for $C_{13}H_{16}N_2O_2Na$ 255.1109; found 255.1110.

3.4: Conclusion

In summary**,** we have developed a Pd-catalysed and amide-assisted multicomponent reaction of 3-diazo oxindole, isocyanide, and water to generate oxazole-fused indole scaffolds. The functional group tolerance at different positions of 3-diazo oxindole along with different isocyanides was tested and the corresponding products were obtained in 37-76% isolated yields. Besides, a DFT study was performed to get an overview of the proposed mechanism which recommended that the reaction involves amide formation at the C-3 position via isocyanide insertion which subsequently assisted [3+1+1] annulation reaction to furnish oxazole-fused indoles. Also, the role of *in-situ* generated amide to assist the annulation reaction was confirmed by the set-up of different control experiments.

3.5: References

1. (a) Khetmalis, Y. M.; Shivani, M.; Murugesan, S.; Chandra Sekhar, K. V. G. Oxindole and its derivatives: A review on recent progress in biological activities. *Biomed.*

Pharmacother. **2021**, *141*, 111842. (b) Rudrangi, S. R. S.; Bontha, V. K.; Manda, V.R.; Bethi, S. Oxindoles and their pharmaceutical significance-an overview. *Asian J. Res. Chem*. **2011**, *4*, 335-338. (c) Yin, L.; Hu, Q.; Emmerich, J.; Lo, M. M. C.; Metzger, E.; Ali, A.; Hartmann, R. W. Novel pyridyl-or isoquinolinyl-substituted indolines and indoles as potent and selective aldosterone synthase inhibitors. *J. Med. Chem*. **2014**, *57*, 5179–5189. (d) Monakhova, N.; Ryabova, S. and Makarov, V. Synthesis and some biological properties of Pyrrolo[1,2-*a*]indoles. *J. Heterocycl. Chem*. **2016**, *53*, 685–709. (e) Bunders, C.; Cavanagh, J.; Melander, C. Flustramine inspired synthesis and biological evaluation of pyrroloindoline triazole amides as novel inhibitors of bacterial biofilms. *Org. Biomol. Chem*. **2011**, *9*, 5476–5481. (f) Gaste, L. M.; Wyman, P. A.; Ellis, E. S.; Brown, A. M.; Young, T. J. 5-HT_4receptor antagonists : oxazolo, oxazino and oxazepino[3,2-a]indole derivatives. *Bioorg. Med. Chem. Lett.* **1994**, *4*, 667-668. (g) Sumpter, W. C. *T H E CHEMISTRY OF ISATIN*, *Chem. Rev.* **1944**, *34*, 393-434.

2. (a) Mei, L. Y.; Wei, Y.; Tang, X. Y.; Shi, M. Catalyst-Dependent Stereodivergent and Regioselective Synthesis of Indole-Fused Heterocycles through Formal Cycloadditions of Indolyl-Allenes. *J. Am. Chem. Soc*, **2015**, *137*, 8131–8137. (b) Pan, G.; Lu, L.; Zhuang, W.; Huang, Q. Synthesis of Indole-Fused Six-, Seven-, or Eight-Membered N,O-Heterocycles via Rhodium-Catalyzed *NH*-Indole-Directed C–H Acetoxylation/Hydrolysis/Annulation. *J. Org. Chem.* **2021**, *86*, 16753–16763. (c) Fang, X.; Gao, S.; Wu, Z.; Yao, H.; Lin, A. Pd (II)-Catalyzed oxidative dearomatization of indoles: substrate-controlled synthesis of indolines and indolones. *Org. Chem. Front.* **2017**, *4*, 292–296. (d) Huang, Y.; Yang, Y.; Song, H.; Liu, Y.; Wang, Q. Synthesis of Structurally Diverse 2,3-Fused Indoles via Microwave-Assisted $AgSbF_6$-Catalysed Intramolecular Difunctionalization of *o*-Alkynylanilines. *Sci. Rep.* **2015**, *5*, 13516. (e) Suzdalev, K. F.; Den'Kina, S. V.; Tkachev, V. V. Formation of the same pyrimido[1,2-*a*]indoles from 1-(oxiran-2-ylmethyl)-1*H*-indole or [1,3]oxazolo[3,2-*a*]indole derivatives in its reactions with aromatic amines. *Tetrahedron*. **2013**, *69*, 8785–8789.
3. Zhang, M.; Duan, Y.; Li, W.; Cheng, Y.; Zhu, C. Visible-light-induced aerobic dearomative reaction of indole derivatives: access to heterocycle fused or spirocyclo indolones. *Chem. Comm.* **2016**, *52*, 4761–4763.
4. Oparina, L. A.; Kolyvanov, N. A.; Ushakov, I. A.; Mal'kina, A. G.; Vashchenko, A. V.; Trofimov, B. A. Metal-and Solvent-free **Synthesis** of Functionalized Dihydrooxazolo [3, 2-a] indoles by One-Pot Tandem Assembly of 3H-Indoles and Propargylic Alcohols. *Synthesis.* **2019**, *51*, 1445–1454.

5. Zhao, Y.; Niu, X.; Yang, H.; Yang, J.; Wang, Z.; Wang, Q. Substrate-directed divergent synthesis of fused indole polycycles through Rh (ii)-catalyzed cascade reactions of bis (diazo) indolin-2-ones. *Chem. Comm.* **2022**, *58*, 8576–8579.
6. (a) Ciulla, M. G.; Zimmermann, S.; Kumar, K. *Org Biomol Chem*, **2019**, *17*, 413–431. (b) Xiang, Y.; Wang, C.; Ding, Q.; Peng, Y. Diazo Compounds: Versatile Synthons for the Synthesis of Nitrogen Heterocycles via Transition Metal-Catalyzed Cascade C–H Activation/Carbene Insertion/Annulation Reactions. *Adv. Synth. Catal.* **2019**, *361*, 919-944. (c) Baccalini, A.; Faita, G.; Zanoni, G.; Maiti, D. Transition Metal Promoted Cascade Heterocycle Synthesis through C−H Functionalization. *Chem. Eur. J.* **2020**, *26*, 9749–9783. (d) Alahyen, I.; Benhamou, L.; Dalla, V.; Taillier, C.; Comesse, S.; 20 Years of Forging N-Heterocycles from Acrylamides through Domino/Cascade Reactions. *Synthesis.* **2021**, *53*, 3409–3439. (e) Connon, R.; Guiry, P. J. Recent advances in the development of one-pot/multistep syntheses of 3, 4-annulated indoles. *Tet. Lett*. **2020**, 61, 151696.
7. (a) Hong, F. L.; Ye, L. W. Transition metal-catalyzed tandem reactions of ynamides for divergent N-heterocycle synthesis. *Acc. Chem. Res*. **2020**, *53*, 2003–2019. (b) D'Souza, D. M.; Mueller, T. J. Multi-component syntheses of heterocycles by transition-metal catalysis. *Chem. Soc. Rev.* **2007**, *36*, 1095-1108. (c) Xia, Y.; Wang, J. Transition-Metal-Catalyzed Cross-Coupling with Ketones or Aldehydes via *N*-Tosylhydrazones. *J. Am. Chem. Soc*. **2020**, *142*, 10592–10605.
8. (a) Qiu, G.; Wang, Q.; Zhu. Palladium-Catalyzed Three-Component Reaction of Propargyl Carbonates, Isocyanides, and Alcohols or Water: Switchable Synthesis of Pyrroles and Its Bicyclic Analogues. J. *Org. Lett*. **2017**, 19, 270–273. (b) Tashrifi, Z.; Khanaposhtani, M. M.; Gholami, F.; Larijani, B.; Mahdavi, M. Rapid Access to Fused Tetracyclic N-Heterocycles via Amino-to-Alkyl 1,5-Palladium Migration Coupled with Intramolecular $C(sp^3)$–$C(sp^2)$ Coupling. *Adv. Synth. Catal*. **2023**, *365*, 926–947. (c) Collet, J. W.; Roose, T. R.; Weijers, B.; Maes, B. U. W.; Ruijter, E.; Orru, R. V. A. Recent advances in palladium-catalyzed isocyanide insertions. *Molecules*. **2020**, *25*, 4906. (d) Zhou, F.; Ding, K.; Cai, Q. Palladium-Catalyzed Amidation of *N*-Tosylhydrazones with Isocyanides. *Chem. Eur. J.* **2011**, *17*, 12268–12271. (e) Tian, Y.; Tian, L.; He, X.; Li, C.; Jia, X.; Li, J. Indium (III) chloride-catalyzed isocyanide insertion reaction to construct complex spirooxindole. *Org. Lett*. **2015**, *17*, 4874–4877.
9. Cao, M.; Fang, Y. L.; Wang, Y. C.; Xu, X. J.; Xi, Z. W.; Tang, S. $Ce(OTf)_3$-Catalyzed Multicomponent Reaction of Alkynyl Carboxylic Acids, *tert*-Butyl Isocyanide, and

Azides for the Assembly of Triazole–Oxazole Derivatives. *ACS Comb. Sci*. **2020**, *22*, 268–273.

10. Sisodiya, S.; Acharya, A.; Nagpure, M.; Roy, N.; Giri, S. K.; Yadav, H. R.; Choudhury, A. R.; Guchhait, S. K. A cascade reaction of indolyl-migratory isocyanide insertion, scaffold rearrangement and redox-neutral event with isocyanide as a $C_{(sp^3)}$H–N synthon efficiently constructs indolylisoindolinones. *Chem. Comm.* **2022**, *58*, 11827–11830.
11. Lu, S.; Ding, C. H. Xu, B. Triple-Consecutive Isocyanide Insertions with Aldehydes: Synthesis of 4-Cyanooxazoles. *Org. Lett*. **2023**, *25*, 849–854.
12. Soam, P.; Gaba, H.; Mandal, D.; Tyagi, V. A Pd-catalyzed one-pot cascade consisting of C–C/C–O/N–N bond formation to access benzoxazine fused 1, 2, 3-triazoles. *Org. Biomol. Chem*. **2021**, *19*, 9936–9945.
13. Soam, P.; Mandal, D.; Tyagi, V. Divergent and Selective Synthesis of 3-Alkylidene Oxindoles Using Pd-Catalyzed Multicomponent Reaction. *J. Org. Chem.* **2023**, *88*, 11023–11035.
14. (a) Vol, B.; McDANIEL, D. H.; Brown, H. C. An extended table of Hammett substitutent constants based on the ionization of substituted benzoic acids. *J. Org. Chem*. **1958**, *23*, 420-427. (b) Yau, H. M.; Haines, R. S.; Harper, J. B.; A Robust, "One-Pot" Method for Acquiring Kinetic Data for Hammett Plots Used To Demonstrate Transmission of Substituent Effects in Reactions of Aromatic Ethyl Esters. *J. Chem. Educ*. **2015**, *92*, 538–542. (c) Khansole, S. V.; Vibhute, Y. B. Kinetic of iodination of phenol and substituted phenols by pyridinium iodochloride in methanol. *J. Iran. Chem. Res.* **2009**, *2*, 151-156.
15. Zhang, X.; Chung, L. W.; Wu, Y. D. New mechanistic insights on the selectivity of transition-metal-catalyzed organic reactions: the role of computational chemistry. *Acc. Chem. Res*. **2016**, *49*, 1302–1310.
16. (a) Xia, Y.; Qiu, D.; Wang, J. Transition-metal-catalyzed cross-couplings through carbene migratory insertion. *Chem. Rev*. **2017**, *117*, 13810–13889. (b) Liu, Y.; Luo, Z.; Zhang, J. Z.; Xia, F. DFT calculations on the mechanism of transition-metal-catalyzed reaction of diazo compounds with phenols: O–H insertion versus C–H insertion. *J. Phys. Chem. A*, **2016**, *120*, 6485–6492. (c) Bi, X.; Liu, Z.; Cao, S.; Wu, J.; Zanoni, G.; Sivaguru, P. Palladium (II)-catalyzed cross-coupling of diazo compounds **and** isocyanides to access ketenimines. *ACS Catal*. **2020**, *10*, 12881–12887. (d) Zhang, H.; Geng, Z. Y.; Tai Wang, K. Theoretical studies on the mechanism

of palladium(II)-catalysed *ortho*-carboxylation of acetanilide with CO. J. *Chem. Sci.* **2014**, *126*, 265-272.

17. (a) Bakulina, O.; Inyutina, A.; Dar'in, D.; Krasavin, M. Multicomponent reactions involving diazo reagents: a 5-year update. *Molecules*. **2021**, *26*, 6563. (b) Gu, H.; Qiu, Z.; Zhang, Z.; Li, J.; Yan, B. A mechanistic study of Pd (OAc) 2-catalyzed intramolecular C–H functionalization reaction involving CO/isonitrile insertion. *Dalton Trans*. **2015**, *44*, 9839–9846.
18. (a) Chen, F.; Zhu, C.; Jiang, H. [3+1+1] Annulation Reaction of Benzo-1,2-Quinones, Aldehydes and Hydroxylamine Hydrochloride: Access to Benzoxazoles with Inorganic Nitrogen Source. *Adv. Synth. Catal.* **2021**, *363*, 2124-2132. (b) Zhu, W.Q.; Fang, Y.C.; Han, W.Y.; Li, F.; Yang, M.G.; Chen, Y.Z. Palladium-catalyzed [2 + 2 + 1] annulation: access to chromone fused cyclopentanones with cyclopropenone as the CO source. *Org. Chem. Front.* **2021**, *8*, 3082-3090.
19. Muthusamy, S.; Gunanathan, C.; Nethaji, M. *J. Org. Chem.* **2004**, *69*, 5631–5637.
20. Murphy, G. K.; Abbas, F. Z.; Poulton, A. V.; *Adv. Synth. Catal*. **2014**, *356*, 2919–2923.Jeankumar, V. U.; Alokam, R.; Sridevi, J. P.; Suryadevara, P.; Matikonda, S. S.; Peddi, S.; Sahithi, S.; Alvala, M.; Yogeeswari, P.; Sriram, D. *Chem. Biol. Drug. Des.* **2014**, *83*, 498–506.
21. Spingler, B.; Schnidrig, S.; Todorova, T.; Wild, F. *CrystEngComm*, **2012**, *14*, 751–757.
22. Chen, X.; Zhu, W.; Qian, W.; Feng, E.; Zhou, Y.; Wang, J.; Jiang, H.; Yao, Z.-J.; Liu, H. *Adv. Synth. Catal*. **2012**, *354*, 2151-2156.
23. Bfuude, F. Lindwall, H.G. *J. Am. Chem. Soc.* **1933**, *55*, 325-327.
24. (a) Becke, A. D. *J. Chem. Phys*. **1993**, *98*, 5648. (b) Lee, C.; Yang, W.; Parr, R. G. *Phys. Rev. B*. **1988**, *37*, 785.
25. (a) Harihara, P. C.; Pople, J. A.; *Theoret. Chimica Acta*. **1973**, *28*, 213; (b) Francl, M. M.; Petro, W. J.; Hehre, W. J.; Binkley, J. S.; Gordon, M. S.; DeFrees, D. J.; Pople, J. A. *J. Chem. Phys*. **1982**, *77*, 3654.
26. Andrae, D.; Haussermann, U.; Dolg, M.; Stoll, H.; Preuss. H. *Theor. Chim. Acta.* **1990**, *77*, 123.
27. Marenich, A.V.; Cramer, C. J.; Truhlar. D. G. *J. Phys. Chem*. B. **2009**, *113*, 6378.
28. Andrienko, G. A. ChemCraft, http://www.chemcraftprog.com.
29. Gaussian 16, Revision C.01, Frisch, M. J.; Trucks, G. W.; Schlegel, H. B.; Scuseria, G. E.; Robb, M. A.; Cheeseman, J. R.; Scalmani, G.; Barone, V.; Petersson, G. A.; Nakatsuji, H.; Li, X.; Caricato, M.; Marenich, A. V.; Bloino, J.; Janesko, B. G.;

Gomperts, R.; Mennucci, B.; Hratchian, H. P.; Ortiz, J. V.; Izmaylov, A. F.; Sonnenberg, J. L.; Williams-Young, D.; Ding, F.; Lipparini, F.; Egidi, F.; Goings, J.; Peng, B.; Petrone, A.; Henderson, T.; Ranasinghe, D.; Zakrzewski, V. G.; Gao, J.; Rega, N.; Zheng, G.; Liang, W.; Hada, M.; Ehara, M.; Toyota, K.; Fukuda, R.; Hasegawa, J.; Ishida, M.; Nakajima, T.; Honda, Y.; Kitao, O.; Nakai, H.; Vreven, T.; Throssell, K.; Montgomery, J. A., Jr.; Peralta, J. E.; Ogliaro, F.; Bearpark, M. J.; Heyd, J. J.; Brothers, E. N.; Kudin, K. N.; Staroverov, V. N.; Keith, T. A.; Kobayashi, R.; Normand, J.; Raghavachari, K.; Rendell, A. P.; Burant, J. C.; Iyengar, S. S.; Tomasi, J.; Cossi, M.; Millam, J. M.; Klene, M.; Adamo, C.; Cammi, R.; Ochterski, J. W.; Martin, R. L.; Morokuma, K.; Farkas, O.; Foresman, J. B.; Fox, D. J. Gaussian, Inc., Wallingford CT, **2016.**

CHAPTER 4

Synthesis of indole-based N-carboxamides via Pd-catalyzed isocyanide insertion into remotely activated N-H bond of oxindoles

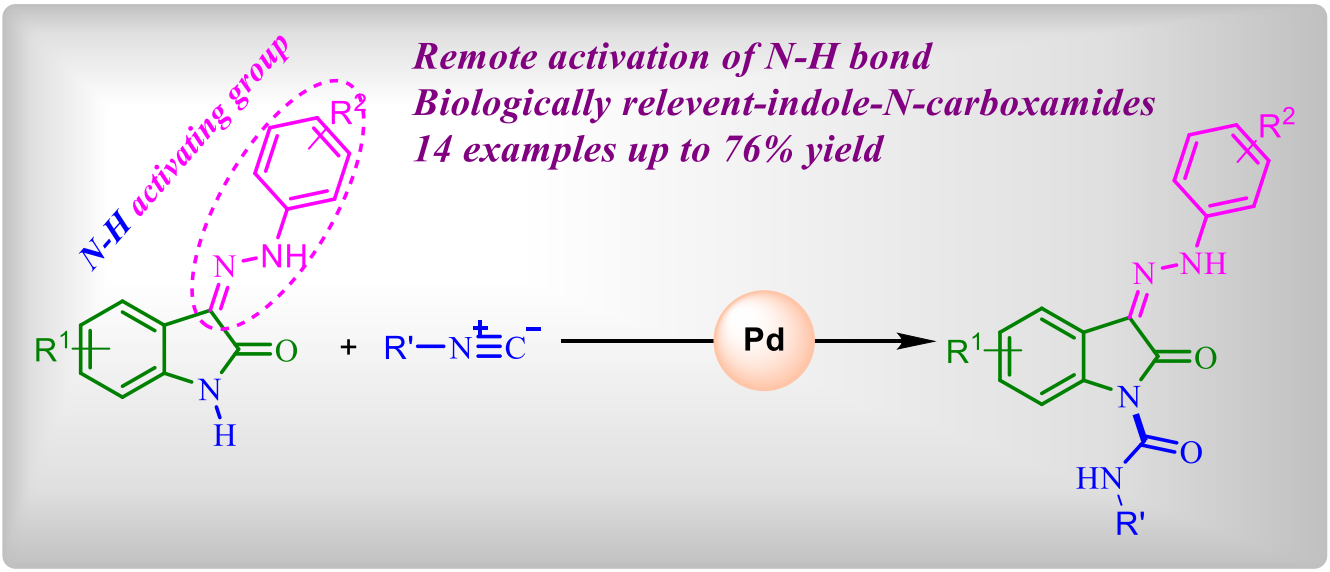

4.1: Introduction

Indole and its analogs represent an important class of nitrogen-containing heterocyclic compounds renowned for their diverse range of biological and pharmacological properties.[1,2] Over the years, several methods have been explored to introduce diverse functional groups onto the indole moiety, facilitating its transformation into captivating molecular frameworks.[3,4] These reactions have not only expanded the understanding of the chemical versatility of indole but have also paved the way for the synthesis of novel compounds with enhanced therapeutic potential and biological activities.[5–7] However, most of the methods primarily concentrated on reactions occurring at the carbon atoms of the pyrrole or phenyl ring of the indole scaffolds.[8,9] Surprisingly, the reactions at the *N*-1 position of indole are considerably less explored, due to the low nucleophilicity of nitrogen.[10] The reported reactions at the *N*-1 position predominantly involve protection strategies such as alkylation or arylation to lessen potential side reactions.[11,12] Nevertheless, *N*-substituted indole derivatives emerged as privileged scaffolds in medicinal chemistry.[13–15] In particular, indole-based N-carboxamide derivatives, including those functioning as a TNF-α modulator, GPR43 antagonist, VEGFR-2 inhibitor, and topoisomerase inhibitor, have been documented as promising anticancer compounds.[16] Additionally, Geldern's research team has disclosed the development of an indole-based *N*-carboxamide derivative as an endothelin antagonist targeting the endothelin A receptor[17], attributed to its capacity to forge distinctive interactions with various proteins facilitated by the presence of two nitrogen atoms (**Scheme 4.1**). Moreover, indole-*N*-carboxamide derivatives are also used as important precursors for several organic transformations.[18]

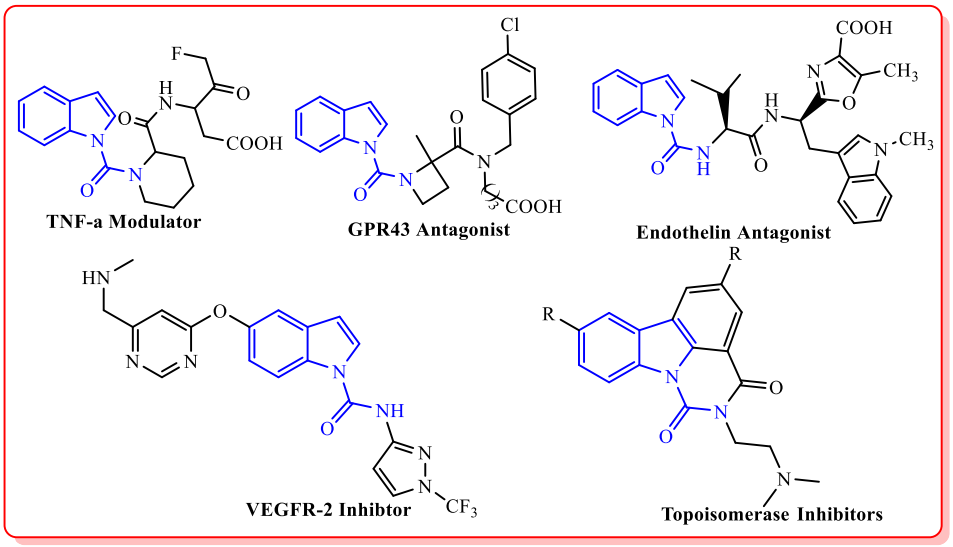

Scheme 4.1: Biologically active indole-based *N*-carboxamide derivatives

Still, there are only a limited number of methods available for the synthesis of indole-based *N*-carboxamide derivatives. Conventionally, the synthesis of indole-based N-carboxamides involves a multistep approach that necessitates the use of highly moisture-sensitive and flammable reagents, in addition to a rigorous work-up procedure.[18] (**Scheme 4.2a**). Besides, Liu's team introduced a gold-catalyzed method for synthesizing indole-*N*-carboxamides via intramolecular hydroamination of terminal alkynes (**Scheme 4.2b**).[19] Recently, Cui's research group unveiled a Ugi multicomponent reaction enabling the synthesis of indole-N-carboxamide amino amide derivatives, utilizing indole-N-carboxylic acid as the starting material (**Scheme 4.2c**).[16] Considering the importance of indole-N-carboxamides and the limitation of previously reported methods there is a significant need for the development of a novel protocol for synthesizing these scaffolds.

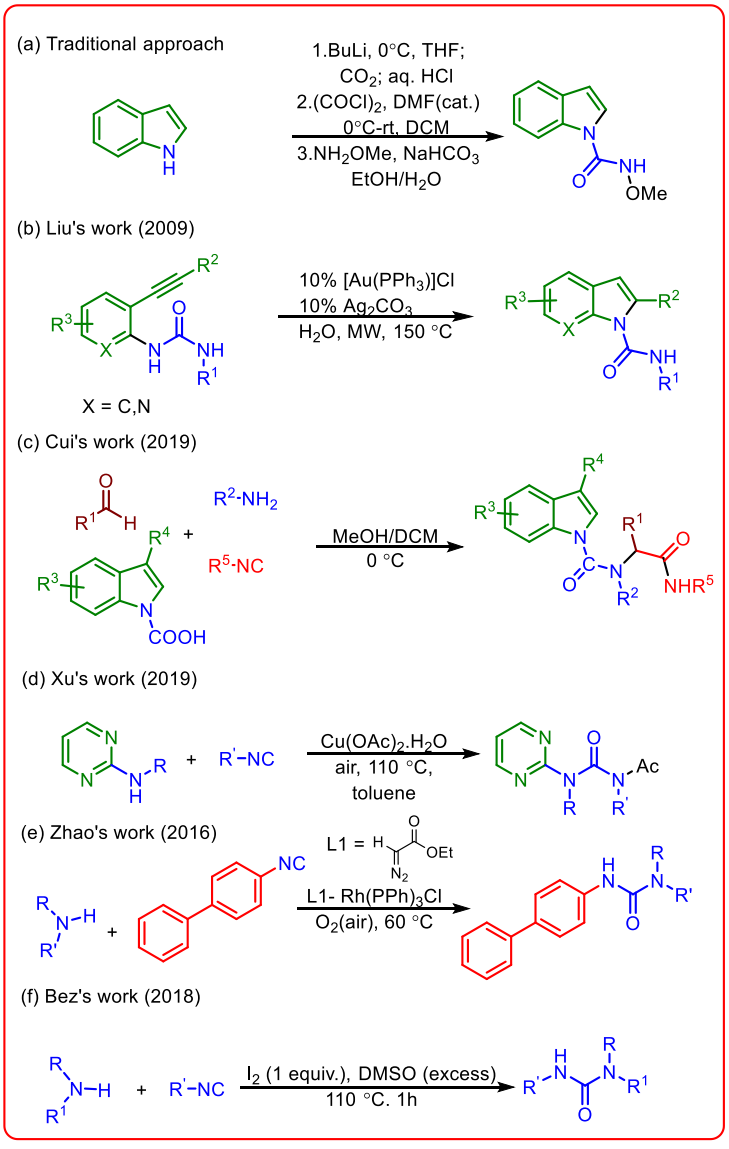

Scheme 4.2: Previous approaches for synthesizing indole-based *N*-carboxamides

On the other side, transition metal-catalyzed isocyanide insertion into the N-H bond has emerged as a valuable strategy for synthesizing *N*-carboxamide derivatives in recent years.[20,21] In this context, Xu's group reported an efficient synthesis of unsymmetrical tetrasubstituted urea derivatives in a one-pot process using a Cu-catalyzed multicomponent reaction (**Scheme 4.2d**).[22] This reaction involves the insertion of isocyanide into the less reactive N-H bond of secondary aryl amines. Zhao and colleagues reported another approach, wherein they developed an Rh-catalyzed aerobic oxidative coupling reaction between isocyanides and amines to produce urea derivatives in an atom-economic manner (**Scheme 4.2e**).[23] Additionally, several transition metal-free approaches have been developed for the generation of N-carboxamide derivatives. Recently, Bez et al. reported an iodine-DMSO-mediated method for isocyanide insertion into the N-H bond (**Scheme 4.2f**).[24] Nevertheless, these approaches were limited to aryl amines and aliphatic amines exclusively. To the best of our knowledge, these methods have never been documented for the amidation of the N-H bond in indole-based heterocycles. In this view, we hypothesized to explore the synthesis of indole-based *N*-carboxamides via transition metal-catalyzed isocyanide insertion into the N-H bond of the indole scaffold.

4.2: Results and discussion

4.2.1: Optimization of the reaction conditions

To actualize our hypothesis, we set up the reactions between indole and *tert*-butyl isocyanide in the presence of various transition metals catalysts *i.e.* $Cu(OAc)_2$, $Pd(OAc)_2$, and $Rh_2(OAc)_4$, however, none of the reaction provided the desired indole-based *N*-carboxamides and it could be due to the low nucleophilicity of nitrogen (**Scheme 4.3a**). Interestingly, the Kanger group has also noted similar types of findings and addressed them by employing 3-phenylimino substituted oxindole as a substrate.[25] The inclusion of 3-phenylimine moiety enhanced the nucleophilicity of the nitrogen atom of oxindole through remote activation. Consequently, they achieved successful asymmetric Michael addition reactions with unsaturated 1,4-ketoesters at the N-1 position of substituted oxindoles. Drawing encouragement from this report, we tried the Pd-catalyzed reaction of *tert*-butyl isocyanide with oxindole, 3-phenylimine substituted oxindole, and 3-phenylhydrozone substituted oxindole, respectively (**Scheme 4.3b-d**). Delightfully, we obtained the indole-based *N*-carboxamide product (**3a**) in 44% yield only when 3-phenylhydrozone substituted oxindole reacted with *tert*-butyl isocyanide only in the presence of Pd-catalyst (**Scheme 4.3d**).

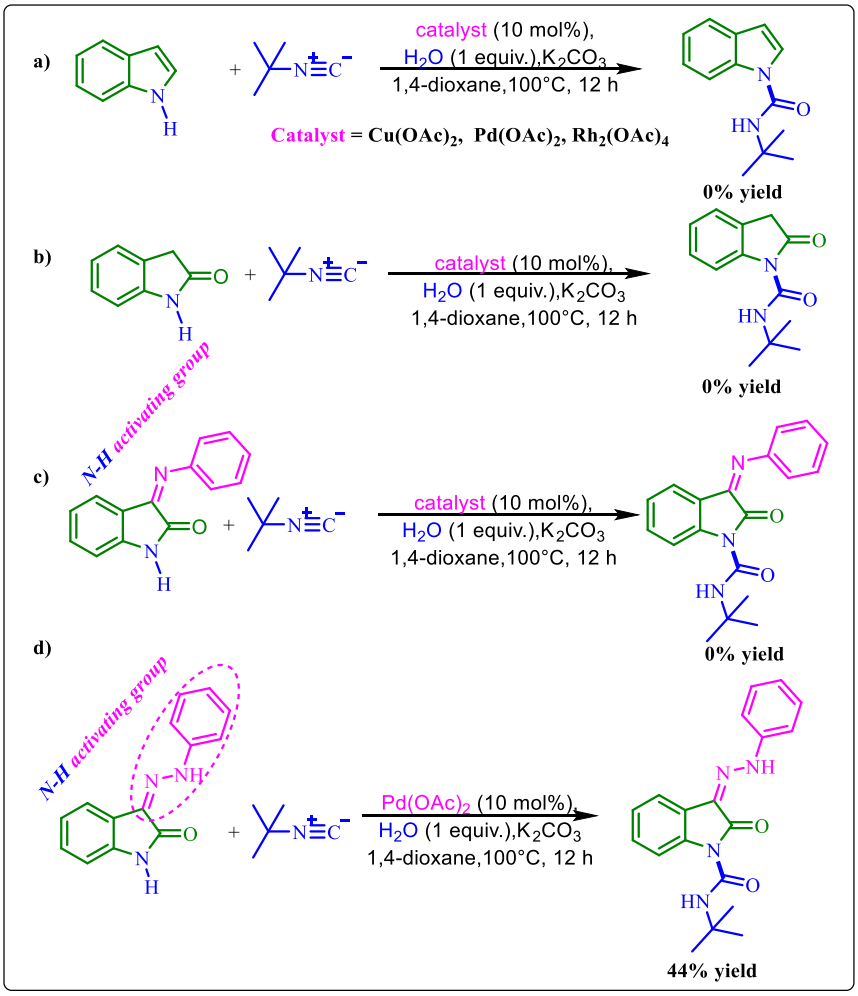

[a]**Reaction conditions:** (Z)-3-(2-phenylhydrazono) indolin-2-one (**1a)** (1.0 equiv.), *tert*-butyl isocyanide (**2a**) (1.2 equiv.), H_2O (1 equiv.), $Pd(OAc)_2$ (10 mol%), K_2CO_3 (1.5 equiv.), 1,4-dioxane (2 ml), temperature=100 °C,12 h.

Scheme 4.3: Our hypothesis to synthesize the indole-based *N*-carboxamide derivative

Based on the preliminary results, we decided to explore this methodology by optimizing various reaction conditions. Initially, we began our investigation for this transformation by selecting 3-(phenylhydrazono)oxindole (**1a**), *tert*-butyl isocyanide (**2a**) as the model substrates and screened various metal catalysts such as $Cu(OAc)_2$, ($Rh_2(OAc)_4$ and $Ni(OAc)_2$ in place of $Pd(OAc)_2$ (**Table 4.1, entries 2-4**). Unfortunately, the reaction didn't occur with $Cu(OAc)_2$ and $Rh_2(OAc)_4$ catalysts, however, only a trace amount of product was observed with $Ni(OAc)_2$. These results underscored the essential role of $Pd(OAc)_2$ as catalysts to make this reaction feasible. Next, we tried $Pd(PPh_3)_4$ and $PdCl_2$ instead of $Pd(OAc)_2$, the reaction provided a lower yield of 31% in the case of $Pd(PPh_3)_4$ and a comparable yield of 41% was observed with $PdCl_2$ (**Table 4.1, entries 5&6**). Also, a reduction of yield up to 36% was noticed when 5 mol% of $Pd(OAc)_2$ was added in place of 10 mol%, and no product formation was observed in the absence of palladium catalyst (**Table 4.1, entries 7&8**). Next, we screened various bases like

Na_2CO_3, KO*t*-Bu, LiO*t*-Bu, NEt_3, and DBU, etc., in the presence of $Pd(OAc)_2$ as a catalyst and found that K_2CO_3 was superior for this reaction (**Table 4.1, entries 9-13**). It was noticed that a mild base provides a higher yield in comparison to a strong base like KO*t*Bu & LiO*t*-Bu which afforded only 37 & 33% isolated yield respectively. Also, organic bases like NEt_3 and DBU weren't found superior for the reaction and provided only 32 & 29% yield respectively. However, when we tried the reaction in the absence of a base it gave the product (**3a**) only in 21% isolated yield which shows the importance of K_2CO_3 in this transformation (**Table 4.1, entry 14**).

Table 4.1. Optimization of the reaction conditions[a]

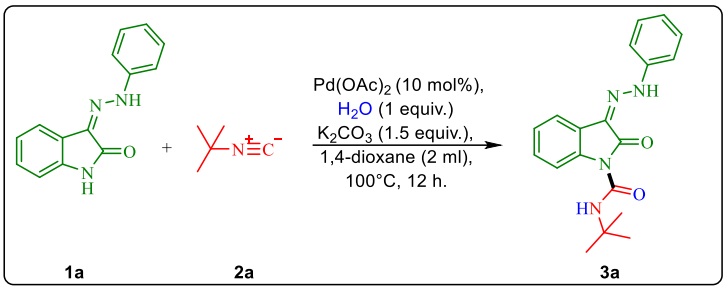

entry	deviation from reaction conditions	isolated yield
1.	**No deviation**	44%
2.	$Cu(OAc)_2$ as a catalyst	-
3.	$Rh_2(OAc)_4$ as a catalyst	-
4.	$Ni(OAc)_2$ as a catalyst	Trace
5.	$Pd(PPh_3)_4$ instead of $Pd(OAc)_2$	31%
6.	$PdCl_2$ instead of $Pd(OAc)_2$	41%
7.	$Pd(OAc)_2$ (5 mol% instead of 10 mol%).	36%
8.	in the absence of a catalyst	-
9.	Na_2CO_3 instead of K_2CO_3	40%
10.	KO*t*-Bu instead of K_2CO_3	37%
11.	LiO*t*-Bu instead of K_2CO_3	33%
12.	NEt_3 instead of K_2CO_3	32%
13.	DBU instead of K_2CO_3	29%
14.	in the absence of a base	21%
15.	Toluene instead of 1,4-dioxane	39%
16.	DMF instead of 1,4-dioxane	31%
17.	DMSO instead of 1,4-dioxane	35%
18.	130 °C	38%
19.	**70 °C**	**61%**
20.	50 °C	37%
21.	2 equiv. of H_2O	43%

[a]**Reaction conditions:** (Z)-3-(2-phenylhydrazono) indolin-2-one (1a) (1.0 equiv.),*tert*-butyl isocyanide (2a) (1.2 equiv.), H_2O (1 equiv.), $Pd(OAc)_2$ (10 mol%), K_2CO_3 (1.5 equiv.), 1,4-dioxane (2 ml), temperature of the reaction (100 °C) for 12 h.

Next, we checked the solvent suitability for the reaction, and it was noticed that 1, 4-dioxane persists as the best solvent for the developed reaction (**Table 4.1, entries 15-17**). Also, it was noticed that increasing the temperature up to 130 ℃ slightly decreases the reaction yield while decreasing the temperature up to 70 ℃ provided the reaction yield to 61% (**Table 4.1, entries 18-19**). However, the reaction yield diminished when the temperature was further reduced to 50 ℃, and only 37% of the product formation occurred (**Table 4.1, entry 20**). Also, it was noticed that increasing the amount of H_2O does not make any improvement in the outcome of the model reaction (**Table 4.1, entry 21**).

4.2.2: Substrate Scope

After having optimized conditions in our hands, we explored the substrate scope to check the feasibility of this transformation. Firstly, we have replaced *tert*-butyl isocyanide with 1,1,3,3-*tetra*methyl butyl isocyanide or cyclohexyl isocyanide, as a result, corresponding carboxamide products **3b** & **3c** were obtained in comparable yield in comparison of the product **3a** (**Scheme 4.4)**. These results represent that the structure of the isocyanide substrate and steric hindrance don't play any effective role in forming the desired product. Next, we checked the presence of electron-donating methoxy- group at oxindole moiety which provide only 46% yield (**Scheme 4.4**, **3d**) and strongly suggest that electron-donating groups diminished the reaction yield. After that, oxindole having halide substituents such as 5-Cl and 5-Br was tested with *tert*-butyl isocyanide respectively and obtained slightly higher yields in the case of 5-Cl (**Scheme 4.4**, **3e**) as compared to 5-Br substituent (**Scheme 4.4**, **3g**) of the product. Further, the reaction provided 64% yield, when 5-Cl substituted oxindole was used along with cyclohexyl isocyanide (**Scheme 4.4**, **3f**). Next, electron-withdrawing groups such as 5-trifluoro methoxy and 5-nitro were implemented and it was observed that electron-poor substituents slightly favored the reaction and provided 68% & 71% (**Scheme 4.4, 3h & 3i**) yields for the desired products. Next, we checked the 6-Cl substituent which again slightly decreased the yield and only provided 52% yield (**Scheme 4.4, 3j**). By encouraging these results, we have checked the effect of substituents at the phenyl ring of hydrazone functionality along with the electron-withdrawing and halogen groups at the C-5 position of oxindole. It was observed that the electron-donating group i.e. *p*-methyl at the phenyl ring of hydrazone and the 5-NO_2 group at the oxindole ring provide a maximum yield of 76% (**Scheme 4.4, 3k**). However, *p*-methyl at the phenyl ring of hydrazone and 5-F group at the oxindole ring provide a lower yield of 58% (**Scheme 4.4, 3l**). Also, when halogen substituents are employed on the *p*- and *o*- positions of phenyl hydrazone, the yield of the reaction decreases up to 51% and 55% (**Scheme 4.4, 3m &**

3n). However, when strong electron-withdrawing group *p*-NO_2 was installed at phenyl hydrazone, no product formation was observed (**Scheme 4.4, 3o**). Also, the reaction provided no yield when the substituent was implemented at 4- and 7-positions of oxindole moiety (**Scheme 4.4, 3p & 3q**). All these experiments proved that reaction outcome is highly dependent on the electronic effect of the substituent.

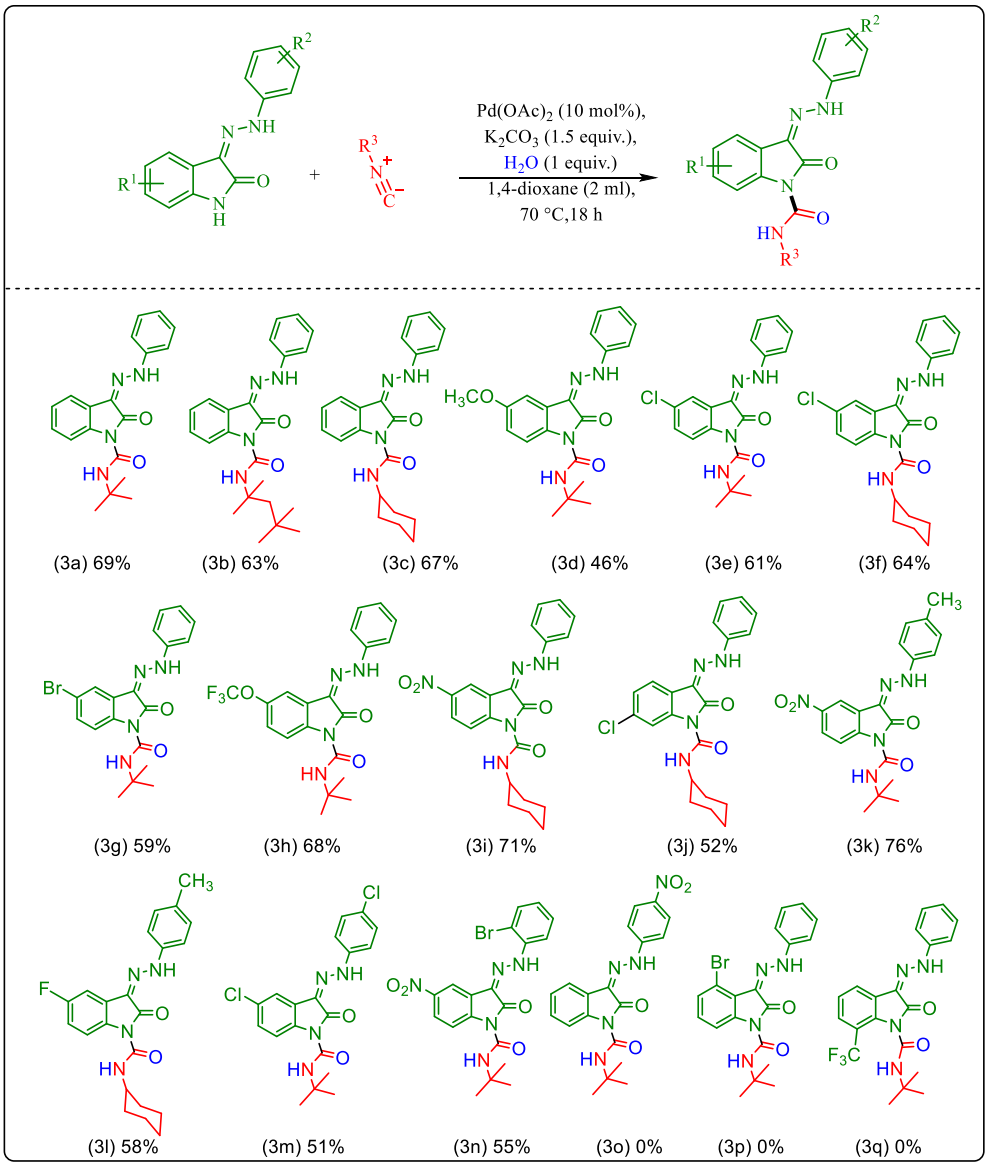

[a]**Reaction conditions:** (*Z*)-3-(2-phenylhydrazono) indolin-2-one (1a) (1.0 equiv.),*tert*-butyl isocyanide (2a) (1.2 equiv.), H_2O (1 equiv.), $Pd(OAc)_2$ (10 mol%), K_2CO_3 (1.5 equiv.), 1,4-dioxane (2 ml), temperature of the reaction (70 °C) for 12 h.

Scheme 4.4: Substrate scope of the Pd-catalysed reaction

4.2.3: Plausible mechanism

Based on these control experiments, we have proposed a mechanistic route for the reaction (**Scheme 4.5**).[20,26] Initially, hydrazone proton abstraction takes place in the presence of a base to open the oxindole ring which on the subsequent reaction with Pd-isocyanide complex (**A**),

which was generated by the reaction of Pd-catalyst and isocyanide, furnished complex (B) on the removal of AcOH. Next, this complex (**B**) went through an isocyanide insertion step to form a tricyclic intermediate (**C)** which again eliminated another AcOH unit to form complex (**D)**. This tricyclic ring can easily open and form a ketenimine-Pd complex (**E**) having electrophilic carbon.[27] Next, nucleophilic attack by water molecule takes place to form intermediate (**F**) which upon reductive elimination of palladium acetate form intermediate (H). This intermediate (**H**) simultaneously undergoes through tautomerization followed by cyclization to provide final product **(3a)**.

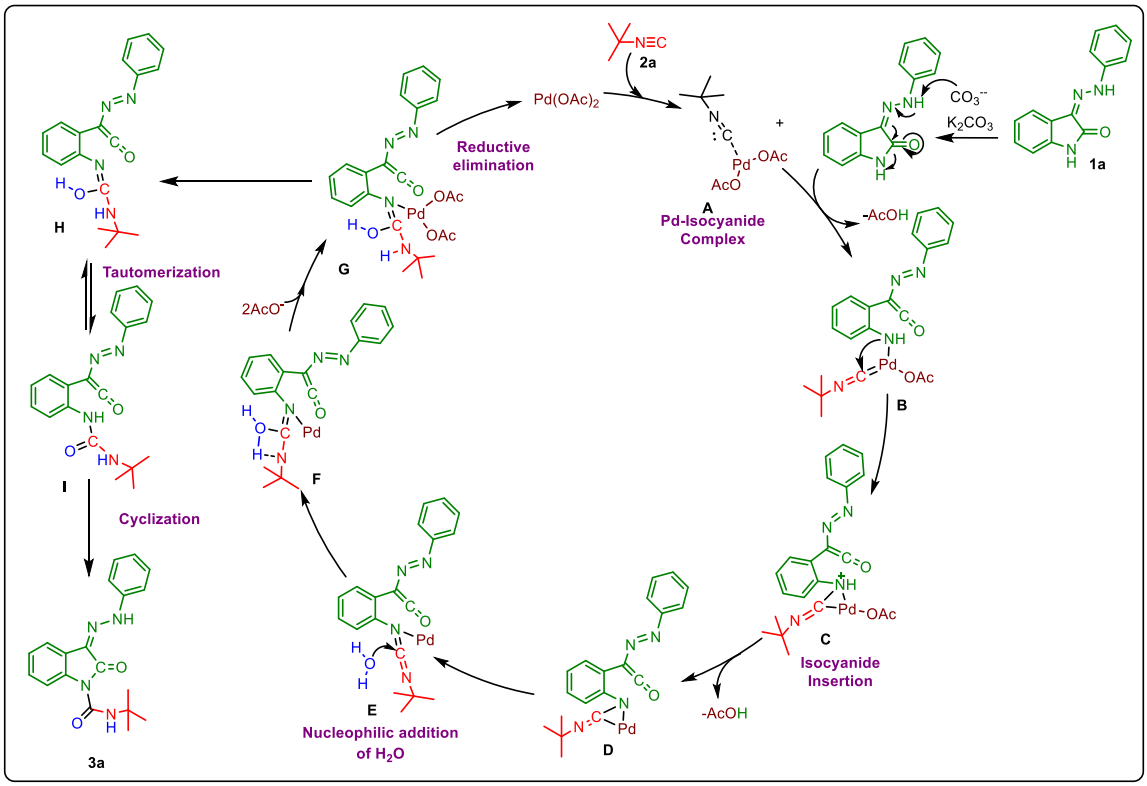

Scheme 4.5: Proposed reaction mechanism for the synthesis of indole-based N-carboxamide

4.3: Experimental section

4.3.1: General Information

All the reagents and solvents were purchased from commercial sources and used without undergoing any further purification. The ^{1}H NMR and $^{13}C\{^{1}H\}$ NMR were recorded on 400 and 100 MHz, respectively using JEOL or Bruker spectrometers in $CDCl_3$ and d_6-DMSO using tetramethylsilane (TMS) as an internal reference. The chemical shift value is denoted by δ (ppm) and the coupling constant in *J* (Hz). Other abbreviations used in NMR follow-up experiments: b, broad; s, singlet; d, doublet; t, triplet; q, quartet; m, multiplet; td or dd, doublet of triplet and double doublet. HRMS data were obtained by using the Water QTOF mass

spectrometer (XEVO G2 XS) in ESI(+ve) mode. Glass plates with silica gel (GF-254) were employed in Thin Layer Chromatography (TLC) to track the development of the reaction. The column chromatography was performed using silica gel (60-120 mesh) as the stationary phase and ethyl acetate in hexane as the mobile phase. All the compounds were characterized using ^{1}H NMR, $^{13}C\{^{1}H\}$ NMR & HRMS data.

4.3.2: General procedure to synthesize Indoline-1-carboxamides (3a-3n)

In a sealed tube having a stirrer bar added (Z)-3-(2-phenylhydrazono)indolin-2-one (1.0 equiv., 100 mg, 0.42 mmol), isocyanide (1.2 equiv., 42.09 mg, 0.50 mmol, 57.2 µl), H_2O (1.0 equiv., 7.59 µl, 0.42 mmol), $Pd(OAc)_2$ (10 mol%, 9.5 mg) and K_2CO_3 (1.5 equiv., 87 mg, 0.63 mmol) in 2 mL 1,4-dioxane as a solvent. The resulting reaction mixture was stirred at 70 ℃ in a preheated oil bath for 18 h and the progress of the reaction was monitored using TLC. After completion of the reaction as indicated by TLC, volatiles were evaporated under reduced pressure and the obtained residue was purified by column chromatography using ethyl acetate in hexane as eluents affording the corresponding indoline-1-carboxamide derivatives (**3a-3n**) in 46- 76% yields.

4.3.3: General procedure to synthesize (Z)-3-(2-phenylhydrazono)indolin-2-one (1a-1q)

In a round bottom flask, a mixture of isatin (1 mmol, 1 equivalent) and phenyl hydrazine (2.5 equiv.) in ethanol (3 mL) was refluxed for 1 h and then cooled to room temperature, resulting in the precipitation of hydrazone that was filtered, dried, and recrystallized from ethanol to provide yellow solid in 70-97% yield.

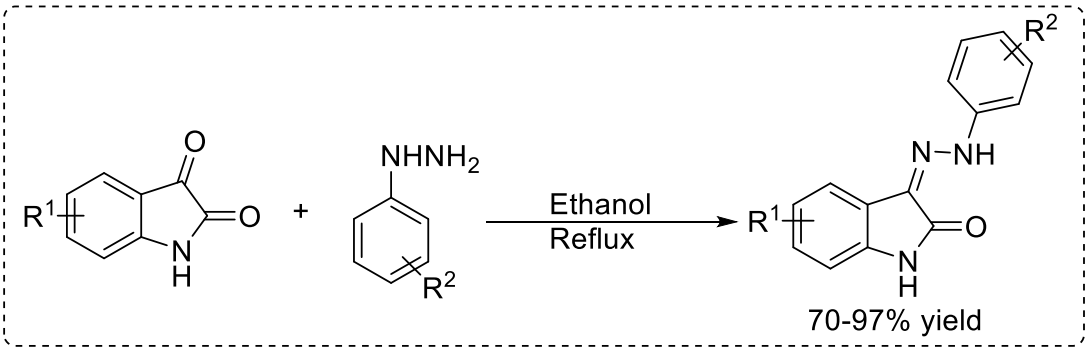

4.3.4: Characterization data

(Z)-3-(2-phenylhydrazono)indolin-2-one (1a)

Purification by recrystallization. Yellow solid, yield = 97%. ^{1}H NMR (400 MHz, DMSO-d_6): δ 12.75 (s, 1H), 11.02 (s, 1H), 7.51 (d, *J* = 8Hz, 1H), 7.40-7.30 (m, 4H), 7.20 (t, *J* = 8Hz, 1H), 7.02-6.98 (m, 2H), 6.88 (d, *J* = 8Hz, 1H) ppm.

(Z)-N-(tert-butyl)-2-oxo-3-(2-phenylhydrazono)indoline-1-carboxamide (3a)

Purification by column chromatography (mobile phase: EtOAc/Hexane, 0.3:9.7 v/v, stationary phase: Silica 60-120 mesh) afforded 3a; Yellow solid, yield = 69% (98 mg, 0.29 mmol), ^{1}H NMR (400 MHz, $CDCl_3$): δ 11.91 (s, 1H), 8.47 (s, 1H), 8.27 (d, *J* = 8Hz, 1H), 7.65 (s, *J* = 8Hz, 1H), 7.39-7.37 (m, 4H), 7.29 (t, *J* = 8Hz, 1H), 7.19 (t, *J* = 8Hz, 1H), 7.13-7.08 (m, 1H), 1.49 (s, 9H) ppm. ^{13}C{^{1}H} NMR (100 MHz, $CDCl_3$): δ 163.1, 150.6, 142.2, 138.0, 129.6, 128.5, 125.7, 124.4, 124.2, 121.3, 118.2, 116.5, 114.8, 51.4, 29.0 ppm. HRMS (ESI-TOF) m/z: $[M + H]^+$ calcd. for $C_{19}H_{21}N_4O_2$ 337.1665 found 337.1649.

(Z)-2-oxo-3-(2-phenylhydrazono)-N-(2,4,4-trimethylpentan-2-yl)indoline-1-carboxamide (3b)

Purification by column chromatography (mobile phase: EtOAc/Hexane, 0.3:9.7 v/v, stationary phase: Silica 60-120 mesh) afforded 3b; Yellow solid, yield = 63% (104 mg, 0.27 mmol), ^{1}H NMR (400 MHz, $CDCl_3$): δ 12.61 (s, 1H) ppm, 8.48 (s, 1H), 8.28 (d, *J* = 8Hz, 1H), 7.66 (s, *J* = 8Hz, 1H), 7.41-7.36 (m, 4H), 7.31-7.27 (m, 1H), 7.21-7.17 (m, 1H), 7.12-7.08 (m, 1H), 1.86, (s, 2H), 1.53 (s, 6H), 1.05 (s, 9H) ppm. ^{13}C{^{1}H} NMR (100 MHz, $CDCl_3$): δ 171.1, 163.1, 150.3, 142.2, 138.1, 129.6, 128.5, 125.7, 124.4, 124.2, 121.4, 118.2, 116.5, 114.9, 55.2, 51.5, 31.8, 31.6, 29.6 ppm.

(Z)-N-cyclohexyl-2-oxo-3-(2-phenylhydrazono)indoline-1-carboxamide (3c)

Purification by column chromatography (mobile phase: EtOAc/Hexane, 0.3:9.7 v/v, stationary phase: Silica 60-120 mesh) afforded 3c; Yellow solid, yield = 67% (102 mg, 0.28 mmol), ^{1}H NMR (400 MHz, $CDCl_3$): δ 12.60 (s, 1H), 8.45 (s, 1H), 8.26 (d, *J* = 8Hz, 1H), 7.65 (s, *J* = 8Hz, 1H), 7.39-7.37 (m, 4H), 7.32 (t, *J* = 8Hz, 1H), 7.19 (t, *J* = 8Hz, 1H), 7.14-7.07 (m, 1H), 3.92-3.85(m, 1H), 2.03-2.00 (m, 2H), 1.78-1.74 (m, 2H), 1.50-1.27 (m, 6H) ppm. ^{13}C{^{1}H} NMR (100 MHz, $CDCl_3$): δ 163.1, 151.2, 142.1, 137.9, 129.6, 128.6, 125.6, 124.5, 124.3, 121.4, 118.3, 116.4, 114.9, 48.8, 33.0, 25.7, 24.6 ppm. HRMS (ESI-TOF) m/z: $[M + H]^+$ calcd. for $C_{21}H_{23}N_4O_2$ 367.1770; found 367.1789.

(Z)-N-(tert-butyl)-5-methoxy-2-oxo-3-(2-phenylhydrazono)indoline-1-carboxamide (3d)

Purification by column chromatography (mobile phase: EtOAc/Hexane, 0.3:9.7 v/v, stationary phase: Silica 60-120 mesh) afforded 3d; Yellow solid, yield = 46% (63 mg, 0.17 mmol), ^{1}H NMR (400 MHz, $CDCl_3$): δ 12.63 (s, 1H), 8.42 (s, 1H), 8.16 (d, *J* = 8Hz, 1H), 7.41-7.36 (m, 4H), 7.29 (t, *J* = 8Hz, 1H), 7.18(d, *J* = 2.4Hz, 1H), 7.13-7.08 (m, 1H), 6.83 (dd, *J*= 9.2, 2.8Hz, 1H), 3.85(s, 1H), 1.47 (s, 9H) ppm. $^{13}C\{^{1}H\}$ NMR (100 MHz, $CDCl_3$): δ 171.2, 163.2, 156.9, 150.6, 142.1, 139.9, 129.6, 125.9, 124.3, 122.3, 117.4, 114.9, 102.9, 55.8, 51.4, 30.0 ppm.

(Z)-N-(tert-butyl)-5-chloro-2-oxo-3-(2-phenylhydrazono)indoline-1-carboxamide (3e)

Purification by column chromatography (mobile phase: EtOAc/Hexane, 0.3:9.7 v/v, stationary phase: Silica 60-120 mesh) afforded 3e; Yellow solid, yield = 61% (83 mg, 0.22 mmol), ^{1}H NMR (400 MHz, $CDCl_3$): δ 12.61 (s, 1H), 8.40 (s, 1H), 8.19 (d, *J* = 12Hz, 1H), 7.59(d, *J* = 2.4, 1H), 7.40-7.35 (m, 4H), 7.22 (dd, *J* = 8.8, 2Hz, 1H), 7.15-7.10 (m, 1H), 1.48 (s, 9H) ppm. $^{13}C\{^{1}H\}$ NMR (100 MHz, $CDCl_3$): δ 170.9, 162.7, 150.2, 141.8, 136.1, 130.0, 129.7, 128.0, 124.8, 124.4, 122.8, 118.1, 117.7, 115.0, 51.5, 28.9 ppm. HRMS (ESI-TOF) m/z: $[M + H]^+$ calcd. for $C_{19}H_{20}ClN_4O_2$ 371.1275; found 371.1267.

(Z)-5-chloro-N-cyclohexyl-2-oxo-3-(2-phenylhydrazono)indoline-1-carboxamide (3f)

Purification by column chromatography (mobile phase: EtOAc/Hexane, 0.3:9.7 v/v, stationary phase: Silica 60-120 mesh) afforded 3f; Yellow solid, yield = 64% (93 mg, 0.23 mmol), ^{1}H NMR (400 MHz, $CDCl_3$): δ 12.61 (s, 1H), 8.38 (d, *J* = 2.4Hz, 1H), 8.35 (d, *J* = 8.8Hz, 1H), 8.29(d, *J* = 7.6, 1H), 7.34 (d, 4H), 7.14-7.09 (m, 1H), 3.81 (s, 3H), 1.97-1.95 (m, 2H), 1.73-1.69 (m, 2H), 1.40-1.24 (m, 6H) ppm. $^{13}C\{^{1}H\}$ NMR (100 MHz, $CDCl_3$): δ 162.6, 150.4, 144.8, 141.3, 129.8, 125.6, 123.6, 123.3, 122.3, 116.5, 115.4, 113.4, 49.2, 32.9, 29.8, 25.6, 24.6 ppm.

(Z)-5-bromo-N-(tert-butyl)-2-oxo-3-(2-phenylhydrazono)indoline-1-carboxamide (3g)

Purification by column chromatography (mobile phase: EtOAc/Hexane, 0.3:9.7 v/v, stationary phase: Silica 60-120 mesh) afforded 3g; Yellow solid, yield = 59% (mg, 0.19 mmol), ^{1}H NMR (400 MHz, $CDCl_3$): δ 12.64 (s, 1H), 8.41 (s, 1H), 8.16 (d, *J* = 8.0Hz, 1H), 7.76(d, *J* = 2Hz, 1H), 7.39-7.37 (m, 5H),), 7.15-7.11 (m, 1H), 1.47 (s, 9H) ppm. $^{13}C\{^{1}H\}$ NMR (100 MHz, $CDCl_3$): δ 162.6, 150.2, 141.8, 136.6, 130.8, 129.7, 124.8, 124.3, 123.2, 121.0, 118.0, 117.6, 115.0, 51.6, 29.0 ppm.

(Z)-N-(tert-butyl)-2-oxo-3-(2-phenylhydrazono)-5-(trifluoromethoxy)indoline-1-carboxamide (3h)

Purification by column chromatography (mobile phase: EtOAc/Hexane, 0.3:9.7 v/v, stationary phase: Silica 60-120 mesh) afforded 3h; Yellow solid, yield = 68% (89 mg, 0.21 mmol), ^{1}H NMR (400 MHz, $CDCl_3$): δ 12.63 (s, 1H), 8.35 (s, 1H), 8.25 (d, *J* = 8.0Hz, 1H), 7.44(d, *J* = 1.6Hz, 1H), 7.36-7.31 (m, 4H),), 7.11-7.06 (m, 2H), 1.42 (s, 9H) ppm. ^{13}C{^{1}H} NMR (100 MHz, $CDCl_3$): δ 170.5, 162.9, 150.2, 146.1, 141.7, 136.0, 129.7, 124.9, 124.6, 122.7, 121.0, 117.6, 115.1, 111.1, 110.9, 51.6, 29.0 ppm.

(Z)-N-cyclohexyl-5-nitro-2-oxo-3-(2-phenylhydrazono)indoline-1-carboxamide (3i)

Purification by column chromatography (mobile phase: EtOAc/Hexane, 0.4:9.6 v/v, stationary phase: Silica 60-120 mesh) afforded 3i; Yellow solid, yield = 71% (102 mg, 0.25 mmol), ^{1}H NMR (400 MHz, $CDCl_3$): δ 12.57 (s, 1H), 8.35 (d, *J* =7.6Hz, 1H), 8.16 (d, *J* = 8.8Hz, 1H), 7.56-7.55(m, 1H), 7.39-7.33 (m, 4H),), 7.22-7.20 (m, 1H), 7.13-7.09 (m, 1H), 3.89-3.81 (m, 1H), 2.03-2.00 (m, 2H), 1.78-1.74 (m, 2H), 1.49-1.24 (m, 6H) ppm. ^{13}C{^{1}H} NMR (100 MHz, $CDCl_3$): δ 162.6, 150.8, 141.7, 136.0, 130.1, 129.7, 128.1, 124.8, 124.3, 122.9, 118.1, 117.5, 115.0, 48.9, 33.0, 25.7, 24.6 ppm.

(Z)-6-chloro-N-cyclohexyl-2-oxo-3-(2-phenylhydrazono)indoline-1-carboxamide (3j)

Purification by column chromatography (mobile phase: EtOAc/Hexane, 0.4:9.6 v/v, stationary phase: Silica 60-120 mesh) afforded 3j; Yellow solid, yield = 52% (73 mg, 0.19 mmol), ^{1}H NMR (400 MHz, $CDCl_3$): δ 12.64 (s, 1H), 8.41 (d, *J* =3.6Hz, 1H), 8.39 (s, *J* = 1H), 7.60(d, *J* = 4.8Hz, 1H), 7.42 (s, 4H),), 7.22 (d, *J* = 4.4Hz, 1H), 7.16 (s, 1H), 3.91-3.90 (m, 1H), 2.06-1.40 (m, 10H), ppm. ^{13}C{^{1}H} NMR (100 MHz, $CDCl_3$): δ 162.8, 150.8, 141.9, 138.2, 134.0, 129.6, 124.7, 124.6, 124.5, 119.8, 117.0, 114.0, 48.9, 32.8, 25.6, 24.5 ppm. HRMS (ESI-TOF) m/z: $[M + H]^+$ calcd. for $C_{21}H_{22}ClN_4O_2$ 397.1431; found 397.1423.

(Z)-N-(tert-butyl)-5-nitro-2-oxo-3-(2-(p-tolyl)hydrazono)indoline-1-carboxamide (3k)

Purification by column chromatography (mobile phase: EtOAc/Hexane, 0.3:9.7 v/v, stationary phase: Silica 60-120 mesh) afforded 3k; Yellow solid, yield = 76% (95 mg, 0.24 mmol), ^{1}H NMR (400 MHz, $CDCl_3$): δ 12.77 (s, 1H), 8.50 (d, *J* = 2.4Hz, 1H), 8.46 (s, 1H), 8.44 (s, 1H), 8.17 (dd, *J* = 8.8, 2.4Hz, 1H), 7.35 (d, *J* =8.4, 2H) 2.37 (s, 3H), 1.48 (s, 9H) ppm. ^{13}C{^{1}H} NMR (100 MHz, $CDCl_3$): δ 162.8, 149.9, 141.3, 139.1, 135.6, 130.4, 123.3, 122.8, 122.4, 116.6, 115.5, 113.4, 51.8, 29.8, 28.9 ppm.

(Z)-N-cyclohexyl-5-fluoro-2-oxo-3-(2-(p-tolyl)hydrazono)indoline-1-carboxamide (3l)

Purification by column chromatography (mobile phase: EtOAc/Hexane, 0.3:9.7 v/v, stationary phase: Silica 60-120 mesh) afforded 3l; Yellow solid, yield = 58% (85 mg, 0.22 mmol), ^{1}H NMR (400 MHz, $CDCl_3$): δ 12.67 (s, 1H), 8.42 (d, *J* = 7.6Hz, 1H), 8.23 (q, *J* =4.4Hz, 1H), 7.34-7.26 (m, 4H), 7.18 (s, 1H), 7.00-6.95 (m, 1H), 3.89-3.87 (m, 1H), 2.35 (s, 3H), 2.04-1.28 (m, 10H) ppm. ^{13}C{^{1}H} NMR (100 MHz, $CDCl_3$): δ 162.9, 161.3, 158.9, 151.0, 139.5, 134.6, 133.4, 130.1, 124.2, 123.1, 123.0, 121.9, 117.6, 117.5, 115.0,114.7, 114.4, 105.0, 104.8, 48.7, 32.9, 25.6, 24.6, 21.0 ppm.

(Z)-N-(tert-butyl)-5-chloro-3-(2-(4-chlorophenyl)hydrazono)-2-oxoindoline-1-carboxamide (3m)

Purification by column chromatography (mobile phase: EtOAc/Hexane, 0.3:9.7 v/v, stationary phase: Silica 60-120 mesh) afforded 3m; Yellow solid, yield = 51% (67 mg, 0.17 mmol), ^{1}H NMR (400 MHz, $CDCl_3$): δ 12.60 (s, 1H), 8.35 (s, 1H), 8.20 (d, *J* = 8Hz, 1H), 7.59 (d, *J* = 2.0Hz, 1H), 7.35-7.29 (m, 4H), 7.26-7.23 (m, 1H), 1.47 (s, 9H) ppm. ^{13}C{^{1}H} NMR (100 MHz, $CDCl_3$): δ 162.8, 150.1, 140.5, 136.3, 130.1, 129.8, 128.4, 125.1, 122.6, 118.3, 117.8, 116.1, 51.6, 29.0 ppm.

(Z)-3-(2-(2-bromophenyl)hydrazono)-N-(tert-butyl)-5-nitro-2-oxoindoline-1-carboxamide (3n)

Purification by column chromatography (mobile phase: EtOAc/Hexane, 0.3:9.7 v/v, stationary phase: Silica 60-120 mesh) afforded 3n; Yellow solid, yield = 55% (70 mg, 0.15 mmol), ^{1}H NMR (400 MHz, $CDCl_3$): δ 12.88 (s, 1H), 8.51 (d, *J* = 2.4Hz, 1H), 8.47 (d, *J* =8.0Hz, 1H), 8.37 (s, 1H), 8.21 (dd, *J* = 8.8, 2.0Hz, 1H), 7.89 (d, *J* = 8.0Hz, 1H), 7.55 (d, *J* = 7.6Hz, 1H), 7.41 (t, *J* = 8Hz, 1H), 7.03 (t, *J* = 7.6Hz, 1H), 1.50 (s, 9H) ppm. ^{13}C{^{1}H} NMR (100 MHz, $CDCl_3$): δ 162.6, 149.7, 144.8, 142.2, 139.2, 133.0, 129.0, 125.9, 125.4, 124.2, 122.0, 116.9, 116.1, 113.9, 110.4 ppm.

4.4: Conclusion

In summary, a significant methodology has been developed for synthesizing indole-based N-carboxamide derivatives via Pd-catalyzed isocyanide insertion into the N-H bond of 3-(phenylhydrazono)oxindole. Notably, the phenylhydrazone moiety positioned at the C3 position exhibits a crucial role in remotely activating the N-H bond of oxindole. To demonstrate the broad applicability and reliability of this approach, various electron-withdrawing, electron-donating, and halide substituents were examined at both the oxindole and hydrazone moieties,

yielding moderate to good results. However, the reaction's outcome was found to be highly influenced by the electronic effects of the substituents and highlights the need for further exploration of this methodology.

4.5: References

(1) Norwood, V. M.; Huigens, R. W. Harnessing the Chemistry of the Indole Heterocycle to Drive Discoveries in Biology and Medicine. *ChemBioChem*. **2019**, *20*, 2273–2297.

(2) Kumar, S.; Ritika. A Brief Review of the Biological Potential of Indole Derivatives. *Futur. J. Pharm. Sci.* **2020**, *6*, 1-19.

(3) Yu, B.; Yu, D. Q.; Liu, H. M. Spirooxindoles: Promising Scaffolds for Anticancer Agents. *Eur. J. Med. Chem.* **2015**, *97*, 673–698.

(4) Sakla, A. P.; Kansal, P.; Shankaraiah, N. Syntheses and Applications of Spirocyclopropyl Oxindoles: A Decade Review. *Eur. J. Org. Chem.* **2021**, *2021*, 757–772.

(5) Dhokne, P.; Sakla, A. P.; Shankaraiah, N. Structural Insights of Oxindole Based Kinase Inhibitors as Anticancer Agents: Recent Advances. *Eur. J. Med. Chem.* **2021**, *216*, 11334.

(6) Varun; Sonam; Kakkar, R. Isatin and Its Derivatives: A Survey of Recent Syntheses, Reactions, and Applications. *MedChemComm*. **2019**, *10*, 351–368.

(7) Khetmalis, Y. M.; Shivani, M.; Murugesan, S.; Chandra Sekhar, K. V. G. Oxindole and Its Derivatives: A Review on Recent Progress in Biological Activities. *Biomed. Pharmacother.* **2021,** *141*, 111842.

(8) Lashgari, N.; Ziarani, G. M. *Synthesis of Heterocyclic Compounds Based on Isatin through 1, 3-Dipolar Cycloaddition Reactions*. ARKIVOC. **2012**.

(9) Tingare, Y. S.; Shen, M. T.; Su, C.; Ho, S. Y.; Tsai, S. H.; Chen, B. R.; Li, W. R. Novel Oxindole Based Sensitizers: Synthesis and Application in Dye-Sensitized Solar Cells. *Org. Lett.* **2013**, *15*, 4292–4295.

(10) Zhao, M. X.; Chen, M. X.; Tang, W. H.; Wei, D. K.; Dai, T. L.; Shi, M. Cinchona Alkaloid Catalyzed Regio- and Enantioselective Allylic Amination of Morita-Baylis-Hillman Carbonates with Isatins. *Eur. J. Org. Chem.* **2012**, *19*, 3598–3606.

(11) Ma, J.; Feng, R.; Dong, Z. B. Recent Advances in Indole Synthesis and the Related Alkylation. *Asian. J. Org. Chem*. **2023,** *6*, e202300092.

(12) Oeser, P.; Koudelka, J.; Petrenko, A.; Tobrman, T. Recent Progress Concerning the N-Arylation of Indoles. *Molecules*. **2021**, *26*, 5079.

(13) Soledade, M.; Pedras, C.; Sorensen, J. L.; Okanga, F. I.; Zaharia, I. L. *WASALEXINS A AND B, NEW PHYTOALEXINS FROM WASABI: ISOLATION, SYNTHESIS, AND ANTIFUNGAL ACTIVITY*. *Bioorg. Med. Chem. Lett.* **1999**, *9*, 3015-3020.

(14) Zou, H.; Zhang, L.; Ouyang, J.; Giulianotti, M. A.; Yu, Y. Synthesis and Biological Evaluation of 2-Indolinone Derivatives as Potential Antitumor Agents. *Eur. J. Med. Chem.* **2011**, *46*, 5970–5977.

(15) Sharma, P. K.; Balwani, S.; Mathur, D.; Malhotra, S.; Singh, B. K.; Prasad, A. K.; Len, C.; Van der Eycken, E. V.; Ghosh, B.; Richards, N. G. J.; Parmar, V. S. Synthesis and Anti-Inflammatory Activity Evaluation of Novel Triazolyl-Isatin Hybrids. *J. Enzyme. Inhib. Med. Chem.* **2016**, *31*, 1520–1526.

(16) Zeng, L.; Sajiki, H.; Cui, S. Multicomponent Ugi Reaction of Indole- N-Carboxylic Acids: Expeditious Access to Indole Carboxamide Amino Amides. *Org. Lett.* **2019**, *21*, 5269–5272.

(17) Von Geldern, T. W.; Kester, J. A.; Bal, R.; Wu-Wong, J. R.; Chiou, W.; Dixon, D. B.; Opgenorth, T. J. Azole Endothelin Antagonists. 2. Structure-Activity Studies. *J. Med. Chem.* **1996**, *39*, 968-981.

(18) Zeng, L.; Lin, Y.; Cui, S. Indole-N-Carboxylic Acids and Indole-N-Carboxamides in Organic Synthesis. *Chem. Asian J*. **2020**, *15*, 973–985.

(19) Ye, D.; Wang, J.; Zhang, X.; Zhou, Y.; Ding, X.; Feng, E.; Sun, H.; Liu, G.; Jiang, H.; Liu, H. Gold-Catalyzed Intramolecular Hydroamination of Terminal Alkynes in Aqueous Media: Efficient and Regioselective Synthesis of Indole-1-Carboxamides. *Green. Chem.* **2009**, *11*, 1201–1208.

(20) Collet, J. W.; Roose, T. R.; Weijers, B.; Maes, B. U. W.; Ruijter, E.; Orru, R. V. A. Recent Advances in Palladium-Catalyzed Isocyanide Insertions. *Molecules*. **2020**, 25, 4906.

(21) Wang, X.; Fu, J. P.; Xie, J. X.; Teng, Q. H.; Tang, H. T.; Pan, Y. M. Palladium-Catalyzed Synthesis of 5-Amino-1,2,4-Oxadiazoles via Isocyanide Insertion. *Org. Biomol. Chem.* **2020**, *18*, 4936–4940.

(22) Huang, X.; Xu, S.; Tan, Q.; Gao, M.; Li, M.; Xu, B. A Copper-Mediated Tandem Reaction through Isocyanide Insertion into N–H Bonds: Efficient Access to Unsymmetrical Tetrasubstituted Ureas. *Chem. Comm.* **2014**, *50*, 1465–1468.

(23) Bu, X. Bin; Wang, Z.; Wang, Y. H.; Jiang, T.; Zhang, L.; Zhao, Y. L. Rhodium-Catalyzed Oxidative Coupling Reaction of Isocyanides with Alcohols or Amines and Molecular Oxygen as Oxygen Source: Synthesis of Carbamates and Ureas. *Eur. J. Org. Chem.* **2017**, *2017*, 1132–1138.

(24) Bora, P.; Bez, G. Chemoselective Isocyanide Insertion into the N-H Bond Using Iodine-DMSO: Metal-Free Access to Substituted Ureas. *Chem. Comm.* **2018**, *54*, 8363–8366.

(25) Žari, S.; Kudrjashova, M.; Pehk, T.; Lopp, M.; Kanger, T. Remote Activation of the Nucleophilicity of Isatin. *Org. Lett.* **2014**, *16*, 1740–1743.

(26) Qin, J.; Li, Z.; Ma, S.; Ye, L.; Jin, G.; Su, W. One-Pot Cascade Ring Enlargement of Isatin-3-Oximes to 2,4-Dichloroquinazolines Mediated by Bis(Trichloromethyl)Carbonate and Triarylphosphine Oxide. *Phosphorus, Sulfur Silicon Relat. Elem.* **2020**, *195*, 1007–1012.

(27) Bi, X.; Liu, Z.; Cao, S.; Wu, J.; Zanoni, G.; Sivaguru, P. Palladium(II)-Catalyzed Cross-Coupling of Diazo Compounds and Isocyanides to Access Ketenimines. *ACS Catal.* **2020**, *10*, 12881–12887.

CHAPTER 5

Pd-catalyzed one-pot cascade consisting C-C/C-O/N-N bond formation to access benzoxazine fused 1,2,3-triazoles

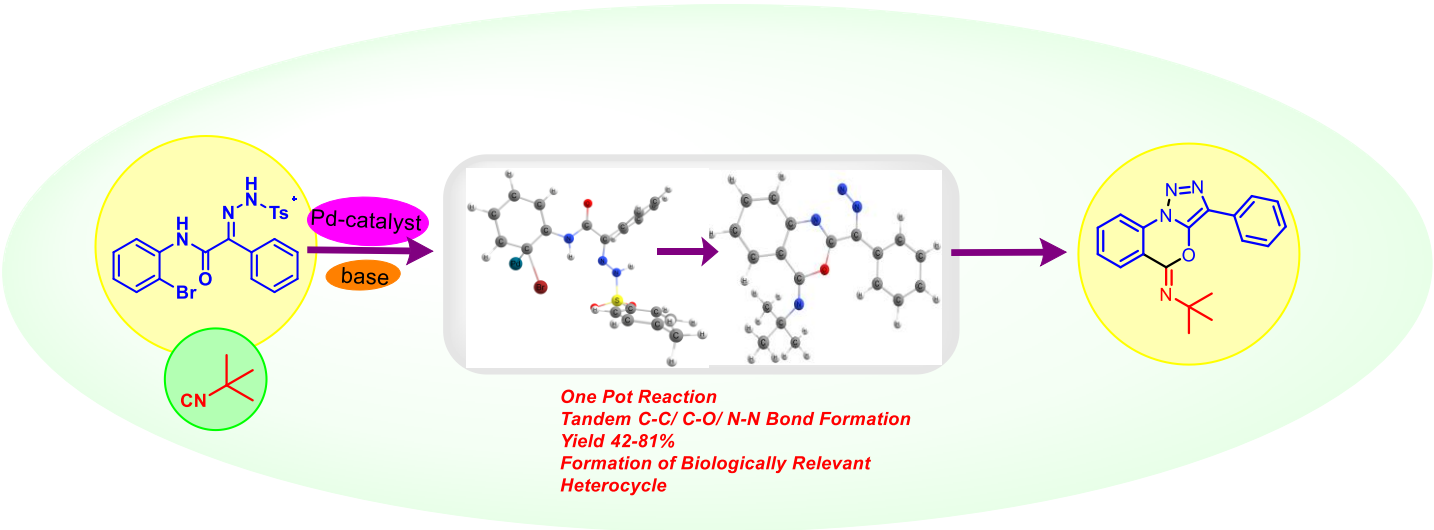

5.1: Introduction

α-Diazoacetamides have been extensively used in the last many years as a starting material to synthesize substituted oxindoles, lactams or other heterocyclic compounds via transition-metal catalysed intramolecular/intermolecular carbene insertion reactions.[1] Recently, Lautens *et al.* reported a Ru-catalysed intramolecular cyclization of diazo-β-ketoanilides in combination with Pd-catalysed asymmetric allylic alkylation in one pot (**Scheme 5.1a**).[2] Further, Kim group reported the synthesis of α-quaternary chiral β-lactam moiety using relay Rh(II)/Pd(0) dual catalysis (**Scheme 5.1b**).[3] A Rh-catalysed coupling of α-diazo-γ-butyrolactams with aromatic amines to generate α-arylamino-γ-butyrolactams was reported by Karsavin research group (**Scheme 5.1c**).[4]

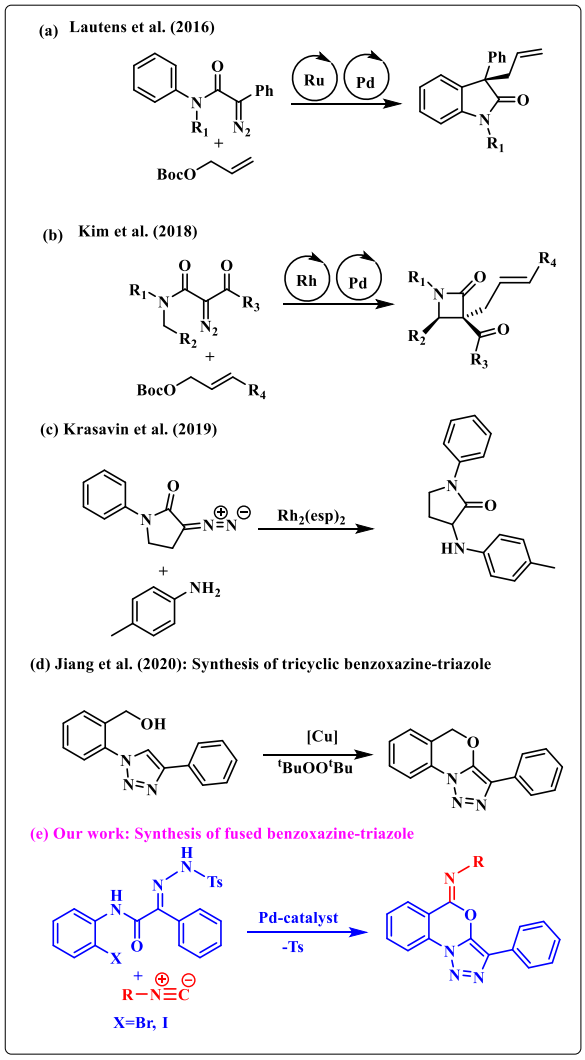

Scheme 5.1: Use of α-diazoacetamides or their N-tosylhydrazone surrogate to synthesize N-heterocycles

Interestingly, previous reports demonstrated that the structure of α-diazoacetamides can dramatically affect the outcome of the reaction mainly in terms of efficiency, chemo-, regio- and stereoselectivity.[5] Thus, the careful designing of the structure of α-diazoacetamides as reacting substrates in transition-metal catalysed reactions is an imperative task.

On the other hand, 1,2,3-triazole fused heterocyclic compounds have attracted continuous growing attention of chemical community due to their significant applications in the various area of chemistry such as material chemistry, supramolecular, medicinal and pharmaceutical chemistry.[6] Further, 1,2,3-triazole fused heterocyclic compounds have been found displaying a wide range of biological activities such as antibacterial, anti-HIV, antitrypanosomal, antiallergic, anti-fungal, cardiovascular, antileishmanial, and chemotherapeutic activities (**Figure 5.1**).[7] The conventional method for synthesizing 1,2,3-triazole ring fused with numerous heterocycles is click chemistry which involved thermal or copper-catalyzed 1,3-dipolar cycloaddition of alkynes to azides.[8] Over the years, several other strategies have been reported for the synthesis of 1,2,3-triazole ring fused with various heterocycles.[9] Additionally, benzoxazine fused triazoles have been interesting scaffolds due to their potential diuretic activities (**Figure 5.1**), however, very few methods are available in the literature to synthesize this scaffold.[10] Very recently, Jiang and co-workers have developed copper-catalyzed intramolecular C−H alkoxylation reaction to synthesize tricyclic benzoxazine-triazoles.[11]

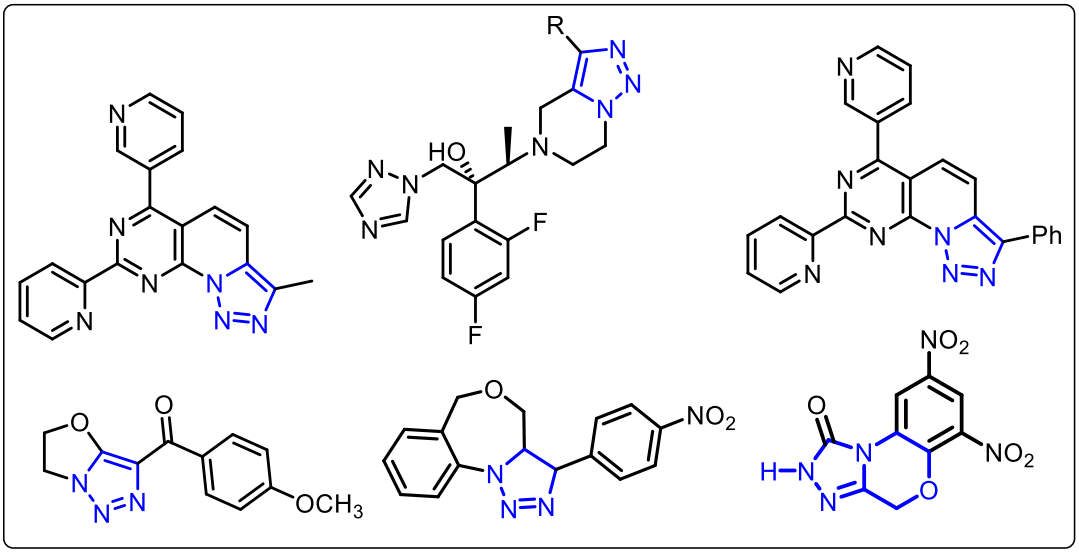

Figure 5.1: Biologically active triazole fused heterocycles

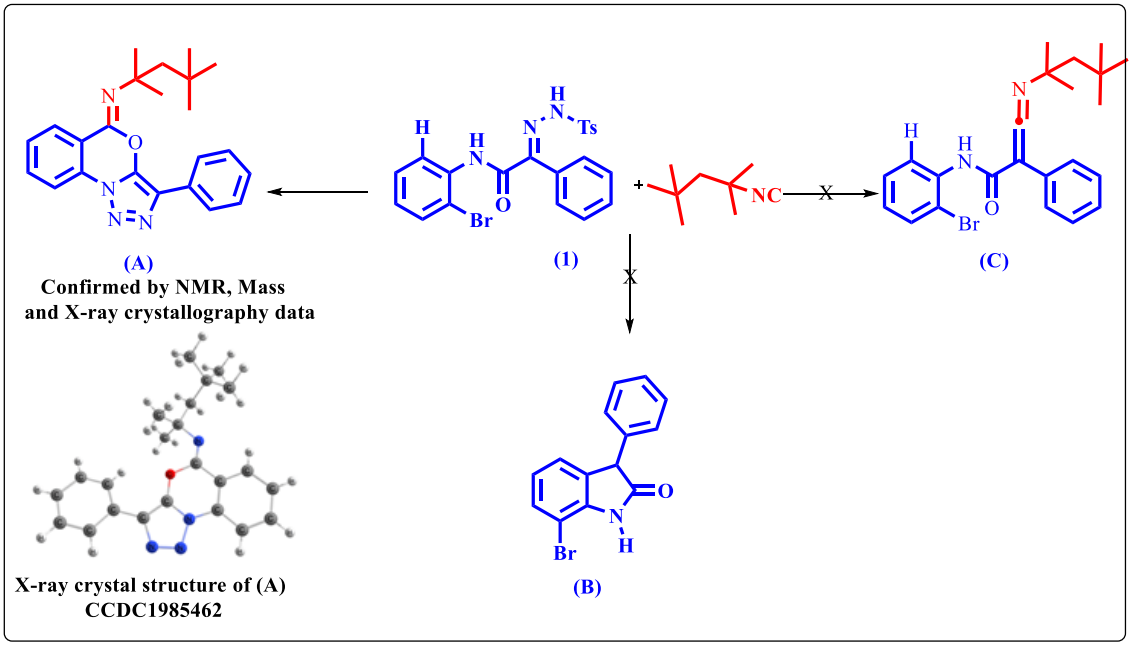

Scheme 5.2: Possible structures under Pd-catalyzed reaction conditions

5.2: Results & discussion

5.2.1: Optimization of the reaction conditions

Initially, we hypothesized to use N-aryl-α-(tosyl hydrazone)acetamide as more easily synthesizable, safe and stable surrogate of α-diazoacetamides with isocyanide under the palladium catalysed conditions to produce substituted ketenimines (C) as reported very recently by Bi et al. (**Scheme 5.2**).[12] To realize our hypothesis, we started a reaction of N-aryl-α-(tosyl hydrazone) acetamide with tetramethylbutyl isocyanide using 10 mol% of $PdCl_2$ and 2 equiv. of KO*t*-Bu as a catalyst and base respectively in 1,4-dioxane at 100°C for overnight in a sealed tube and obtained the isolated product in 56% yield. However, formation of benzoxazine fused 1,2,3-triazoles (A) was unexpectedly obtained (**Scheme 5.2**). Drawing motivation by the clinical application of benzoxazine fused triazoles, herein, we decided to optimize the newly discovered reaction and screen various Pd-catalysts, bases and solvents in this context and selected N-aryl-α-(tosyl hydrazone)acetamides (1a) and tert-butyl isocyanide (2a) as the model substrates (**Table 5.1**). Initially, the reaction was carried out using a series of Pd-catalysts with KO*t*Bu as a base in 1,4-dioxane at 110°C (**Table 5.1, entries 1-6**), and the results exhibited that $Pd(OAc)_2$ was superior than other Pd-catalysts and gave the product (3a) in 78% yield (**Table 5.1, entry 2**). Also,

$Pd(DPPF)Cl_2$ showed similar catalytic activity and gave the product (3a) in 75% yield (**Table 5.1, entry 4**). Beside these catalysts, $PdCl_2(NCC_6H_5)_2$ and $Pd(dba)_3$ furnished the product (3a) in significant yield that was 50% and 47% respectively (**Table 5.1, entries 3 and 5**). In addition, when reaction was initiated using $PdCl_2$ or $Pd(PPh_3)_4$ as catalyst, a comparatively lower yield of (3a) was obtained (**Table 5.1, entries 1&6**). Next, we screened several bases for example K_2CO_3, Cs_2CO_3, KOH, NaH, $NaHCO_3$, DBU and LiO*t*Bu with $Pd(OAc)_2$ as a catalyst in 1,4-dioxane at 110°C (**Table 5.1, entries 7-13**). When, we used K_2CO_3, KOH, NaH as the base, the product was formed in considerable amount and the isolated yield was between 50-63% (**Table 5.1, entries 7, 9, 10 and 13**). Furthermore, when Cs_2CO_3, $NaHCO_3$ and DBU were implemented as the base, the product was obtained in inferior yield (**Table 5.1, entries 8, 11 & 12**). These results showed that KO*t*Bu remained the best choice with $Pd(OAc)_2$ as a catalyst in 1,4-dioxane (**Table 5.1, entry 2**). Having, $Pd(OAc)_2$ and KO*t*Bu as the best catalyst and base, next, we screened various solvents including toluene, THF, DMF and DMSO, and obtained the product in 33-59% yield (**Table 5.1, entries 14-17**). This showed that variations in solvent have a substantial effect on the product formation in this reaction. Consequently, 1,4-dioxane persisted the best solvent in the presence of $Pd(OAc)_2$ and KO*t*Bu as a catalyst and base respectively (**Table 5.1, entry 1**). In addition, when the molar ratio of $Pd(OAc)_2$ was decreased from 10 mol% to 5 mol%, the reaction provided the product only in 51% yield (**Table 5.1, entry 18**). Moreover, the procedure was unfavorable when catalyst was omitted from the reaction (**Table 5.1, entry 19**). It is interesting to note that 110°C temperature and 2.0 equiv. of KO*t*Bu was essential in this reaction to obtain the maximum conversion.

Table 5.1. Optimization of the reaction conditions[a]

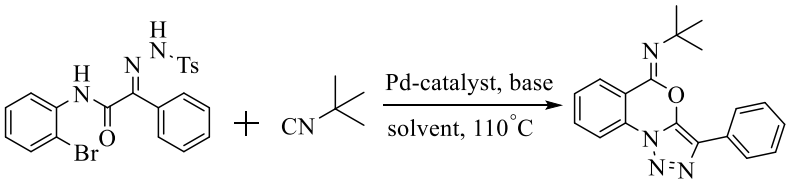

(1a) **(2a)** **(3a)**

entry	catalyst	base	solvent	yield[b] (%)
1	$PdCl_2$	KO*t*-Bu	1,4-dioxane	26
2	**$Pd(OAc)_2$**	**KO*t*-Bu**	**1,4-dioxane**	**78**

3	$PdCl_2(NCC_6H_5)_2$	KO*t*-Bu	1,4-dioxane	50
4	$Pd(DPPF)Cl_2$	KO*t*-Bu	1,4-dioxane	75
5	$Pd(dba)_3$	KO*t*-Bu	1,4-dioxane	47
6	$Pd(PPh_3)_4$	KO*t*-Bu	1,4-dioxane	20
7	$Pd(OAc)_2$	K_2CO_3	1,4-dioxane	55
8	$Pd(OAc)_2$	Cs_2CO_3	1,4-dioxane	26
9	$Pd(OAc)_2$	KOH	1,4-dioxane	50
10	$Pd(OAc)_2$	NaH	1,4-dioxane	60
11	$Pd(OAc)_2$	$NaHCO_3$	1,4-dioxane	25
12	$Pd(OAc)_2$	DBU	1,4-dioxane	38
13	$Pd(OAc)_2$	LiOt-Bu	1,4-dioxane	63
14	$Pd(OAc)_2$	KO*t*-Bu	Toluene	59
15	$Pd(OAc)_2$	KO*t*-Bu	DMF	35
16	Pd(OAc)2	KO*t*-Bu	DMSO	47
17	$Pd(OAc)_2$	KO*t*-Bu	THF	33
18	$Pd(OAc)_2$	KO*t*-Bu	1,4-dioxane	51[c]
19	-	KO*t*-Bu	1,4-dioxane	nr[d]

[a]**Reaction conditions**: substrate 1a (1.0 equivalent), *tert*-butyl isocyanide 2a (1.2 equivalents), Pd-catalyst (10 mol%), base (2.0 equivalents), solvent (2 ml), temperature of the reaction (110°C) for 3 hr. [b]isolated yield, [c]Pd-catalyst (5 mol%), [d]nr= desired product was not obtained.

5.2.2: Substrate scope

After having the optimized conditions (**Table 5.1, entry 2**), we investigated the effect of various substitutions on aryl groups attached to the N-atom (anilide moiety) of the N-aryl-α-(tosyl hydrazone)acetamides (1) with different isocyanides (2) and briefed the results in **Scheme 5.2**.

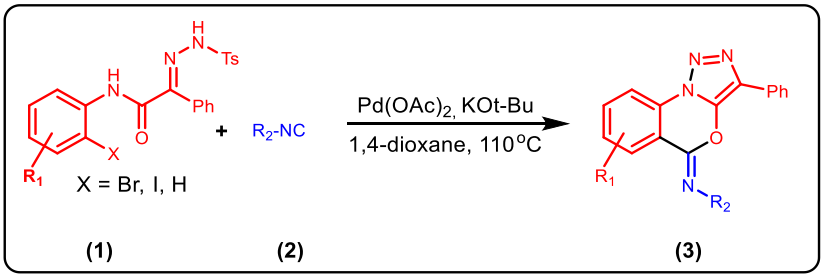

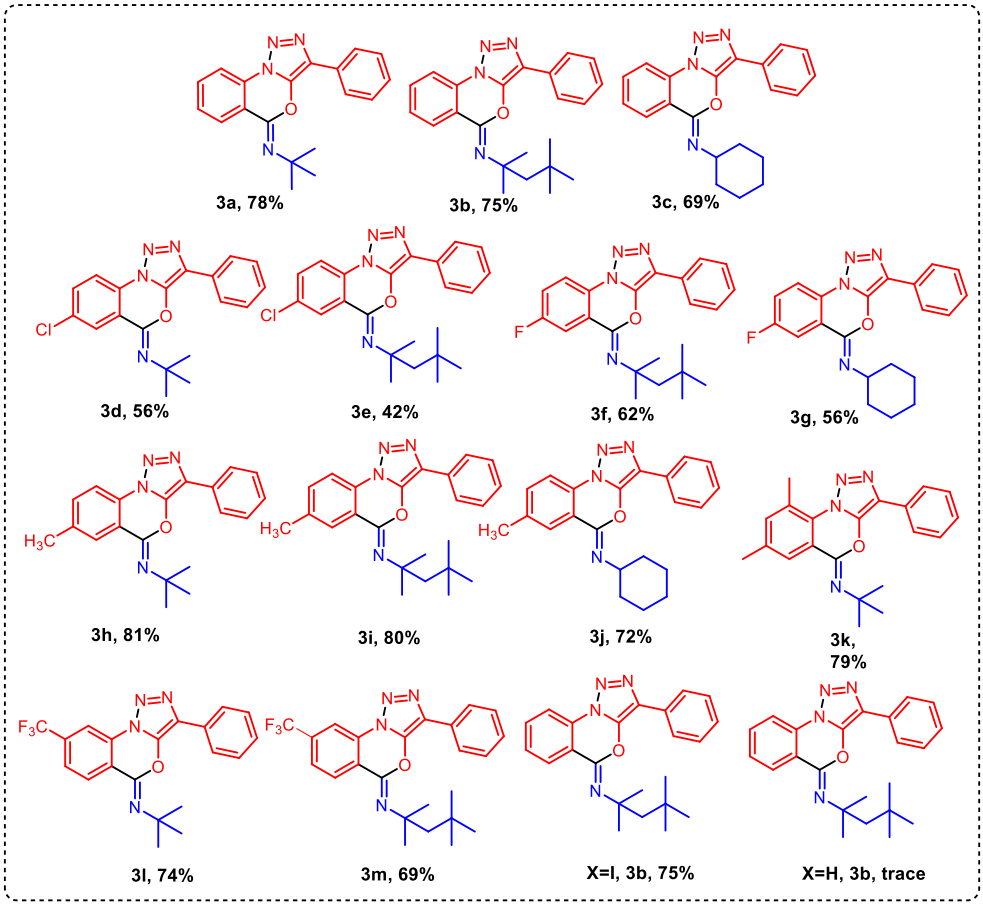

[a]**Reaction conditions**: hydrazones **1** (1.0 equivalent), isocyanides **2** (1.2 equivalents), $Pd(OAc)_2$ (10 mol%), KOt-Bu (2.0 equivalents), 1,4-dioxane (2 ml), temperature of the reaction (110°C) for 2-3 hr. [b]isolated yield.

Scheme 5.3. Scope of the substrate in the Pd-catalysed cascade reaction[a]

In this context, when reacted tosylhydrazone (1a) with 1,1,3,3-tetramethylbutyl isocyanide, we obtained the product (3b) in very good yield (**Scheme 5.3, entry 2**) and the yield of (3b) was close to the product attained from the reaction of tosylhydrazone (1a) with tert-butyl isocyanide (**Scheme 5.3, entry 1**). But, in the case of cyclohexyl isocyanide, the yield of product (3c) was slightly lower (**Scheme 5.3, entry 3**). These results showed that there was no significant change in the yield of products from moving one isocyanide to others (**Scheme 5.3, entries 1-3**). Further, we verified the effect of halide substitutions on the *para*-position of anilide moiety and in case of 4-Cl substitution the reaction gave inferior yield of the products with both tert-butyl isocyanide as well as 1,1,3,3-tetramethylbutyl isocyanide (**Scheme 5.3, entries 4-5**). However, when 4-chloro was replaced with 4-fluoro substitution, yield of the corresponding products was found 62% and 56% respectively with 1,1,3,3-tetramethylbutyl isocyanide and cyclohexyl isocyanide (**Scheme 5.3,**

entries 6-7). Next, we tested the effect of mild electron-donating group such as methyl on anilide moiety and observed that substrate bearing 4-Me or 4,6-dimethyl groups were more facile to react under the optimized reaction conditions and afforded the corresponding products in 72-81% isolated yield (**Scheme 5.3, entries 8-11**). Furthermore, the effect of electron-withdrawing group was examined and we got the corresponding product (3l) in 74% yield, when reacted 5-CF_3 containing hydrazone (1f) with tert-butyl isocyanide (**Scheme 5.3, entry 12**). There was no significant change in the course of the reaction when reacted 5-CF_3 containing hydrazone (1f) with 1,1,3,3-tetramethyl butyl isocyanide (**Scheme 5.3, entry 13**). In addition, the effect of halide at the *ortho*-position of anilide moiety was investigated by replacing bromo with iodo, gratifyingly, there was no significant change in the yield of the corresponding product (**Scheme 5.3, entry 14**). However, in the absence of any halide on ortho-position of tosylhydrazone, the product was formed only in trace amount (**Scheme 5.3, entry 15**). So, this explained the significance of the presence of a halide on the *ortho*-position of anilide moiety (**Scheme 5.3, entry 15**).

5.2.3: Plausible mechanism and DFT calculations

Next, we proposed two plausible mechanisms (route 1&2) for the formation of benzoxazine fused 1,2,3-triazole as depicted in **Figure 5.2**. According to route 1, which comprises generation of benzoxazine ring first followed by triazole ring, reaction starts with the oxidative insertion of palladium to the N-aryl-α-(tosyl hydrazone) acetamides (1a) and leads to the INT (i). This species evolves to palladacyclic INT (ii) which on insertion of tert-butyl isocyanide furnish INT (iii). Next, INT (iii) converted to INT (iv) via subsequent reductive elimination of palladium. Further, base mediated removal of tosyl group leads to α-diazoimino intermediate (v) which converted to product (3a) through 5-endo-dig cyclization.[13] According to plausible route 2, which includes formation of triazole ring first then benzoxazine ring as depicted in **Figure 5.2**, N-aryl-α-(tosyl hydrazone) acetamides (1a) converts to INT (vi) in the presence of base followed by the conversion of INT (vi) into INT (vii) through intramolecular N-N cyclization reaction. Next, oxidative addition of palladium to INT (vii) leads to the formation of INT (viii). Additionally, base mediated removal of HBr furnish six membered palladacyclic INT (ix) which converted into seven membered palladacyclic INT (x) after the insertion of tert-butyl isocyanide. Finally, reductive elimination of palladium leads to the formation of product (3a). Then, we have performed control experiments to get evidences about most possible mechanism between two probable routes presented in **Figure 5.2**. In this context, when the N-H group of N-Aryl amide was protected

reaction didn't work {**Figure 5.11(i)**}. Also, there was no reaction in the absence of Pd-catalyst {**Figure 5.11(ii)**}. These experiments indicated that benzoxazine ring generates first and favors to route 1 over the route 2. Subsequently, to validate the proposed mechanisms and to find the favorable routes between 1 & 2, a computational investigation has been performed. First, we have discussed about the route 1and the potential energy surface (PES) related to the reaction has been shown in **Figure 5.3**. It is worthy to mention here that in the PES all the steps have been considered explicitly which involves few extra intermediate structures, whereas, the minimum numbers of steps have been stated in the schematic mechanism (**Figure 5.2a**). So, during the discussion of PES, we will indicate the important structures to correlate with the proposed mechanism. B3LYP density functional method was employed for this investigation along with SDD for Pd, Br and 6-31+G(d,p) basis set for rest of the atoms. This particular level of theory was successfully used in earlier typical investigations.[14] As presented in **figure 5.2a**, the first step is oxidative insertion which undergoes through the formation of π-complex (2) by releasing ~25 kcal mol^{-1} energy followed by the addition of Pd(0) into C-Br bond to furnished complex 3. Then, complex 3 proceeds through a low barrier (~3 kcal mol-1) transition state (TS_{3-4}) to form the complex 4 (implies the INT(i) in figure 5.2a), which exists ~45 kcal mol-1 lower point in the PES with respect to separated reactant (1a+Pd). The oxidative addition mechanism towards Carbon-halogen bond is fairly common as provided by Diefenbach et.al.[15] It further stabilized by ~ 19 kcal mol^{-1} after a conformational change through rotation of aryl C-N bond and converts to complex 5. In the next step, the abstraction of proton from complex 5 along with releasing of bromine taken place in the presence of strong base. Here we have followed most favorable inter-molecular base assisted mechanism compares to intra-molecular base assisted or non-assisted mechanism as proposed by García-Cuadrado et.al.[16] It is found as one of the key steps which explains the explicit role of strong base in this reaction. This conclusion was drawn after analyzing the relaxed PES scan of the N-H bond cleavage of complex 5, which exposed a barrier-less down ward path (**Figure 5.4, section 5.3.4**). On the other hand, in absence of base the proton abstraction barrier was quite high ~40 kcal mol^{-1} (**Figure 5.5, section 5.3.4**). These results were also supported by our controlled experiments as the reaction was not occurred in the absence of base (**Figure 5.11(iii), section 5.3.5**). Though, the proton abstraction is barrier-less but the pathway between 5 and 6 is found endothermic and complex 6 is found only at the 14.5 kcal mol^{-1} lower point compare to the initial reactants (1a+Pd). The elimination of Br^- leads to the formation of six membered palladacyclic

intermediate 6 (implies the INT(ii) in figure 5.2a). This step does not involve any transition state as indicated by the relax PES scan along the reaction co-ordinates for Pd-Br bond cleavage (**Figure 5.6, section 5.3.4**).

Next, isocyanide co-ordinates with the palladium atom of complex 6 to generate complex 7. It is also found to be barrier-less which was further confirmed by PES scan (**Figure 5.7, section 5.3.4**) and revealed a smooth downward path from complex 6 to 7 after releasing of energy ~24 kcal mol^{-1}. Afterwards, isocyanide inserted into the C-Pd bond, leads to the formation of 7-membered cyclic intermediate 8 (implies the INT(iii) structure in figure 5.2a) with the increment of energy of about ~16.0 kcal mol^{-1} from complex 7. Further, the complex 8 was converted into complex 9 (implies the INT(iv) in figure 5.2a) by the removal of Pd-atom with slight increment in energy (1 kcal mol^{-1}). Subsequently, base molecule abstracts the proton from the nitrogen of tosyl hydrazone in complex 9 to form complex 10. This conversion takes place through a highly exothermic pathway (~41 kcal mol^{-1}).

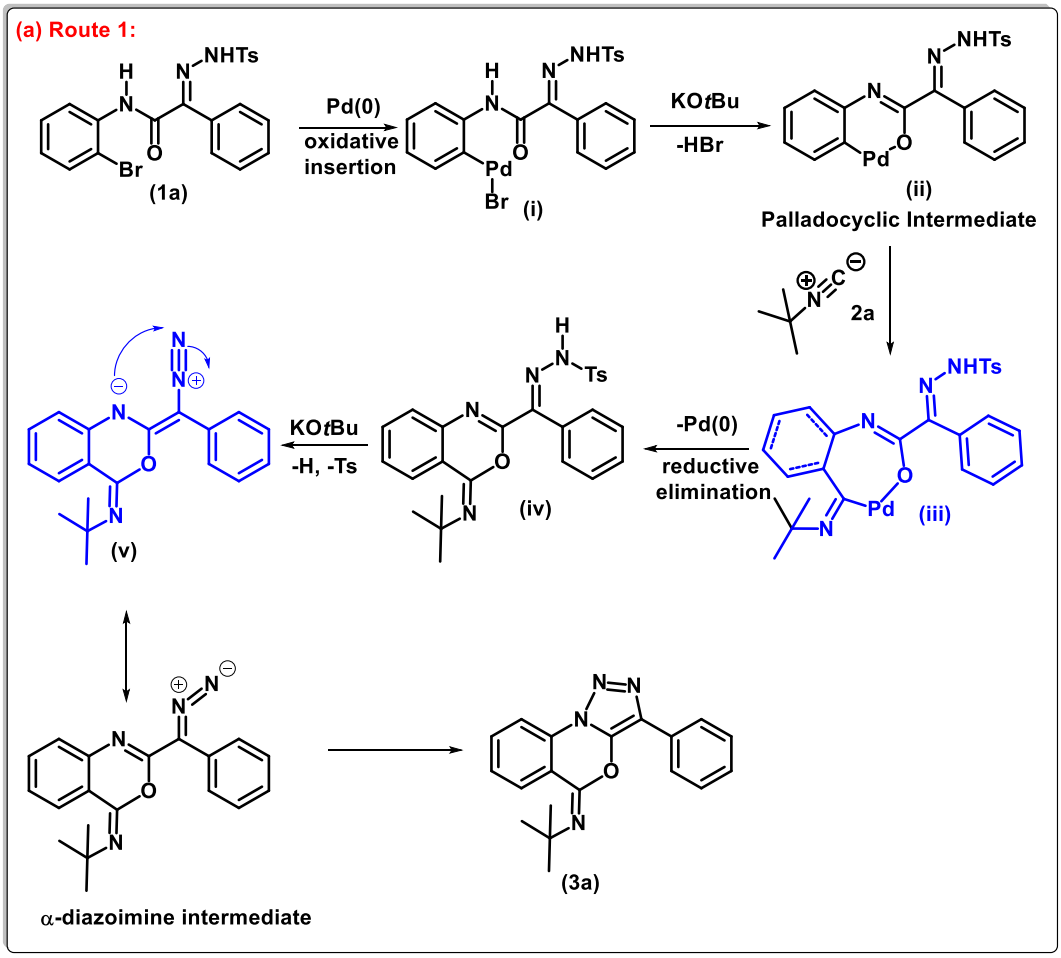

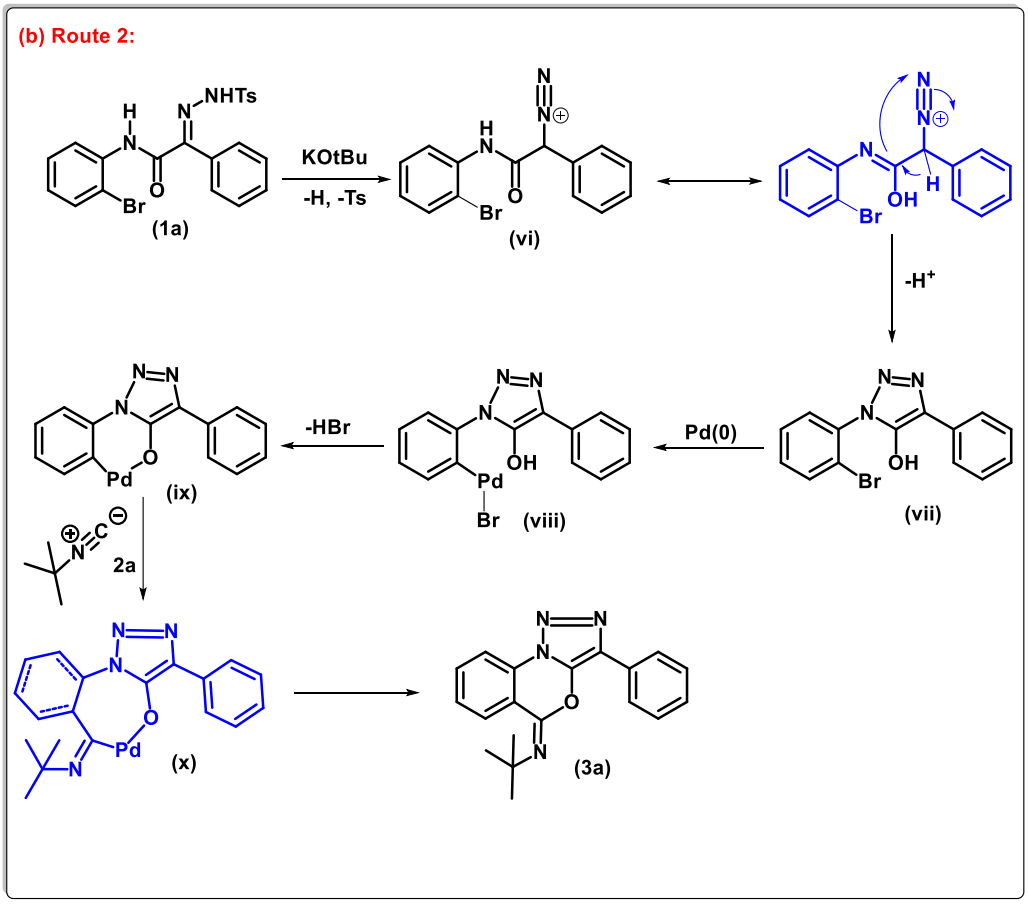

Figure 5.2: Plausible mechanisms for the synthesis of benzoxazine fused triazoles

The second H-abstractions (proton on the nitrogen of tosyl hydrazone of complex 9) also happen through a barrier-less pathway shown by PES scan of N-H bond (**Figure 5.8, section 5.3.4**). Also, in the absence of base the proton abstraction barrier is quite high ~38 kcal mol^{-1} (**Figure 5.9, section 5.3.4**). After releasing of proton, the elimination of tosyl group taken place which formed highly reactive diazo-intermediate complex 11 (implies the INT(v) in **figure 5.2a**). This diazo intermediate readily cyclize to form stable benzoxazine fused triazole ring (implies the 3a structure in **figure 5.2a**) through transition state (TS_{11-12}) with an activation energy barrier of 12.2 kcal mol^{-1}(**Figure 5.10, section 5.3.4**). This N-N bond forming cyclization follows five endo dig cyclization mechanism.[17]

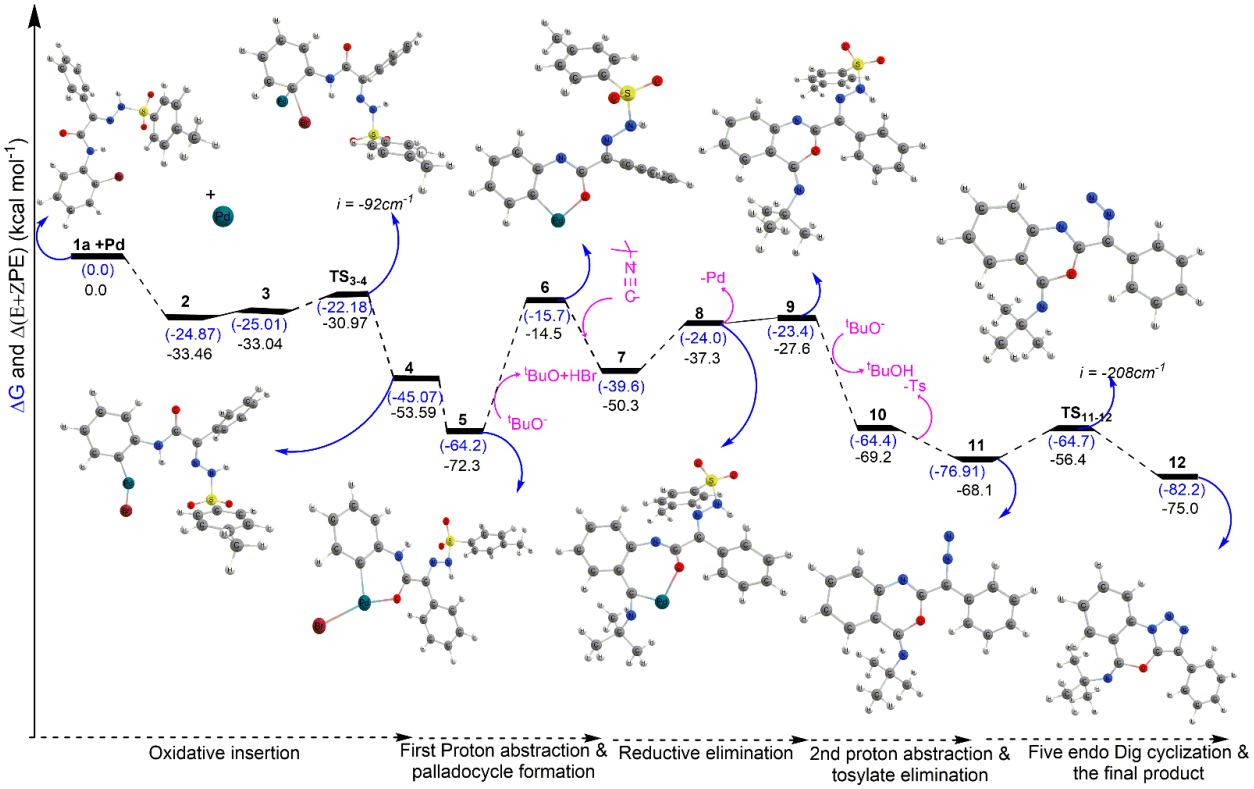

Figure 5.3: The potential energy profiles computed at B3LYP/6-31+G(d,p) level of theory related to the plausible mechanism depicted in figure 5.2a.

Next, we started investigating route 2 as depicted in figure 5.2b, however, the first step of route 2 involves the tautomerization of amide group and for this a prior rotation along H-N-C-O bond of amide is required. The PES scan implies that it requires around 20 kcal mol^{-1} energy to rotate (**Figure 5.11, section 5.3.4**). It was showing that when dihedral angle along H-N-C-O is near to 0°, it formed less stable (8 $kcalmol^{-1}$) intermediate than N-aryl-α-(tosyl hydrazone)acetamides (1a) in which dihedral angle was near about 180°. Also, the tautomer was 7.2 kcal mol^{-1} higher in energy than N-aryl-α-(tosyl hydrazone)acetamides (1a). On the other hand, route 1contains the highly exothermic oxidative insertion as the initial step, which suggests that route 1 is more favourable than route 2, so, we did not investigate the route 2 further.

5.3: Experimental details

5.3.1: General method for the synthesis of N-aryl-α-(tosyl hydrazone)acetamides derivatives (1a-1h)

A mixture of aniline (1.0 equivalent, 500 mg, 2.91mmol), benzoyl formic acid (1.5 equivalents, 655 mg, 4.36mmol), DMAP (1.5 equivalents, 532.5 mg, 4.36 mmol) and DCC (1.5 equivalents,

900 mg, 4.36 mmol) were added in dichloromethane as solvent (~ 10 mL) at 25℃ and stirred the resulting mixture for overnight. Upon complete conversion of the starting materials, work up of the reaction with ethyl acetate and distilled water in 2:1 ratio was done and the volatiles were removed using high vacuum. The mixture was purified using gradient column chromatography to obtain the corresponding acetamides. To the corresponding acetamides (1.0 equivalent, 500 mg, 1.64 mmol), tosyl hydrazine (1.5 equivalents, 458.1 mg, 2.46 mmol) and p-TSA (catalytic amount) in methanol (10 mL) were added and the resulted mixture was heated at 70℃ for 3 hrs. The reaction progress was monitored by TLC and upon complete consumption of the reactants, the volatiles were removed and the desired product was purified by column chromatography to obtain N-aryl-α-(tosyl hydrazone)acetamides derivatives (1a-1h).

5.3.2: General method for the preparation of benzoxazine fused 1,2,3 triazole derivatives (3a-3m)

In a sealed tube having a stirrer bar added N-aryl-α-(tosyl hydrazone)acetamides (1.0 equiv., 100 mg), base (2.0 equiv.), Pd-catalyst (10 mol%) and isocyanide (1.2 equiv.) in 2 mL 1,4-dioxane as a solvent. The resulting reaction mixture was refluxed at 110℃ for 2-3 hrs and the progress of the reaction was monitored using TLC. After completion of the reaction as indicated by TLC, the resulting mixture was filtered through a small pad of cellite followed by washing of the cellite pad with ethyl acetate (2x5 ml). The volatiles were evaporated under reduced pressure and the residue was purified by column chromatography using ethyl acetate in hexane as eluents affording the corresponding products 3a-3m in 42- 81% yields.

5.3.3: Computational details

All the species involved in the current investigation were fully optimized using DFT-B3LYP method. This method is the most popularly used DFT functional which uses Becke's three parameters hybrid exchange correlation functional along with Lee Yang and Parr (LYP) correlation functional.[18] For Pd & Br, Stuttgart/Dresden ECP containing basis set SDD[19] and for rest of the atoms pople's double zeta 6-31+G(d,p) basis set was used.[20] Further, frequency calculations were also performed to ensure the optimized stationary points either minima (no imaginary frequencies) or transition state (one imaginary frequency) and free energy correction at the same level of theory. Intrinsic reaction coordinate (IRC) calculations were performed to further verify that obtained transition states are connecting the exact minima or not. The Minnesota

continuum solvation model, SMD, was applied to consider the influence of solvent 1,4- Di-oxane on the reaction.[21] All the calculations were performed using Gaussian 16 program[22] and for the visualization and result analysis Chemcraft[23] software is used.

5.3.4: PES and Transition state

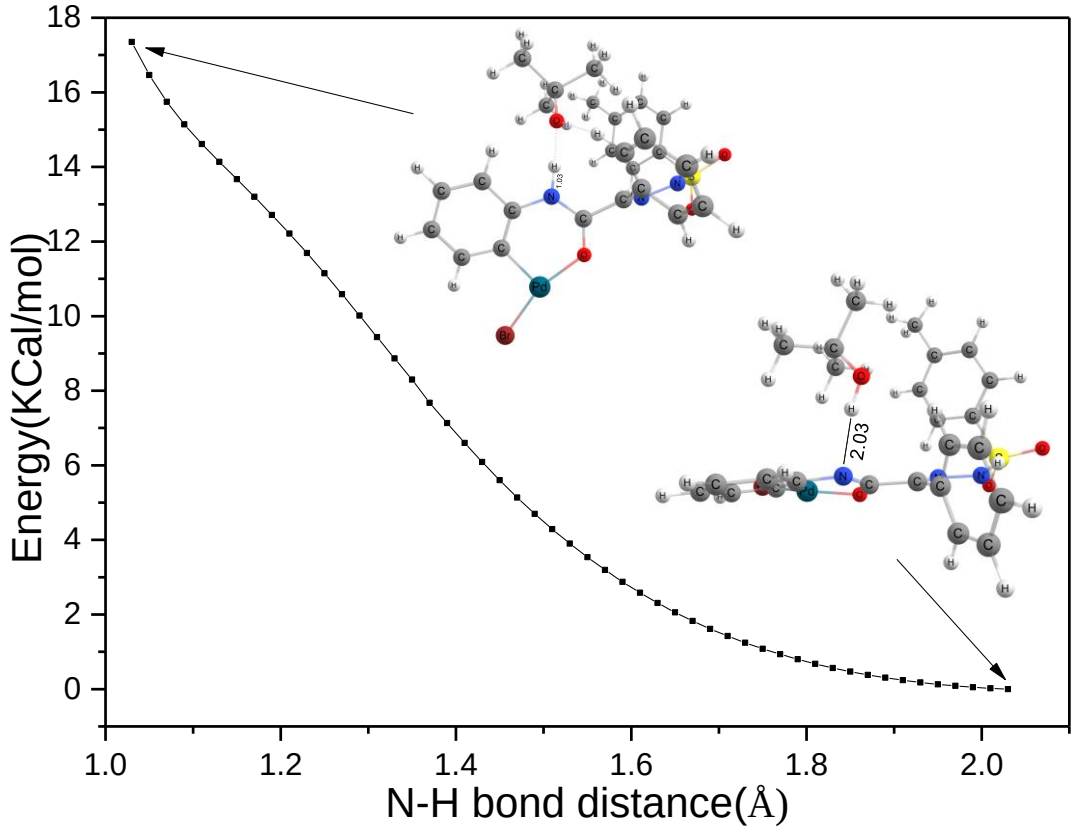

Figure 5.4: Relaxed potential energy surface scan for N-H proton abstraction from N-aryl amide in presence of strong base (KO*t*Bu)

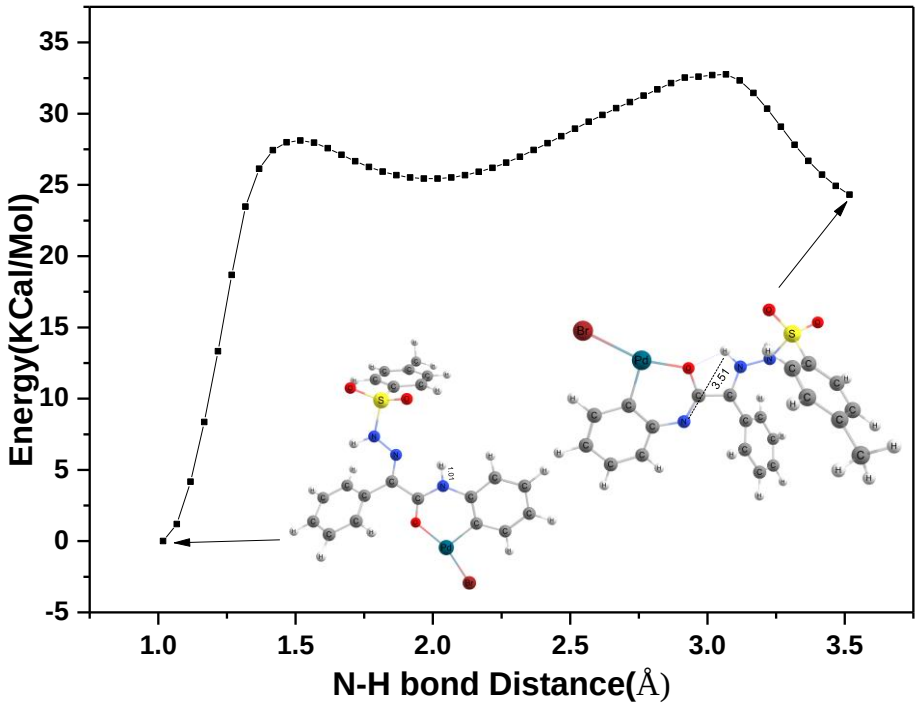

Figure 5.5: Relaxed potential energy surface scan for N-H proton abstraction from N-aryl amide in absence of strong base

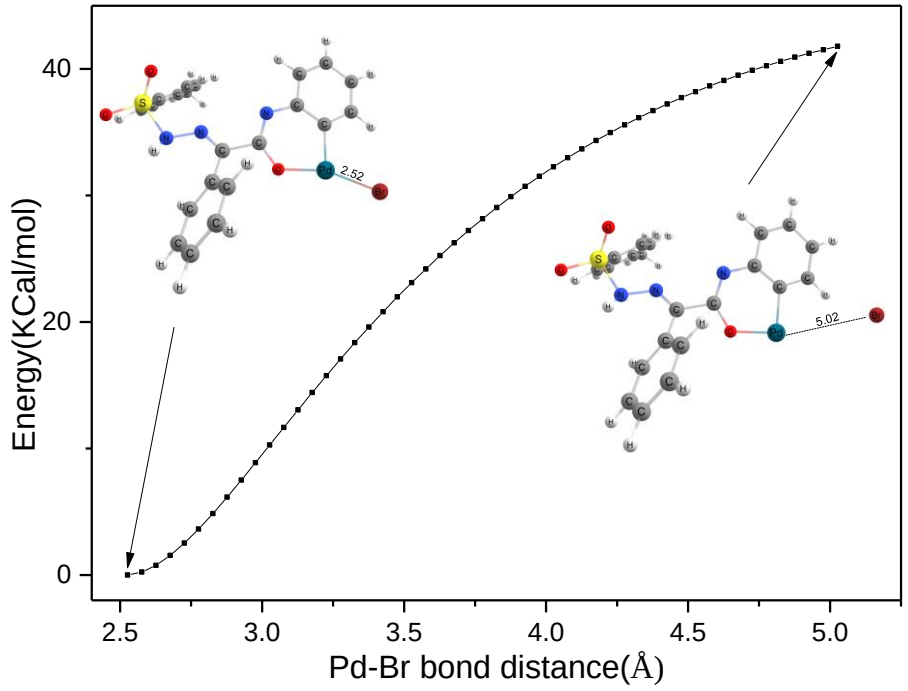

Figure 5.6: Relaxed potential energy surface scan for Pd-Br bond breaking

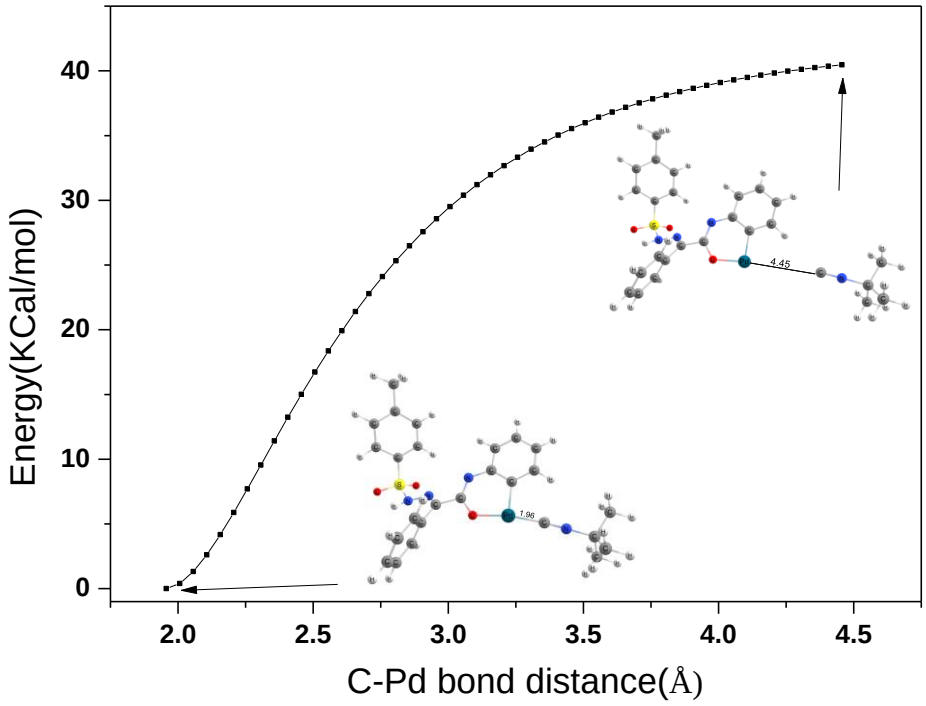

Figure 5.7: Relaxed potential energy surface for C-Pd bond formation

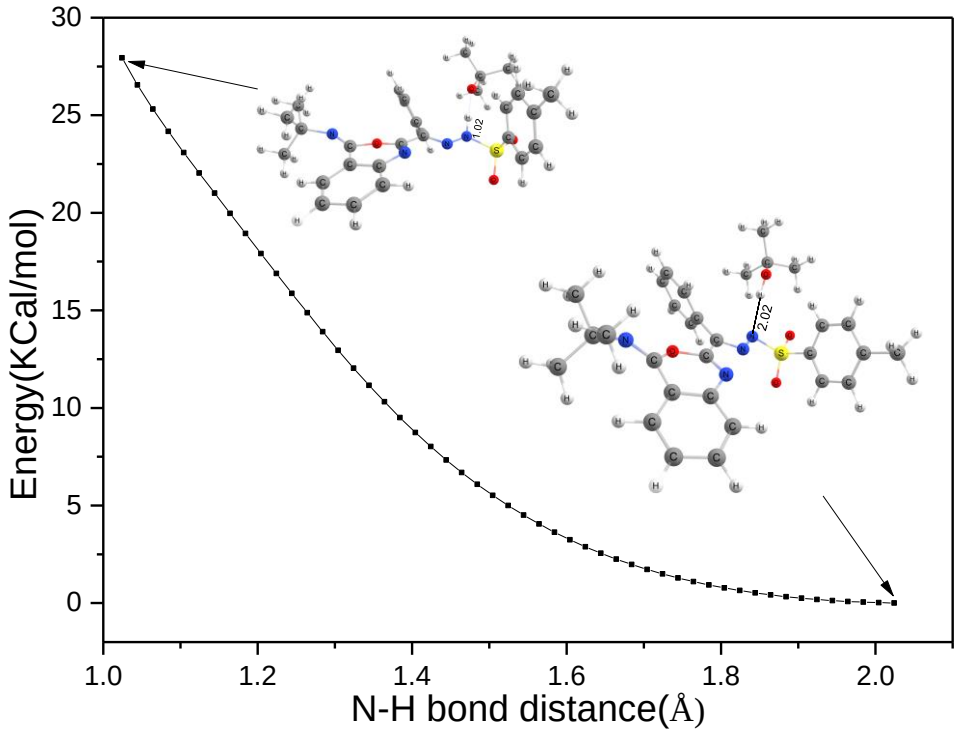

Figure 5.8: PES Scan for N-H proton abstraction from tosyl hydrazone in presence of base

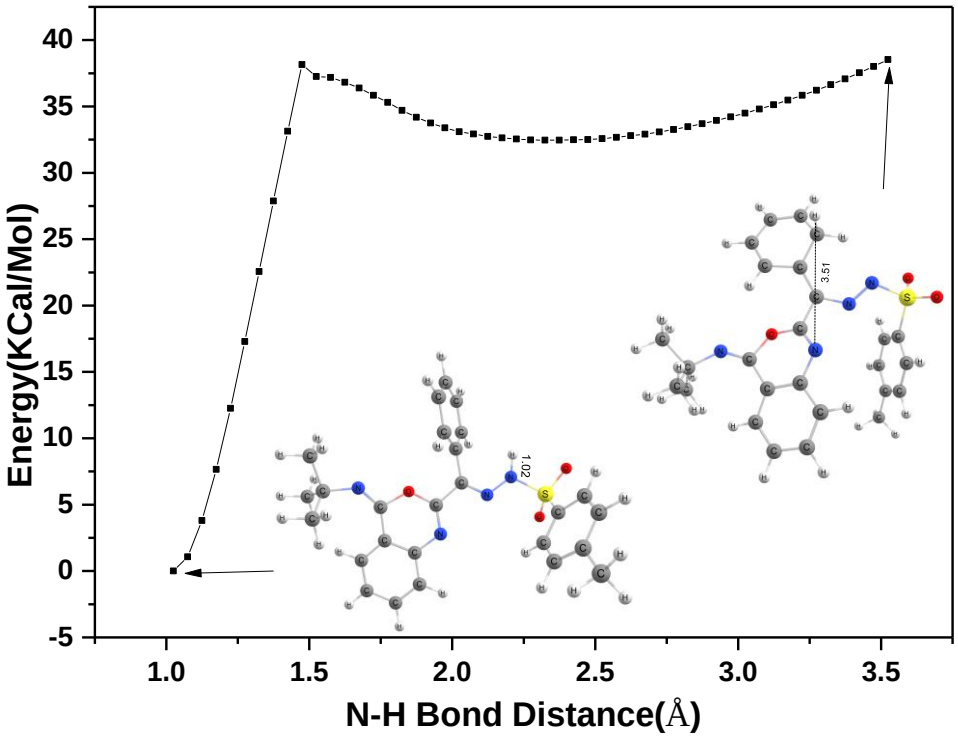

Figure 5.9: PES Scan for N-H proton abstraction from tosyl hydrazone in absence of base

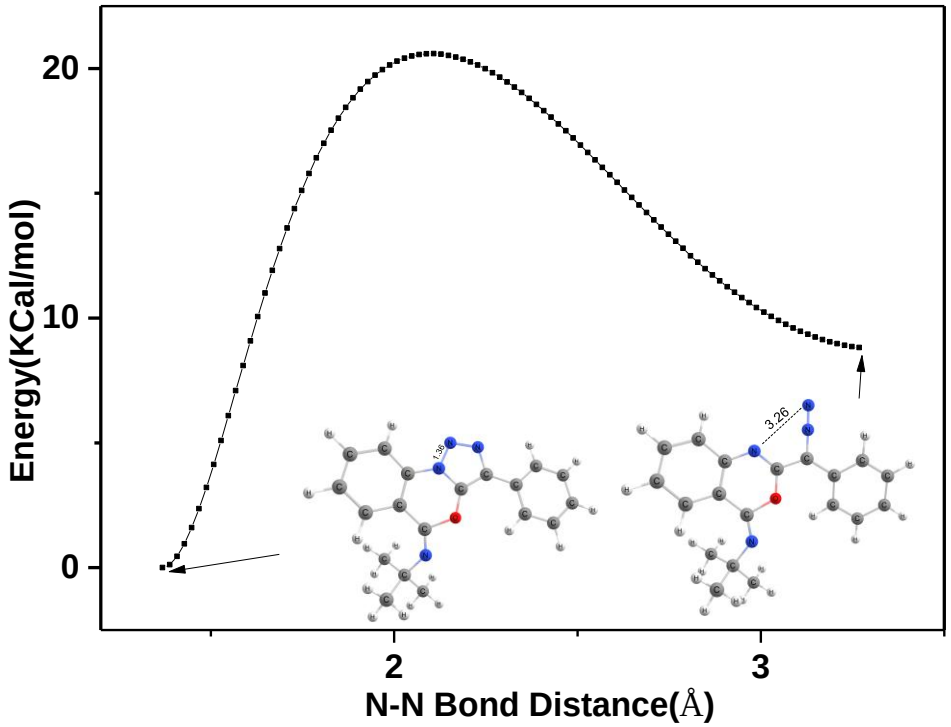

Figure 5.10: PES scan calculation for $TS_{11\text{-}12}$

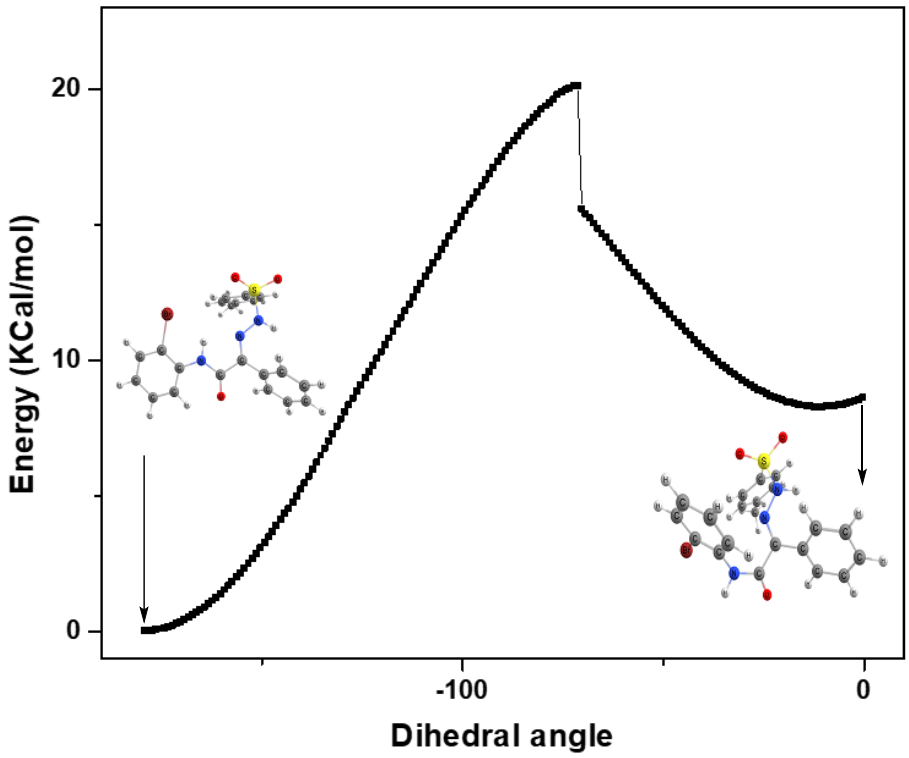

Figure 5.11: PES Scan for rotation along O-C-N-H dihedral

5.3.5: Control experiments

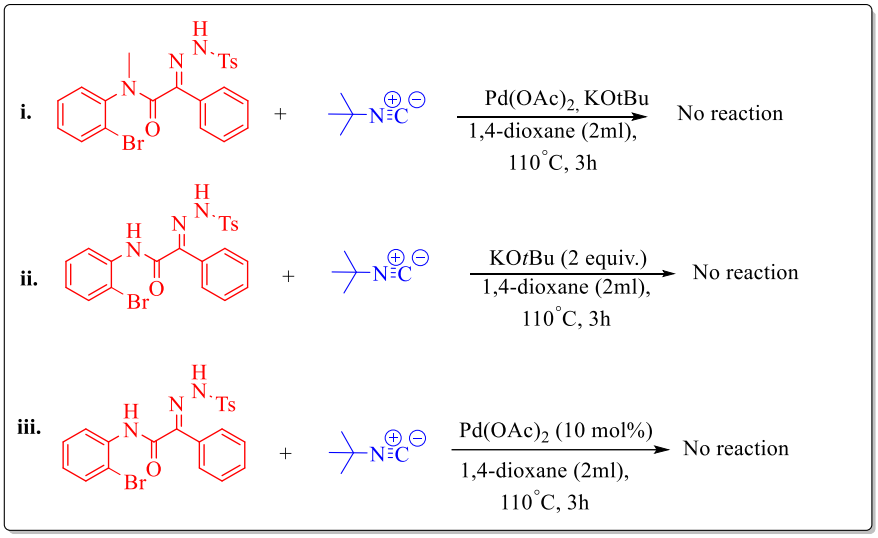

Figure 5.12: Control experiments

5.3.6: Characterization data

N-(tert-butyl)-3-phenyl-5*H*-benzo[d][1,2,3]triazolo[5,1-b][1,3]oxazin-5-imine (3a):

Solid, yield = 78% (49 mg, 0.15 mmol), ^{1}H NMR (400 MHz, $CDCl_3$): δ 8.19-8.14 (m, 2H), 8.04-8.02 (m, 2H), 7.66 (t, *J* = 8.0 Hz, 1H), 7.50-7.40 (m, 3H), 7.34 (t, *J* = 8.0 Hz, 1H), 1.51 (s, 9H) ppm, ^{13}C NMR (100 MHz, $CDCl_3$): δ 141.8, 138.6, 133.2, 132.4, 129.4, 129.0, 128.3, 128.0, 127.9, 125.4, 115.3, 114.9, 55.0, 30.0 ppm, HRMS calculated for $C_{19}H_{19}N_4O$ $[M+H]^+$ 319.3800 Found 319.3871.

3-phenyl-N-(2,4,4-trimethylpentan-2-yl)-5*H*-benzo[d][1,2,3]triazolo[5,1-b][1,3]oxazin-5-imine (3b):

Solid, yield = 75% (56 mg, 0.15 mmol), ^{1}H NMR (400 MHz, $CDCl_3$): δ 8.21 (d, *J* = 8.4 Hz, 2H), 8.09 (d, *J* = 7.6, 2H), 7.72 (t, *J* = 8.4 Hz, 1H), 7.53-7.45 (m, 3H), 7.40 (t, *J* = 7.2 Hz, 1H), 2.01(s, 2H), 1.61 (s, 6H), 1.08 (s, 9H) ppm, ^{13}C NMR (100 MHz, $CDCl_3$): δ 141.9, 137.1, 133.0, 132.4, 129.4, 129.3, 128.8, 128.2, 127.9, 127.8, 125.4, 115.5, 114.9, 58.7, 55.8, 32.0, 31.8, 30.1 ppm, HRMS calculated for $C_{22}H_{25}N_4O$ $[M+H]^+$ 361.4610 Found 361.4681.

N-cyclohexyl-3-phenyl-5*H*-benzo[d][1,2,3]triazolo[5,1-b][1,3]oxazin-5-imine (3c):

Solid, yield = 69% (47.4mg, 0.13mmol), ^{1}H NMR (400 MHz, $CDCl_3$): δ 8.28 (d, *J* = 8.0 Hz, 1H), 8.21 (d, *J* = 8.0 Hz, 1H), 8.05 (d, *J* = 8.0 Hz, 2H), 7.74 (t, *J* = 8.4 Hz, 1H), 7.54-7.46 (m, 3H), 7.40 (t, *J* = 6.8 Hz, 1H), 4.11-4.05 (m, 1H), 1.96-1.89 (m, 4H), 1.62-1.45 (m, 6H) ppm, ^{13}C NMR (100 MHz, $CDCl_3$): δ 141.8, 141.1, 133.3, 132.3, 129.4, 128.9, 128.6, 128.2, 127.8, 125.0, 114.9, 114.5, 55.7, 33.4, 25.8, 24.7 ppm, HRMS calculated for $C_{21}H_{21}N_4O$ $[M+H]^+$ 345.4180 Found 345.4181.

N-(tert-butyl)-7-chloro-3-phenyl-5*H*-benzo[d][1,2,3]triazolo[5,1-b][1,3]oxazin-5-imine (3d):

Solid, yield = 56% (39.2 mg, 0.11 mmol), ^{1}H NMR (400 MHz, $CDCl_3$): δ 8.20 (d, 1H), 8.15 (d, *J* = 8.4 Hz, 1H), 8.05 (d, *J* = 7.6 Hz, 2H), 7.67 (dd, *J* = 4.4 Hz, 1H), 7.51 (t, *J* = 8.0 Hz, 2H), 7.40-7.37 (m, *J* = 7.6 Hz, 1H), 1.55 (s, 9H) ppm, ^{13}C NMR (100 MHz, $CDCl_3$): δ 141.5, 137.4, 134.0, 133.3, 130.8, 129.1, 129.0, 128.9, 128.0, 127.9, 125.4, 116.7, 116.5, 55.2, 29.9 ppm, HRMS calculated for $C_{19}H_{18}N_4OCl$ $[M+H]^+$ 353.8220 Found 353.8224.

7-chloro-3-phenyl-N-(2,4,4-trimethylpentan-2-yl)-5*H*-benzo[d][1,2,3]triazolo[5,1-b][1,3]oxazin-5-imine (3e) :

Solid, yield = 42% (33.8 mg, 0.08 mmol), ^{1}H NMR (400 MHz, $CDCl_3$): δ 8.16 (d, *J* = 2 MHz, 1H), 8.13 (s, 1H), 8.06 (d, *J* = 8.4 Hz, 2H), 7.6 (dd, *J* = 2.4, 8.8Hz, 1H), 7.51 (t, *J* = 8.0 Hz, 2H), 7.40 (t, *J* = 7.6 Hz, 1H), 2.7 (s, 2H), 1.59 (s, 6H), 1.07 (s, 9H) ppm, ^{13}C NMR (100 MHz, $CDCl_3$): δ 141.6, 136.0, 134.1, 133.2, 130.9, 129.1, 129.0, 128.9, 128.0, 127.9, 125.4, 116.9, 116.5, 59.0, 55.5, 32.0, 31.8, 30.1 ppm, HRMS calculated for $C_{22}H_{24}N_4OCl$ $[M+H]^+$ 395.9030 Found 395.9032.

7-fluoro-3-phenyl-N-(2,4,4-trimethylpentan-2-yl)-5*H*-benzo[d][1,2,3]triazolo[5,1-b][1,3]oxazin-5-imine (3f):

Solid, Yield = 62% (49.6 mg, 0.12 mmol), ^{1}H NMR (400 MHz, $CDCl_3$): δ 8.21-8.18 (m, 1H), 8.06-8.04 (m, 2H), 7.88 (dd, *J*=2.8, 8.8 Hz, 1H), 7.51 (t, *J* = 7.6 Hz, 2H), 7.43-7.38 (m, 2H), 1.89 (s, 2H), 1.60 (s, 6H), 1.07 (s, 9H) ppm, ^{13}C NMR (100 MHz, $CDCl_3$): δ 162.9, 160.4, 141.5, 136.4, 129.2, 128.8, 127.9, 127.9, 125.4, 120.8, 120.6, 117.7, 117.6, 117.2, 117.1, 115.7,115.5, 58.9, 55.7, 32.0, 31.8, 30.0 ppm, HRMS for $C_{22}H_{24}FN_4O$ $[M+H]^+$ 379.4514 Found 379.4512.

N-cyclohexyl-7-fluoro-3-phenyl-5*H*-benzo[d][1,2,3]triazolo[5,1-b][1,3]oxazin-5-imine (3g):

Solid, Yield = 56% (41.4 mg, 0.11 mmol), ^{1}H NMR (400 MHz, $CDCl_3$): δ 8.21-8.17 (m, 1H), 8.02 (d, *J* = 8.0 Hz, 2H), 7.96(d, *J*= 8.8 Hz, 1H), 7.53 (t, *J* = 6.8 Hz, 2H), 7.44-7.36 (m, 2H), 4.10-4.04 (m, 1H), 1.93-1.91 (m, 4H), 1.65-1.39 (m, 6H) ppm, ^{13}C NMR (100 MHz, $CDCl_3$): δ 162.9, 160.4, 141.4, 140.3, 129.2, 128.9, 128.8, 127.8, 127.8, 125.0, 121.1, 120.8, 117.3, 117.2, 116.7, 116.6, 115.1, 114.9, 55.8, 33.3, 25.7, 24.6 ppm, HRMS for $C_{21}H_{20}FN_4O$ $[M+H]^+$ 363.4084 Found 363.4085.

N-(tert-butyl)-7-methyl-3-phenyl-5H-benzo[d][1,2,3]triazolo[5,1-b][1,3]oxazin-5-imine (3h):

Solid, yield = 81% (55.08 mg, 0.16 mmol), ^{1}H NMR (400 MHz, $CDCl_3$): δ 8.08-8.05 (m, 3H), 8.01 (s, 1H), 7.56-7.48 (m, 3H), 7.39 (t, *J* = 7.2 Hz, 1H), 2.47 (s, 3H), 1.55 (s, 9H) ppm, ^{13}C NMR (100 MHz, $CDCl_3$): δ 141.5, 138.9, 138.5, 134.1, 130.2, 129.4, 129.1, 128.8, 127.8, 127.7, 125.3,

114.9, 114.8, 54.9, 29.9, 21.3 ppm, HRMS calculated for $C_{20}H_{21}N_4O$ $[M+H]^+$ 332.4070 Found 332.4083.

7-methyl-3-phenyl-N-(2,4,4-trimethylpentan-2-yl)-5*H*-benzo[d][1,2,3]triazolo[5,1-b][1,3]oxazin-5-imine (3i):

Solid, yield = 80% (56 mg, 0.16 mmol), ^{1}H NMR (400 MHz, $CDCl_3$): δ 8.09-8.06 (m, 3H), 7.98 (s, 1H), 7.52-7.48 (m, 3H), 7.39 (t, *J* = 7.6 Hz, 1H), 2.48 (s, 3H), 1.91(s, 2H), 1.60 (s, 6H), 1.08 (s, 9H) ppm, ^{13}C NMR (100 MHz, $CDCl_3$): δ 141.6, 138.4, 137.4, 133.9, 130.3, 129.5, 129.1, 128.8, 127.8, 127.7, 125.4, 115.2, 114.8, 58.6, 55.5, 32.0, 31.8, 30.1, 21.4 ppm, HRMS calculated for $C_{23}H_{27}N_4O$ $[M+H]^+$ 375.4880 Found 375.4881.

N-cyclohexyl-7-methyl-3-phenyl-5*H*-benzo[d][1,2,3]triazolo[5,1-b][1,3]oxazin-5-imine (3j):

Solid, yield = 72% (52 mg, 0.14 mmol), ^{1}H NMR (400 MHz, $CDCl_3$): δ 8.09-8.02 (m, 4H), 7.53-7.49 (m, 3H), 7.39-7.35 (m, 1H), 4.11-4.06 (m, 1H), 2.48 (s, 3H), 1.97-1.89 (m, 4H), 1.62-1.44 (m, 6H) ppm, ^{13}C NMR (100 MHz, $CDCl_3$): δ 141.6, 141.5, 138.6, 134.3, 130.2, 129.5, 128.4, 127.7, 125.0, 114.9, 114.2, 55.8, 33.4, 25.8, 24.8, 21.3 ppm, HRMS calculated for $C_{22}H_{23}N_4O$ $[M+H]^+$ 359.4450 Found 359.4452.

N-(tert-butyl)-7,9-dimethyl-3-phenyl-5*H*-benzo[d][1,2,3]triazolo[5,1-b][1,3]oxazin-5-imine (3k):

Solid, yield = 79% (54.6 mg, 0.16 mmol), ^{1}H NMR (400 MHz, $CDCl_3$): δ 8.10 (d, *J* = 8.0 Hz, 2H), 7.95 (s, 1H), 7.55-7.49 (m, 2H), 7.39-7.34 (m, 2H), 2.90 (s, 3H), 2.43 (s, 3H), 1.54 (s, 9H) ppm, ^{13}C NMR: δ 137.6, 137.3, 129.4, 128.8, 127.9, 127.6, 127.1, 125.4, 116.1, 54.7, 29.9, 22.3, 20.9 ppm, HRMS for $C_{21}H_{23}N_4O$ $[M+H]^+$ 346.4340 Found 346.4361.

N-(tert-butyl)-3-phenyl-7-(trifluoromethyl)-5*H*-benzo[d][1,2,3]triazolo[5,1-b][1,3]oxazin-5-imine (3l):

Solid, Yield = 74% (52.9 mg, 0.14 mmol), ^{1}H NMR (400 MHz, $CDCl_3$): δ 8.44 (s, 1H), 8.35 (d, *J* = 8.4 Hz, 1H), 8.04 (d, *J* = 8.0 Hz, 2H), 7.68 (d, *J* = 8.0 Hz, 1H), 7.52-7.48 (m, 2H), 7.40-7.35 (m, 1H), 1.55 (s, 9H), ^{13}C NMR (100 MHz, $CDCl_3$): δ 141.7, 137.3, 135.1, 134.8, 132.5, 130.4, 128.9,

128.1, 128.0, 125.3, 124.4, 124.4, 121.6, 118.16, 112.4, 112.4, 55.4, 29.8 ppm, HRMS for $C_{20}H_{18}F_3N_4O$ $[M+H]^+$ 387.3782 Found 387.3783.

3-phenyl-7-(trifluoromethyl)-N-(2,4,4-trimethylpentan-2-yl)-5*H* benzo[d][1,2,3]triazolo[5,1-b][1,3]oxazin-5-imine (3m):

Solid, Yield = 69% (56.6 mg, 0.13 mmol), ^{1}H NMR (400 MHz, $CDCl_3$): δ 8.46 (s, 1H), 8.33 (d, *J* = 8.4 Hz, 1H), 8.06 (d, *J* = 7.2 Hz, 2H), 7.73(d, *J* = 7.2 Hz, 1H), 7.56-7.49 (m, 2H), 7.40 (t, *J* = 7.2 Hz, 1H), 1.90 (s, 2H), 1.61 (s, 6H), 1.08 (s, 9H) ppm, ^{13}C NMR (100 MHz, $CDCl_3$): δ 141.8, 136.0, 135.0, 132.5, 130.4, 128.9, 128.1, 128.0, 125.4, 124.5, 124.5, 124.3, 121.6, 118.3, 112.5, 112.4, 59.1, 55.7, 32.0, 31.7, 29.9 ppm, HRMS for $C_{23}H_{24}F_3N_4O$ $[M+H]^+$ 429.4592 Found 429.4592.

5.4: Conclusion

In summary, we have described a Pd-catalyzed one-pot tandem synthesis of medicinally important benzoxazine fused 1,2,3-triazoles using N-aryl-α-(tosyl hydrazone)acetamides as a safe and stable surrogate of α-diazoacetamides with isocyanides. Next, the compatibility of this protocol to generate a library of benzoxazine fused 1,2,3-triaoles derivatives was tested using various substitutions on N-aryl part of acetamide along with isocyanides. Besides, two possible mechanistic routes were proposed, however, one of them consisting formation of benzoxazine ring first followed by the generation of triazole ring was more favorable as suggested by control experiments and theoretical study. Additionally, the DFT calculation of more favourable mechanistic route have been performed to get insight about the mechanism which suggested Pd(II)-isocyanide complex and α-diazoimino intermediate formation as a key steps during this catalytic cycle. Interestingly, this work extends the application of α-diazoacetamides based precursors in the synthesis of medicinally interested heterocycles.

5.5: References

(1) (a) Zhang, B.; Wee, A. G. H. Di- and Trisubstituted γ-Lactams via Rh(II)-Carbenoid Reaction of N -Cα-Branched, N -Bis(Trimethylsilyl)Methyl α-Diazoamides. Synthesis of (±)-α-Allokainic Acid. *Org. Lett.* **2010**, *12*, 5386–5389. (b) Solé, D.; Pérez-Janer, F.; Bennasar, M. L.; Fernández, I. Palladium Catalysis in the Intramolecular Carbene C–H

Insertion of α-Diazo-α-(Methoxycarbonyl)Acetamides to Form β-Lactams. *European J. Org. Chem.* **2018**, *2018*, 4446–4455. (c) Zheng, Y.; Bao, M.; Qiu, L.; Xu, X. Thermally Induced Reaction of Diazoamides with Isatins: A Complementary Approach to the 3,3′-Bioxindole Derivatives. *Tetrahedron Lett.* **2017**, *58*, 3390–3393. (d) Chen, L. H.; Ma, Y. T.; Yang, F.; Huang, X. Y.; Chen, S. W.; Ji, K.; Chen, Z. S. Chemo-Selective Rh(II)/Pd(0) Dual Catalysis: Synthesis of All-Carbon C3-Quaternary Allylic Oxindoles from n-Aryl-a-Diazo-b-Keto-Amides with Functionalized Allyl Carbonates. *Adv. Synth. Catal.* **2019**, *361*, 1307–1312. (e) Ring, A.; Ford, A.; Maguire, A. R. Substrate and Catalyst Effects in C–H Insertion Reactions of α-Diazoacetamides. *Tetrahedron Lett.* **2016**, *57*, 5399–5406. (f) Candeias, N. R.; Gois, P. M. P.; Afonso, C. A. M. Rh(II)-Catalyzed Intramolecular C-H Insertion of Diazo Substrates in Water: Scope and Limitations. *J. Org. Chem.* **2006**, *71*, 5489–5497.

(2) Yamamoto, K.; Qureshi, Z.; Tsoung, J.; Pisella, G.; Lautens, M. Combining Ru-Catalyzed C-H Functionalization with Pd-Catalyzed Asymmetric Allylic Alkylation: Synthesis of 3-Allyl-3-Aryl Oxindole Derivatives from Aryl α-Diazoamides. *Org. Lett.* **2016**, *18* (19), 4954–4957.

(3) Huang, L. Z.; Xuan, Z.; Jeon, H. J.; Du, Z. T.; Kim, J. H.; Lee, S. G. Asymmetric Rh(II)/Pd(0) Relay Catalysis: Synthesis of α-Quaternary Chiral β-Lactams through Enantioselective C-H Insertion/Diastereoselective Allylation of Diazoamides. *ACS Catal.* **2018**, *8*, 7340–7345.

(4) Zhukovsky, D.; Dar'in, D.; Krasavin, M. Rh2(Esp)2-Catalyzed Coupling of α-Diazo-γ-Butyrolactams with Aromatic Amines. *European J. Org. Chem.* **2019**, *2019*, 4377–4383.

(5) (a) Martín, C.; Belderraín, T. R.; Pérez, P. J. Rediscovering Copper-Based Catalysts for Intramolecular Carbon-Hydrogen Bond Functionalization by Carbene Insertion. *Org. Biomol. Chem.* **2009**, *7*, 4777–4781. (b) Slattery, C. N.; Ford, A.; Maguire, A. R. Catalytic Asymmetric C-H Insertion Reactions of α-Diazocarbonyl Compounds. *Tetrahedron* **2010**, *66*, 6681–6705. (c) Young, C. J.; Cheol, H. Y.; Turos, E.; Kyung, S. Y.; Kyung, W. J. Total Syntheses of (-)-α-Kainic Acid and (+)-α-Allokainic Acid via Stereoselective C-H Insertion and Efficient 3,4-Stereocontrol. *J. Org. Chem.* **2007**, *72*, 10114–10122. (d) Gois, P. M. P.; Afonso, C. A. M. Regio- and Stereoselective Dirhodium(II)-Catalysed Intramolecular C-H Insertion Reactions of α-Diazo-α-(Dialkoxyphosphoryl)Acetamides and -Acetates.

European J. Org. Chem. **2003**, *3*, 3798–3810. (e) Grohmann, M.; Buck, S.; Schäffler, L.; Maas, G. Diruthenium(I,I) Catalysts for the Formation of β- and γ-Lactams via Carbenoid C-H Insertion of α-Diazoacetamides. *Adv. Synth. Catal.* **2006**, *348*, 2203–2211.

(6) (a) Huo, J.; Hu, H.; Zhang, M.; Hu, X.; Chen, M.; Chen, D.; Liu, J.; Xiao, G.; Wang, Y.; Wen, Z. A Mini Review of the Synthesis of Poly-1,2,3-Triazole-Based Functional Materials. *RSC Adv.* **2017**, *7*, 2281–2287. (b) Kantheti, S.; Narayan, R.; Raju, K. V. S. N. The Impact of 1,2,3-Triazoles in the Design of Functional Coatings. *RSC Adv.* **2015**, *5*, 3687–3708. (c) Ginalska, G.; Pachuta-stec, A.; Pitucha, M. And Docking Studies. **2020**, 1–18; (d) Hozien, Z. A.; EL-Mahdy, A. F. M.; Abo Markeb, A.; Ali, L. S. A.; El-Sherief, H. A. H. Synthesis of Schiff and Mannich Bases of News-Triazole Derivatives and Their Potential Applications for Removal of Heavy Metals from Aqueous Solution and as Antimicrobial Agents. *RSC Adv.* **2020**, *10*, 20184–20194. (e) Niu, T. F.; Gu, L.; Wang, L.; Yi, W. Bin; Cai, C. Chemoselective Preparation of Unsymmetrical Bis(1,2,3-Triazole) Derivatives and Application in Bis(1,2,3-Triazole)-Modified Peptidomimetic Synthesis. *European J. Org. Chem.* **2012**, *34*, 6767–6776.

(7) (a) Zhang, S.; Xu, Z.; Gao, C.; Ren, Q.C.; Chang, L.; Lv, Z.S.; Feng, L.S. Triazole derivatives and their anti-tubercular activity. *European J. Med. Chem.*, **2017**, *138*, 501-513. (b) Ayati, A.; Emami, S.; Foroumadi, A. The importance of triazole scaffold in the development of anticonvulsant agents. *Eur. J. Med. Chem.* **2016**, *109*, 380–392. (c) El-Sherief, H.A.; Youssif, B.G.; Bukhari, S.N.A.; Abdelazeem, A.H.; Abdel-Aziz, M.; Abdel-Rahman, H.M. Synthesis, anticancer activity and molecular modeling studies of 1, 2, 4-triazole derivatives as EGFR inhibitors. *Eur. J. Med. Chem.* **2018**, *156*, 774–789.

(8) (a) Ma, N.; Wang, Y.; Zhao, B. X.; Ye, W. C.; Jiang, S. The Application of Click Chemistry in the Synthesis of Agents with Anticancer Activity. *Drug Des. Devel. Ther.* **2015**, *9*, 1585–1599. (b) Thirumurugan, P.; Matosiuk, D.; Jozwiak, K. Click Chemistry for Drug Development and Diverse Chemical-Biology Applications. *Chem. Rev.* **2013**, *113*, 4905–4979. (c) Totobenazara, J.; Burke, A. J. New Click-Chemistry Methods for 1,2,3-Triazoles Synthesis: Recent Advances and Applications. *Tetrahedron Lett.* **2015**, *56*, 2853–2859. (d) Rostovtsev, V. V.; Green, L. G.; Fokin, V. V.; Sharpless, K. B. A Stepwise Huisgen Cycloaddition Process: Copper(I)-Catalyzed Regioselective "Ligation" of Azides and Terminal Alkynes. *Angew. Chemie - Int. Ed.* **2002**, *41*, 2596–2599. (e) Boren, B. C.;

Narayan, S.; Rasmussen, L. K.; Zhang, L.; Zhao, H.; Lin, Z.; Jia, G.; Fokin, V. V. Ruthenium-Catalyzed Azide-Alkyne Cycloaddition: Scope and Mechanism. *J. Am. Chem. Soc.* **2008**, *130*, 8923–8930. (f) Gholampour, M.; Ranjbar, S.; Edraki, N.; Mohabbati, M.; Firuzi, O.; Khoshneviszadeh, M. Click Chemistry-Assisted Synthesis of Novel Aminonaphthoquinone-1,2,3-Triazole Hybrids and Investigation of Their Cytotoxicity and Cancer Cell Cycle Alterations. *Bioorg. Chem.* **2019**, *88*, 102967. (g) Hou, W.; Luo, Z.; Zhang, G.; Cao, D.; Li, D.; Ruan, H.; Ruan, B. H.; Su, L.; Xu, H. Click Chemistry-Based Synthesis and Anticancer Activity Evaluation of Novel C-14 1,2,3-Triazole Dehydroabietic Acid Hybrids. *Eur. J. Med. Chem.* **2017**, *138*, 1042–1052.

(9) (a) Bakherad, M.; Keivanloo, A.; Amin, A. H.; Farkhondeh, A.; Access, O. Through a Copper-Catalyzed Click Reaction. **2019**, 122–129; (b) Ibraheem, T.; Abdul, W.; Abdul, R.; Shneshil, M. K. Synthesis of 1 , 2 , 3-Triazole Derivatives from Azidoacetamide via Cyclo-Addition Reaction. **2019**, *11*, 540–544; (c) Giel, M.; Smedley, C. J.; Mackie, E. R. R.; Guo, T.; Dong, J.; Soares, T. P. Metal-Free Click Synthesis of Functional 1-Substituted-1 , 2 , 3-Triazoles. No. I; (d) Nemallapudi, B. R.; Guda, D. R.; Ummadi, N.; Avula, B.; Zyryanov, G. V.; Reddy, C. S.; Gundala, S. New Methods for Synthesis of 1,2,3-Triazoles: A Review. *Polycycl. Aromat. Compd.* **2020**, *2020*, 1–19. (e) Espinoza-Vázquez, A.; Rodríguez-Gómez, F. J.; Vergara-Arenas, B. I.; Lomas-Romero, L.; Angeles-Beltrán, D.; Negrón-Silva, G. E.; Morales-Serna, J. A. Synthesis of 1,2,3-Triazoles in the Presence of Mixed Mg/Fe Oxides and Their Evaluation as Corrosion Inhibitors of API 5L X70 Steel Submerged in HCl. *RSC Adv.* **2017**, *7*, 24736–24746. (f) Efimov, I. V. [InlineMediaObject Not Available: See Fulltext.] Recent Methods for the Synthesis of NH-1,2,3-Triazoles (Microreview). *Chem. Heterocycl. Compd.* **2019**, *55*, 28–30. (g) Ashok, D.; Reddy, M. R.; Dharavath, R.; Ramakrishna, K.; Nagaraju, N.; Sarasija, M. Microwave-Assisted Synthesis of Some New 1,2,3-Triazole Derivatives and Their Antimicrobial Activity. *J. Chem. Sci.* **2020**, *132*, 1–9.

(10) (a) Liu, Y.; Zhang, W.; Xie, K.; Jiang, Y. Silver-Catalyzed Intramolecular C(5)-H Acyloxylation of 1,4-D-Substituted 1,2,3-Triazoles. *Synlett.* **2017**, *28*, 1496–1500.; (b) Ravikumar, K.; Sridhar, B.; Nanubolu, J. B.; Hariharakrishnan, V.; Singh, A. N. Structures of Benzoxazine-Fused Triazoles as Potential Diuretic Agents. *Acta Crystallogr. Sect. C Cryst. Struct. Commun.* **2012**, *68*. (c) Nagavelli, V. R.; Nukala, S. K.; Narsimha, S.; Battula, K. S.; Tangeda, S. J.; Reddy, Y. N. Synthesis, Characterization and Biological Evaluation

of 7-Substituted- 4-((1-Aryl-1H-1,2,3-Triazol-4-Yl) Methyl)-2H-Benzo[b][1,4]Oxazin-3(4H)-Ones as Anticancer Agents. *Med. Chem. Res.* **2016**, *25*, 1781–1793.

(11) Ma, X.; Li, H.; Xin, H.; Du, W.; Anderson, E. A.; Dong, X.; Jiang, Y. Copper-Catalyzed Intramolecular C-H Alkoxylation of Diaryltriazoles: Synthesis of Tricyclic Triazole Benzoxazines. *Org. Lett.* **2020**, *22*, 5320–5325.

(12) Liu, Z.; Cao, S.; Wu, J.; Zanoni, G.; Sivaguru, P.; Bi, X. Palladium (II)-catalyzed cross-coupling of diazo compounds and isocyanides to access ketenimines. *ACS Catal.* **2020**, *10*, 12881–12887.

(13) (a) Santiago, J.V.; Burtoloso, A.C. Synthesis of Fused Bicyclic [1, 2, 3]-Triazoles from γ-Amino Diazoketones. *ACS Omega.,* **2019**, *4*, 159–168. (b) Sajid, M.A.; Khan, Z.A.; Shahzad, S.A.; Naqvi, S.A.R.; Usman, M.; 5-endo-dig cyclizations in organic syntheses. *Mol. Divers.,* **2020**, *24*, 295–317.

(14) (a) Mandal, N.; Datta, A. Harnessing the efficacy of 2-pyridone ligands for Pd-catalyzed (β/γ)-c (sp3)–H activations. *J. Org. Chem.*, **2020**, *85*, 13228–13238. (b) López-Serrano, J.; Duckett, S.B.; Lledós, A.Palladium-catalyzed hydrogenation: Detection of palladium hydrides. A joint study using para-hydrogen-enhanced NMR spectroscopy and density functional theory. *J. Am. Chem. Soc.,* **2006**, *128*, 9596–9597. (c) Lam, K.C.; Marder, T.B.; Lin, Z. DFT Studies on the Effect of the Nature of the Aryl Halide Y− C6H4− X on the Mechanism of Its Oxidative Addition to Pd0L versus Pd0L2. *Organometallics.,* **2007,** *26*, 758-760. (d) Tang, Y.; Bi, S.; Liu, Y.; Liu, C.; Liang, H.; Ling, B. Theoretical study on Pd-catalyzed reaction of aryl iodide with unsymmetrical alkyne. *J. Organomet. Chem.* **2016**, 803**,** 134-141.

(15) Diefenbach, A.; Bickelhaupt, F.M. Oxidative addition of Pd to C–H, C–C and C–Cl bonds: Importance of relativistic effects in DFT calculations. *J. Chem. Phys.,* **2001**, *115*, 4030–4040.

(16) García-Cuadrado, D.; De Mendoza, P.; Braga, A.A.; Maseras, F.; Echavarren, A.M. Proton-abstraction mechanism in the palladium-catalyzed intramolecular arylation: substituent effects. *J. Am. Chem. Soc.,* **2007**, *129*, 6880–6886.

(17) Evans, L.E.; Cheeseman, M.D.; Jones, K. N–N bond-forming cyclization for the one-pot synthesis of N-aryl [3, 4-d] pyrazolopyrimidines. *Org. Lett.,* **2012**, *14*, 3546–3549.

(18) (a) Becke, A. D. Phys. Rev. A: At., Mol., Opt. Phys. **1988**, 38, 3098 DOI:

0.1103/PhysRevA.38.3098. (b) Lee, C.; Yang, W.; Parr, R. G. *Phys. Rev. B: Condens. Matter Mater. Phys*. **1988**, 37, 785. (c) Miehlich, B.; Savin, A.; Stoll, H.; Preuss, H. Chem. Phys. Lett. **1989**, *157*, 200.

(19) Andrae, D.; Haussermann, U.; Dolg, M.; Stoll, H.; Preuss, H. Theor. Chim. Acta **1990**, *77*, 123.

(20) Hehre, W. J.; Radom, L.; Schleyer, P. v. R.; Pople, J. A. *Ab Initio Molecular Orbital Theory*; Wiley-Interscience: New York, **1986**.

(21) Marenich, A. V.; Cramer, C. J.; Truhlar, D. G. *J. Phys. Chem*. B **2009**, *113*, 6378.

(22) Frisch, M. J.; Trucks, G. W.; Schlegel, H. B.; Scuseria, G. E.; Robb, M. A.; Cheeseman, J. R.; Scalmani, G.; Barone, V.; Petersson, G. A.; Nakatsuji, H.; Li, X.; Caricato, M.; Marenich, A. V.; Bloino, J.; Janesko, B. G.; Gomperts, R.; Mennucci, B.; Hratchian, H. P.; Ortiz, J. V.; Izmaylov, A. F.; Sonnenberg, J. L.; Williams-Young, D.; Ding, F.; Lipparini, F.; Egidi, F.; Goings, J.; Peng, B.; Petrone, A.; Henderson, T.; Ranasinghe, D.; Zakrzewski, V. G.; Gao, J.; Rega, N.; Zheng, G.; Liang, W.; Hada, M.; Ehara, M.; Toyota, K.; Fukuda, R.; Hasegawa, J.; Ishida, M.; Nakajima, T.; Honda, Y.; Kitao, O.; Naka, H.; Vreven, T.; Throssell, K.; J.A. Montgomery, J.; Peralta, J. E.; Ogliaro, F.; Bearpark, M. J.; Heyd, J. J.; Brothers, E. N.; Kudin, K. N.; Staroverov, V. N.; Keith, T. A.; Kobayashi, R.; Normand, J.; Raghavachari, K.; Rendell, A. P.; Burant, J. C.; Iyengar, S. S.; Tomasi, J.; Cossi, M.; Millam, J. M.; Klene, M.; Adamo, C.; Cammi, R.; Ochterski, J. W.; Martin, R. L.; Morokuma, K.; Farkas, O.; Foresman, J. B.; Fox, D. J. *Gaussian 16*, Revision C.01, Gaussian Inc., Wallingford, CT, **2016**.

(23) Zhurko, G. A.ChemCraft software, http://www.chemcraftprog.com

Conclusion of the thesis:

Over the past few years, a lot of work has been done to develop transition metal-mediated processes to synthesize new heterocyclic compounds that are clinically significant. Furthermore, in recent years, there has been a lot of interest in the synthesis of essential heterocyclic scaffolds via tandem or cascade processes mediated by transition metals. These reactions decrease the overall number of reaction steps and the need for intermediate purifications by forming numerous bonds in a single pot without varying the reaction conditions. Cascade reactions are considered extremely cost-effective and environmentally benign due to the reduction of wastage of chemicals used for purifications. To carry out these kinds of reactions, a variety of transition metal catalysts, including Rh, Pd, Cu, Ru, Ir, Fe, etc., have been used. In this view, Pd-based catalysts are widely used for isocyanide insertion and carbene insertion cascade methodologies. Also, computational chemistry is becoming a more versatile tool for a variety of chemists from various fields of chemistry. DFT studies are particularly useful for mechanistic investigations and are regarded as a crucial technique for the discovery of novel synthesis routes in organic synthesis. This thesis's first chapter highlights some noteworthy recent efforts to synthesize novel heterocyclic moieties that are highly significant by employing palladium-catalyzed cascade reactions, with carbene transfer, isocyanide insertion, C-H activation, and cyclization serving as crucial steps. These reports also cover mechanistic inquiry through a variety of experimental and computational studies, further transformation and applications, etc.

- In **Chapter 2**, a multicomponent reaction involving a carbene insertion strategy has been reported to produce therapeutically relevant 3-alkylidene oxindoles. A one-pot strategy includes aniline, isocyanides, and 3-diazo oxindole catalyzed by palladium acetate, which in turn produced (*E*)-3-alkylidene oxindole derivatives having two amino substituents that can be utilized for various functionalization were synthesized in moderate to good yields. The possible pathway that proposed the production of Pd(II)-carbene complex, migratory insertion of isocyanides which was then followed by the nucleophilic addition of aniline was next investigated using DFT calculations.
- In **Chapter 3,** we have developed a Pd-catalysed and amide-assisted multicomponent reaction of 3-diazo oxindole, isocyanide, and water to generate tricyclic oxazole-fused indole scaffolds. Besides, a sophisticated route for the mechanistic path followed by the reaction was proposed which is further validated by using DFT calculations recommended that the reaction involves

amide formation at the C-3 position via isocyanide insertion which subsequently assisted [3+1+1] annulation reaction to furnish oxazole-fused indoles.

- In **Chapter 4**, we have developed a hydrazone-promoted isocyanide insertion strategy towards Indole-*N*-carboxamide scaffolds which can be used as valuable precursors for the synthesis of various biologically active moieties. A diverse range of substrate scopes have been developed to validate the feasibility of the protocol. The hydrazone group acts as a reaction promoter to facilitate the weak nucleophilic N-H insertion reaction.
- **Chapter 5** includes a Pd-catalyzed one-pot tandem synthesis of medicinally important benzoxazine fused 1,2,3-triazoles using N-aryl-α-(tosyl hydrazone)acetamides with isocyanides. Besides, two possible mechanistic routes were proposed, the DFT calculation of a more favorable mechanistic route has been performed to get deep insight into the mechanism which suggested Pd(II)-isocyanide complex and α-diazo imino intermediate formation as a key step during this catalytic cycle.

This work extends the detailed experimental and theoretical study of various palladium-catalyzed cascade strategies for the synthesis of novel heterocyclic scaffolds which can be utilized for various applications.

Outlook:

- The indole-based heterocycles have great importance in various fields of biological as well as pharmaceuticals. From this perspective, this multi-component strategy towards the synthesis of (*E*)- 3-alkylidene oxindole derivative having two amino groups via palladium-catalyzed cascade carbenoid insertion methodology has been developed. This approach can play an important role in synthesizing various biologically active pharmaceutical ingredients (APIs) as precursors as there is the presence of two amino substituents that can easily be functionalized.
- Also, a novel indole-based tricyclic scaffold has been developed via another tandem multicomponent strategy involving carbenoid generation, isocyanide insertion, and [3+1+1] annulation approach. A good combination of important reactions involving great organic chemistry concepts is seen in this methodology which can be further extended towards various poly heterocycles molecules in the future. DFT studies done to get a deep understanding of this multi-component strategy opened new directions from mechanistic aspects.
- An amazing concept of remote activation was involved during the synthesis of valuable precursors of indole-*N*-carboxamide scaffolds in which the nucleophilicity was influenced by the phenyl hydrazone group at the third position of oxindole moiety. In this view, these kinds

of strategies which are accelerated by any functional group presence can be an interesting strategy for the synthesis of valuable molecules.

- Another isocyanide insertion, intramolecular cyclization methodology towards biologically relevant triazoles has been studied. However, the limited substrate scope doesn't limit its applications. These synthesized scaffolds can act as good precursors for various organic synthetic transformations.

Representative ^{1}H NMR (400 MHz, $CDCl_3$) and $^{13}C\{^{1}H\}$ NMR (100 MHz, $CDCl_3$) spectra of Chapter 2

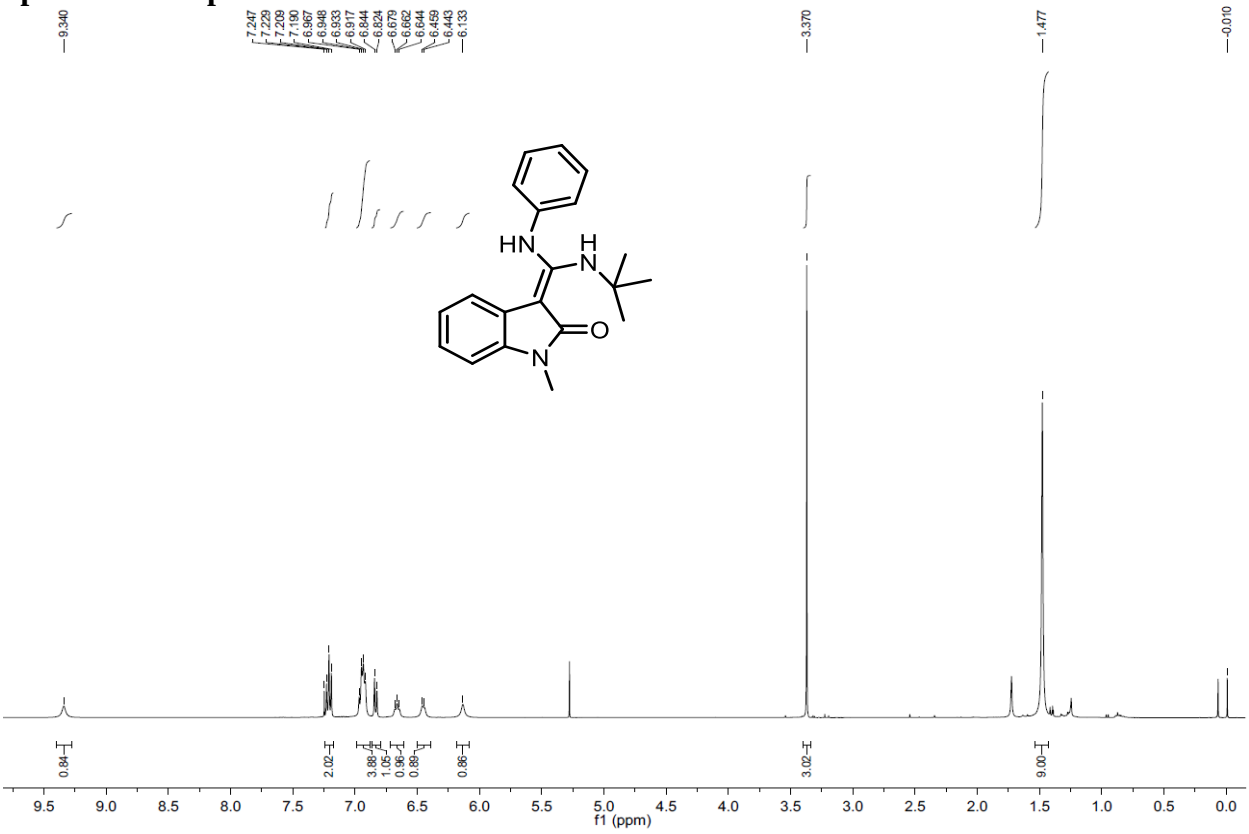

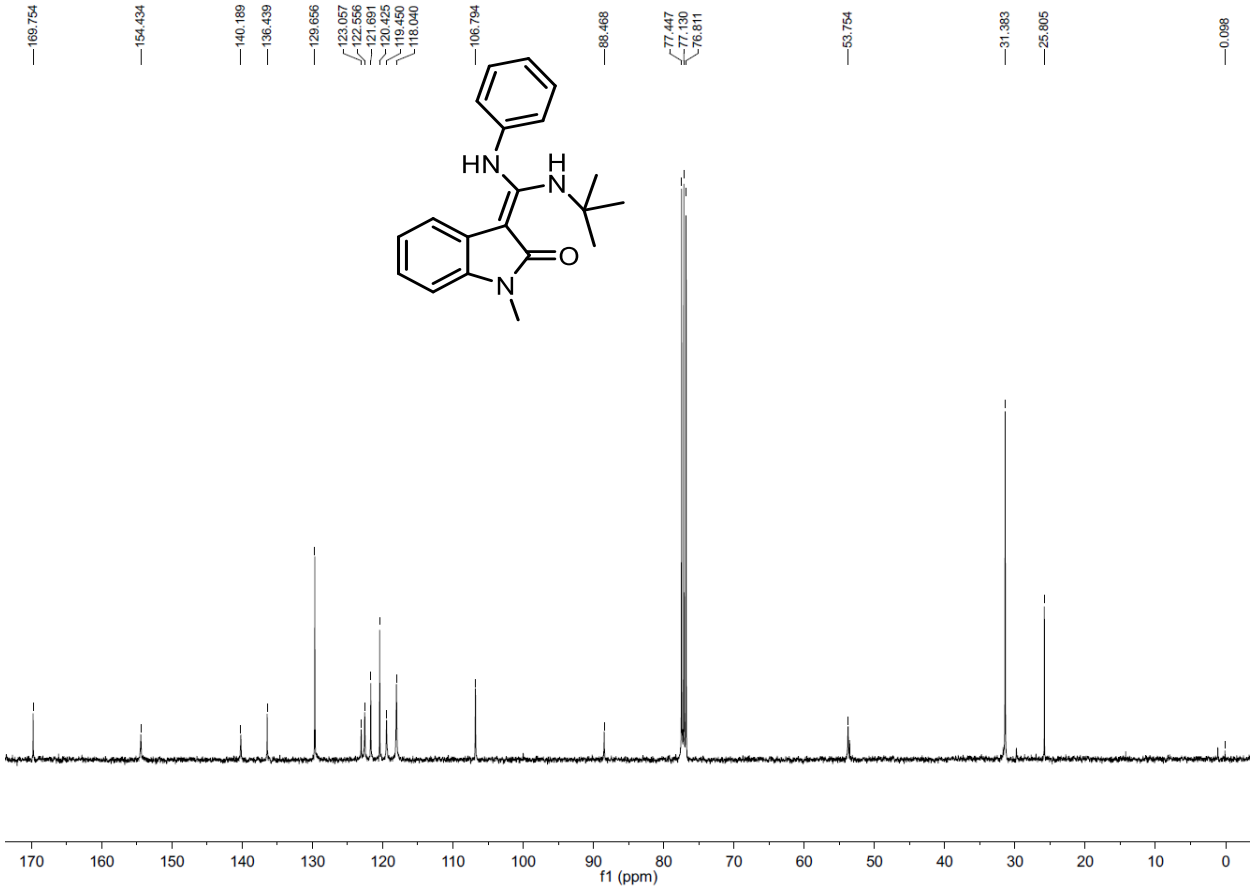

Representative Crystallographic Data of Chapter 2

Identification code	PS-309
Empirical formula	C20H22ClN3O
Formula weight	355.85
Temperature/K	293(2)
Crystal system	Monoclinic
Space group	P21/c
a/Å	14.7035(5)
b/Å	10.4600(3)
c/Å	12.2462(5)
α/°	90
β/°	101.646(4)
γ/°	90
Volume/Å3	1844.68(11)
Z	4
ρcalcg/cm3	1.281
μ/mm-1	0.220
F(000)	752.0
Crystal size/mm3	0.045 × 0.03 × 0.025
Radiation	MoKα (λ = 0.71073)
2Θ range for data collection/°	6.794 to 52.742
Index ranges	-18 ≤ h ≤ 18, -13 ≤ k ≤ 13, -14 ≤ l ≤ 15
Reflections collected	13923
Independent reflections	3583 [Rint = 0.0526, Rsigma = 0.0437]
Data/restraints/parameters	3583/0/230
Goodness-of-fit on F2	1.092
Final R indexes [I>=2σ (I)]	R1 = 0.0513, wR2 = 0.1341
Final R indexes [all data]	R1 = 0.0736, wR2 = 0.1563
Largest diff. peak/hole / e Å-3	0.34/-0.34
Ellipsoid contour % probability	50%

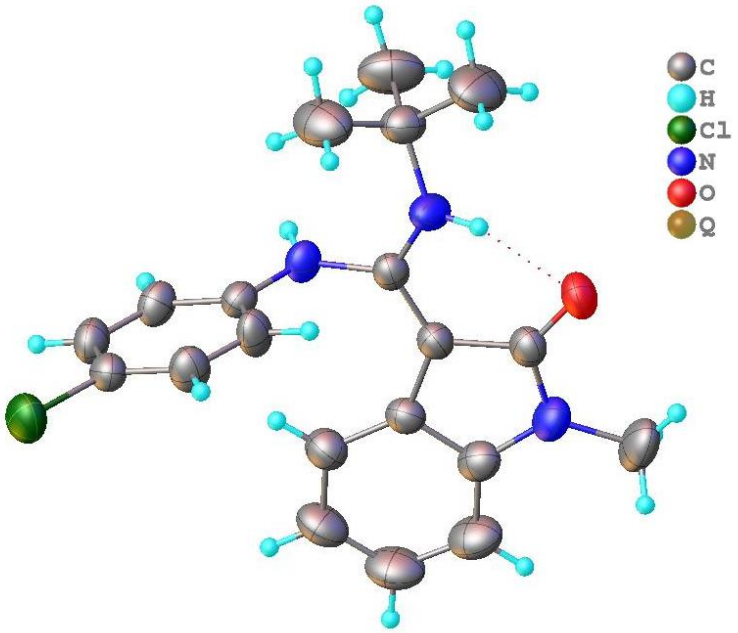

Figure (i): X-ray crystal structure of 4w (CCDC: 222643), ellipsoid contour 50 %

Representative ^{1}H NMR (400 MHz, $CDCl_3$) and $^{13}C\{^{1}H\}$ NMR (100 MHz, $CDCl_3$) spectra of Chapter 3

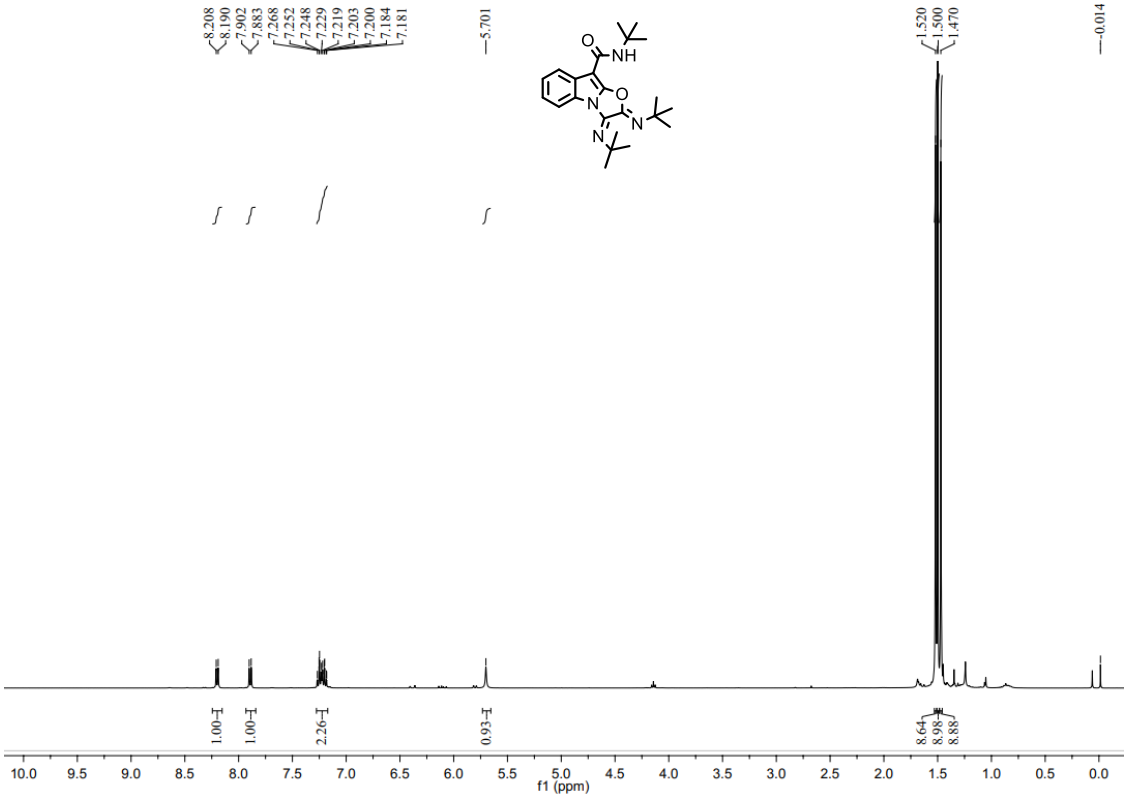

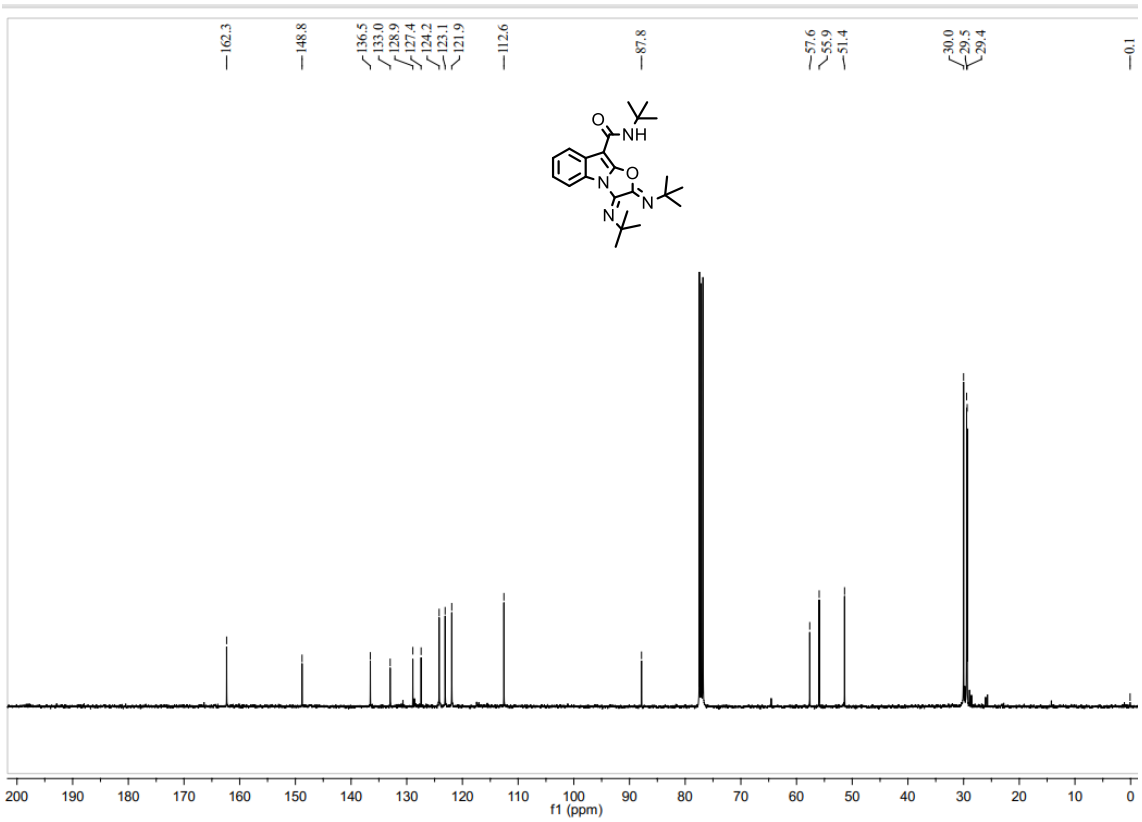

Representative Crystallographic Data of Chapter 3

Identification code	Ex-Thapar-pooja
Empirical formula	C23H32N4O2
Formula weight	396.52
Temperature/K	293(2)
Crystal system	triclinic
Space group	P-1
a/Å	9.59358(18)
b/Å	10.5593(2)
c/Å	11.9248(3)
α/°	103.8143(19)
β/°	97.5949(17)
γ/°	98.8737(17)
Volume/Å^3	1140.89(4)
Z	2

ρcalcg/cm^3	1.154
μ/mm^{-1}	0.075
F(000)	428.0
Crystal size/mm^3	0.05 × 0.04 × 0.03
Radiation	MoKα (λ = 0.71073)
2Θ range for data collection/°	6.474 to 52.74
Index ranges	-11 ≤ h ≤ 11, -13 ≤ k ≤ 12, -14 ≤ l ≤ 14
Reflections collected	15515
Independent reflections	4625 [Rint = 0.0351, Rsigma = 0.0350]
Data/restraints/parameters	4625/0/275
Goodness-of-fit on F^2	1.066
Final R indexes [I>=2σ (I)]	R_1 = 0.0497, wR_2 = 0.1260
Final R indexes [all data]	R_1 = 0.0698, wR_2 = 0.1399
Largest diff. peak/hole / e Å^{-3}	0.16/-0.23

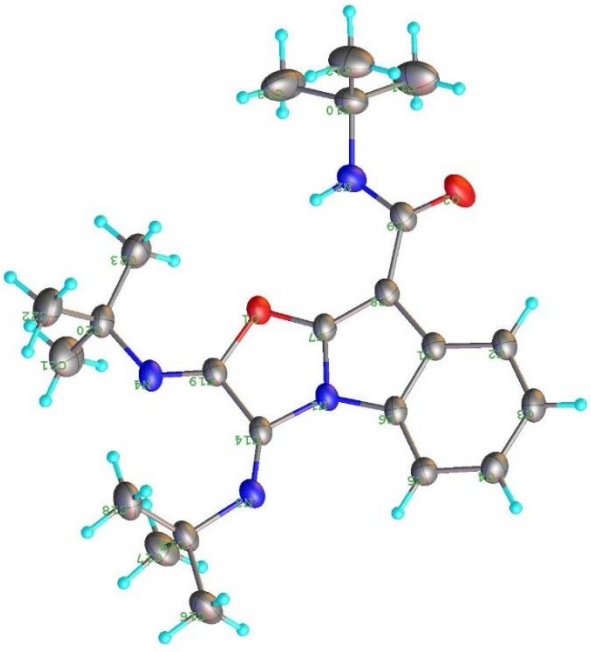

Figure (ii): ORTEP diagram for the crystal structure of 3a (CCDC: 2291510) (Ellipsoid = 50%)

Representative ^{1}H NMR (400 MHz, $CDCl_3$) and $^{13}C\{^{1}H\}$ NMR (100 MHz, $CDCl_3$) spectra of Chapter 4

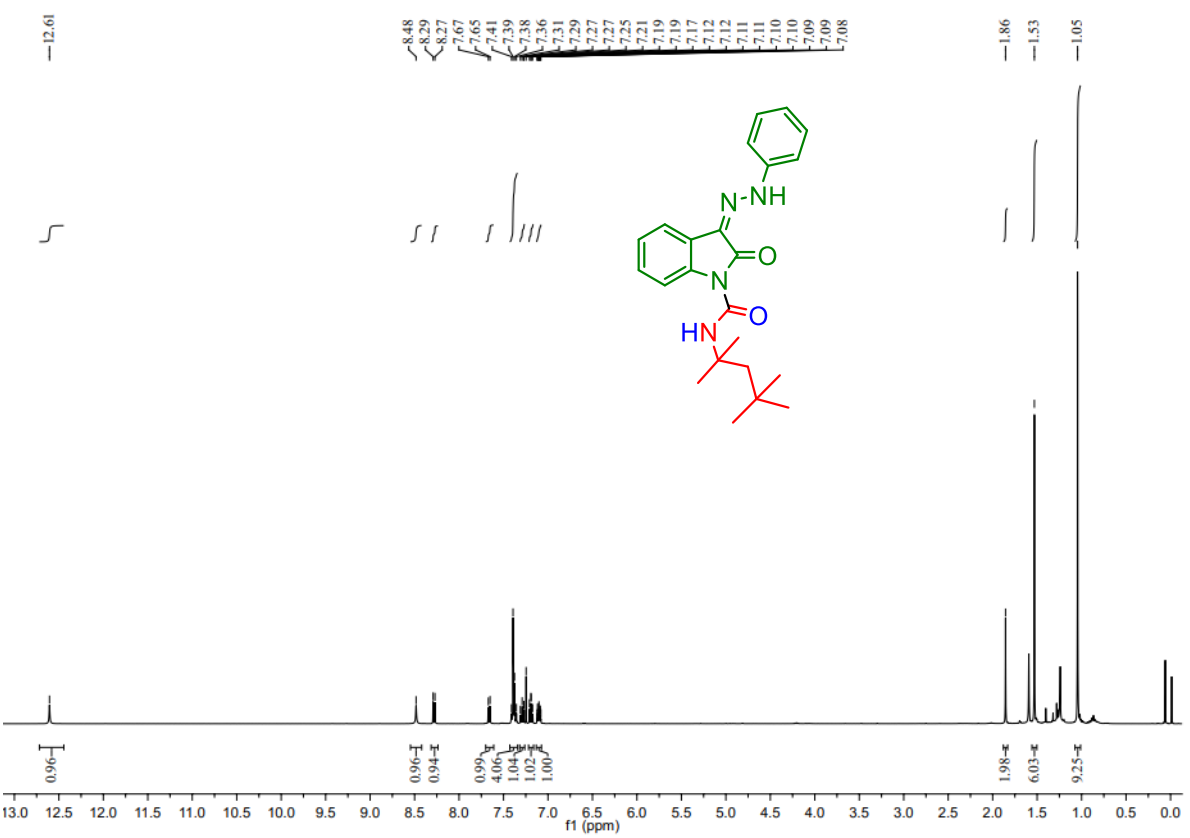

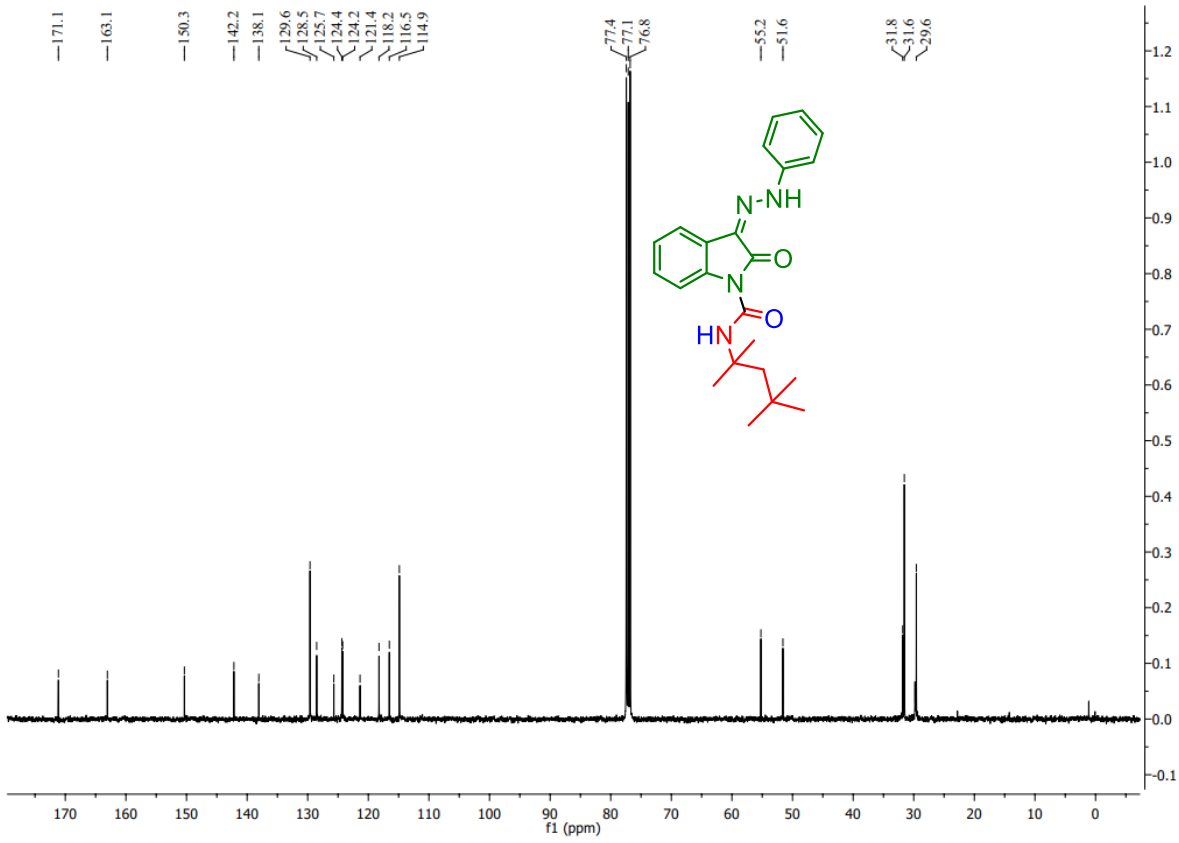

Representative ^{1}H NMR (400 MHz, $CDCl_3$) and $^{13}C\{^{1}H\}$ NMR (100 MHz, $CDCl_3$) spectra of Chapter 5

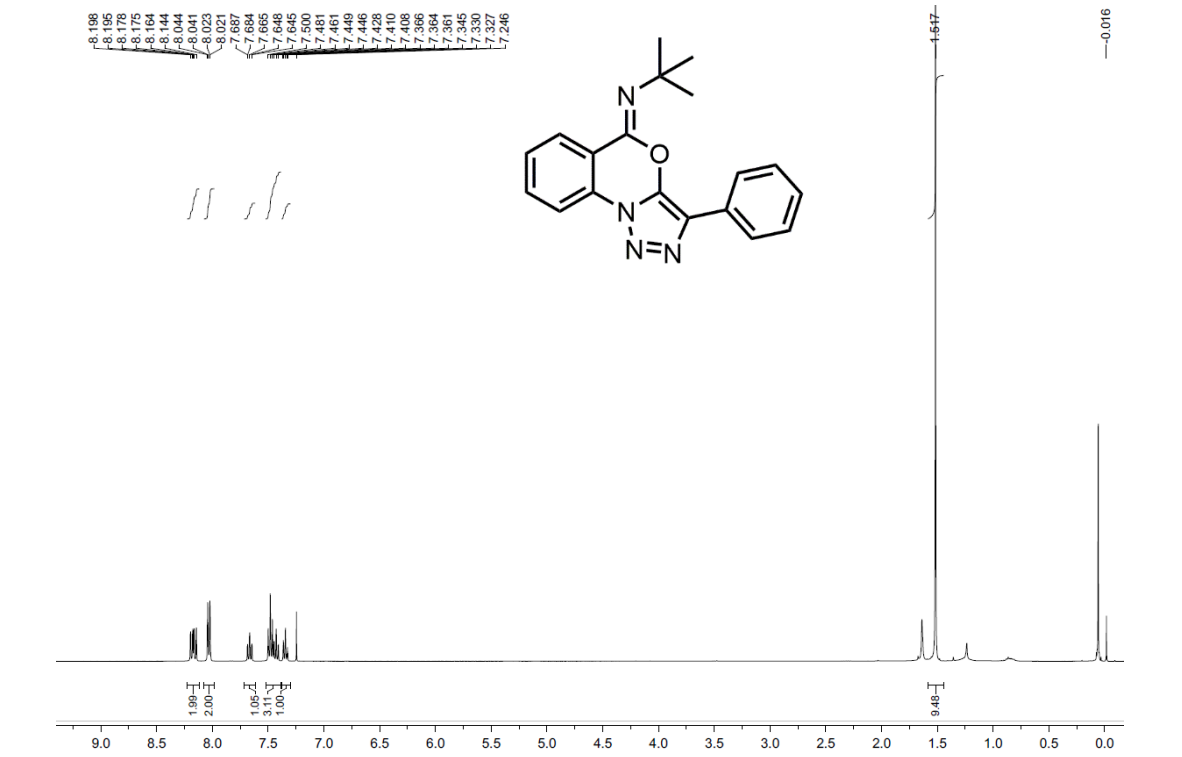

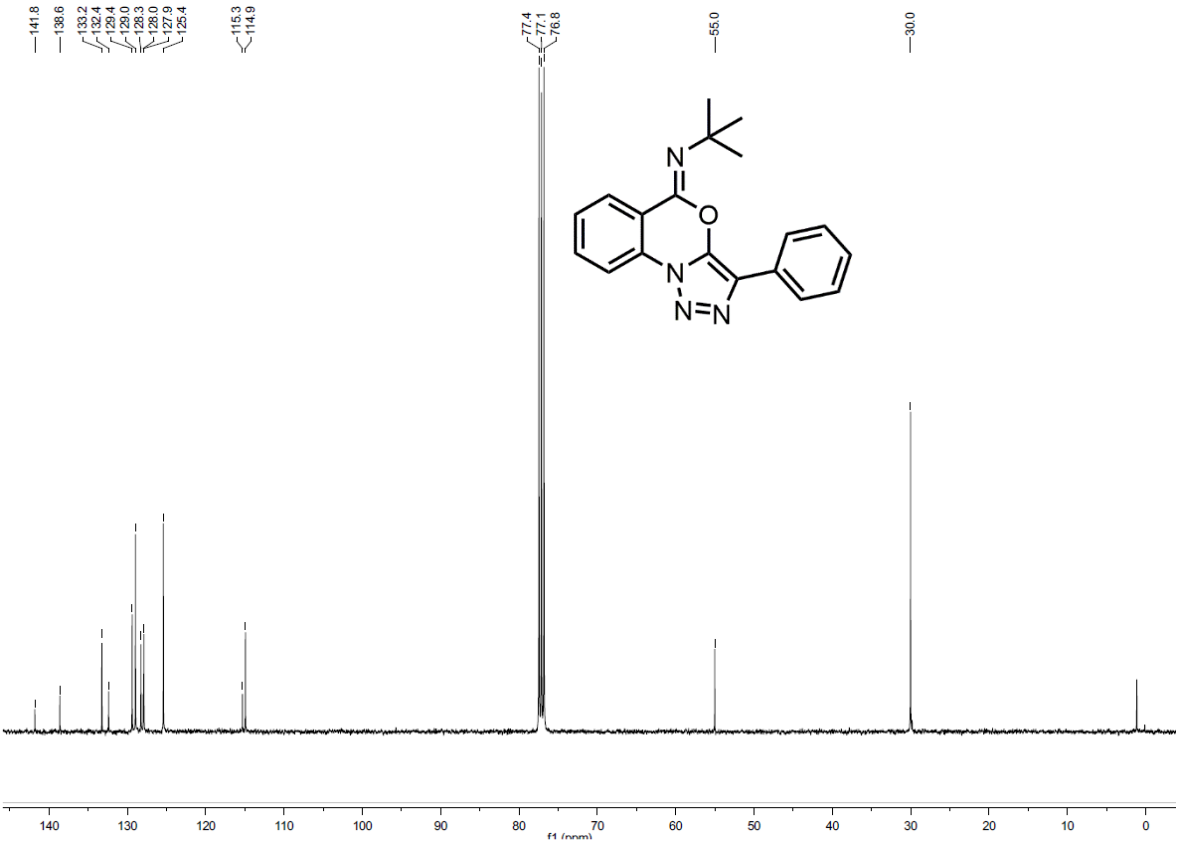

Representative Crystallographic Data of Chapter 5

Identification code	3b (dd-hg-11)
Empirical formula	C23 H26 N4 O
Formula weight	374.48
Temperature/K	150^{o}
Crystal system	monoclinic
Space group	P 1
a/Å	15.2432(13)
b/Å	6.8557(4)
c/Å	19.6543(15)
α/°	90
β/°	99.415(7)
γ/°	90
Volume/Å3	2026.3(3)
Z	4
ρ_{calc}g/cm^3	1.228
μ/mm^{-1}	0.077
F(000)	800
Crystal size/mm^3	0.15 x 0.28 x 0.4
Radiation MoKα	0.71073
2θ range for data collection/°	2.679- 25.999
Index ranges	-18 ≤ h ≤ 14, -6 ≤ k ≤ 8, -24 ≤ l ≤ 20
Reflections collected	3991
Independent reflections	2822
parameters	258
Goodness-of-fit on F2	1.080
Final R indexes [I>=2σ (I)]	0.0559
Final R indexes [all data]	0.0831
Largest diff. peak/hole / e Å-3	0.299/ -0.311
CCDC Number	**1985462**

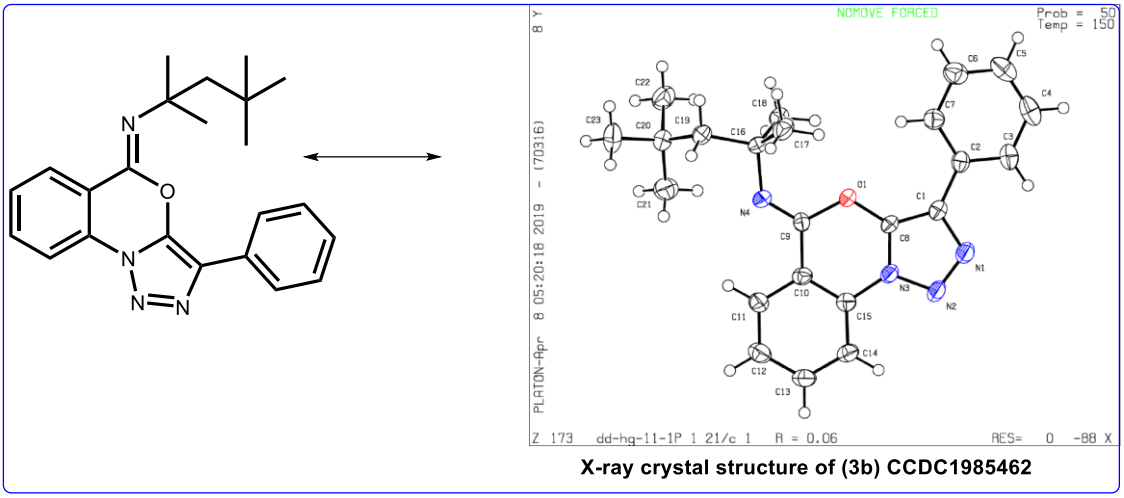

Figure (iii): ORTEP diagram for the crystal structure (CCDC: 1985462) (Ellipsoid = 50%)

1. **Soam, P**.; Mandal, D.; Tyagi, V. Divergent and Selective Synthesis of 3-Alkylidene Oxindoles Using Pd-Catalyzed Multicomponent Reaction. *J. Org. Chem.* **2023**, 88, 11023–11035.
2. **Soam, P.**; Mandal, D.; Tyagi, V. Synthesis of *N*-fused polycyclic indoles *via* a Pd-catalyzed multicomponent cascade reaction consisting of an amide-directed [3+1+1] annulation reaction of 3-diazo oxindole and isocyanides. *New J. Chem.* **2024,** *48*, 2639–2648.
3. **Soam, P**.; Gaba, H.; Mandal, D.; Tyagi, V. A Pd-catalyzed one-pot cascade consisting of C–C/C–O/N–N bond formation to access benzoxazine fused 1,2,3-triazoles. *Org. Biomol. Chem.* **2021**, *19*, 9936-9945.
4. **Soam, P**.; Kamboj, P.; Tyagi, V. Rhodium-Catalyzed Cascade Reactions using Diazo Compounds as a Carbene Precursor to Construct Diverse Heterocycles. *Asian. J. Org. Chem.* **2022**, *11*, e202100570.
5. **Soam, P**.; Mandal, D.; Tyagi, V. Palladium-Catalyzed Isocyanide Insertion into the Remotely Activated N-H bond of 3-(Phenylhydrazono)oxindoles: Facile Access to Indole-N-Carboxamide Derivatives. *Eur. J. Org. Chem.* **2024,** e202400439.

thesis pooja soam

ORIGINALITY REPORT

12%	10%	9%	7%
SIMILARITY INDEX	INTERNET SOURCES	PUBLICATIONS	STUDENT PAPERS

PRIMARY SOURCES

1	epublications.marquette.edu Internet Source	2%
2	pubs.rsc.org Internet Source	2%
3	nrl.northumbria.ac.uk Internet Source	2%
4	Chen, Andrew Dyhan. "New Radical Reactivity at the Interface of Synthetic Methodology Development and Computational Modeling", The Ohio State University, 2023 Publication	1%
5	Submitted to Rutgers University, New Brunswick Student Paper	1%
6	www.freepatentsonline.com Internet Source	1%
7	Submitted to Indian Institute of Technology Patna Student Paper	1%
	Submitted to Osmania University, Hyderabad	